INTERNATIONAL
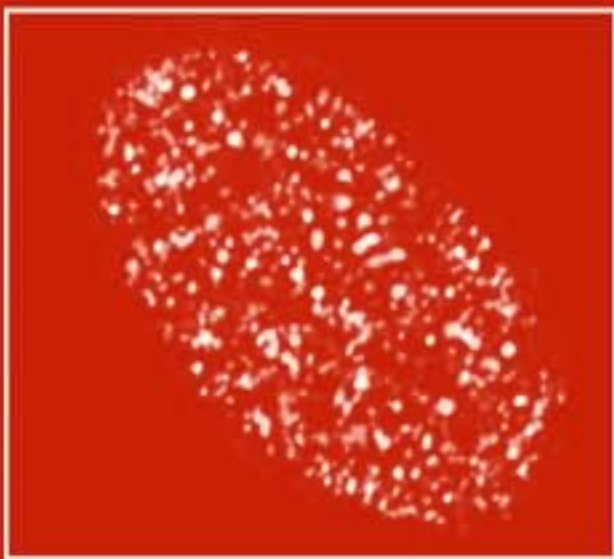# REVIEW OF CELL AND
MOLECULAR BIOLOGY

Edited by
Kwang W. Jeon

Volume 277

INTERNATIONAL REVIEW OF
CELL AND MOLECULAR BIOLOGY

INTERNATIONAL REVIEW OF CELL AND MOLECULAR BIOLOGY

Series Editors

GEOFFREY H. BOURNE	*1949–1988*
JAMES F. DANIELLI	*1949–1984*
KWANG W. JEON	*1967–*
MARTIN FRIEDLANDER	*1984–1992*
JONATHAN JARVIK	*1993–1995*

INTERNATIONAL REVIEW OF
CELL AND MOLECULAR BIOLOGY

EDITED BY

KWANG W. JEON
Department of Biochemistry
University of Tennessee
Knoxville, Tennessee

Contents

CONTRIBUTORS

Etienne Boulter
Department of Cell and Developmental Biology and Lineberger Comprehensive Cancer Center, CB#7295, University of North Carolina, Chapel Hill, North Carolina 27599

Keith Burridge
Department of Cell and Developmental Biology and Lineberger Comprehensive Cancer Center, CB#7295, University of North Carolina, Chapel Hill, North Carolina 27599

Kin-Chow Chang
School of Veterinary Medicine and Science, University of Nottingham, Sutton Bonington LE12 5RD, United Kingdom

Renee Doughman
Department of Cell and Developmental Biology and Lineberger Comprehensive Cancer Center, CB#7295, University of North Carolina, Chapel Hill, North Carolina 27599

Adi D. Dubash
Department of Cell and Developmental Biology and Lineberger Comprehensive Cancer Center, CB#7295, University of North Carolina, Chapel Hill, North Carolina 27599

Rafael García-Mata
Department of Cell and Developmental Biology and Lineberger Comprehensive Cancer Center, CB#7295, University of North Carolina, Chapel Hill, North Carolina 27599

Seiichiro Hasezawa
Institute for Bioinformatics Research and Development (BIRD), Japan Science and Technology Agency (JST), Tokyo 102-8666, Japan; and Department of Integrated Biosciences, Graduate School of Frontier Sciences, The University of Tokyo, Chiba 277-8562, Japan

Takumi Higaki
Institute for Bioinformatics Research and Development (BIRD), Japan Science and Technology Agency (JST), Tokyo 102-8666, Japan; and Department of Integrated Biosciences, Graduate School of Frontier Sciences, The University of Tokyo, Chiba 277-8562, Japan

Hartwig Höcker
DWI an der RWTH Aachen e.V. Pauwelsstrasse 8, D–52056 Aachen, Germany

Muthugapatti K. Kandasamy
Department of Genetics, Davison Life Sciences Building, University of Georgia,
Athens, Georgia 30602

Natsumaro Kutsuna
Institute for Bioinformatics Research and Development (BIRD), Japan Science
and Technology Agency (JST), Tokyo 102-8666, Japan; and Department of
Integrated Biosciences, Graduate School of Frontier Sciences, The University of
Tokyo, Chiba 277-8562, Japan

Joanne Mallinson
School of Veterinary Medicine and Science, University of Nottingham,
Sutton Bonington LE12 5RD, United Kingdom

Elizabeth C. McKinney
Department of Genetics, Davison Life Sciences Building, University of Georgia,
Athens, Georgia 30602

Richard B. Meagher
Department of Genetics, Davison Life Sciences Building, University of Georgia,
Athens, Georgia 30602

Joachim Meissner
Department of Physiology, OE4220, Hannover Medical School, D–30623
Hannover, Germany

Marisa M. Menold
Department of Cell and Developmental Biology and Lineberger Comprehensive
Cancer Center, CB#7295, University of North Carolina, Chapel Hill,
North Carolina 27599

Yoshihisa Oda
Department of Biological Sciences, Graduate School of Science, The University of
Tokyo, Tokyo 113-0033, Japan

Crisan Popescu
University ''Aurel Vlaicu,'' Bd. Revolutiei 77, RO–310130 Arad, Romania; and
DWI an der RWTH Aachen e.V. Pauwelsstrasse 8, D–52056 Aachen, Germany

Eileen Roy
Department of Genetics, Davison Life Sciences Building, University of Georgia,
Athens, Georgia 30602

Thomas Samson
Department of Cell and Developmental Biology and Lineberger Comprehensive Cancer Center, CB#7295, University of North Carolina, Chapel Hill, North Carolina 27599

Liudmila V. Solovjeva
Institute of Cytology, Russian Academy of Sciences, 194064 St. Petersburg, Russian Federation

Maria P. Svetlova
Institute of Cytology, Russian Academy of Sciences, 194064 St. Petersburg, Russian Federation

Nikolai V. Tomilin
Institute of Cytology, Russian Academy of Sciences, 194064 St. Petersburg, Russian Federation

Focal Adhesions: New Angles on an Old Structure

Adi D. Dubash, Marisa M. Menold, Thomas Samson,
Etienne Boulter, Rafael García-Mata, Renee Doughman,
and Keith Burridge

Contents

Department of Cell and Developmental Biology and Lineberger Comprehensive Cancer Center, CB#7295, University of North Carolina, Chapel Hill, North Carolina 27599

Abstract

Focal adhesions have been intensely studied ever since their discovery in 1971. The last three decades have seen major advances in understanding the structure of focal adhesions and the functions they serve in cellular adhesion, migration, and other biological processes. In this chapter, we begin with a historical perspective of focal adhesions, provide an overview of focal adhesion biology, and highlight recent major advances in the field. Specifically, we review the different types of matrix adhesions and the role different Rho GTPases play in their formation. We discuss the relative contributions of integrin and syndecan adhesion receptors to the formation of focal adhesions. We also focus on new insights gained from studying focal adhesions on biomaterial surfaces and from the growing field of mechanotransduction. Throughout this chapter, we have highlighted areas of focal adhesion biology where major questions still remain to be answered.

Key Words: Focal adhesion, Extracellular matrix, Integrins, Syndecan-4, GEF, Rho GTPase, RhoA, Biomaterial surfaces, Mechanotransduction, Focal adhesion disassembly. © 2009 Elsevier Inc.

ABBREVIATIONS

CBD	cell–binding domain
CG	collagen
DH	Dbl homology
ECM	extracellular matrix
EM	electron microscopy
FA	focal adhesion
FAK	focal adhesion kinase

FBA	fibrillar adhesion
FCX	focal complex
FN	fibronectin
GAG	glycosaminoglycan
GAP	GTPase-activating protein
GDI	GTPase dissociation inhibitor
GEF	guanine nucleotide exchange factor
GFP	green fluorescent protein
HBD	heparin-binding domain
HSPG	heparan sulfate proteoglycan
IRM	interference reflection microscopy
LPA	lysophosphatidic acid
MT	microtubule
PH	pleckstrin homology
$PtdIns(4,5)P_2$	phosphatidylinositol 4,5-bisphosphate
PKCα	protein kinase Cα
PM	plasma membrane
ROCK	Rho kinase
SAM	self-assembled monolayers
SF	stress fiber
Syn (1–4)	syndecan (1–4)
VN	vitronectin

1. INTRODUCTION

Adhesive interactions are critical to the lives of metazoan cells. Essentially, two types of adhesion exist: those made between adjacent cells, and others made between cells and components of the extracellular matrix (ECM). Adhesion to the ECM is required for survival and growth of cells, and influences both cell morphology and migration. Today, ECM adhesions are known to be composed of more than 50 different proteins. Structural proteins provide a scaffold linking transmembrane ECM-binding integrins to the actin cytoskeleton, thereby anchoring cells to the substratum. The signaling proteins (kinases, phosphatases, exchange factors, etc.) respond to different environmental cues, and transmit signals to the intracellular environment. Numerous signaling pathways are activated by focal adhesion (FA) proteins, including those that control cell survival, division, differentiation, and migration (Zaidel–Bar et al., 2004; Zamir and Geiger, 2001).

Whereas this field has become much too large to review here in its entirety, we will focus mainly on discussing new insights gained in several different areas of FA biology, such as their structure, function, and the

mechanisms involved in their formation and disassembly. Besides classic FAs, other ECM adhesion structures will be discussed, such as focal complexes (FCXs), fibrillar adhesions (FBAs), and podosomes. We will first describe the roles integrin and syndecan adhesion receptors play in FA formation, and discuss the interplay between these two types of receptors. In addition, we will discuss in detail two fields that are currently active areas of study—the analysis of FA structure on biomimetic surfaces, and the transduction of mechanical forces into adhesion-regulated signaling events (a process known as mechanotransduction). We refer the reader to other excellent reviews which discuss areas of FA biology we do not cover in detail here (Geiger et al., 2001; Lock et al., 2008; Romer et al., 2006; Webb et al., 2003; Zaidel-Bar et al., 2004, 2007a). To begin, we will present a historical perspective detailing the first studies involving adhesions to the ECM. Adhesions to the underlying substratum were first observed by electron microscopy (EM), where they were described as dense plaques which appeared to anchor bundles of microfilaments [stress fibers (SFs)] at the ventral plasma membrane (PM) (Abercrombie et al., 1971). These structures were originally termed *adhesion plaques*, but nothing was known of their composition or protein complexity. At the light microscope level, the technique of interference reflection microscopy (IRM) was developed to visualize how close the ventral surface of a cell approaches the substratum (Curtis, 1964). This technique was used to show that the adhesion plaques seen by EM coincided with regions that came closest to the substratum, appearing most dark by IRM (Abercrombie and Dunn, 1975). IRM was also used to distinguish two types of adhesion made by cells: *focal contacts,* with the separation of the PM being 10–15 nm from the substratum, and *close contacts* which have a separation of about 30 nm (Izzard and Lochner, 1976). Whereas much is now known about focal contacts, close contacts remain poorly characterized and relatively unstudied.

At about the same time that IRM was being used to identify the adhesions made between cells in culture and their underlying substratum, immunofluorescence microscopy was beginning to be used to visualize the distribution of cytoskeletal proteins. The first localization of α-actinin within fibroblasts revealed that it was not only distributed periodically along the length of SFs, but that it was also enriched in "patches" at their ends (Lazarides and Burridge, 1975). This localization led to the speculation that it might correspond to the adhesion plaques described by Abercrombie and coworkers, and that α-actinin might be involved in anchoring the bundles of actin filaments to the PM at these sites. Whereas α-actinin is distributed both along SFs as well as at their ends, the distribution of vinculin, another cytoskeletal protein was striking because it was the first to be localized exclusively to the termini of SFs (Geiger, 1979). Over time, the use of antibodies against proteins like vinculin, or the expression of these proteins tagged with green fluorescent protein (GFP) or its derivatives, became the standard way to visualize adhesions made to the ECM.

However, these techniques have also revealed that not all adhesions are the same and that there is heterogeneity with respect to their components.

The terms *adhesion plaque* and *focal contact* were used essentially interchangeably for several years and are still used by some authors, but FA has become the most commonly used term to describe the large adhesions that anchor SFs in cells (Fig. 1.1B). The term *focal adhesion* was coined when adhesion plaques visualized by EM were shown to be the same as focal contacts by IRM (Heath and Dunn, 1978). FAs have been studied for a long time and the reader is referred to earlier reviews for older information about their composition, assembly, and structure (Burridge and Chrzanowska-Wodnicka, 1996; Burridge et al., 1988; Jockusch et al., 1995; Schwartz et al., 1995; Woods and Couchman, 1988).

The term *focal complex* was introduced by Nobes and Hall in 1995 to refer to a distinct set of smaller adhesions (Nobes and Hall, 1995; Wang et al., 1997) (Fig. 1.1A). Earlier work had demonstrated that the formation of FAs and SFs is regulated by the GTP-binding protein, Rho (Ridley and Hall, 1992). When Rho activity was inhibited, but the related proteins Rac1 or Cdc42 were activated, small adhesions were induced to form at the cell periphery (Nobes and Hall, 1995). These FCXs are less stable than FAs and can mature into FAs in response to active GTP-bound Rho.

A third type of adhesion is associated with the long fibrillar arrays formed by the assembly of ECM components such as fibronectin (FN). Over time, FN fibrils can assemble to form a dense meshwork, but early in cell culture, when the fibrils first form, they are often seen to parallel the distribution of SFs (Hynes and Destree, 1978). Indeed, a transmembrane relationship between FN fibrils on the outside of cells with actin filaments on the inside led to this complex being referred to as the *fibronexus* (Singer, 1979), although this term has largely been dropped. When the protein vinculin was microinjected into cells, it was recruited both to FAs and to a fibrillar pattern, which aligned with FN fibrils on the cell surface (Burridge and Feramisco, 1980). EM also revealed vinculin within the fibronexus (Singer and Paradiso, 1981). Only much later were FAs compared to the adhesions made to FN fibrils. Multiple differences were noted both in the assembly of these structures and in their protein composition, leading the authors to distinguish FBAs from FAs (Zamir et al., 1999, 2000) (Fig. 1.1C). While discussing FAs will be the major focus of this chapter, FCXs and FBAs will also be briefly discussed.

2. Formation of ECM Adhesions

2.1. ECM adhesion receptors: Integrins and syndecans

In tissues, cells interact with many different ECM components, including FN, collagen (CG), laminin (LN), and many proteoglycans. However, most research performed on cell adhesion in 2D tissue culture models has focused

A   Focal complex   B   Focal adhesion   C   Fibrillar adhesion

D   Podosome   E   Invadopodia
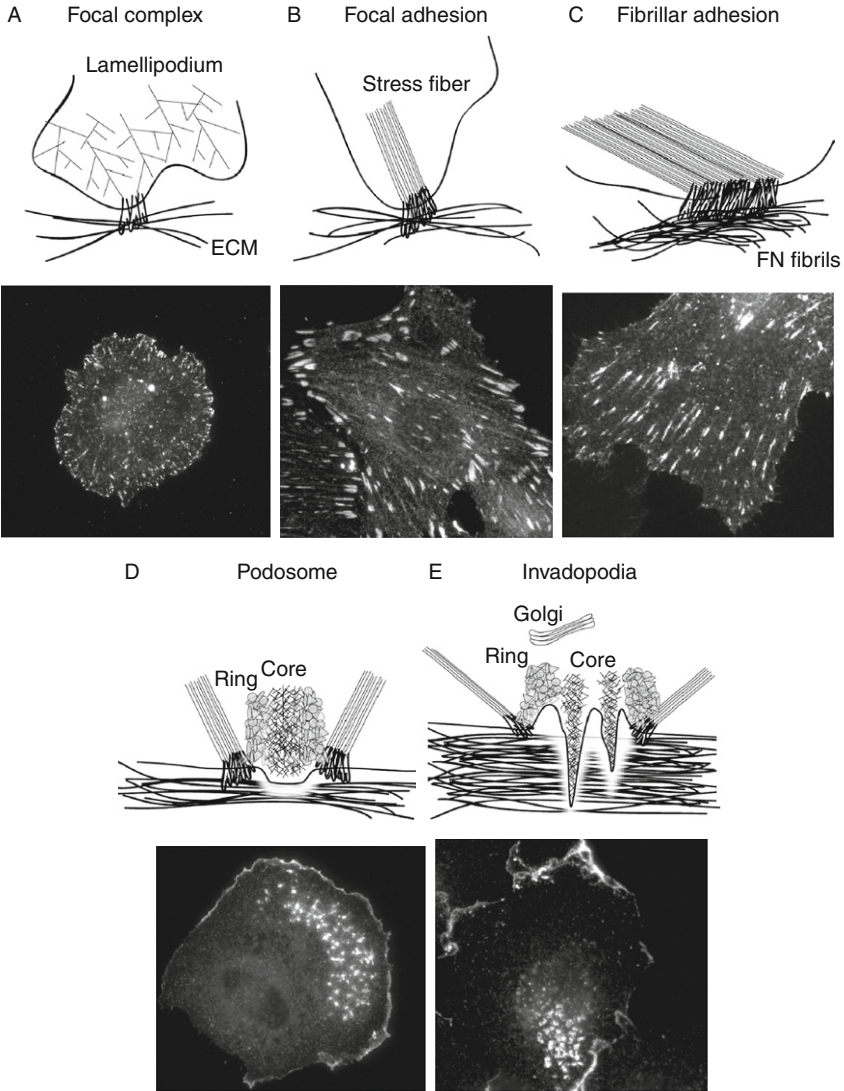
Figure 1.1 Types of ECM adhesions. Structural differences between the different types of ECM adhesions. (A) Focal complexes (FCXs) and (B) focal adhesions (FAs) were visualized by staining with anti–Paxillin. (C) Fibrillar adhesions (FBAs) were visualized by transfecting cells with GFP-tagged tensin. (D) Podosomes and (E) invadopodia were observed by staining cells for F-actin.

on adhesion of cells to FN, or to surfaces to which the serum protein vitronectin (VN) has been adsorbed (either intentionally or often simply because the cells have been grown in the presence of serum). Most cells do not adhere well to glass surfaces to which proteins have not been adsorbed,

although various leukocytes are an exception. The major cell surface proteins that bind FN and VN belong to the integrin family of cell adhesion receptors. Integrins are heterodimeric, transmembrane receptors that are made up of noncovalently linked α and β subunits (Hynes, 2002). It is this α/β combination that confers ligand specificity on the particular integrin (Humphries et al., 2006). So far, 18 α subunits and 8 β subunits have been identified in humans, and these can combine to generate 24 different integrins.

Integrins have large extracellular domains that mediate binding to different ECM ligands. Each subunit spans the membrane once, and the cytoplasmic domains of both α and β chains are short and lack enzymatic activity. The cytoplasmic domain of the β_4 subunit is a notable exception, as it is long and provides attachment for keratin filaments (in hemidesmosomes) rather than actin filaments (Borradori and Sonnenberg, 1999). Multiple different integrins have been identified in FAs in culture, but the integrins most studied are the canonical FN- and VN-binding integrins, $\alpha_5\beta_1$ and $\alpha_v\beta_3$. Whereas $\alpha_5\beta_1$ binds almost exclusively to FN, $\alpha_v\beta_3$ binds to FN, VN, and other ECM proteins (Hynes, 1992). The specific roles integrins play in the formation and structure of FAs have been well studied and are discussed in detail below. A second type of adhesion receptor, syndecan-4 (syn4), has also been shown to be important for the formation of mature FAs. Syn4 is a ubiquitously expressed heparan sulfate proteoglycan (HSPG) that binds to several different ECM proteins (Bass and Humphries, 2002; Couchman, 2003).

The extracellular domains of integrins and syndecans bind to different regions of FN. The mature FN molecule is a dimer of two disulfide-linked chains, and each monomer chain contains multiple repeat domains (Fig. 1.2). The tripeptide RGD sequence in FN repeat III_{10}, part of the cell-binding domain (CBD), is the central recognition sequence required for most FN-binding integrins (Hynes, 2002; Pankov and Yamada, 2002). A different region containing FN repeats III_{12-14} is the major heparin-binding domain (HBD or HepII), and serves as the attachment site for syndecans (Bass and Humphries, 2002) (Fig. 1.2).
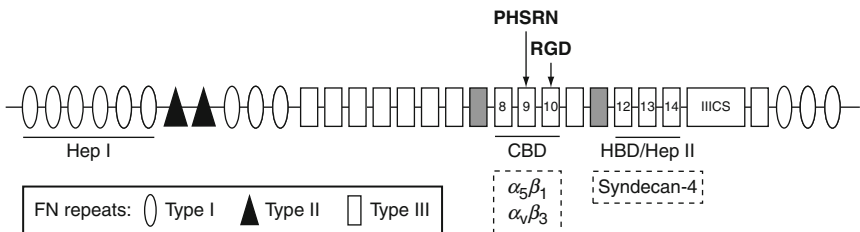
Figure 1.2 Structure of fibronectin (FN). The FN molecule is made up of three different types of domain repeats, type I, II, and III. Type III repeats 9–10 (CBD) support adhesion to integrins, and repeats 12–14 (HBD/HepII) support adhesion to syn4.

2.2. Regulation of focal adhesion assembly by Rho GTPases

Integrins and syn4 are both involved in the process of FCX and FA assembly through the regulation of Rho GTPases (Arthur and Burridge, 2001; Arthur et al., 2000, 2002; Bass and Humphries, 2002; Chrzanowska-Wodnicka and Burridge, 1996; Hotchin and Hall, 1995; Humphries et al., 2005; Ren et al., 1999; Ridley and Hall, 1992; Saoncella et al., 1999). The Rho GTPases are a major subfamily of the Ras superfamily, containing at least 20 members, with RhoA, Rac1, and Cdc42 being among the best characterized GTPases. These proteins function by switching between an active GTP-bound form that can interact with downstream effectors, and an inactive form that is bound to GDP (Wennerberg and Der, 2004; Wennerberg et al., 2005) (Fig. 1.3). The activation state of the GTPase is regulated by three types of proteins. Guanine nucleotide exchange factors (GEFs) activate GTPases by causing the exchange of GDP for GTP. GTPase-activating proteins (GAPs) inactivate GTPases by promoting the intrinsic hydrolytic activity of the proteins. Guanine nucleotide dissociation inhibitors (GDIs) bind to GTPases and sequester them in the cytosol in their inactive conformation (Rossman et al., 2005) (Fig. 1.3).

Activation of Rho GTPases downstream of ECM adhesion triggers signaling cascades that regulate cytoskeletal architecture and FA formation, thereby allowing the cells to spread and migrate on ECM substrates. The different GTPases have distinct effects on SF and FA structure. Initially, Rac and Cdc42 stimulate the formation of broad lamellipodia, filopodia, and punctate FCXs at the cell periphery, allowing for initial cell attachment and spreading. At later time points, RhoA induces the assembly of SFs and FAs (Kozma et al., 1995; Nobes and Hall, 1995; Ridley and Hall, 1992).

While it had been demonstrated previously that RhoA was necessary for the formation of SFs (Chardin et al., 1989; Paterson et al., 1990; Rubin et al., 1988), a seminal study in 1992 showed that RhoA was also required for the assembly of FAs (Ridley and Hall, 1992). Microinjection of constitutively active mutants of RhoA into quiescent serum-starved cells led to the rapid formation of SFs and FAs, an effect that was also seen when cells were treated with serum or lysophosphatidic acid (LPA). These effects could be blocked by the addition of C3 exotransferase (which ADP-ribosylates and inactivates RhoA), indicating that RhoA activity was critical for the formation of FAs. Adhesion to the ECM was also shown to be necessary for RhoA-induced FA assembly, as its effects were not evident in the absence of integrin-specific matrix adhesion (Hotchin and Hall, 1995).

Later studies developed the use of the RhoA activity assay, which allows for a direct assessment of RhoA GTPase activity. This pull-down assay uses the Rho-binding domain (RBD) of the RhoA effector protein Rhotekin to selectively precipitate active GTP-bound RhoA (Ren et al., 1999). These studies showed that when cells are plated on FN, RhoA activity undergoes a
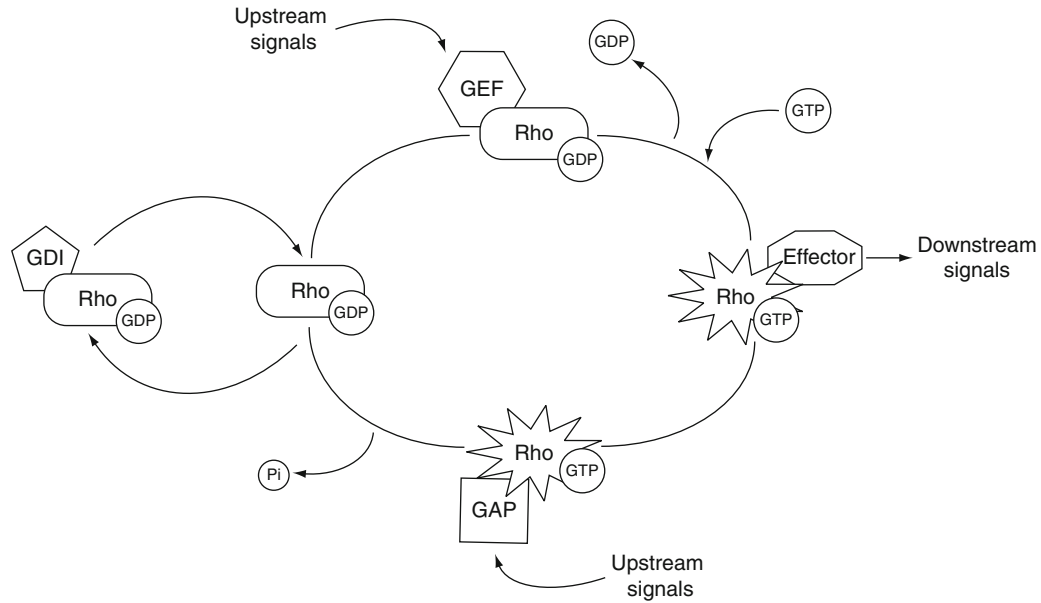
Figure 1.3 Rho GTPase cycle. Rho proteins cycle between a GTP-bound ''on'' state and a GDP-bound ''off'' state. This cycle is controlled by three types of regulatory proteins, guanine nucleotide exchange factors (GEFs), GTPase–activating proteins (GAPs), and GTPase dissociation inhibitors (GDIs).

biphasic transition (Fig. 1.4). Initially, RhoA activity is briefly inhibited, allowing the cells to spread on the matrix. This transient dip is followed by a sustained increase in RhoA activity levels which coincides with the formation of SFs and FAs (Ren et al., 1999).

It has been shown that engagement of integrins causes the initial decrease in RhoA activity through the activation of the Src kinase, which phosphorylates and activates a negative regulator of RhoA, p190 RhoGAP (Arthur and Burridge, 2001; Arthur et al., 2000). The subsequent increase in RhoA activity is caused by activation of several different RhoA-specific GEFs downstream of ECM adhesion (Dubash et al., 2007; Lim et al., 2008) (Fig. 1.4). The mechanisms involved in regulating this biphasic transition of RhoA is discussed in detail in the next section.

Activation of RhoA leads to SF and FA formation via activation of several different effector proteins. Specifically, activation of Rho kinase (ROCK) causes an increase in myosin light chain (MLC) phosphorylation, via phosphorylation (and inactivation) of the MLC phosphatase, as well as direct phosphorylation of MLC itself (Fig. 1.5). Increase in MLC phosphorylation promotes the assembly of myosin II into bipolar filaments and stimulates the interaction of myosin II with actin filaments, resulting in an increase in contractility and bundling of the existing actin filaments into SFs
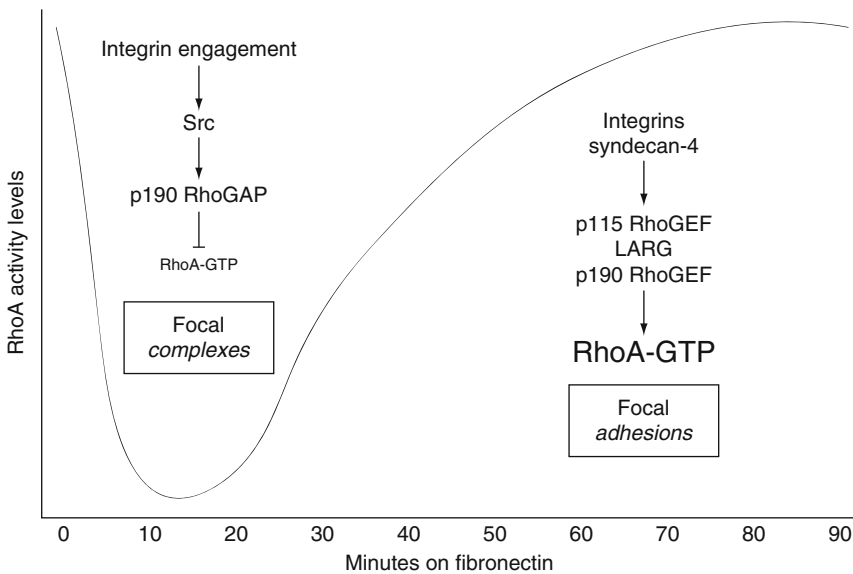
Figure 1.4   Regulation of RhoA activity by FN. RhoA activity undergoes a biphasic transition upon adhesion of cells to FN, where a brief inactivation phase is followed by a sustained reactivation phase. This biphasic transition is regulated by different GAPs and GEFs.
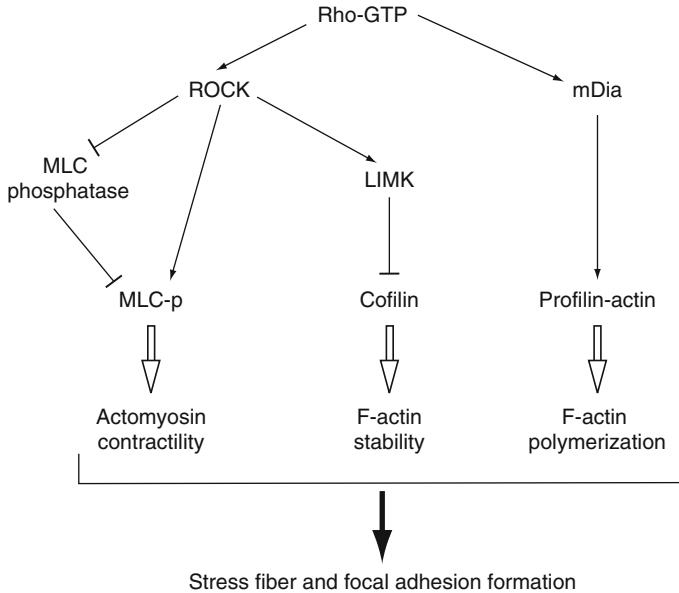
Figure 1.5 RhoA effector pathways. RhoA activity regulates various pathways to SF and FA formation via different effector proteins. Activation of ROCK downstream of GTP-bound RhoA promotes actomyosin contractility, and activation of mDia increases F-actin polymerization and SF organization.

(Pellegrin and Mellor, 2007). This increase in tension and the bundling lead to integrin clustering and formation of large FAs at the ends of the SFs (Chrzanowska–Wodnicka and Burridge, 1996). Other RhoA effector pathways also affect SF and FA formation. Phosphorylation of LIM kinase by ROCK causes phosphorylation and inactivation of cofilin, which leads to stabilization of F-actin filaments (Bishop and Hall, 2000). Activation of mDia, another RhoA effector, is required in addition to ROCK for proper SF formation. mDia, in conjunction with profilin, causes an increase in F-actin polymerization and SF organization (Bishop and Hall, 2000; Watanabe et al., 1997) (Fig. 1.5).

SFs and FAs are closely linked, with FAs rarely if ever being seen without an associated bundle of actin filaments. One of the favorite models for studying the assembly of FAs has been to use quiescent, well spread cells in which RhoA activity is low and in which SFs and FAs are either absent or very reduced (Ridley and Hall, 1992). Activation of RhoA, for example, by addition of LPA or introduction of constitutively active RhoA, rapidly leads to the assembly of both SFs and FAs (Ridley and Hall, 1992). This model was used to show that Rho acts by activating myosin II, resulting in bundling of actin filaments and increased tension leading to the formation

of SFs and the clustering of dispersed integrins to form FAs (Chrzanowska-Wodnicka and Burridge, 1996). The SFs developed in this situation are ventral SFs. Other types of actin bundle organization have been described in more dynamic, motile cells, and cells that are spreading on an ECM-coated surface (Small et al., 1998). Whereas ventral SFs are attached at each end to FAs and appear to be under isometric tension, dorsal SFs arise at the cell periphery and are attached only at one end to a FA or FCX. The dorsal SF rises up from the ventral attachment passing into the dorsal cortex of the cell. In an elegant study, Hotulainen and Lappalainen observed the behavior of dorsal SFs and showed that in some situations the ends of two opposing dorsal SFs come into contact, fuse, and the tension developed converts these into ventral SFs (Hotulainen and Lappalainen, 2006). These investigators demonstrated that growth of dorsal SFs occurs by a formin-mediated (mDia1/DRF1) polymerization of actin. In addition to ventral and dorsal SFs, many cells that are spreading or migrating develop dorsal ''arcs'' that form in the lamellipodia and move centripetally toward the nucleus (Heath and Holifield, 1993; Soranno and Bell, 1982). Hotulainen and Lappalainen found that arcs can also give rise to ventral SFs, by annealing with dorsal SFs thereby becoming attached to FAs (Hotulainen and Lappalainen, 2006). In the case of arcs, they provided evidence that these arise from actin polymerization driven by the Arp2/3 complex.

2.3. The role of GEFs and GAPs in focal adhesion formation

Activity of the Rho family of GTPases is mainly controlled by two major regulatory protein families, GEFs and GAPs. The Dbl proteins are the major family of GEFs for Rho GTPases, containing approximately 70 members. Dbl family proteins are characterized by tandem Dbl homology (DH) and Pleckstrin homology (PH) domains. The DH domain is responsible for catalytic activity of the proteins, by facilitating binding to GTPases and destabilization of the nucleotide-binding pocket, leading to rapid exchange of GDP for GTP (Rossman et al., 2005). A second smaller family of GEFs known as CZH proteins, catalyze activation of Rac and Cdc42 by binding to a DH-unrelated DOCKER or CZH2 (Ced5-Dock180-Myoblast city (CDM)-zizimin homology 2) domain (Meller et al., 2005).

GAPs for Rho GTPases also comprise a large family of approximately 80 members, all of which contain a RhoGAP domain that is capable of binding GTP-bound Rho proteins and stimulating their intrinsic GTPase activity (Moon and Zheng, 2003). Of the approximately 70 known GEFs and 80 known GAPs, few have been extensively studied. In addition, while much is known about how Rho proteins regulate FA formation downstream of FN adhesion, comparatively little is known about the role of specific GEFs or GAPs in this process.

Activation of Rac upon cell spreading causes the recruitment of a complex of the Rac GEF Pix and the Arf GAP PKL/GIT to FCXs. In turn, the PKL/GIT–Pix complex is responsible for recruitment of the Rac downstream effector PAK to FAs (Brown et al., 2002; Rosenberger and Kutsche, 2006). Importantly, both Pix and PAK play a role in the maintenance of paxillin-containing FAs (Stofega et al., 2004). Interestingly, PKL/GIT binds another Rac GEF, Vav2, and recruits it to FAs. The ability of PKL/GIT to recruit Vav2 to FAs is also dependent on the FA protein Paxillin (Jamieson et al., 2009). The signaling complex involving Pix, Paxillin, PAK, and PKL/GIT has been reviewed extensively elsewhere (Rosenberger and Kutsche, 2006).

As already mentioned, RhoA activity is initially decreased when cells are plated onto FN. This transient dip in RhoA activity is caused by activation of p190 RhoGAP, by activation of Src in an integrin-dependent manner (Arthur et al., 2000) (Fig. 1.4). Loss of p190 RhoGAP function causes a premature activation of RhoA, SF, and FA formation, thereby hindering cell spreading in response to matrix adhesion (Arthur and Burridge, 2001).

Besides phosphorylation by Src, several different mechanisms have been shown to regulate p190 RhoGAP downstream of FN adhesion. The Arg kinase has also been shown to phosphorylate p190 RhoGAP in response to integrin-mediated adhesion. Arg-dependent phosphorylation of p190 RhoGAP promotes its binding to p120 RasGAP, which is required for proper membrane localization of p190 RhoGAP (and hence RhoA inactivation) (Bradley et al., 2006). The importance of p120 RasGAP for RhoA signaling downstream of adhesion was demonstrated in a study using p120 RasGAP null cells. In wound healing experiments, p120 RasGAP cells were unable to reorient their FAs for proper wound closure, a likely consequence of deregulated RhoA signaling (Kulkarni et al., 2000).

The reactivation of RhoA in FN adhered cells is regulated by a subfamily of GEFs known as RGS-GEFs, which includes Lsc/p115 RhoGEF and Leukemia associated RhoGEF (LARG) (Dubash et al., 2007) (Fig. 1.4). Importantly, knockdown of these GEFs causes a major defect in the ability of cells to form FAs when plated onto FN. Also, both these GEFs can localize subcellularly in patch-like structures that partially colocalize with paxillin-containing FAs (Dubash et al., 2007). The mechanism by which these GEFs localize to these regions remains to be determined. Interestingly, RGS-GEFs also play a major role in controlling RhoA activity downstream of activation of G-protein-coupled receptors by LPA or thrombin (Fukuhara et al., 1999, 2000, 2001; Hart et al., 1998; Majumdar et al., 1999; Suzuki et al., 2003; Wang et al., 2004).

p190 RhoGEF (an exchange factor closely related to the RGS-GEF family) was also shown to be involved in regulating FN-induced RhoA activation via its association with focal adhesion kinase (FAK) (Lim et al., 2008). The functional redundancy caused by a number of

related RhoA GEFs being involved in regulating FA formation down-
stream of FN adhesion highlights the importance of tight spatiotemporal
regulation of this process. In addition to controlling FA formation, there is
also evidence to show that RGS–GEFs are directly involved in regulating
adhesion dynamics in fibroblasts. Knockdown of the RGS–GEF PDZ
RhoGEF causes a decrease in the movement of FAs in response to LPA
treatment (Iwanicki et al., 2008). Cells lacking PDZ RhoGEF demon-
strate an inability to retract their tails when stimulated, an effect presum-
ably due to the defect in FA turnover, and/or a loss of Rho–generated
contractility in these cells (Iwanicki et al., 2008).

   The FA protein FAK has been shown to phosphorylate p190 RhoGEF
and several members of the RGS–GEF family, suggesting that FAK plays a
role in regulating RhoA activation downstream of FN (Chikumi et al.,
2002; Zhai et al., 2003). However, FAK has also been shown to bind to
p190 RhoGAP (Masiero et al., 1999), and there is evidence to suggest that
FAK plays a role in activation of p190 RhoGAP downstream of matrix
adhesion (Holinstat et al., 2006; Ren et al., 2000; Zrihan–Licht et al., 2000).
It is seemingly contradictory that FAK could be responsible for activation of
both GEFs and GAPs involved in the regulation of Rho function down-
stream of matrix adhesion. However, it is possible that, upon matrix
adhesion, FAK signaling to different GEFs and GAPs occurs sequentially,
and is spatially controlled through the action of different scaffold proteins,
allowing for an initial GAP–induced inhibition of RhoA followed by a
GEF–induced reactivation phase. Also, considering the number of RhoA
GEFs being activated by FN adhesion, it is likely that there are other
intermediate signaling components besides FAK that are responsible for
regulating GEF activity.

   Several additional studies have identified other GEFs and GAPs that
are important for FA formation. The Rap GEF C3G has been shown to
be required for formation of paxillin- and integrin β_1- (but not β_3)
containing FAs (Voss et al., 2003). The Rac GEF Def-6 can localize
to FAs in undifferentiated C2C12 myoblasts, presumably as a result of its
interaction with the α7A integrin chain (Samson et al., 2007). The Rho
and Cdc42 GAP DLC-1 (deleted in liver cancer) localizes strikingly to
FAs, and this localization is dependent on its interaction with the protein
cten (C-terminal tensin like) (Kim et al., 2009). Interestingly, the localiza-
tion of DLC-1 to FAs is critical for its tumor suppressor activities (Liao
et al., 2007).

   It is clear from the above examples that many different GEFs and
GAPs associate with FCXs and FAs, and regulate their formation. It will
therefore be crucial for future studies to determine which GEFs and
GAPs are activated by which specific extracellular signals, as this will help
resolve some of the questions in the field regarding GTPase signaling
specificity.

2.4. The role of integrins in RhoA activation and focal adhesion formation

2.4.1. Differential activation of RhoA by different integrins

Activation of RhoA on an ECM substrate such as FN could potentially be regulated via different integrin receptors ($\alpha_v\beta_3$ and/or $\alpha_5\beta_1$), and several groups have focused on investigating this question. For one study, the authors compared RhoA activity levels in normal CHO cells (which do not express endogenous β_3) to those overexpressing either β_3, β_1, or a chimera (β_{1-3-1}) that contained a β_1 cytoplasmic domain, but adhered to β_3 ligands (Miao et al., 2002). When plated on FN, the cells overexpressing either β_3 or the β_{1-3-1} chimera showed an increase in RhoA activation with concomitant SF formation. In contrast, CHO cells overexpressing β_1 did not show any increase in RhoA activity, but instead had increased Rac1-GTP levels with lamellipodia formation (Miao et al., 2002). A second study in the same year reported contradictory results, potentially due to the different cell types used by the two groups (Danen et al., 2002). In the second study, GD25 (β_1-deficient fibroblastic cells) and GE11 (β_1-deficient epithelioid cells) cells were transfected with either β_1 or β_3 subunits. Plating of these cells on FN revealed that β_1-expressing cells, but not β_3-expressing cells, showed the biphasic regulation of RhoA (dip and reactivation) that had previously been described to occur upon FN adhesion. Interestingly, while FAs were formed by cells expressing either the β_1 or β_3 subunits, the patterns were different. When plated on just the CBD of FN, the β_3-expressing cells formed FA that looked the same as those formed on FN, but the β_1-expressing cells could not assemble FA on CBD unless the HBD of FN was also present. Interestingly, RhoA activity levels in β_1-expressing cells were similar on both full-length FN and CBD (Danen et al., 2002).

A later report by this group investigated the effects the different integrins had on the ability of cells to migrate on FN (Danen et al., 2005). Adhesion to FN through β_1 integrins (causing high RhoA activity) promoted random migration, whereas adhesion through β_3 integrins (causing lower RhoA activity) promoted migration in a persistent and polarized manner. Inhibition of RhoA activity in the β_1-expressing cells allowed for persistent migration similar to those expressing β_3. Interestingly, the type of integrin involved significantly affected the dynamics of the FAs. Cells adhering through $\alpha_5\beta_1$ had FAs that were very dynamic and turned over rapidly, while those formed by $\alpha_v\beta_3$ were more stable and promoted migration in a directed manner (Danen et al., 2005).

2.4.2. Integrin occupancy and clustering

Several studies have investigated whether ligand density has an effect on the formation of FAs. CHO cells plated on different concentrations of FN demonstrated that the morphology of their adhesions differed based on

the density of the substrate, with FCXs being predominant at intermediate concentrations of FN, and larger well-developed FAs forming only at higher concentrations of FN. When GTPase activity levels were measured, Rac1 and Cdc42 activity was highest at the intermediate amount, while RhoA activity increased with increasing FN concentration, remaining high at the highest substrate levels (Cox et al., 2001).

As mentioned before, RhoA activity undergoes a biphasic transition upon plating of cells onto FN, with a transient inactivation being followed by a period of sustained activation. Simple engagement of an integrin to a monovalent RGD ligand has been shown to be sufficient to trigger the initial decrease in the amount of active RhoA (Arthur et al., 2000). However, we have also observed that engagement of integrins by just RGD is not sufficient to cause the reactivation of RhoA (William Arthur and Keith Burridge, unpublished observations), suggesting that later activation of RhoA might require additional clustering or aggregation of integrins. In support of this, a study looking at the neuronal surface molecule Thy-1, which is known to bind to β_3 integrin on astrocytes showed that clustering β_3 integrins with Thy-1 led to a measurable increase in RhoA-GTP (Avalos et al., 2004).

However, it is widely believed in the field that RhoA activation (leading to contractility) is a prerequisite for FA formation (and significant integrin clustering), leading one to question how integrin clustering might occur before RhoA activation. Several related studies have suggested mechanisms for clustering of integrins that do not require RhoA activity. A recent paper showed that expression of the integrin coreceptor tissue transglutaminase (tTG) can cause clustering of integrins and a concomitant increase in RhoA activity levels (Janiak et al., 2006). Also, gamma-PAK (p21-activated kinase), a Rac/Cdc42 effector protein, has been shown to directly phosphorylate MLC, suggesting an increase in contractility (Chew et al., 1998). Both these studies, therefore, suggest a positive feedback loop mechanism, whereby RhoA-independent mechanisms trigger the formation of small integrin aggregates or "microclusters" which lead to an initial low level of RhoA activation. RhoA activation will lead to further integrin clustering, setting up the positive feedback loop and sustained FA formation. In support of this, experiments conducted in our laboratory have shown that pretreatment of cells with the contractility inhibitor blebbistatin causes a reduction in the ability of FN to activate RhoA, indicating that sustained and significant RhoA activation requires a positive feedback signal (Renee Doughman and Keith Burridge, unpublished observations).

2.5. Fibrillar adhesions

It is often difficult to differentiate between the more common types of ECM adhesions (FCXs and FAs), as they share many protein components, and are highly interdependent and interconvertible (Geiger et al., 2001). However,

FBAs are a unique kind of differentiated adhesion complex. Their main function is to remodel the ECM, and therefore, they recruit a unique subset of proteins required to fulfill this particular function. Originally, FBAs were defined by EM in chicken fibroblasts as α–actinin– and/or vinculin–containing complexes associated with extracellular FN fibrils (Chen and Singer, 1982), and it is clear that FBAs are involved in FN fibrillogenesis.

2.5.1. Formation of fibrillar adhesions and fibronectin fibrillogenesis

FBAs are fiber-like complexes with a variable length ranging from 3 to 20 μm. Their structure is similar to other ECM adhesion complexes (with an integrin receptor (usually $\alpha_5\beta_1$) bridging the PM between the ECM and the actin cytoskeleton), and they are the last step in the maturation process of ECM adhesions. Just like FAs evolve from FCXs, FBAs are generated from FAs (Pankov et al., 2000; Zamir et al., 1999) (Fig. 1.1C).

During the formation of FBAs, the $\alpha_5\beta_1$ integrin receptor is pulled out from $\alpha_v\beta_3$ and $\alpha_5\beta_1$–containing FAs, and translocates to form a new FBA (Pankov et al., 2000). This translocation requires an intact and dynamic actin cytoskeleton, as agents that disrupt (cytochalasin D) or stabilize (jasplakinolide) actin filaments inhibit this process (Pankov et al., 2000). Similarly, inhibition of cellular contractility by different inhibitors (H7 or BDM) blocks the formation of FBAs (Zhong et al., 1998). This process may seem analogous to the maturation of FAs, but certain differences exist. While isometric tension is required for FA maturation (Riveline et al., 2001), FBA formation requires dynamic forces to actively pull out several components from FAs (Pankov et al., 2000).

Assembly of the extracellular network of FN and the conversion of FAs to FBAs are tightly interlaced processes. Both RhoA and ROCK signaling are required for not only FBA formation, but FN fibrillogenesis as well (Pankov et al., 2000; Yoneda et al., 2007; Zhong et al., 1998). Since their first characterization in the early 1980s, FBAs were shown to align along extracellular FN fibrils (Chen and Singer, 1982). More recently, it has been demonstrated that inhibiting the formation of FBAs impairs the assembly of FN fibrils, demonstrating a critical role for FBAs in ECM assembly (Pankov et al., 2000).

2.5.2. Composition of fibrillar adhesions

Almost two decades after the initial characterization of adhesion complexes, Zamir and Geiger attempted to categorize them on the basis of their protein composition and their morphological features in order to unify the field around common definitions (Geiger et al., 2001; Zamir and Geiger, 2001; Zamir et al., 1999, 2000). Besides integrins, the proteins classified as being part of FBAs included tensin, parvins (α–actinin–related proteins), and FN (Katz et al., 2000; Olski et al., 2001; Pankov et al., 2000; Zamir et al., 1999). Although being

extremely helpful and carefully documented, this classification appears too harsh now, defining clear and strict boundaries to a continuum of evolving adhesion complexes. Indeed, numerous other proteins have been shown to be transiently or stably recruited to FBAs, such as ILK (Vouret-Craviari et al., 2004), PINCH (Stanchi et al., 2005), paxillin (Zaidel-Bar et al., 2007b), vinculin, and α-actinin (Burridge and Feramisco, 1980; Chen and Singer, 1982). More generally, it seems reasonable to hypothesize that the composition of FBAs may vary from cell type to cell type, with different cells recruiting different proteins to achieve similar properties.

Nevertheless, the composition of FBAs is fundamentally different from other adhesion complexes. For instance, none of the proteins that localize to FBAs possess any enzymatic activity (besides ILK, which is discussed below). This suggests that FBAs may be devoid of any "classical" signaling properties as compared to FCXs or FAs. This is further supported by observations that tyrosine phosphorylation cannot be detected in FBAs (Zamir et al., 1999). Indeed, some phosphorylated proteins such as paxillin are even dephosphorylated prior to FBA formation (Zaidel-Bar et al., 2007b). The case of ILK is interesting, because while ILK has been reported to phosphorylate some proteins (including Akt/PKB) (Delcommenne et al., 1998), more recent genetic and biochemical studies have cast doubt on this activity, and have instead established ILK as a scaffold protein necessary for ECM adhesion stabilization and further maturation (Hill et al., 2002; Lynch et al., 1999; Mackinnon et al., 2002; Sakai et al., 2003; Vouret-Craviari et al., 2004; Zervas et al., 2001). Therefore, localization of ILK to FBAs fits into the model of FBAs as matrix assembling complexes mostly devoid of signaling properties, as opposed to FAs.

2.5.3. The role of tensin in fibrillar adhesion formation

Tensin has emerged as the molecular link between integrins and the actin cytoskeleton required to provide the dynamic forces needed in order to form FBAs and assemble the ECM. Tensin was originally identified as an SH2 domain–containing actin-binding protein localized in ECM adhesions (Davis et al., 1991). In humans, there are three genes coding for three tensin proteins, all of which are highly conserved at their N- and C-terminal regions which are involved in FA targeting. However, of these two domains, only the C-terminal PTB domain binds directly to the classical NPXY motif of β integrin tails (McCleverty et al., 2007). Additionally, a fourth gene encodes a shorter form of tensin named cten. Cten only contains the most C-terminal FA-targeting domain, which is sufficient to localize the protein to ECM adhesions (Lo and Lo, 2002).

Tensins are actin-binding proteins which interact differently with actin filaments: tensin 1, 2, and 3 cap the barbed end of actin filaments whereas only tensin 1 can also bundle them (Lo et al., 1994). On the other hand, cten does not bind actin filaments at all (Lo and Lo, 2002). So far, several

genetic studies have investigated tensin function. In *Drosophila* (which express only one tensin), tensin knockout induces destabilization of muscle cell attachments, which are structures homologous to FAs in mammalian cells (Torgler et al., 2004). In mice, tensin 1 knockout leads to kidney degeneration and renal function failure due to defective assembly of cell-matrix adhesions (Lo et al., 1997). It has been previously shown that renal function and kidney histology are affected by alterations in ECM assembly and FN deposition resulting in diseases such as diabetic nephropathy, glomerulosclerosis, or glomerulonephritis (Terukina and Aoki, 1985). Therefore, it is likely that tensin 1 knockout interferes with proper FN matrix assembly. Consistent with its name, tensin may be mechanically required to provide tension to ECM adhesions.

Intriguingly, tensin can bind directly to the RhoA-specific GAPs DLC1–3 (Liao et al., 2007; Qian et al., 2007). More precisely, the shortest tensin molecule, cten, targets DLC1 to ECM adhesions, and stimulates its tumor suppressor activities. This also raises the interesting possibility that a feedback regulatory mechanism exists to regulate the levels of local RhoA activity via the recruitment of DLC1 to FBAs.

2.6. Podosomes and invadopodia

In addition to all the above-mentioned FA structures, cells also interact with the ECM using podosomes and invadopodia. Podosomes and invadopodia are highly dynamic, punctate structures that form at the ventral surface of the cell and consist of a densely packed actin core, surrounded by a ring of components commonly found in FA structures (Linder and Aepfelbacher, 2003) (Fig. 1.1D and E). Podosomes are typically formed in monocyte-derived cells such as macrophages, osteoclasts, and dendritic cells (Amato et al., 1983; Burns et al., 2001; Destaing et al., 2003; Lehto et al., 1982; Linder et al., 1999). They have also been described in other cell types like smooth muscle, epithelial, and endothelial cells (Hai et al., 2002; Osiak et al., 2005; Spinardi et al., 2004; Tatin et al., 2006; Varon et al., 2006). In addition, podosomes have been found in Src-transformed fibroblasts and malignant B-cells (Caligaris-Cappio et al., 1986; Marchisio et al., 1988; Tarone et al., 1985).

Like FAs, podosomes and invadopodia have a common basic set of molecular components, including adhesion receptors such as integrins, adaptor proteins connecting the cytoskeletal elements, and signaling molecules. What is unique about podosomes and invadopodia is that in addition to adhering to the substrate, they are also involved in matrix degradation and tissue invasion (Chen, 1989, 1990; Linder, 2007). Podosomes are thought to be involved in a variety of physiological processes, such as sealing ring formation in osteoclasts, monocyte extravasation, and tissue transmigration, or in pathological conditions, such as atherosclerosis or cancer (Buccione

et al., 2004; Carman et al., 2007; Destaing et al., 2003; Jurdic et al., 2006; Linder and Aepfelbacher, 2003; Moreau et al., 2003; Yamaguchi et al., 2006).

2.6.1. Comparing podosomes and invadopodia

Classifying podosomes and invadopodia separately is still a matter of active debate. Since their molecular components and functions seem to be mostly indistinguishable, it is not clear if they do represent different structures. Current convention is to use the term podosomes for the structures found in normal cells (such as monocytic cells, endothelial cells, and smooth muscle cells) and in Src-transformed fibroblasts, and the term invadopodia for the structures found in cancer cells (Gimona et al., 2008).

Based on the current definitions, some structural and functional differences can be found between podosomes and invadopodia. First, podosomes tend to form in the periphery of the cell, and invadopodia are almost invariably localized below the nucleus, often close to the Golgi complex (Baldassarre et al., 2003). Second, invadopodia are longer lived and more stable than podosomes. Podosomes turn over on a minute time scale while invadopodia are stable for hours (Baldassarre et al., 2003; Destaing et al., 2003; Evans et al., 2003; Yamaguchi et al., 2005). Third, while invadopodia are motile structures (Yamaguchi et al., 2005), individual podosomes are not motile. Movement of podosomes can be achieved by *de novo* assembly at the front and disassembly at the rear (Destaing et al., 2003). Finally, at the ultrastructural level, podosomes look like small PM protrusions (Gavazzi et al., 1989). In contrast, invadopodia not only extend their protrusions much deeper into the ECM, but also form profound invaginations in the ventral surface of the cell, in close contact with the Golgi apparatus (Baldassarre et al., 2003).

2.6.2. Differences from focal adhesions

While podosomes and invadopodia share many components with FAs, they differ in several different structural and functional aspects. The center of podosomes is filled with a densely packed meshwork of newly polymerized actin filaments (the actin core) (Fig. 1.1D and E). This actin core represents the main structural difference between podosomes/invadopodia and FAs, and consists primarily of F–actin and proteins involved in actin nucleation like cortactin, the Arp2/3 complex and WASP (which are absent in FAs) (Artym et al., 2006; Bowden et al., 1999; Linder et al., 1999, 2000; Luxenburg et al., 2006; Mizutani et al., 2002; Pfaff and Jurdic, 2001; Tehrani et al., 2006; Webb et al., 2007). FAs are elongated in shape, and do not have a core/ring structure (Block et al., 2008) (Fig. 1.1B). The actin core in podosomes forms a column that orients perpendicular to the substrate. In contrast, actin fibers in FAs are oriented tangentially to the substrate (Block et al., 2008). The localization of cortactin and the Arp2/3–dependent actin polymerization machinery at the core is consistent with dynamic reorganization of actin.

A wide variety of proteins have been found at podosomes, including integrins, cytoskeletal components, adaptor proteins, tyrosine kinases, ser/thr kinases, Rho GTPases, and other signaling molecules (Block et al., 2008; Linder and Aepfelbacher, 2003). The podosome ring also contains proteins commonly found in FAs and other ECM adhesions, such as vinculin, paxillin, talin, and integrins (Marchisio et al., 1984; Pfaff and Jurdic, 2001). The ring proteins function to link the cytoskeleton to the ECM (Buccione et al., 2004; Linder and Aepfelbacher, 2003). For a comparative list of proteins found in podosomes and FAs, we refer the reader to a review by Block and colleagues (Block et al., 2008).

The major functional difference is that while podosomes and invadopodia actively degrade the surrounding ECM, FAs usually do not participate in matrix degradation. Different types of proteases have been found associated with invadopodia and podosomes, including members of the matrix metalloproteinase (MMP) and serine proteinase families (Linder, 2007; Weaver, 2006). The transmembrane MT1-MMP and the secreted MMP2 and MMP9 have been found in both podosomes and invadopodia (Linder, 2007). Metalloproteinases of the ADAM (a disintegrin and metalloproteinase) family have also been found in invadopodia and podosomes (Linder, 2007; Weaver, 2006). Rather than degrading the matrix, ADAMs function by cleaving receptors and growth factors at the cell surface, thereby releasing their ectodomains (sheddases). ADAM12 binds to the adaptor protein Tsk5/Fish, and the complex relocates to podosomes in Src-transformed fibroblasts (Abram et al., 2003).

2.6.3. Formation of podosomes and invadopodia

Very little is known about the sequence of events that leads to the formation of podosomes. Live imaging of cells has revealed that one of the first events during podosome formation is the recruitment of cortactin into small clusters that grow in size. Arp2/3 is recruited shortly after, and actin polymerization is initiated (Burgstaller and Gimona, 2004; Zhou et al., 2006). Other proteins are recruited at later times. However, the detailed temporal sequence of protein recruitment to podosomes/invadopodia is still a matter of debate. One of the key components required for the formation of podosomes/invadopodia is the nonreceptor tyrosine kinase Src (Gimona and Buccione, 2006; Linder and Aepfelbacher, 2003). Src activation is both necessary and sufficient for podosome formation (Brandt et al., 2002; Chen et al., 1984, 1985). In addition, several of the proteins found associated with podosomes are Src substrates, such as cortactin, AFAP110, paxillin, Tks5t/FISH, p130Cas, and Pyk2 (Buccione et al., 2004).

Downstream of Src, Rho GTPases play a central role in the formation of podosomes. Specifically, RhoA, Cdc42, and Rac1 have been shown to be required for their formation (Linder and Aepfelbacher, 2003). Cdc42 is essential for podosome formation in many different cell types, including

macrophages and dendritic cells (Linder and Aepfelbacher, 2003). Silencing of Cdc42 inhibits invadopodia formation in metastatic carcinoma cells, while overexpression of constitutively active Cdc42 can promote formation of podosome-like structures in cells which normally do not form podosomes (Linder et al., 1999). Surprisingly, active RhoA has been shown to localize to podosomes in Src-transformed fibroblasts (Berdeaux et al., 2004). In addition, different GEFs (α-PIX) and GAPs (p190 RhoGAP and DLC-1) have been shown to play a role in the formation of podosomes (Burgstaller and Gimona, 2004; Gringel et al., 2006; Schramp et al., 2008; Webb et al., 2005). p190 RhoGAP is recruited to sites of podosome assembly in smooth muscle cells, and it is believed to play a role in the local inhibition of contractility that precedes podosome formation (Burgstaller and Gimona, 2004).

While the importance of Rho GTPases is undisputed, there are several reports which describe contradictory results for the role of GTPases in the formation of these structures. In some cases, activation of a certain GTPase induces podosome formation (in a particular cell line), while it inhibits podosome formation in others. For example, overexpression of both constitutively active and dominant negative Rac1 mutants has been shown to induce podosome disassembly in different cell lines including chicken osteoclasts, human and mouse dendritic cells (Burns et al., 2001; Castellano et al., 2001; Ory et al., 2000). Similarly, constitutively active RhoA stimulated podosome formation in osteoclasts, whereas it disrupted podosomes in osteoclast-like cells (Chellaiah et al., 2000; Ory et al., 2000). Inhibition of Rho can also promote podosome disruption in human and mouse dendritic cells, in mouse osteoclast-like cells, and in avian osteoclast-like cells and osteoclasts (Burns et al., 2001; Castellano et al., 2001; Chellaiah et al., 2000; Ory et al., 2000; Zhang et al., 1995). These discrepancies can possibly be explained by differences in the experimental setup, or by differences between cell types. Regardless, these studies clearly underline the requirement for exquisite regulation of GTPases activity in the formation of podosomes and invadopodia. The small GTPases of the ARF family have been also implicated in invadopodia formation. These proteins may function as a link between invadopodia and the secretory pathway, which is required for delivering proteases and other components, as well as localized actin remodeling at the site of invadopodia formation (Hashimoto et al., 2004; Tague et al., 2004).

There is increasing evidence to suggest that phosphoinositides (PIs) play a role in podosome formation. In osteoclasts, integrin activation leads to the recruitment of phosphoinositide 3-Kinase (PI3K) to podosomes, leading to increased local levels of PIs (Chellaiah and Hruska, 1996). PIs at podosomes direct the association of signaling proteins with gelsolin through phospholipid–protein interactions (Chellaiah et al., 2001). In addition, several components of the podosomal complex (including talin, vinculin, and WASP) can be regulated by PIs like phosphatidylinositol 4,5-bisphosphate (PtdIns(4,5)P$_2$) (Gilmore and Burridge, 1996; Ling et al., 2003; Sechi and

Wehland, 2000; Steimle et al., 1999). Recently, work from Oikawa and colleagues has shown that PtdIns(3,4)P$_2$ accumulates very early at podosomes, and helps to stabilize the scaffolding protein Tsk5 at the PM (Oikawa et al., 2008). Tsk mediates the recruitment of N-WASP through its SH3 domain, causing an increase in actin polymerization (Oikawa et al., 2008).

During the past few years, substantial progress has been made in understanding the molecular mechanisms that govern podosomes and invadopodia formation. However, several key issues remain unresolved; among them, the role of podosome/invadopodia *in vivo* and their role in transmigration and invasion.

3. Role of Syndecan-4 in Focal Adhesion Formation

While it is widely accepted that integrin signaling is necessary for the assembly of FAs, there is also a body of literature that provides evidence that integrin adhesion alone is not sufficient for the formation of FAs. These studies have indicated that complementary adhesion of syn4 to the HBD of FN is required for the proper formation of FAs (Bloom et al., 1999; Couchman and Woods, 1999; Izzard et al., 1986; Saoncella et al., 1999; Woods and Couchman, 1998, 2001; Woods et al., 2000). While the exact role that syn4 plays in FA formation (and significantly, RhoA activity) remains unclear, it is nevertheless clear that a synergy exists between integrins and syn4, and that at least in certain cases, proper FA formation does not occur without signaling from both types of adhesion receptors.

3.1. Structure of syndecan-4

The syndecan family of transmembrane HSPGs is composed of four members (syn1–4), all of which are made up of a core protein with attached sulfated glycosaminoglycan (GAG) chains. They all contain highly homologous cytoplasmic and transmembrane domains, with unique extracellular regions (Couchman, 2003) (Fig. 1.6). Unlike syn1–3 which are tissue specific, syn4 is ubiquitously expressed (Woods and Couchman, 1994). When cells are plated on FN, syn4 binds with greatest affinity to the C-terminal HBD of FN (HBD/HepII), comprising the 12–14 type III FN repeats. Specifically, the interaction is mediated via a cluster of basic residues that form a pocket in FN type III repeat 13 (Bloom et al., 1999). While HBD/HepII is the major HBD of FN, other lower affinity HBDs are present at the N-terminal type I repeat region (HepI) (Couchman, 2003) and the type III connecting segment (IIICS) (Mostafavi-Pour et al., 2001; Wayner et al., 1989) (Fig. 1.2).

The ectodomain (ED) of syn4 is modified mainly by the addition of heparan sulfate GAG chains. While these heparan sulfate chains are
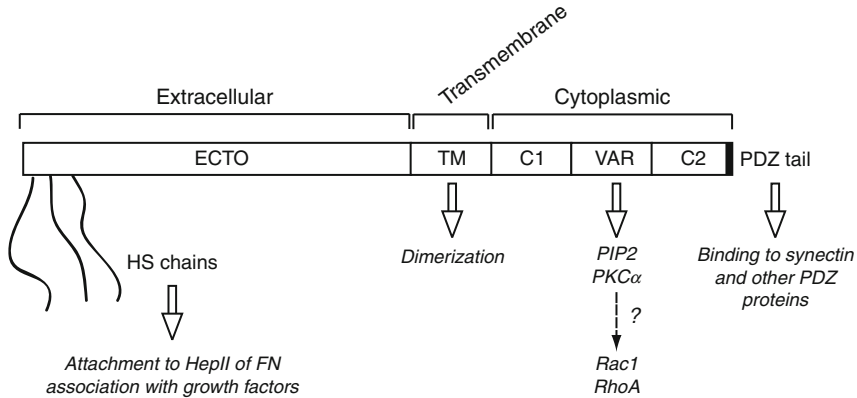
Figure 1.6 Structure of syndecan-4 (syn4). The Syn4 molecule has a large extracellular domain (which contains large heparin sulfate chains that bind FN), a transmembrane domain (involved in dimerization), and various cytoplasmic domains (involved in intracellular signaling).

important for binding to FN and interacting with growth factors (Mahalingam et al., 2007), overexpression of the core protein alone appears to be enough to lead to the formation of FAs in cells adhered through integrins (Echtermeyer et al., 1999). The ED of syn4 can also be shed during wound healing, and has been shown to act as a substrate for some mesenchymal cells through an integrin-binding site (Whiteford and Couchman, 2006; Whiteford et al., 2007). Syn4 also contains a transmembrane region that passes once through the membrane and a short (28 amino acids) cytoplasmic tail that is devoid of intrinsic activity. The cytoplasmic domains of all four syndecans share homologous conserved regions (C1 and C2), a C-terminal PDZ-binding motif, and unique variable regions (V) (Fig. 1.6).

Much work in recent years has focused on the role of syn4 in the regulation of numerous signaling pathways, its binding partners, and biological function. While this chapter will focus specifically on detailing what we know about the role of syn4 in activation of Rho GTPases and FA formation, we refer the reader to the following reviews for more information about other syn4 signaling pathways: Bass and Humphries (2002), Couchman (2003), Couchman et al. (2001), Morgan et al. (2007), Simons and Horowitz (2001), Tkachenko et al. (2005), Wilcox–Adelman et al. (2002b).

3.2. Evidence for a role for syndecan-4 in RhoA activation and focal adhesion formation

Early experiments using proteolytic fragments of FN showed that while cells could adhere and spread on the RGD region in the CBD of FN, they could not form SFs and FAs unless the HBD of FN was also engaged by a

HSPG (Izzard et al., 1986; Pierschbacher and Ruoslahti, 1984; Woods et al., 1986). The formation of SFs and FAs by the additional engagement of a HSPG could be blocked by pretreating FN with heparin, essentially blocking any binding to the HBD of FN. Interestingly, while cells could also be shown to adhere to HBD alone, they did not spread well or form SFs and FAs (Bloom et al., 1999; Woods et al., 2000). These data seemed to indicate that binding of a cell surface HSPG to the HBD of FN might be generating a signal that was required (but not sufficient) for the formation SFs and FAs. Later work using an antibody specific for a portion of the cytoplasmic domain of syn4 determined that it colocalized with FAs (Woods and Couchman, 1994). Further, it was also shown that cells adhered to the CBD would only form FAs when they are treated with an antibody which clusters syn4 (Saoncella et al., 1999). Both of these results, therefore, implicate syn4 as the HSPG required for FA formation.

Syn4 activates several different kinases that might be involved in FA formation. Studies have shown that activation of syn4 leads to the phosphorylation of FAK (Wilcox–Adelman et al., 2002a). Protein Kinase C α (PKCα) is also activated by syn4. The V region of syn4 contains binding sites for both PKC and PtdIns(4,5)P$_2$ (Oh et al., 1997a,b). The binding of PtdIns(4,5)P$_2$ and PKCα to the V region of syn4 leads to activation of PKCα (Lim et al., 2003; Woods and Couchman, 1992; Woods et al., 1986). Importantly, it was demonstrated that activation of PKCα by HBD treatment was needed to stimulate the assembly of SFs and FAs in cells preadhered to the CBD of FN (Woods and Couchman, 1992).

Syn4 knockout mice have been created by two separate groups using homologous recombination techniques (Echtermeyer et al., 2001; Ishiguro et al., 2000). The syn4 null mice in both cases were viable, fertile, and demonstrated no gross abnormalities. However, upon closer examination, they were shown to possess defects in both wound healing and angiogenesis (Echtermeyer et al., 2001; Ishiguro et al., 2000). Interestingly, fibroblasts derived from syn4 null mice still form FAs when plated onto full-length FN. However, in contrast to wild-type cells which form FAs on CBD only after addition of soluble HBD, syn4 null cells plated on CBD are unresponsive to soluble HBD addition, and do not form FAs. These data suggest that a separate signaling factor might be compensating for the lack of syn4 when cells are plated on full-length FN, one that does not respond to soluble forms of the HBD ligand (Ishiguro et al., 2000). It is also possible that one of the other syndecans (1–3) could offset the loss of syn4 under such conditions (Ishiguro et al., 2000; Woods and Couchman, 2001). Unfortunately, our current knowledge about a possible role for other syndecans in FA formation is limited. Unlike syn4, other syndecans do not localize to FAs (Baciu and Goetinck, 1995; Woods and Couchman, 1994). However, it has been shown that in P29 cells (lewis lung carcinoma), syn2 can act in concert with integrin $\alpha_5\beta_1$ to induce SF formation on FN (Kusano et al., 2000).

As mentioned before, previous experiments have shown that many cell types adhered to the CBD of FN do not form FAs unless they are treated with soluble HBD or antibodies which cluster syn4 (Saoncella et al., 1999). If RhoA activation is blocked, FA formation can no longer be induced by clustering syn4, suggesting that syn4 controls FA formation by regulation of RhoA activity (Saoncella et al., 1999). Further, using an enzyme-linked immunosorbent assay (ELISA) to measure levels of active RhoA, it was shown that activation of RhoA does not occur on CBD alone, and requires the addition of soluble HBD. Using pharmacological inhibitors, these authors demonstrated that RhoA activation in response to HBD occurs via activation of PKCα (Dovas et al., 2006). These data support findings that basal levels of RhoA are lower in syn4 null cells compared to normal cells (Wilcox-Adelman et al., 2002a), and therefore implicate syn4 in the activation of RhoA (and hence FA assembly).

A recent study has also implicated syn4 in regulating p190 RhoGAP during cell spreading (Bass et al., 2008). Plating of cells onto just CBD was not sufficient to cause the initial inactivation of RhoA, a consequence attributed to mislocalizion of p190 RhoGAP in the absence of soluble HBD (Bass et al., 2008). These authors also show that PKCα activation downstream of syn4 is required for proper membrane localization of p190 RhoGAP. However, taken in concert with previous work, these results suggest that PKCα signaling downstream of Syn4 contributes to both the initial inactivation and the later reactivation of RhoA, seemingly opposite roles for the same signaling pathway (Bass et al., 2008; Dovas et al., 2006). While it is possible PKCα is modulating these two opposite effects in a temporally regulated manner, there is no data to suggest how this might occur, and more work will have to be done to address this question.

Other studies have indirectly suggested a role for syn4 in regulating RhoA activity. In particular, a recent study reported that the PDZ tail of the RhoA GEF Syx1 binds to synectin, a protein that binds to the cytoplasmic tail of syn4 (Liu and Horowitz, 2006). Localization of Syx1 to the PM in response to LPA treatment is synectin dependent, and FRET assays showed that expression of Syx1 causes an increase in PM-localized RhoA activity in response to LPA treatment. Importantly, a splice variant of Syx1 (Syx2) that lacks the PDZ tail (and hence cannot bind to synectin) does not localize to the PM in response to LPA treatment. Cells expressing Syx2 have a much higher basal level of RhoA activity than those expressing Syx1, and do not demonstrate an increase in PM-localized RhoA activity in response to LPA treatment. These data indicate that synectin is responsible for restricting activation of RhoA at the PM by regulating the localization of Syx1 (Liu and Horowitz, 2006). While syn4 was not directly examined in this study, one can hypothesize that recruitment of Syx1 to the PM by synectin is dependent on syn4, suggesting that syn4 might regulate RhoA activity by restricting localization of a RhoA GEF.

3.3. Is syndecan-4 signaling essential for focal adhesion formation?

All of the above data seem to suggest that syn4 plays a major role in regulating RhoA activity, and is required for the formation of FAs. However, some contradictory studies suggest that syn4 may only play an accessory role in this process. Interestingly, there is evidence to suggest that the requirement of syn4 for FA formation may depend on the type of integrin. Cells containing only $\alpha_5\beta_1$ were shown to require HBD (in addition to CBD) for the formation of FAs, while in contrast, FA formation in cells containing $\alpha_v\beta_3$ was indistinguishable in the presence or absence of HBD (Danen et al., 2002). Further, a study by Wang and colleagues demonstrated that signaling through syn4 is not needed for FA formation if the cells can achieve a threshold level of integrin clustering (Wang et al., 2005). Specifically, FN null cells were shown to efficiently form FAs when plated on high concentrations of CBD in the absence of a ligand for syn4 (Fig. 1.7). Addition of HBD was required to generate FAs only when cells were plated onto low amounts of CBD (which were insufficient to induce FA formation). Integrin binding led to the activation of RhoA and an increase in actomyosin contractility through downstream ROCK signaling (Wang et al., 2005). In support of these data, it has also been shown that integrin adhesion to CBD alone (in the absence of adhesion to HBD or serum factors) is sufficient to activate Lsc/p115RhoGEF, a GEF that has been directly implicated in the activation of RhoA by FN adhesion (Dubash et al., 2007). These data, therefore, suggest that ligand density is an important factor for the ability of cells to form FAs, and that CBD is indeed sufficient for FA formation once a threshold level of integrin clustering is achieved (Fig. 1.7).
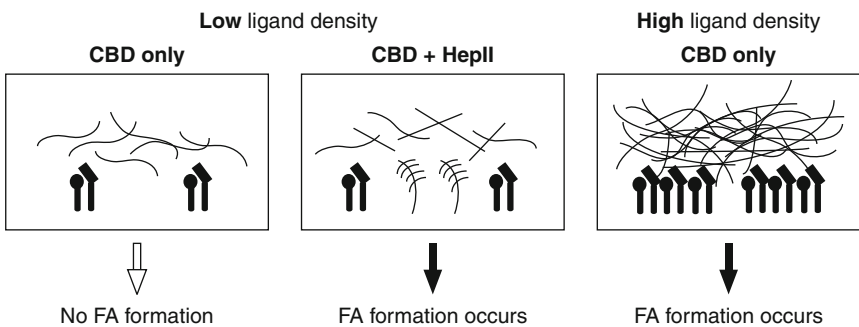

Figure 1.7 The contributions of integrins and syn4 to FA formation. In cases of high FN ligand density, attachment of cells to CBD alone is sufficient to allow FA formation. In cases of low ligand density, attachment to both CBD and HBD is required for FA formation.

Wang and colleagues also emphasized an important factor in FN adhesion studies that could explain some of the conflicting results obtained by different groups with regards to the involvement of syn4 in FA formation. This group demonstrated that the efficiency of adsorption of FN fragments to a surface depends upon conditions such as pH of the coating buffer, whether or not the FN fragment is tagged (His or GST), and even the type of surface to which the fragment is being adsorbed (plastic, glass, or tissue culture-treated plastic). Using ELISA, this group determined that the coating efficiency of FN fragments was extremely low under certain conditions, such as using a CAPS buffer for coating, certain kinds of tissue culture-treated plastic, or a His–tagged fragment. These data, therefore, implied that previous studies may have been using CBD (and other FN fragments) at concentrations suboptimal for generating the amount of integrin clustering required for FA formation. In such cases, additional engagement of syn4 by HBD presumably acts synergistically to activate signaling pathways that lead to proper FA formation.

The pattern of RhoA activation in cells plated on the CBD of FN is similar to the pattern of activity on full-length FN, with a transient dip in activity being followed by a sustained increase active RhoA-GTP levels (Arthur et al., 2000; Bass et al., 2007a; Ren et al., 1999; Wang et al., 2005). Wang and colleagues also found that while cocoating of HBD (with suboptimal amounts of CBD) did, in fact, lead to FA formation, this occurred *without a measurable increase in active RhoA levels* (Wang et al., 2005). These data, therefore, suggest that the synergistic function of syn4 leading to FA formation does not involve RhoA. It will, therefore, be crucial for future studies to determine which specific signaling pathways activated downstream of syn4 are responsible for this synergistic role of syn4 in the formation of FAs.

3.4. Syndecan-4 and Rac1 signaling

Syn4 has also been shown to play a role in Rac1 signaling in response to FN adhesion. Plating of wild-type cells onto CBD does not lead to a measurable increase in Rac activity unless soluble HBD is added. This activation of Rac1 in response to syn4 engagement is dependent on the activation of PKCα. Syn4 null cells plated on full–length FN also show no increase in Rac activity, directly implicating syn4 in the activation of Rac by FN (Bass et al., 2007b; Humphries et al., 2005). These cells also demonstrate a decreased rate of migration in a scratch wound assay, a result that explains the slower rate of skin repair seen in the syn4 null mice (Echtermeyer et al., 2001). Interestingly, however, FRET assays suggested that syn4 null fibroblasts seem to have elevated basal levels of Rac1 activity all over the cell, unlike wild-type cells that demonstrate a more localized and concentrated amount of active Rac at the leading edge. These results suggest that syn4 might

regulate the ability of cells to migrate by correctly localizing active Rac1 in the cell, a hypothesis supported by data showing that syn4 null cells demonstrate random migration (Bass et al., 2007b).

Regulation of Rac1 activation by syn4 is not unique to fibroblasts, however, as it has been previously demonstrated in endothelial cells. Clustering of syn4 in this cell type similarly leads to concentration of the receptor in the leading edge, with localized activation of Rac1 and initiation of cell migration (Tkachenko et al., 2004, 2006). The C-terminal PDZ tail of syn4 is necessary for this response to occur, and it was suggested that clustering of syn4 leads to the release of synectin from the PDZ tail, with the subsequent downstream increase in Rac1 activity. Endothelial cells lacking either synectin (syn4-binding partner) or the PDZ tail of syn4, have high basal levels of Rac1, just as in the syn4 null fibroblasts, demonstrating the need for syn4 and synectin in the regulation of Rac1 activity (Bass et al., 2007b; Saoncella et al., 2004; Tkachenko et al., 2004, 2006).

Interestingly, these results mirror those obtained for RhoA by Horowitz's group, who showed that synectin is responsible for restricted localization of active RhoA at the PM via proper localization of the RhoA GEF Syx1 (Liu and Horowitz, 2006). It is, therefore, plausible to suggest a similar mechanism for the regulation of Rac1 activity by syn4 and synectin, where Rac1 activity is restricted to the leading edge of cells by specific recruitment of a Rac1 GEF to the PM by association with synectin.

3.5. Cross talk between integrins and syndecans

Deciphering the specific roles of integrins and syndecans in FA formation has been complicated by the fact that these different adhesion receptors do not activate linear and mutually exclusive signaling pathways. Indeed, there is signaling cross talk between the receptors. Signaling links from syndecans to integrins have been reported between syn1 and integrins $\alpha_v\beta_5$ and $\alpha_v\beta_3$ (Beauvais and Rapraeger, 2003; Beauvais et al., 2004; McQuade et al., 2006). These studies have shown that plating of human mammary carcinoma cells (MB-231) onto a surface coated with syn1 antibodies leads to the activation of integrin $\alpha_v\beta_3$ regardless of whether the integrins are engaged or not, leading to cell spreading. Activation of integrin $\alpha_v\beta_3$ is dependent on adhesion through syn1, as inhibition of the syn1 ED prevents the activation of $\alpha_v\beta_3$ (and inhibits cell spreading) even when a ligand for $\alpha_v\beta_3$ is provided by plating the cells onto VN (Beauvais et al., 2004). Interestingly, cell spreading caused by syn1 signaling to $\alpha_v\beta_3$ is inhibited when the integrin β_1 subunit is activated by the addition of activating antibodies. These data suggest that signaling through β_1 integrins can block the link between syn1 and $\alpha_v\beta_3$, indicating additional levels of cross talk (Beauvais and Rapraeger, 2003).

The interaction between syn1 and integrin $\alpha_v\beta_5$ differs somewhat from that with $\alpha_v\beta_3$ (McQuade et al., 2006). In B82L mouse fibroblasts, engagement of syn1 by its specific antibodies leads to filopodial extension and activation of $\alpha_v\beta_5$, but does not result in cell spreading unless an integrin ligand (FN or VN) is present, even in amounts that are normally suboptimal for spreading. The cells will also spread when plated on a high concentration of FN or VN, but only if syn1 is present. Knockdown of syn1 inhibits spreading on FN or VN, and it is suggested that the syndecan and integrin are in a complex that is necessary to activate the integrin, thus leading to enhanced adhesion and a downstream response (McQuade et al., 2006).

An interesting variation on the interaction between syn4 and integrin β_1 occurs in cells adhering to ADAM12 (a disintegrin and metalloprotease). The cysteine-rich domain of this protein provides a binding site for syn4 which must first be engaged in order to activate β_1 integrin and induce cell spreading (Iba et al., 2000; Thodeti et al., 2003). Cells that cannot adhere first through syn4 cannot adhere through β_1 integrins either. This cross talk appears to be absent in some carcinoma cells or CHO-K1 cells, which can adhere through syn4 but not spread unless treated with Mn^{2+} or β_1 integrin–activating antibodies (Iba et al., 2000; Thodeti et al., 2003). Importantly, it was shown that the activation of β_1 integrins downstream of syn4 adhesion seems to occur through inside-out signaling by PKCα (Thodeti et al., 2003).

From the above-mentioned studies, it is clear that a synergy exists between integrins and syndecans, and they may complement each other functionally. It is, however, as yet unclear which specific biochemical signals link these two types of receptors, and how this cross talk is regulated. It will, therefore, be important to investigate in detail the mechanisms of cross talk between these two types of adhesion receptors, in order to fully develop an understanding of the specific roles of integrins and syndecans in Rho GTPase–related signaling pathways.

4. Focal Adhesions on Biomaterial Surfaces

Adhesion of cells to specially prepared artificial surfaces containing a ligand with a specific conformation, pattern, or density, can be used to study the effects of manipulating integrin adhesion on the actin cytoskeleton. Biomimetic or biomaterial surfaces can be prepared in many different ways, and the techniques used have been extensively reviewed (Ariga et al., 2006; Blattler et al., 2006; Chan and Yousaf, 2006; Falconnet et al., 2006; Lazzari et al., 2006; Shin et al., 2006; Whitesides et al., 2005). Many of the groups that create and use these surfaces are primarily interested in how cells would react to them when they are implanted into the body.

However, a lot of basic information about cell behavior can be found in these studies, especially data that specifically look at FA assembly under well-controlled conditions. We have selected examples from the literature showing how these surfaces have been used to further our knowledge on the formation of FAs on specific ligands. For more in-depth information about the use of biomaterial surfaces in cell biology, we direct the reader to several reviews (Falconnet et al., 2006; Gallant et al., 2007; Garcia, 2005; Gates et al., 2005; Petrie et al., 2006; Spatz and Geiger, 2007; Whitesides et al., 2005).

Biomaterial surfaces provide a reactive surface on which to couple a ligand of interest, and a nonadhesive (passivated) region in the areas between ligands. The nonadhesive portion of the surface prevents both cells and proteins (either from the growth medium or those produced and secreted by the cells) from adhering to it (Ariga et al., 2006; Blattler et al., 2006; Chan and Yousaf, 2006; Falconnet et al., 2006; Lazzari et al., 2006; Shin et al., 2006; Whitesides et al., 2005). To study integrin adhesion in cells on artificial surfaces, several features are typically varied, such as ligand structure, conformation, and spatial orientation. The ligand to which the integrin will bind can be either a full-length ECM protein (McClary and Grainger, 1999), a minimal binding peptide such as RGD (Hersel et al., 2003), or larger fragments or domains of an ECM protein (Cutler and Garcia, 2003). The presentation of a peptide ligand can also be altered so that it is presented in different molecular conformations (Hersel et al., 2003) or in a single or clustered formation (Maheshwari et al., 2000). Some other methods allow for specific placement of the ligands in regions of a particular size or shape, while also varying the distances between these adhesive areas (Brock et al., 2003; Cavalcanti-Adam et al., 2006, 2007). Such fine-tuned manipulations of the adhesive surface allows for a detailed analysis of which aspects of integrin adhesion are required for transmitting signals to the actin cytoskeleton.

4.1. Focal adhesions formed on linear RGD versus cyclic RGD

The tripeptide RGD, derived from the CBD of FN, is the minimal peptide ligand that can support cell adhesion (Pierschbacher and Ruoslahti, 1984), and many variations of it have been used on biomaterial surfaces to study integrin adhesion (Hersel et al., 2003). It had been shown previously that Swiss 3T3 fibroblasts can adhere, spread, and form SFs and FAs on surfaces containing only a linear RGD peptide (Houseman and Mrksich, 1998, 2001). However, studies looking at inhibition of cell adhesion showed that cells have a higher affinity for cyclized RGD (Kumagai et al., 1991; Lieb et al., 2005). Other studies have specifically investigated how FA formation occurs on linear RGD (lower affinity) versus cyclic RGD (higher affinity ligand). Using either linear or cyclic

RGD ligands coupled to self-assembled monolayers (SAMs) of alkanethiolates on gold, these studies showed that cells grown on cyclic RGD had nearly twice as many FAs as those grown on linear RGD (Kato and Mrksich, 2004). Interestingly, the FA size was smaller on average in the cells adhered to the cyclic ligand. The distribution of the FAs within the cells also varied, with the cells on cyclic RGD presenting more FAs in the interior of the cell compared to those plated on linear RGD. These data suggested that FA formation is influenced by both rate of nucleation and rate of growth. Nucleation occurs at a faster rate on the higher affinity cyclic RGD (resulting in more FAs). However, growth on cyclic RGD would be slower due to longer association times, thereby limiting the number of mobile receptors available to diffuse into the clusters (resulting in smaller FAs) (Kato and Mrksich, 2004).

4.2. Effect of ligand density and presentation on focal adhesion formation

A study by Massia and colleagues was one of the earliest to show that the density of integrin ligand affected the ability of a cell to spread and form SFs and FAs (Massia and Hubbell, 1991). Human foreskin fibroblasts were plated on RGD-coated glass surfaces of various densities in serum-free conditions. While the cells were able to adhere and spread on the low density of ligand, SFs and FAs only formed on the higher density of ligand. It was concluded that RGD peptides at a density of 1 fmol/cm^2 was sufficient for cell adhesion and spreading, but that a 10-fold higher concentration (10 fmol/cm^2) was necessary for the assembly of SFs and FAs. These values correspond to a peptide-to-peptide spacing of 440 and 140 nm, respectively (Massia and Hubbell, 1991).

Other studies have investigated whether ligand presentation (single vs. clustered) has an effect on SF and FA assembly. Surfaces were made with RGD peptides that were either single or in clusters of five or nine, with a varying surface density (i.e., the average distance between clusters) ranging from 6 to 300 nm (Maheshwari et al., 2000). When SF and FA formation were examined on the various surfaces, it was seen that the clustered ligand was more efficient than the single ligand at inducing the formation of both. This was true even if the single ligands were presented at a uniform density.

The ability of cells to migrate is closely linked with the formation of SFs and FAs. The highest rates of migration are achieved with intermediate amounts of adhesion and contractility, and large SFs and FAs are often inhibitory to the ability of cells to migrate (Cox et al., 2001; Huttenlocher et al., 1996). Considering that clustering of the ligand increased SF and FA formation, it is not surprising that similar effects were seen for cell migration. Presentation of ligand in a clustered format supported increased migration speeds at all densities, with the larger clusters requiring less density to see the same response (Maheshwari et al., 2000).

However, the estimation of the spacing between clusters required for maximal SF and FA assembly determined by this group (9 nm for clusters of five ligands and 60 nm for clusters of nine ligands) was much lower than that concluded by Massia and Hubbell (140 nm) (Massia and Hubbell, 1991). The reason for this is unclear, but may reflect differences in cell type and experimental design. Both groups used peptide ligands, but the Maheshwari study displayed the ligand at the end of flexible polymers. As discussed below (section 5.2) there is evidence that flexible substrata are less able to form FAs than rigid substrata (Pelham and Wang, 1997).

4.3. Using micropatterned substrates to study focal adhesion formation

To study the behavior of cells plated on a surface with uniformly spaced patterns of different sized ECM-coated dots, a technique called microcontact printing can be employed (Mrksich and Whitesides, 1996). This technique allows production of specific patterns of SAMs of alkanethiols on gold, to which an ECM protein can be coupled. Using this technique, Lehnert and colleagues looked at the early events regulating cell adhesion and spreading on surfaces containing ECM squares with a size range of $0.1–12\ \mu\text{m}^2$, coated with either FN or VN, and separated by a distance of $1–30\ \mu\text{m}$ (Lehnert et al., 2004). B16–F1 melanoma cells plated on surfaces made up of $1\ \mu\text{m}^2$ FN-coated squares separated by a distance of $5\ \mu\text{m}$, adhered and began to spread within 10 min. All FA proteins examined were shown to colocalize with the ECM–coated squares and actin SFs formed between these areas of concentrated FA proteins. Cells did not adhere to squares without an integrin ligand attached. Cells plated on poly-L-lysine-coated squares were able to adhere, but they did not accumulate FA proteins at these regions and did not form actin bundles between them, supporting the evidence for the requirement of integrin-based adhesion for the formation of FAs (Lehnert et al., 2004). When the distance between the ECM squares was increased, the B16–F1 melanoma cells continued to be able to adhere and spread from square to square until the distance between them exceeded $25\ \mu\text{m}$. At this point, the cells could adhere to only one ECM square, and could not bridge the nonadhesive region to adhere to an adjacent square (Lehnert et al., 2004). Not surprisingly, the value of this maximum distance varies by cell type. REF52 fibroblasts spreading on striped surfaces of alternating adhesive/nonadhesive domains, could not cross a nonadhesive region greater than $8\ \mu\text{m}$ (Zimerman et al., 2004).

Another method that can be used to create patterned substrates is based on the self-assembly of diblock copolymer micelles, which results in a regular hexagonal pattern of gold nanodots on a substrate such as glass. Each nanodot is about 8 nm in diameter, which is approximately the size of an integrin head and is biofunctionalized by binding the cyclic RGD peptide to it. The distance

between these gold dots can be controlled, and the region between dots is made nonadhesive by the application of polyethylene glycol (Arnold et al., 2004). Since integrin clustering is an important first step in the formation of FAs, these surfaces can be used to measure the lateral spacing between individual integrins that is needed for adequate cluster formation and subsequent FA assembly. Using this technique to position gold nanodots at a spacing of 28, 58, 73, and 85 nm apart, it was shown that a distance between 58 and 73 nm supported cell adhesion, spreading, and formation of FAs that contained β_3 integrin, FAK, and vinculin (Arnold et al., 2004). Actin SFs were also shown to terminate in these adhesive regions. Cells plated on surfaces containing nanodots positioned greater than 73 nm apart did not adhere well or spread, and did not form FAs or SFs, indicating that specific lateral spacing was important for the ability to form integrin clusters that could support FA formation (Arnold et al., 2004). These data also confirmed that the spacing between ligands is a limiting factor in FA and SF assembly, not simply the total number of ligands on a surface.

4.4. Measuring RhoA activity on biomaterial surfaces

To date, we are not aware of any studies that have attempted to measure RhoA activity on biomaterial surfaces using the Rhotekin RBD pull–down assay (Ren et al., 1999). This is probably due to the fact that these surfaces are expensive to make, and can only be prepared in small sizes. As a result, the number of adherent cells per surface would not yield adequate amounts of protein needed for the measurements. However, this may be possible in the future as newer, larger, and less expensive biomaterial surfaces can be developed. In addition, more sensitive ELISA assays have recently been developed for assaying RhoA activity, which require significantly less protein amounts.

However, other indirect methods for measuring RhoA activity on biomaterial surfaces have been used. One group was able to measure relative RhoA levels by separating cell lysates into membrane and cytosolic fractions, then blotting for either RhoA or RhoGDI (McClary and Grainger, 1999). Cells were grown in serum on either $-CH_3-$ or $-COOH$-terminated SAMs, with the expectation that ECM proteins contained in the serum and those secreted by the cell would adhere to the monolayers. Importantly, RhoA activity (measured by this indirect method) was higher in cells plated on the $-COOH$-terminated SAMs. In support of this, cells grown on the $-COOH$-terminated SAMs were shown to adhere better, spread, and form FAs and SFs, while those on the $-CH_3$-terminated SAMs did not adhere well or form FAs or SFs. These differences were attributed to better adsorption of ECM proteins to the carboxyl group (McClary and Grainger, 1999).

Even when a constitutively active mutant of RhoA was overexpressed in the cells grown on the $-CH_3$-terminated SAMs, FA assembly did not occur due to inadequate adhesion via integrins to the ECM ligand (McClary and Grainger, 1999). This showed that adhesion of cells to the ECM via

integrins was necessary at some minimal level for FA assembly, even in the presence of high levels of RhoA-GTP. These data supported previous work which showed that microinjection of active RhoA into cells plated on poly-L–lysine does not lead to formation of FAs (Hotchin and Hall, 1995).

A second group used a FRET-based RhoA biosensor to measure RhoA activation in cells on biomaterial surfaces. Cells transfected with the RhoA biosensor were plated onto patterned SAMs on gold surfaces that contained discrete regions of immobilized FN surrounded by nonadhesive regions (Hodgson et al., 2007). The cells that adhered to the FN ligand were confined within the patterned regions, but could extend and retract membrane protrusions onto the nonadhesive surfaces. When RhoA activation was compared in the cells on SAMs versus those on FN-coated glass, it was seen that RhoA was active at the edges of the protrusions in cells on both surfaces. On normal surfaces, RhoA activity decreased at the edge of the protrusion once it adhered to the FN surface (Pertz et al., 2006). In contrast, on the patterned SAMs, RhoA activity remained high in the protrusions which could not adhere to the surrounding nonadhesive surfaces (Hodgson et al., 2007). These data are consistent with previous results showing that early integrin engagement leads to a decrease in RhoA activity (Arthur and Burridge, 2001; Arthur et al., 2000; Bass and Humphries, 2002; Hotchin and Hall, 1995; Humphries et al., 2005; Ren et al., 1999; Saoncella et al., 1999).

5. MECHANOTRANSDUCTION

Cells can sense and react to mechanical tension. In fact, the normal growth and behavior of many tissues are influenced by physical forces, including gravity, tension, stiffness, compression, pressure, and shear (Ingber, 1997, 2006). Integrins are known to be critically involved in force sensing processes and many studies on mechanotransduction have focused on integrins and associated proteins present in FAs and their pre-cursors (Katsumi et al., 2004; Schwartz and DeSimone, 2008). FAs and FCXs are considered to be major sites of force sensation, and in addition, their own formation and disassembly is strongly influenced by mechanical changes (Chrzanowska-Wodnicka and Burridge, 1996; Riveline et al., 2001). Interestingly, recent findings suggest that podosomes also have the ability to sense force (Alexander et al., 2008; Collin et al., 2008).

We will begin this section of the chapter with a discussion of the different types of tension, followed by a comparison between tension generated in a 2D versus 3D environment and the corresponding effect on FA structure. Finally, we will discuss examples of cellular mechanor-esponses, and how a mechanical force can be translated into a biochemical signal (the primary sensory processes of force).

5.1. Types of mechanical forces acting on cells

Mechanical forces acting on cells can be of several different types and origins. Fibroblasts and epithelial cells in their natural environment are usually exposed to uni- or multiaxial forces originating from passive movements of the ECM substrate that is attached to or surrounds the cells. In contrast, endothelial cells lining blood vessels are continuously exposed to fluid shear forces by the blood flow on their luminal side. In addition, the ventral surface of endothelial cells attached to the basement membrane experiences stretching forces during cycles of diastole and systole.

Besides such external forces, cells are subject to internally generated forces that derive from actomyosin contractility. It is important to realize that any tension which originates from intracellular contractility in adherent cells is also totally dependent on the stiffness of the substrate the cell is attached to. Hence, the mechanical strain experienced by adherent cells reflects the integration of both their own contractility and the rigidity of the substrate to which they are attached (Discher et al., 2005; Vogel and Sheetz, 2006). Importantly, several different studies show that many different cell types (including fibroblasts, endothelial cells, and muscle cells) are able to ''measure'' the local stiffness of their environment and eventually react to it (Deroanne et al., 2001; Engler et al., 2004; Pelham and Wang, 1998; Vogel and Sheetz, 2006).

To study the effects of forces on cells, different experimental protocols have been used in the past. To investigate the effects of uni- or multiaxial stretch, experiments have been performed with cells plated onto elastic membranes which can be stretched. For most of these experiments, cells are usually stretched in the range of 10–15% of their original length. The mode of stretching used is either a single stretching event (static strain) or continuous cycles of stretch followed by relaxation (cyclic strain). Different methods have also been developed to apply locally restricted forces on single cells, in order to observe any spatially restricted effects within single cells at the microscopic level. These methods include adhesive pipette tips (Riveline et al., 2001), magnetic beads (Glogauer and Ferrier, 1998), or laser tweezers (Choquet et al., 1997; Kuo and Sheetz, 1992). Finally, flow chambers are usually used to simulate shear stress on the surface of endothelial cells by the blood flow.

Consequences of stretching cells can easily be observed by conventional light microscopy. A monolayer of cells will tend to reorient and specifically align themselves in response to a force applied to the whole cell. The type of alignment depends on both the type of force applied and the type of cell. Fibroblasts were reported to align along the axis of static stretch (Haston et al., 1983). In contrast, endothelial cells and rat cardiac myocytes align perpendicular to the direction of force when they are exposed to cyclic stretch (Yano et al., 1996a,b). Endothelial cells exposed to fluid shear align parallel to the direction of flow (Levesque and Nerem, 1985; Tzima et al.,

2001). It is interesting to note that the two forces endothelial cells typically experience in their natural environment lead independently to the same alignment within blood vessels: perpendicular to the stretch caused by diastole/systole cycling and parallel to the blood flow.

5.2. Comparing focal adhesion structure in 2D versus 3D cell attachment

FAs and SFs are very prominent in cells grown in tissue culture, and culturing cells in a 2D environment has been used by most groups attempting to study the role of FAs and FCXs as mechanosensors. Obviously, this reflects the historical ease of growing cells in tissue culture dishes or on coverslips, as well as the advantage of cells growing on a flat surface for microscopy. However, it should be noted that a 2D culture is artificial relative to the natural environment of most cells embedded in tissues within multicellular organisms (Discher et al., 2005). For instance, while fibroblasts are usually nonpolarized cells *in vivo*, they tend to polarize when grown in conventional tissue culture, with a basal surface attached to the substrate and an apical surface exposed to the tissue culture fluid. Not surprisingly, fibroblasts grown in a ''normal'' 3D environment exhibit an altered morphology from that seen in a 2D environment, and rarely develop FAs or lamellipodia (Beningo et al., 2004; Cukierman et al., 2001; Tamariz and Grinnell, 2002). SFs are also rarely observed in most tissues *in vivo*. These observations have led many to question the physiological relevance of studying cells cultured on 2D substrates (Discher et al., 2005).

Several factors seem to contribute to the prominence of SFs and FAs in 2D tissue culture. Firstly, tissue culture medium contains high amounts of serum that contains factors (such as LPA and sphingosine-1–phosphate) that cause activation of RhoA and a concomitant increase in contractility. Secondly, the rigidity of the underlying surface of tissue culture dish plays a major role in the formation of SFs and FAs in 2D culture. The stiffness or elasticity of a material is defined by the elastic modulus (measured in Pascals). Tissues in the body have varying stiffness with bone being the most rigid with an elastic modulus of 18,000 Pa. In contrast, the mammary gland is very soft with an elasticity of 150 Pa. The microenvironment surrounding a tumor is approximately 4000 Pa making them very rigid compared to the normal surrounding tissue. Compared to tissue *in vivo*, the elastic modulus of glass coverslips or tissue culture plastic ranges from 10^9 to 10^{10} Pa (Paszek et al., 2005). These huge differences in elasticity, therefore, bring into question the relevance of using conventional 2D tissue culture to study cell behavior, and in particular, SF and FA formation. Experiments culturing cells on surfaces of different rigidity or compliance have demonstrated convincingly that cells react to different rigidities. Cells cultured on relatively soft CG-coated polyacrylamide gels do

not develop FAs, but those cultured on more rigid polyacrylamide gels can form FAs (Pelham and Wang, 1997).

Interestingly, fibroblasts growing in 3D CG gels that are free floating and relatively compliant do not develop SFs. In these gels, the cells contract the CG gels so that it visibly shrinks in size, often to as little as a tenth of its initial area. However, if the gels are anchored so that they cannot be contracted, fibroblasts develop isometric tension and now display SFs (Grinnell, 1994; Halliday and Tomasek, 1995; Mochitate et al., 1991; Tomasek et al., 1992). Release of the gels from attachment to their dishes results in rapid contraction of the gels and a concomitant disassembly of the SFs. These results are similar to those obtained on 2D polyacrylamide gel cultures, and support the general conclusion that the development of isometric tension is crucial to the formation of SFs and FAs.

However, while some consider SFs and FAs to be artifacts of tissue culture, equivalent structures are seen in different cell types *in vivo*. Parallel arrays of intracellular filaments in the spiral ligament of the cochlea contain actin and other SF-associated proteins (Henson et al., 1985). SFs have also been observed in endothelial cells *in vivo* (Wong et al., 1983). The myofibrils of smooth muscle resemble SFs in their organization, and attach to the PM at dense plaques, structures which resemble FAs. Integrins are concentrated in dense plaques, along with many of the proteins traditionally found in FAs. Like FAs, dense plaques also provide a transmembrane link between the intracellular cytoskeleton and the ECM.

Myofibroblasts are fibroblasts with several characteristics of smooth muscle cells. Specifically, they express an actin isoform that is found in smooth muscle, α-SM actin (Skalli et al., 1986). Myofibroblasts reveal prominent bundles of actin filaments, similar to stress fibers, attached to sites where integrins are clustered and which mediate attachment to the surrounding ECM (Tomasek et al., 2002). These structures might be functionally important for myofibroblasts, as they are responsible for the contraction of wound granulation tissue (Gabbiani et al., 1971). Myofibroblasts also generate the contractile forces involved in several disease situations, such as in Dupuytren's disease, which is a connective tissue disorder characterized by tissue contracture and fibrosis (Tomasek et al., 1986).

Myotendenous junctions (the physical links between muscle fibers and tendons) display prominent FA-equivalent features. Mammalian muscles express a splice isoform of the integrin $\beta 1$ chain (β_{1D}), which differs from the generally expressed isoform (β_{1A}) in sections of the intracellular domain (Belkin et al., 1996). Solid-phase assays have revealed a much stronger binding of talin to the β_{1D} tail compared to β_{1A}, thereby suggesting that talin contributes significantly to the required mechanical stability of myotendenous junctions *in vivo* (Belkin et al., 1997).

5.3. Mechanotransduction by focal adhesions: From sensing to responding

As mentioned before, numerous examples exist which clearly show that mechanical forces influence cellular behavior. The major question that remains to be answered is which molecules or structures are involved. Molecules which sense mechanical forces and thereby change properties do not necessarily need to be inside the cell. For example, on the extracellular side of FCXs or FAs, integrin receptors form noncovalent bonds to the ECM. The connections between noncovalently linked proteins exposed to a mechanical pulling force have a modest lifetime, with a decreasing bond lifetime when the force increases (Evans, 2001; Merkel et al., 1999). Obviously, the characteristic of these so–called slip bonds requires further strategies of the cell so that it does not lose its hold over time. One important property of integrin receptors is that they are not constitutively active, but their affinity can be regulated (Hynes, 2002). Integrin receptors are usually activated by allosteric mechanisms originating from inside or outside the cell (Tadokoro et al., 2003; Takagi et al., 2002). Interestingly, recent molecular dynamics studies indicate that mechanical forces acting on $\alpha_v\beta_3$ integrin promote an allosteric change in the extracellular domain of the receptor which results in an increased binding strength to the ECM (catch bond) (Puklin–Faucher and Sheetz, 2009; Puklin–Faucher et al., 2006). Besides this scenario where physical properties of FAs are changed by force, mechanotransduction usually refers to intracellular biochemical reactions in response to force.

Mechanotransduction comprises several steps, starting with the *initial sensory process,* followed by further *transducing mechanisms,* and the final integration of these signals into the *mechanoresponse* (Vogel and Sheetz, 2006). Mechanotransduction has become an area that is being increasingly studied, and many signaling molecules are now known to be involved in the process, including membrane receptors (Katsumi et al., 2005), Ca^{2+}-ion channels (Munevar et al., 2004), kinases, phosphatases (von Wichert et al., 2003), and small GTPases (Katsumi et al., 2002).

Mechanoresponses can be further classified into short- and long-termed responses. Cell spreading and migration are typical examples of short-term mechanoresponses. Plating cells on CG-coated polyacrylamide gels of various densities revealed that the spreading and migration behavior of cells depends on the "stiffness" or compliance of the substrate (Pelham and Wang, 1997). When plated on a surface with an internal rigidity gradient, isolated fibroblasts were found to orient and migrate preferentially toward the stiffer environment (Lo et al., 2000). FA formation is another example of a short-term mechanoresponse (Riveline et al., 2001). Long-term mechanoresponses include changes in gene expression and cell differentiation (Engler et al., 2004; Georges and Janmey, 2005).

The signaling events which regulate the short- and long-term mechanoresponses are diverse and numerous. We will discuss a few representative examples of mechanoresponses, and refer the reader to more comprehensive reviews of the process (Chen, 2008; Giannone and Sheetz, 2006; Katsumi et al., 2004). In almost all cases of mechanotransduction, integrins or associated FA proteins are involved, and it is clear that the translation of mechanical force to biochemical signals occurs in these structures. Notably, the activity of many FA-associated proteins is known to be influenced by mechanical stimuli, leading downstream to different signaling events.

In particular, activation of several GTPases of the Ras superfamily has been shown to be influenced by stretching cells. For instance, Ras is inactivated when L929 fibroblasts are stretched (Sawada et al., 2001). Similarly, Rac1 activity is transiently inhibited after biaxial stretching of vascular smooth muscle cells (Katsumi et al., 2002). In contrast, RhoA activity is upregulated in stretched portal veins (Albinsson et al., 2004), and in endothelial cells which were exposed to cyclic stretch (Shikata et al., 2005). Activity of the GTPase Rap1 is also increased in response to stretch, leading to activation of the p38 mitogen-activated protein kinase (MAPK) pathway (Sawada et al., 2001). Nevertheless, it should be mentioned that some conflicting results about the regulation of Rho GTPases by stretch may originate from different responses in different cell types (Liu et al., 2007). For example, Liu and coworkers found that active RhoA is decreased by stretch in endothelial cells, whereas the same stimulus increased RhoA activity in smooth muscle cells (Liu et al., 2007). Future work should, therefore, focus on the molecular reasons for these different reactions.

Applying cyclic strain on fibroblasts also leads to activation of src, which results in tyrosine phosphorylation of FAK, paxillin, and p130Cas (Sai et al., 1999). Several different MAPKs such as extracellular signal-regulated kinase 2 (ERK2) and c-jun amino-terminal kinase (JNK) are also activated in response to stretch in fibroblasts, and this activity is dependent on the type of integrin involved. Stretching of cells plated on FN leads to ERK2 and JNK activation, whereas in the same experimental setup using VN or LN, stretch specifically activated only JNK (MacKenna et al., 1998). Similar to stretch-induced activation of ERK and JNK, the stimulation of PDGF production in vascular smooth muscle cells also depends on the interaction between specific integrins and the stretched ECM involved (Wilson et al., 1993, 1995).

5.4. Specific mechanisms of primary force sensing

Whereas the mechanoresponses described so far demonstrate that cells do react to mechanical inputs, none of them answer specific questions about the mechanisms involved, such as which proteins are directly participating in sensing force, where or how the signaling cascade starts, and how the mechanical signal is converted into a biochemical reaction. The techniques

being developed to answer these questions are still comparatively young (Vogel and Sheetz, 2006), but we will discuss examples which identify mechanisms of force sensing in mechanotransduction.

5.4.1. Reinforcement

Talin can bind simultaneously to both integrins and actin (Nayal et al., 2004). Besides its role in integrin activation (inside-out signaling) (Calderwood et al., 1999; Tadokoro et al., 2003; Vinogradova et al., 2002), the function of talin as a mechanosensor has been extensively investigated. Specifically, talin plays a pivotal role in the first steps of mechanosensation by initiating a process called *reinforcement* (del Rio et al., 2009; Giannone et al., 2003). This process describes the ability of cells to tighten or reinforce the integrin–actin cytoskeleton connection in response to force (Choquet et al., 1997). Interestingly, reinforcement is a local event in a cell, only occurring where the force is applied. In response to mechanical force, talin causes the recruitment of other FCX and FA components, and acts as a core scaffold in a mechano-stress-dependent manner.

Talin is one of the first proteins to localize to newly formed ECM-integrin connections (Izzard and Izzard, 1987), and it provides the first weak mechanical resistance (Jiang et al., 2003). These first ECM-integrin connections (named *initial adhesions*) are precursors to FCXs, and lack typical FCX markers like vinculin (Galbraith et al., 2002; Izzard, 1988). Measurements by Jiang and coworkers showed that initial contacts between FN fragments and the cytoskeleton (through $\alpha_v\beta_3$) resist to a mechanical force of 2 pN (Jiang et al., 2003), which is much less than that of a single integrin-FN bond (20 pN) (Thoumine et al., 2000). Interestingly, this 2 pN slip bond disappears in talin null cells, but can be rescued by reexpression of talin (Jiang et al., 2003). Inhibition of known enzymatic activities important for reinforcement of the integrin–cytoskeleton connection did not affect the 2 pN slip bond, suggesting that formation of these initial adhesions is independent of other enzymatic activities.

The crucial event for reinforcement is the subsequent appearance of vinculin in initial adhesions, which can now be termed FCXs (DePasquale and Izzard, 1987; Galbraith et al., 2002; Izzard, 1988). Recent findings have shown that recruitment of vinculin to FAs greatly enhances their mechanical stability (Humphries et al., 2007). Vinculin is only recruited to initial adhesions if a minimal amount of mechanical strain is achieved, either by endogenous myosin-II-derived force or exogenous force applied on the initial adhesions (Galbraith et al., 2002). Importantly, reinforcement does not occur without recruitment of vinculin, a process that requires talin (del Rio et al., 2009; Giannone et al., 2003). The mechanisms involved in the ability of talin to recruit vinculin to initial adhesions in response to mechanical force were recently investigated by Lee and coworkers (Lee et al., 2007). This study revealed that a masked vinculin binding site in a five-

helix-bundle of the talin rod domain becomes accessible after the application of an *unfolding* force on this domain (Lee et al., 2007) (Fig. 1.8A).

5.4.2. Activation of Rap1 by unfolding of p130Cas

One member of the Ras superfamily of small GTPases found to be regulated by stretch is Rap1, via a mechanism involving the protein p130Cas. p130Cas is a FA-scaffolding protein which does not possess any intrinsic enzymatic activity (Defilippi et al., 2006). Localization of p130Cas to FAs depends on N- and C-terminal flanking regions of the molecule. Src family kinases can phosphorylate p130Cas in the central substrate domain, leading to the recruitment of Crk, another adaptor protein. Interestingly, stretching cells stimulated tyrosine phosphorylation of p130Cas in a Src-dependent manner (Tamada et al., 2004). Activation of the GTPase Rap1 in response to stretch was shown to depend upon the GEF C3G, which binds to Crk (Sawada et al., 2006). These data, therefore, suggest that mechanoactivation of Rap1 occurs by recruitment of the Crk/C3G complex to p130Cas upon its phosphorylation (Tamada et al., 2004).

Using *in vitro* cell-free systems, Sawada and coworkers determined a mechanism by which mechanical forces stretch p130Cas to generate biochemical signals in this pathway (Sawada et al., 2006). Specifically, purified p130Cas molecules were attached to a membrane by both of their N- and C-terminus. The authors showed that subsequent stretching of the membrane leads to extension of the p130Cas molecules. When these p130Cas-bound membranes were incubated with active Src, tyrosine phosphorylation of p130Cas only occurred in prestretched membranes. This is most likely due to unmasking of the substrate tyrosine, making it accessible to phosphorylation by Src (Fig. 1.8B). Importantly, however, total Src activity (measured by antibodies to its activating and inactivating phosphorylation sites) remained unchanged by stretching. These studies showed that the p130Cas–Src complex can be seen as a primary force sensing unit, able to convert mechanical stretch into a phosphorylation signal.

The concept common to the above two discussed mechanisms of mechanosensation is that in both cases the primary force perception molecule is unfolded (or undergoes a conformational change) by forces pulling on both sides of the molecule in opposing directions, allowing another molecule to access a cryptic site (Fig. 1.8). This mechanism of mechanosensation can possibly be applied to other FA proteins, as a number of them adopt open (unfolded) versus closed (folded) conformations, and are hence possibly regulated by stretch in a similar manner. For example, vinculin exists in a closed conformation (restricting binding to other cytoskeletal components), but binding of several different ligands can cause an "opening" conformational change (Gilmore and Burridge, 1996; Johnson and Craig, 2000; Zamir and Geiger, 2001; Ziegler et al., 2006). Further, it has shown that FAK also undergoes an "opening" conformational change
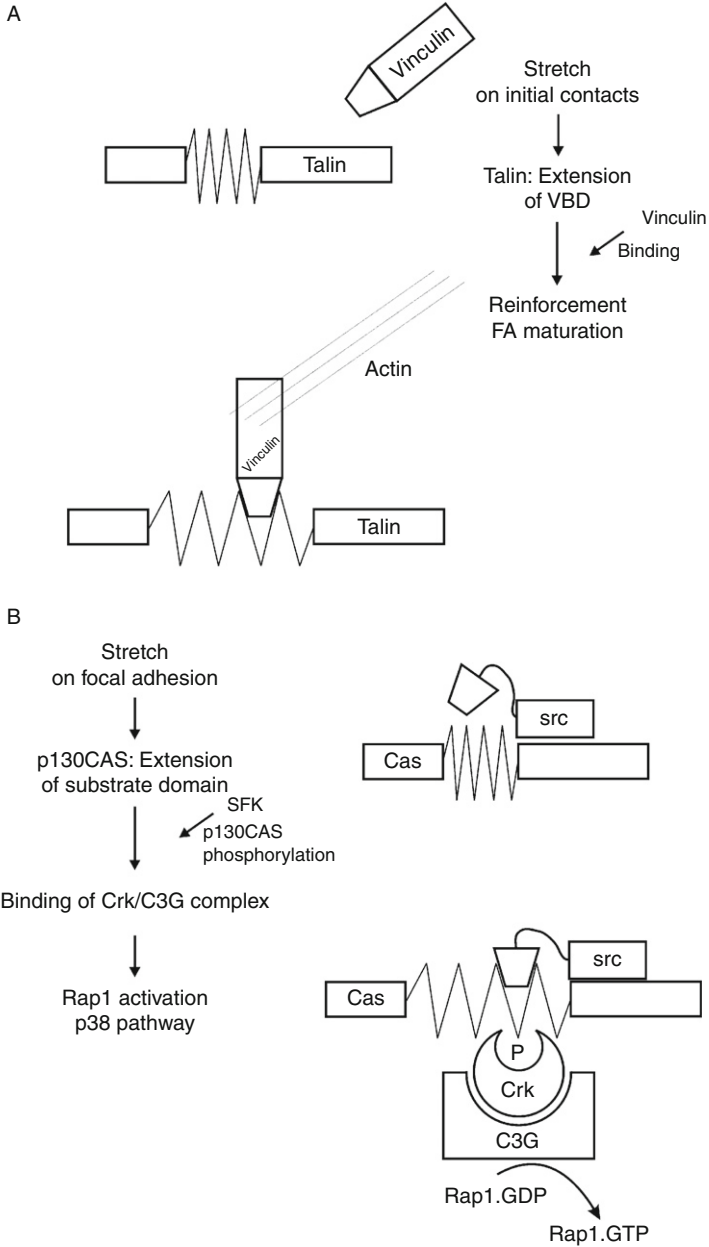
Figure 1.8 Models of mechanotransduction. Mechanical stress regulates different FA proteins by affecting their structural conformations and initiating different signaling pathways.

when it is activated, and that the open conformation of FAK is present in FAs (Cai et al., 2008). It is also likely that unfolding due to tension may be a general principle. A recent study using shotgun labeling of newly exposed cysteine residues in cells has revealed that tension causes the ''opening'' of numerous proteins such as vimentin, myosin, and spectrin (Johnson et al., 2007).

6. Disassembly of Focal Adhesions

Despite the fact that productive cell migration requires active FA disassembly in addition to assembly, we know much less about the mechanisms involving the former. It is easy to imagine that disassembly simply occurs by inhibiting the mechanisms controlling assembly of FAs, leading to the dispersal of integrin clusters and their associated proteins. There is some evidence to support this—Rho activity is critical for maintaining FAs (Ridley and Hall, 1992), and agents that inhibit contractility or ROCK result in the rapid disassembly of FAs (Chrzanowska-Wodnicka and Burridge, 1996; Narumiya et al., 2000; Ren et al., 2000; Ridley and Hall, 1992).

However, whether local inhibition of RhoA or its effectors is responsible for FA disassembly has not been established. Also, why tension is required for the maintenance of FAs is not entirely clear. The loss of tension could potentially result in a decrease in integrin affinity for ECM ligands. However, once a FA has been formed by the clustering of integrins, the simple release of tension seems insufficient to cause a dispersal of integrins, unless there is some counterforce acting to dissociate them. This section of the chapter will focus on several different mechanisms which have been proposed for the regulation of FA disassembly in cells.

6.1. FAK/Src signaling in focal adhesion disassembly

Horwitz and his colleagues have studied the disassembly of two populations of adhesions, those at the rear and those at the front of cells. During fibroblast migration, large FAs at the rear of the cell have to be disassembled in order for cells to move forward. Early work using permeabilized cells indicated that tension and tyrosine kinase activity are required for the detachment of rear FAs (Crowley and Horwitz, 1995). The term *turnover* (as opposed to disassembly) is used to denote the behavior of adhesions at the front of the cell, because as some are disassembling, other adhesions nearby are assembling. In a detailed study, Horwitz and colleagues measured the rate of change of fluorescence intensity of FA markers (like paxillin) as FAs assemble and disassemble, allowing them to calculate rate constants for

assembly and disassembly. These studies allowed the investigators to examine specific signaling molecules that affected rate of disassembly of FAs but not assembly (Webb et al., 2004). For example, in FAK null cells, the rate of FA disassembly was decreased approximately 14-fold, but the rate of assembly was normal (Webb et al., 2004). Reexpression of wild-type FAK, but not kinase-dead FAK, restored the rate of FA disassembly. These data support previous work showing that FAK null cells have long-lived FAs, suggesting a major role for FAK in the disassembly of FAs (Ilic et al., 1995). Similarly, the rate of FA disassembly was greatly decreased in cells lacking Src family kinases. Appropriately, phosphorylation of different FAK and Src substrates (such as p130cas and Paxillin) was also required to maintain the normal rate of FA disassembly. Somewhat surprisingly, however, expression of constitutively active Rac or dominant negative Rho did not affect the rate of FA disassembly. Instead, expression of dominant negative forms of MEK or treatment with MEK inhibitors also decreased the rate of FA disassembly, implicating the MAPK pathway (downstream of Src) in regulation of FA disassembly (Sieg et al., 1999; Webb et al., 2004).

6.2. Proteolytic cleavage of focal adhesion components by calpain

In addition to the studies above highlighting signaling proteins involved in FA disassembly, other work has focused on the physical mechanisms by which these structures are dismantled. One of these mechanisms involves proteolytic cleavage of FA components via the protease calpain. The possibility that proteolysis of FA proteins may play a role in FA disassembly has been considered ever since the calcium-activated protease calpain was discovered in FAs (Beckerle et al., 1987). The importance of calpain in adhesion dynamics was supported by studies showing that either deletion of the small subunit of many calpains (calpain 4) (Huttenlocher et al., 1997; Palecek et al., 1998) or pharmacological inhibition of calpain (Dourdin et al., 2001) causes a decrease in the rates of migration and FA disassembly.

Interestingly, knockdown of calpain 2 (a ubiquitously expressed calpain isoform) by siRNA results in cells which contain large peripheral FAs while lacking central FAs (Franco et al., 2004a). This phenotype is likely not just a result of effects on FA stability, as decreased FA turnover usually results in more central FAs, not less. However, considering the large number of calpain substrates that have been identified, diverse effects on cytoskeletal organization and behavior are not unexpected in cells deficient in calpain 2 activity. Further, determining which calpain target is critical for FA disassembly is complicated by the large number of calpain substrates that are prominent structural or signaling components of FAs (such as talin, filamin, α-actinin, vinculin, integrins, FAK, Src, paxillin, and RhoA). One study focused on this question by creating a mutant of talin that

was resistant to cleavage by calpain and expressed it in talin null fibroblasts. Cells expressing the calpain–resistant talin mutant demonstrated increased FA lifetimes, indicating that proteolysis of talin by calpain 2 does contribute significantly to FA turnover and disassembly in normal cells (Franco et al., 2004b).

6.3. Focal adhesion disassembly by microtubule targeting and endocytosis

One of the problems with studying FA disassembly is that in migrating cells, the event is typically asynchronous, that is, different populations of FAs are disassembling and assembling simultaneously. As a result, it is difficult to analyze the factors that specifically affect FA disassembly. A novel approach to synchronize FA disassembly events was taken by Ezratty and colleagues, who have studied mechanisms of FA disassembly by microtubule (MT) targeting (Ezratty et al., 2005). It has been known that disruption of MTs elevates Rho activity and promotes contractility and FA assembly (Bershadsky et al., 1996; Danowski, 1989; Liu et al., 1998; Ren et al., 1999). Conversely, MTs have been observed to target FAs and this targeting has been correlated with FA disassembly (Kaverina et al., 1999). To coordinate FA disassembly, MTs were first depolymerized with nocodazole treatment, inducing the formation of prominent FAs. Nocodazole washout then allowed for rapid MT regrowth and the targeting of FAs, resulting in a wave of FA disassembly that was nearly synchronous (Ezratty et al., 2005). Interestingly, expression of constitutively active RhoA demonstrated that disassembly was not due to the repression of RhoA activity by MT growth, and that FA disassembly can occur in the presence of high RhoA activity.

Previous work has shown that integrins can recycle from the back of cells to the front, via an endocytic/exocytic pathway (Powelka et al., 2004; White et al., 2007). To investigate whether the disassembly of FAs might involve the endocytic machinery, a dominant negative form of dynamin was expressed in cells, which blocked FA disassembly induced by MT regrowth (Ezratty et al., 2005). Moreover, it was found that dynamin localized in regions overlapping with FAs. In addition, FAK null cells (which have FAs with reduced turnover rates) failed to respond to MT-induced FA disassembly. Notably, dynamin was shown to interact with FAK prior to FA disassembly (via its proline-rich domain), and the localization of dynamin to FAs is lost in FAK null cells. Interestingly, Grb2 has also been shown to bind to the proline-rich region of dynamin, and expression of a mutant of FAK which lacks binding to Grb2 could not rescue the low-FA disassembly rates seen in FAK null cells (Ezratty et al., 2005). While these studies have not characterized the role of FAK/Grb2/dynamin complexes in FA disassembly in detail, they raise intriguing possibilities about an endocytic mechanism for the disassembly of FAs.

▶ 7. Concluding Remarks

From their humble beginnings in 1971, when they were first detected as electron dense plaques at the end of bundles of actin filaments in fibroblasts grown in culture (Abercrombie et al., 1971), FAs have come a very long way. They have been the objects of intense study and much has been learned about many of their major components, about their structure, assembly, and the signaling pathways that emanate from them. However, without doubt, much remains to be learned about these structures. For example, the field has been dominated by studies of FAs in cells adhering to FN, but there are many other ECM components to which cells adhere *in vivo*. Much less is known about the adhesions made to these ECM proteins. Similarly, with respect to integrins, most of our knowledge of their role in FAs derives from $\alpha_5\beta_1$ or $\alpha_V\beta_3$, the integrins that bind FN. Do other integrins generate equivalent adhesions when they are engaging their corresponding ECM ligands? Another area where we suspect much remains to be discovered is the disassembly of FAs. In comparison with assembly, relatively little is known about disassembly, although both must be equally important for the cell. We anticipate that additional pathways will be discovered that contribute to FA disassembly. Understanding more completely how FAs are disassembled will be important in the study of cell migration and invasion.

For many years, essentially all the adhesions made by cells to ECM on a substratum were considered to be FAs, but then it was appreciated that several types of adhesion could be distinguished, including FAs, FCXs, and FBAs. Are there more distinct types of adhesion to be discovered or is the situation more of a continuum, in which there is a gradation of adhesions between some extremes? We favor the latter situation and suspect that many intermediates may exist between these adhesion types. We suspect that the composition of a particular adhesion will depend on the adhesive surface and the matrix to which cells are adhering, the cell type and its repertoire of integrins and other adhesion molecules, as well as on the signaling pathways that have been activated within the cell. The situation will most likely be resolved by the application of imaging techniques that allow simultaneous quantification of different components in real time in living cells. The first steps in such an analysis have already been made (Digman et al., 2009; Zamir et al., 2008).

Finally, the field of FA research has been transitioning into analyzing the adhesions made by cells in three-dimensional matrices. Technically these adhesions are more difficult to analyze, but they are clearly more relevant to the situation *in vivo*. In general, the organization of these adhesions is more reminiscent of FBAs. Whereas the prominence of FAs in tissue culture cells

is something of an artifact of culturing cells on rigid 2D surfaces in situations that activate RhoA, they nevertheless have advantages. They are easily imaged, are often large, and are formed under highly reproducible conditions. Consequently, we believe that they will continue to provide a valuable model for studying ECM adhesions, whether 2D or 3D, as well as for studying the signals that affect adhesions and for investigating the signaling pathways that adhesion to ECM initiates.

ACKNOWLEDGMENTS

REFERENCES

Abercrombie, M., Dunn, G.A., 1975. Adhesions of fibroblasts to substratum during contact inhibition observed by interference reflection microscopy. Exp. Cell Res. 92, 57–62.

Abercrombie, M., Heaysman, J.E., Pegrum, S.M., 1971. The locomotion of fibroblasts in culture. IV. Electron microscopy of the leading lamella. Exp. Cell Res. 67, 359–367.

Abram, C.L., Seals, D.F., Pass, I., Salinsky, D., Maurer, L., Roth, T.M., et al., 2003. The adaptor protein fish associates with members of the ADAMs family and localizes to podosomes of Src-transformed cells. J. Biol. Chem. 278, 16844–16851.

Albinsson, S., Nordstrom, I., Hellstrand, P., 2004. Stretch of the vascular wall induces smooth muscle differentiation by promoting actin polymerization. J. Biol. Chem. 279, 34849–34855.

Alexander, N.R., Branch, K.M., Parekh, A., Clark, E.S., Iwueke, I.C., Guelcher, S.A., et al., 2008. Extracellular matrix rigidity promotes invadopodia activity. Curr. Biol. 18, 1295–1299.

Amato, P.A., Unanue, E.R., Taylor, D.L., 1983. Distribution of actin in spreading macrophages: a comparative study on living and fixed cells. J. Cell Biol. 96, 750–761.

Ariga, K., Nakanishi, T., Michinobu, T., 2006. Immobilization of biomaterials to nano-assembled films (self-assembled monolayers, Langmuir-Blodgett films, and layer-by-layer assemblies) and their related functions. J. Nanosci. Nanotechnol. 6, 2278–2301.

Arnold, M., Cavalcanti-Adam, E.A., Glass, R., Blummel, J., Eck, W., Kantlehner, M., et al., 2004. Activation of integrin function by nanopatterned adhesive interfaces. Chemphyschem 5, 383–388.

Arthur, W.T., Burridge, K., 2001. RhoA inactivation by p190RhoGAP regulates cell spreading and migration by promoting membrane protrusion and polarity. Mol. Biol. Cell 12, 2711–2720.

Arthur, W.T., Petch, L.A., Burridge, K., 2000. Integrin engagement suppresses RhoA activity via a c-Src-dependent mechanism. Curr. Biol. 10, 719–722.

Arthur, W.T., Noren, N.K., Burridge, K., 2002. Regulation of Rho family GTPases by cell-cell and cell-matrix adhesion. Biol. Res. 35, 239–246.

Artym, V.V., Zhang, Y., Seillier-Moiseiwitsch, F., Yamada, K.M., Mueller, S.C., 2006. Dynamic interactions of cortactin and membrane type 1 matrix metalloproteinase at

invadopodia: defining the stages of invadopodia formation and function. Cancer Res. 66, 3034–3043.

Avalos, A.M., Arthur, W.T., Schneider, P., Quest, A.F., Burridge, K., Leyton, L., 2004. Aggregation of integrins and RhoA activation are required for Thy-1-induced morphological changes in astrocytes. J. Biol. Chem. 279, 39139–39145.

Baciu, P.C., Goetinck, P.F., 1995. Protein kinase C regulates the recruitment of syndecan-4 into focal contacts. Mol. Biol. Cell 6, 1503–1513.

Baldassarre, M., Pompeo, A., Beznoussenko, G., Castaldi, C., Cortellino, S., McNiven, M.A., et al., 2003. Dynamin participates in focal extracellular matrix degradation by invasive cells. Mol. Biol. Cell 14, 1074–1084.

Bass, M.D., Humphries, M.J., 2002. Cytoplasmic interactions of syndecan-4 orchestrate adhesion receptor and growth factor receptor signalling. Biochem. J. 368, 1–15.

Bass, M.D., Morgan, M.R., Humphries, M.J., 2007a. Integrins and syndecan-4 make distinct, but critical, contributions to adhesion contact formation. Eur. Phys. J. E Soft Matter 3, 372–376.

Bass, M.D., Roach, K.A., Morgan, M.R., Mostafavi-Pour, Z., Schoen, T., Muramatsu, T., et al., 2007b. Syndecan-4-dependent Rac1 regulation determines directional migration in response to the extracellular matrix. J. Cell Biol. 177, 527–538.

Bass, M.D., Morgan, M.R., Roach, K.A., Settleman, J., Goryachev, A.B., Humphries, M.J., 2008. p190RhoGAP is the convergence point of adhesion signals from alpha 5 beta 1 integrin and syndecan-4. J. Cell Biol. 181, 1013–1026.

Beauvais, D.M., Rapraeger, A.C., 2003. Syndecan-1-mediated cell spreading requires signaling by alphavbeta3 integrins in human breast carcinoma cells. Exp. Cell Res. 286, 219–232.

Beauvais, D.M., Burbach, B.J., Rapraeger, A.C., 2004. The syndecan-1 ectodomain regulates alphavbeta3 integrin activity in human mammary carcinoma cells. J. Cell Biol. 167, 171–181.

Beckerle, M.C., Burridge, K., DeMartino, G.N., Croall, D.E., 1987. Colocalization of calcium-dependent protease II and one of its substrates at sites of cell adhesion. Cell 51, 569–577.

Belkin, A.M., Zhidkova, N.I., Balzac, F., Altruda, F., Tomatis, D., Maier, A., et al., 1996. Beta 1D integrin displaces the beta 1A isoform in striated muscles: localization at junctional structures and signaling potential in nonmuscle cells. J. Cell Biol. 132, 211–226.

Belkin, A.M., Retta, S.F., Pletjushkina, O.Y., Balzac, F., Silengo, L., Fassler, R., et al., 1997. Muscle beta1D integrin reinforces the cytoskeleton-matrix link: modulation of integrin adhesive function by alternative splicing. J. Cell Biol. 139, 1583–1595.

Beningo, K.A., Dembo, M., Wang, Y.L., 2004. Responses of fibroblasts to anchorage of dorsal extracellular matrix receptors. Proc. Natl. Acad. Sci. USA 101, 18024–18029.

Berdeaux, R.L., Diaz, B., Kim, L., Martin, G.S., 2004. Active Rho is localized to podosomes induced by oncogenic Src and is required for their assembly and function. J. Cell Biol. 166, 317–323.

Bershadsky, A., Chausovsky, A., Becker, E., Lyubimova, A., Geiger, B., 1996. Involvement of microtubules in the control of adhesion-dependent signal transduction. Curr. Biol. 6, 1279–1289.

Bishop, A.L., Hall, A., 2000. Rho GTPases and their effector proteins. Biochem. J. 348 (Pt. 2), 241–255.

Blattler, T., Huwiler, C., Ochsner, M., Stadler, B., Solak, H., Voros, J., et al., 2006. Nanopatterns with biological functions. J. Nanosci. Nanotechnol. 6, 2237–2264.

Block, M.R., Badowski, C., Millon-Fremillon, A., Bouvard, D., Bouin, A.P., Faurobert, E., et al., 2008. Podosome-type adhesions and focal adhesions, so alike yet so different. Eur. J. Cell Biol. 87, 491–506.

Bloom, L., Ingham, K.C., Hynes, R.O., 1999. Fibronectin regulates assembly of actin filaments and focal contacts in cultured cells via the heparin-binding site in repeat III13. Mol. Biol. Cell 10, 1521–1536.

Borradori, L., Sonnenberg, A., 1999. Structure and function of hemidesmosomes: more than simple adhesion complexes. J. Invest. Dermatol. 112, 411–418.

Bowden, E.T., Barth, M., Thomas, D., Glazer, R.I., Mueller, S.C., 1999. An invasion-related complex of cortactin, paxillin and PKCmu associates with invadopodia at sites of extracellular matrix degradation. Oncogene 18, 4440–4449.

Bradley, W.D., Hernandez, S.E., Settleman, J., Koleske, A.J., 2006. Integrin signaling through Arg activates p190RhoGAP by promoting its binding to p120RasGAP and recruitment to the membrane. Mol. Biol. Cell 17, 4827–4836.

Brandt, D., Gimona, M., Hillmann, M., Haller, H., Mischak, H., 2002. Protein kinase C induces actin reorganization via a Src- and Rho-dependent pathway. J. Biol. Chem. 277, 20903–20910.

Brock, A., Chang, E., Ho, C.C., LeDuc, P., Jiang, X., Whitesides, G.M., et al., 2003. Geometric determinants of directional cell motility revealed using microcontact printing. Langmuir 19, 1611–1617.

Brown, M.C., West, K.A., Turner, C.E., 2002. Paxillin-dependent paxillin kinase linker and p21-activated kinase localization to focal adhesions involves a multistep activation pathway. Mol. Biol. Cell 13, 1550–1565.

Buccione, R., Orth, J.D., McNiven, M.A., 2004. Foot and mouth: podosomes, invadopodia and circular dorsal ruffles. Nat. Rev. Mol. Cell Biol. 5, 647–657.

Burgstaller, G., Gimona, M., 2004. Actin cytoskeleton remodelling via local inhibition of contractility at discrete microdomains. J. Cell Sci. 117, 223–231.

Burns, S., Thrasher, A.J., Blundell, M.P., Machesky, L., Jones, G.E., 2001. Configuration of human dendritic cell cytoskeleton by Rho GTPases, the WAS protein, and differentiation. Blood 98, 1142–1149.

Burridge, K., Chrzanowska-Wodnicka, M., 1996. Focal adhesions, contractility, and signaling. Annu. Rev. Cell Dev. Biol. 12, 463–518.

Burridge, K., Feramisco, J.R., 1980. Microinjection and localization of a 130K protein in living fibroblasts: a relationship to actin and fibronectin. Cell 19, 587–595.

Burridge, K., Fath, K., Kelly, T., Nuckolls, G., Turner, C., 1988. Focal adhesions: transmembrane junctions between the extracellular matrix and the cytoskeleton. Annu. Rev. Cell Biol. 4, 487–525.

Cai, X., Lietha, D., Ceccarelli, D.F., Karginov, A.V., Rajfur, Z., Jacobson, K., et al., 2008. Spatial and temporal regulation of focal adhesion kinase activity in living cells. Mol. Cell Biol. 28, 201–214.

Calderwood, D.A., Zent, R., Grant, R., Rees, D.J., Hynes, R.O., Ginsberg, M.H., 1999. The Talin head domain binds to integrin beta subunit cytoplasmic tails and regulates integrin activation. J. Biol. Chem. 274, 28071–28074.

Caligaris-Cappio, F., Bergui, L., Tesio, L., Corbascio, G., Tousco, F., Marchisio, P.C., 1986. Cytoskeleton organization is aberrantly rearranged in the cells of B chronic lymphocytic leukemia and hairy cell leukemia. Blood 67, 233–239.

Carman, C.V., Sage, P.T., Sciuto, T.E., de la Fuente, M.A., Geha, R.S., Ochs, H.D., et al., 2007. Transcellular diapedesis is initiated by invasive podosomes. Immunity 26, 784–797.

Castellano, F., Chavrier, P., Caron, E., 2001. Actin dynamics during phagocytosis. Semin. Immunol. 13, 347–355.

Cavalcanti-Adam, E.A., Micoulet, A., Blummel, J., Auernheimer, J., Kessler, H., Spatz, J.P., 2006. Lateral spacing of integrin ligands influences cell spreading and focal adhesion assembly. Eur. J. Cell Biol. 85, 219–224.

Cavalcanti-Adam, E.A., Volberg, T., Micoulet, A., Kessler, H., Geiger, B., Spatz, J.P., 2007. Cell spreading and focal adhesion dynamics are regulated by spacing of integrin ligands. Biophys. J. 92, 2964–2974.

Chan, E.W., Yousaf, M.N., 2006. Immobilization of ligands with precise control of density to electroactive surfaces. J. Am. Chem. Soc. 128, 15542–15546.

Chardin, P., Boquet, P., Madaule, P., Popoff, M.R., Rubin, E.J., Gill, D.M., 1989. The mammalian G protein rhoC is ADP-ribosylated by *Clostridium botulinum* exoenzyme C3 and affects actin microfilaments in Vero cells. EMBO J. 8, 1087–1092.

Chellaiah, M., Hruska, K., 1996. Osteopontin stimulates gelsolin-associated phosphoinositide levels and phosphatidylinositol triphosphate-hydroxyl kinase. Mol. Biol. Cell 7, 743–753.

Chellaiah, M.A., Soga, N., Swanson, S., McAllister, S., Alvarez, U., Wang, D., et al., 2000. Rho-A is critical for osteoclast podosome organization, motility, and bone resorption. J. Biol. Chem. 275, 11993–12002.

Chellaiah, M.A., Biswas, R.S., Yuen, D., Alvarez, U.M., Hruska, K.A., 2001. Phosphatidylinositol 3, 4, 5-Trisphosphate Directs Association of Src Homology 2-containing Signaling Proteins with Gelsolin. J. Biol. Chem. 276, 47434–47444.

Chen, W.T., 1989. Proteolytic activity of specialized surface protrusions formed at rosette contact sites of transformed cells. J. Exp. Zool. 251, 167–185.

Chen, W.T., 1990. Transmembrane interactions at cell adhesion and invasion sites. Cell Differ. Dev. 32, 329–335.

Chen, C.S., 2008. Mechanotransduction—a field pulling together? J. Cell Sci. 121, 3285–3292.

Chen, W.T., Singer, S.J., 1982. Immunoelectron microscopic studies of the sites of cell-substratum and cell-cell contacts in cultured fibroblasts. J. Cell Biol. 95, 205–222.

Chen, W.T., Olden, K., Bernard, B.A., Chu, F.F., 1984. Expression of transformation-associated protease(s) that degrade fibronectin at cell contact sites. J. Cell Biol. 98, 1546–1555.

Chen, W.T., Chen, J.M., Parsons, S.J., Parsons, J.T., 1985. Local degradation of fibronectin at sites of expression of the transforming gene product pp 60src. Nature 316, 156–158.

Chew, T.L., Masaracchia, R.A., Goeckeler, Z.M., Wysolmerski, R.B., 1998. Phosphorylation of non-muscle myosin II regulatory light chain by p21-activated kinase (gamma-PAK). J. Muscle Res. Cell Motil. 19, 839–854.

Chikumi, H., Fukuhara, S., Gutkind, J.S., 2002. Regulation of G protein-linked guanine nucleotide exchange factors for Rho, PDZ-RhoGEF, and LARG by tyrosine phosphorylation: evidence of a role for focal adhesion kinase. J. Biol. Chem. 277, 12463–12473.

Choquet, D., Felsenfeld, D.P., Sheetz, M.P., 1997. Extracellular matrix rigidity causes strengthening of integrin-cytoskeleton linkages. Cell 88, 39–48.

Chrzanowska-Wodnicka, M., Burridge, K., 1996. Rho-stimulated contractility drives the formation of stress fibers and focal adhesions. J. Cell Biol. 133, 1403–1415.

Collin, O., Na, S., Chowdhury, F., Hong, M., Shin, M.E., Wang, F., et al., 2008. Self-organized podosomes are dynamic mechanosensors. Curr. Biol. 18, 1288–1294.

Couchman, J.R., 2003. Syndecans: proteoglycan regulators of cell-surface microdomains? Nat. Rev. Mol. Cell Biol. 4, 926–937.

Couchman, J.R., Woods, A., 1999. Syndecan-4 and integrins: combinatorial signaling in cell adhesion. J. Cell Sci. 112 (Pt. 20), 3415–3420.

Couchman, J.R., Chen, L., Woods, A., 2001. Syndecans and cell adhesion. Int. Rev. Cytol. 207, 113–150.

Cox, E.A., Sastry, S.K., Huttenlocher, A., 2001. Integrin-mediated adhesion regulates cell polarity and membrane protrusion through the Rho family of GTPases. Mol. Biol. Cell 12, 265–277.

Crowley, E., Horwitz, A.F., 1995. Tyrosine phosphorylation and cytoskeletal tension regulate the release of fibroblast adhesions. J. Cell Biol. 131, 525–537.

Cukierman, E., Pankov, R., Stevens, D.R., Yamada, K.M., 2001. Taking cell-matrix adhesions to the third dimension. Science 294, 1708–1712.

Curtis, A.S., 1964. The mechanism of adhesion of cells to glass. A study by interference reflection microscopy. J. Cell Biol. 20, 199–215.

Cutler, S.M., Garcia, A.J., 2003. Engineering cell adhesive surfaces that direct integrin alpha5-beta1 binding using a recombinant fragment of fibronectin. Biomaterials 24, 1759–1770.

Danen, E.H., Sonneveld, P., Brakebusch, C., Fassler, R., Sonnenberg, A., 2002. The fibronectin-binding integrins alpha5beta1 and alphavbeta3 differentially modulate RhoA-GTP loading, organization of cell matrix adhesions, and fibronectin fibrillogenesis. J. Cell Biol. 159, 1071–1086.

Danen, E.H., van Rheenen, J., Franken, W., Huveneers, S., Sonneveld, P., Jalink, K., et al., 2005. Integrins control motile strategy through a Rho-cofilin pathway. J. Cell Biol. 169, 515–526.

Danowski, B.A., 1989. Fibroblast contractility and actin organization are stimulated by microtubule inhibitors. J. Cell Sci. 93 (Pt. 2), 255–266.

Davis, S., Lu, M.L., Lo, S.H., Lin, S., Butler, J.A., Druker, B.J., et al., 1991. Presence of an SH2 domain in the actin-binding protein tensin. Science 252, 712–715.

Defilippi, P., Di Stefano, P., Cabodi, S., 2006. p130Cas: a versatile scaffold in signaling networks. Trends Cell Biol. 16, 257–263.

Delcommenne, M., Tan, C., Gray, V., Rue, L., Woodgett, J., Dedhar, S., 1998. Phosphoinositide-3-OH kinase-dependent regulation of glycogen synthase kinase 3 and protein kinase B/AKT by the integrin-linked kinase. Proc. Natl. Acad. Sci. USA 95, 11211–11216.

del Rio, A., Perez-Jimenez, R., Liu, R., Roca-Cusachs, P., Fernandez, J.M., Sheetz, M.P., 2009. Stretching single talin rod molecules activates vinculin binding. Science 323, 638–641.

DePasquale, J.A., Izzard, C.S., 1987. Evidence for an actin-containing cytoplasmic precursor of the focal contact and the timing of incorporation of vinculin at the focal contact. J. Cell Biol. 105, 2803–2809.

Deroanne, C.F., Lapiere, C.M., Nusgens, B.V., 2001. *In vitro* tubulogenesis of endothelial cells by relaxation of the coupling extracellular matrix-cytoskeleton. Cardiovasc. Res. 49, 647–658.

Destaing, O., Saltel, F., Geminard, J.C., Jurdic, P., Bard, F., 2003. Podosomes display actin turnover and dynamic self-organization in osteoclasts expressing actin-green fluorescent protein. Mol. Biol. Cell 14, 407–416.

Digman, M.A., Wiseman, P.W., Choi, C., Horwitz, A.R., Gratton, E., 2009. Stoichiometry of molecular complexes at adhesions in living cells. Proc. Natl. Acad. Sci. USA 106, 2170–2175.

Discher, D.E., Janmey, P., Wang, Y.L., 2005. Tissue cells feel and respond to the stiffness of their substrate. Science 310, 1139–1143.

Dourdin, N., Bhatt, A.K., Dutt, P., Greer, P.A., Arthur, J.S., Elce, J.S., et al., 2001. Reduced cell migration and disruption of the actin cytoskeleton in calpain-deficient embryonic fibroblasts. J. Biol. Chem. 276, 48382–48388.

Dovas, A., Yoneda, A., Couchman, J.R., 2006. PKCbeta-dependent activation of RhoA by syndecan-4 during focal adhesion formation. J. Cell Sci. 119, 2837–2846.

Dubash, A.D., Wennerberg, K., Garcia-Mata, R., Menold, M.M., Arthur, W.T., Burridge, K., 2007. A novel role for Lsc/p115 RhoGEF and LARG in regulating RhoA activity downstream of adhesion to fibronectin. J. Cell Sci. 120, 3989–3998.

Echtermeyer, F., Baciu, P.C., Saoncella, S., Ge, Y., Goetinck, P.F., 1999. Syndecan-4 core protein is sufficient for the assembly of focal adhesions and actin stress fibers. J. Cell Sci. 112 (Pt. 20), 3433–3441.

Echtermeyer, F., Streit, M., Wilcox-Adelman, S., Saoncella, S., Denhez, F., Detmar, M., et al., 2001. Delayed wound repair and impaired angiogenesis in mice lacking syndecan-4. J. Clin. Invest. 107, R9–R14.

Engler, A., Bacakova, L., Newman, C., Hategan, A., Griffin, M., Discher, D., 2004. Substrate compliance versus ligand density in cell on gel responses. Biophys. J. 86, 617–628.

Evans, E., 2001. Probing the relation between force—lifetime—and chemistry in single molecular bonds. Annu. Rev. Biophys. Biomol. Struct. 30, 105–128.

Evans, J.G., Correia, I., Krasavina, O., Watson, N., Matsudaira, P., 2003. Macrophage podosomes assemble at the leading lamella by growth and fragmentation. J. Cell Biol. 161, 697–705.

Ezratty, E.J., Partridge, M.A., Gundersen, G.G., 2005. Microtubule-induced focal adhesion disassembly is mediated by dynamin and focal adhesion kinase. Nat. Cell Biol. 7, 581–590.

Falconnet, D., Csucs, G., Grandin, H.M., Textor, M., 2006. Surface engineering approaches to micropattern surfaces for cell-based assays. Biomaterials 27, 3044–3063.

Franco, S., Perrin, B., Huttenlocher, A., 2004a. Isoform specific function of calpain 2 in regulating membrane protrusion. Exp. Cell Res. 299, 179–187.

Franco, S.J., Rodgers, M.A., Perrin, B.J., Han, J., Bennin, D.A., Critchley, D.R., et al., 2004b. Calpain-mediated proteolysis of talin regulates adhesion dynamics. Nat. Cell Biol. 6, 977–983.

Fukuhara, S., Murga, C., Zohar, M., Igishi, T., Gutkind, J.S., 1999. A novel PDZ domain containing guanine nucleotide exchange factor links heterotrimeric G proteins to Rho. J. Biol. Chem. 274, 5868–5879.

Fukuhara, S., Chikumi, H., Gutkind, J.S., 2000. Leukemia-associated Rho guanine nucleotide exchange factor (LARG) links heterotrimeric G proteins of the G(12) family to Rho. FEBS Lett. 485, 183–188.

Fukuhara, S., Chikumi, H., Gutkind, J.S., 2001. RGS-containing RhoGEFs: the missing link between transforming G proteins and Rho? Oncogene 20, 1661–1668.

Gabbiani, G., Ryan, G.B., Majne, G., 1971. Presence of modified fibroblasts in granulation tissue and their possible role in wound contraction. Experientia 27, 549–550.

Galbraith, C.G., Yamada, K.M., Sheetz, M.P., 2002. The relationship between force and focal complex development. J. Cell Biol. 159, 695–705.

Gallant, N.D., Charest, J.L., King, W.P., Garcia, A.J., 2007. Micro- and nano-patterned substrates to manipulate cell adhesion. J. Nanosci. Nanotechnol. 7, 803–807.

Garcia, A.J., 2005. Get a grip: integrins in cell-biomaterial interactions. Biomaterials 26, 7525–7529.

Gates, B.D., Xu, Q., Stewart, M., Ryan, D., Willson, C.G., Whitesides, G.M., 2005. New approaches to nanofabrication: molding, printing, and other techniques. Chem. Rev. 105, 1171–1196.

Gavazzi, I., Nermut, M.V., Marchisio, P.C., 1989. Ultrastructure and gold-immunolabelling of cell-substratum adhesions (podosomes) in RSV-transformed BHK cells. J. Cell Sci. 94 (Pt. 1), 85–99.

Geiger, B., 1979. A 130K protein from chicken gizzard: its localization at the termini of microfilament bundles in cultured chicken cells. Cell 18, 193–205.

Geiger, B., Bershadsky, A., Pankov, R., Yamada, K.M., 2001. Transmembrane crosstalk between the extracellular matrix—cytoskeleton crosstalk. Nat. Rev. Mol. Cell Biol. 2, 793–805.

Georges, P.C., Janmey, P.A., 2005. Cell type-specific response to growth on soft materials. J. Appl. Physiol. 98, 1547–1553.

Giannone, G., Sheetz, M.P., 2006. Substrate rigidity and force define form through tyrosine phosphatase and kinase pathways. Trends Cell Biol. 16, 213–223.

Giannone, G., Jiang, G., Sutton, D.H., Critchley, D.R., Sheetz, M.P., 2003. Talin1 is critical for force-dependent reinforcement of initial integrin-cytoskeleton bonds but not tyrosine kinase activation. J. Cell Biol. 163, 409–419.

Gilmore, A.P., Burridge, K., 1996. Regulation of vinculin binding to talin and actin by phosphatidyl-inositol-4-5-bisphosphate. Nature 381, 531–535.

Gimona, M., Buccione, R., 2006. Adhesions that mediate invasion. Int. J. Biochem. Cell Biol. 38, 1875–1892.

Gimona, M., Buccione, R., Courtneidge, S.A., Linder, S., 2008. Assembly and biological role of podosomes and invadopodia. Curr. Opin. Cell Biol. 20, 235–241.

Glogauer, M., Ferrier, J., 1998. A new method for application of force to cells via ferric oxide beads. Pflugers Arch. 435, 320–327.

Gringel, A., Walz, D., Rosenberger, G., Minden, A., Kutsche, K., Kopp, P., et al., 2006. PAK4 and alphaPIX determine podosome size and number in macrophages through localized actin regulation. J. Cell. Physiol. 209, 568–579.

Grinnell, F., 1994. Fibroblasts, myofibroblasts, and wound contraction. J. Cell Biol. 124, 401–404.

Hai, C.M., Hahne, P., Harrington, E.O., Gimona, M., 2002. Conventional protein kinase C mediates phorbol-dibutyrate-induced cytoskeletal remodeling in a7r5 smooth muscle cells. Exp. Cell Res. 280, 64–74.

Halliday, N.L., Tomasek, J.J., 1995. Mechanical properties of the extracellular matrix influence fibronectin fibril assembly *in vitro*. Exp. Cell Res. 217, 109–117.

Hart, M.J., Jiang, X., Kozasa, T., Roscoe, W., Singer, W.D., Gilman, A.G., et al., 1998. Direct stimulation of the guanine nucleotide exchange activity of p115 RhoGEF by Galpha13. Science 280, 2112–2114.

Hashimoto, S., Onodera, Y., Hashimoto, A., Tanaka, M., Hamaguchi, M., Yamada, A., et al., 2004. Requirement for Arf6 in breast cancer invasive activities. Proc. Natl. Acad. Sci. USA 101, 6647–6652.

Haston, W.S., Shields, J.M., Wilkinson, P.C., 1983. The orientation of fibroblasts and neutrophils on elastic substrata. Exp. Cell Res. 146, 117–126.

Heath, J.P., Dunn, G.A., 1978. Cell to substratum contacts of chick fibroblasts and their relation to the microfilament system. A correlated interference-reflexion and high-voltage electron-microscope study. J. Cell Sci. 29, 197–212.

Heath, J.P., Holifield, B.F., 1993. On the mechanisms of cortical actin flow and its role in cytoskeletal organisation of fibroblasts. Symp. Soc. Exp. Biol. 47, 35–56.

Henson, M.M., Burridge, K., Fitzpatrick, D., Jenkins, D.B., Pillsbury, H.C., Henson Jr., O.W., 1985. Immunocytochemical localization of contractile and contraction associated proteins in the spiral ligament of the cochlea. Hear. Res. 20, 207–214.

Hersel, U., Dahmen, C., Kessler, H., 2003. RGD modified polymers: biomaterials for stimulated cell adhesion and beyond. Biomaterials 24, 4385–4415.

Hill, M.M., Feng, J., Hemmings, B.A., 2002. Identification of a plasma membrane Raft-associated PKB Ser473 kinase activity that is distinct from ILK and PDK1. Curr. Biol. 12, 1251–1255.

Hodgson, L., Chan, E.W., Hahn, K.M., Yousaf, M.N., 2007. Combining surface chemistry with a FRET-based biosensor to study the dynamics of RhoA GTPase activation in cells on patterned substrates. J. Am. Chem. Soc. 129, 9264–9265.

Holinstat, M., Knezevic, N., Broman, M., Samarel, A.M., Malik, A.B., Mehta, D., 2006. Suppression of RhoA activity by focal adhesion kinase-induced activation of p190Rho-GAP: role in regulation of endothelial permeability. J. Biol. Chem. 281, 2296–2305.

Hotchin, N.A., Hall, A., 1995. The assembly of integrin adhesion complexes requires both extracellular matrix and intracellular rho/rac GTPases. J. Cell Biol. 131, 1857–1865.

Hotulainen, P., Lappalainen, P., 2006. Stress fibers are generated by two distinct actin assembly mechanisms in motile cells. J. Cell Biol. 173, 383–394.

Houseman, B.T., Mrksich, M., 1998. Efficient solid-phase synthesis of peptide-substituted alkanethiols for the preparation of substrates that support the adhesion of cells. J. Org. Chem. 63, 7552–7555.

Houseman, B.T., Mrksich, M., 2001. The microenvironment of immobilized Arg-Gly-Asp peptides is an important determinant of cell adhesion. Biomaterials 22, 943–955.

Humphries, M.J., Mostafavi-Pour, Z., Morgan, M.R., Deakin, N.O., Messent, A.J., Bass, M.D., 2005. Integrin-syndecan cooperation governs the assembly of signalling complexes during cell spreading. Novartis Found. Symp. 269, 178–188; discussion 188–192, 223–230.

Humphries, J.D., Byron, A., Humphries, M.J., 2006. Integrin ligands at a glance. J. Cell Sci. 119, 3901–3903.

Humphries, J.D., Wang, P., Streuli, C., Geiger, B., Humphries, M.J., Ballestrem, C., 2007. Vinculin controls focal adhesion formation by direct interactions with talin and actin. J. Cell Biol. 179, 1043–1057.

Huttenlocher, A., Ginsberg, M.H., Horwitz, A.F., 1996. Modulation of cell migration by integrin-mediated cytoskeletal linkages and ligand-binding affinity. J. Cell Biol. 134, 1551–1562.

Huttenlocher, A., Palecek, S.P., Lu, Q., Zhang, W., Mellgren, R.L., Lauffenburger, D.A., et al., 1997. Regulation of cell migration by the calcium-dependent protease calpain. J. Biol. Chem. 272, 32719–32722.

Hynes, R.O., 1992. Integrins: versatility, modulation, and signaling in cell adhesion. Cell 69, 11–25.

Hynes, R.O., 2002. Integrins: bidirectional, allosteric signaling machines. Cell 110, 673–687.

Hynes, R.O., Destree, A.T., 1978. Relationships between fibronectin (LETS protein) and actin. Cell 15, 875–886.

Iba, K., Albrechtsen, R., Gilpin, B., Frohlich, C., Loechel, F., Zolkiewska, A., et al., 2000. The cysteine-rich domain of human ADAM 12 supports cell adhesion through syndecans and triggers signaling events that lead to beta1 integrin-dependent cell spreading. J. Cell Biol. 149, 1143–1156.

Ilic, D., Furuta, Y., Kanazawa, S., Takeda, N., Sobue, K., Nakatsuji, N., et al., 1995. Reduced cell motility and enhanced focal adhesion contact formation in cells from FAK-deficient mice. Nature 377, 539–544.

Ingber, D.E., 1997. Tensegrity: the architectural basis of cellular mechanotransduction. Annu. Rev. Physiol. 59, 575–599.

Ingber, D.E., 2006. Cellular mechanotransduction: putting all the pieces together again. FASEB J. 20, 811–827.

Ishiguro, K., Kadomatsu, K., Kojima, T., Muramatsu, H., Tsuzuki, S., Nakamura, E., et al., 2000. Syndecan-4 deficiency impairs focal adhesion formation only under restricted conditions. J. Biol. Chem. 275, 5249–5252.

Iwanicki, M.P., Vomastek, T., Tilghman, R.W., Martin, K.H., Banerjee, J., Wedegaertner, P.B., et al., 2008. FAK, PDZ-RhoGEF and ROCKII cooperate to regulate adhesion movement and trailing-edge retraction in fibroblasts. J. Cell Sci. 121, 895–905.

Izzard, C.S., 1988. A precursor of the focal contact in cultured fibroblasts. Cell Motil. Cytoskeleton 10, 137–142.

Izzard, S.L., Izzard, C.S., 1987. Actin-associated proteins related to focal and close cell-substrate contacts in murine fibroblasts. Exp. Cell Res. 170, 214–227.

Izzard, C.S., Lochner, L.R., 1976. Cell-to-substrate contacts in living fibroblasts: an interference reflexion study with an evaluation of the technique. J. Cell Sci. 21, 129–159.

Izzard, C.S., Radinsky, R., Culp, L.A., 1986. Substratum contacts and cytoskeletal reorganization of BALB/c 3T3 cells on a cell-binding fragment and heparin-binding fragments of plasma fibronectin. Exp. Cell Res. 165, 320–336.

Jamieson, J.S., Deakin, N.O., Machida, K., Mayer, B.J., Turner, C.E., 2009. Paxillin-PKL-Vav2 interactions coordinate adhesion-dependent Rho GTPase signaling. J. Cell Biol. (in press).

Janiak, A., Zemskov, E.A., Belkin, A.M., 2006. Cell surface transglutaminase promotes RhoA activation via integrin clustering and suppression of the Src-p190RhoGAP signaling pathway. Mol. Biol. Cell 17, 1606–1619.

Jiang, G., Giannone, G., Critchley, D.R., Fukumoto, E., Sheetz, M.P., 2003. Two-pico-newton slip bond between fibronectin and the cytoskeleton depends on talin. Nature 424, 334–337.

Jockusch, B.M., Bubeck, P., Giehl, K., Kroemker, M., Moschner, J., Rothkegel, M., et al., 1995. The molecular architecture of focal adhesions. Annu. Rev. Cell Dev. Biol. 11, 379–416.

Johnson, R.P., Craig, S.W., 2000. Actin activates a cryptic dimerization potential of the vinculin tail domain. J. Biol. Chem. 275, 95–105.

Johnson, C.P., Gaetani, M., Ortiz, V., Bhasin, N., Harper, S., Gallagher, P.G., et al., 2007. Pathogenic proline mutation in the linker between spectrin repeats: disease caused by spectrin unfolding. Blood 109, 3538–3543.

Jurdic, P., Saltel, F., Chabadel, A., Destaing, O., 2006. Podosome and sealing zone: specificity of the osteoclast model. Eur. J. Cell Biol. 85, 195–202.

Kato, M., Mrksich, M., 2004. Using model substrates to study the dependence of focal adhesion formation on the affinity of integrin-ligand complexes. Biochemistry 43, 2699–2707.

Katsumi, A., Milanini, J., Kiosses, W.B., del Pozo, M.A., Kaunas, R., Chien, S., et al., 2002. Effects of cell tension on the small GTPase Rac. J. Cell Biol. 158, 153–164.

Katsumi, A., Orr, A.W., Tzima, E., Schwartz, M.A., 2004. Integrins in mechanotransduction. J. Biol. Chem. 279, 12001–12004.

Katsumi, A., Naoe, T., Matsushita, T., Kaibuchi, K., Schwartz, M.A., 2005. Integrin activation and matrix binding mediate cellular responses to mechanical stretch. J. Biol. Chem. 280, 16546–16549.

Katz, B.Z., Zamir, E., Bershadsky, A., Kam, Z., Yamada, K.M., Geiger, B., 2000. Physical state of the extracellular matrix regulates the structure and molecular composition of cell-matrix adhesions. Mol. Biol. Cell 11, 1047–1060.

Kaverina, I., Krylyshkina, O., Small, J.V., 1999. Microtubule targeting of substrate contacts promotes their relaxation and dissociation. J. Cell Biol. 146, 1033–1044.

Kim, T.Y., Vigil, D., Der, C.J., Juliano, R.L., 2009. Role of DLC-1, a tumor suppressor protein with RhoGAP activity, in regulation of the cytoskeleton and cell motility. Cancer Metastasis Rev. 28, 77–83.

Kozma, R., Ahmed, S., Best, A., Lim, L., 1995. The Ras-related protein Cdc42Hs and bradykinin promote formation of peripheral actin microspikes and filopodia in Swiss 3T3 fibroblasts. Mol. Cell Biol. 15, 1942–1952.

Kulkarni, S.V., Gish, G., van der Geer, P., Henkemeyer, M., Pawson, T., 2000. Role of p120 Ras-GAP in directed cell movement. J. Cell Biol. 149, 457–470.

Kumagai, H., Tajima, M., Ueno, Y., Giga-Hama, Y., Ohba, M., 1991. Effect of cyclic RGD peptide on cell adhesion and tumor metastasis. Biochem. Biophys. Res. Commun. 177, 74–82.

Kuo, S.C., Sheetz, M.P., 1992. Optical tweezers in cell biology. Trends Cell Biol. 2, 116–118.

Kusano, Y., Oguri, K., Nagayasu, Y., Munesue, S., Ishihara, M., Saiki, I., et al., 2000. Participation of syndecan 2 in the induction of stress fiber formation in cooperation with integrin alpha5beta1: structural characteristics of heparan sulfate chains with avidity to COOH-terminal heparin-binding domain of fibronectin. Exp. Cell Res. 256, 434–444.

Lazarides, E., Burridge, K., 1975. Alpha-actinin: immunofluorescent localization of a muscle structural protein in nonmuscle cells. Cell 6, 289–298.

Lazzari, M., Rodriguez-Abreu, C., Rivas, J., Lopez-Quintela, M.A., 2006. Self-assembly: a minimalist route to the fabrication of nanomaterials. J. Nanosci. Nanotechnol. 6, 892–905.

Lee, S.E., Kamm, R.D., Mofrad, M.R., 2007. Force-induced activation of talin and its possible role in focal adhesion mechanotransduction. J. Biomech. 40, 2096–2106.

Lehnert, D., Wehrle-Haller, B., David, C., Weiland, U., Ballestrem, C., Imhof, B.A., et al., 2004. Cell behaviour on micropatterned substrata: limits of extracellular matrix geometry for spreading and adhesion. J. Cell Sci. 117, 41–52.

Lehto, V.P., Hovi, T., Vartio, T., Badley, R.A., Virtanen, I., 1982. Reorganization of cytoskeletal and contractile elements during transition of human monocytes into adherent macrophages. Lab. Invest. 47, 391–399.

Levesque, M.J., Nerem, R.M., 1985. The elongation and orientation of cultured endothelial cells in response to shear stress. J. Biomech. Eng. 107, 341–347.

Liao, Y.C., Si, L., deVere White, R.W., Lo, S.H., 2007. The phosphotyrosine-independent interaction of DLC-1 and the SH2 domain of cten regulates focal adhesion localization and growth suppression activity of DLC-1. J. Cell Biol. 176, 43–49.

Lieb, E., Hacker, M., Tessmar, J., Kunz-Schughart, L.A., Fiedler, J., Dahmen, C., et al., 2005. Mediating specific cell adhesion to low-adhesive diblock copolymers by instant modification with cyclic RGD peptides. Biomaterials 26, 2333–2341.

Lim, S.T., Longley, R.L., Couchman, J.R., Woods, A., 2003. Direct binding of syndecan-4 cytoplasmic domain to the catalytic domain of protein kinase C alpha (PKC alpha) increases focal adhesion localization of PKC alpha. J. Biol. Chem. 278, 13795–13802.

Lim, Y., Lim, S.T., Tomar, A., Gardel, M., Bernard-Trifilo, J.A., Chen, X.L., et al., 2008. PyK2 and FAK connections to p190Rho guanine nucleotide exchange factor regulate RhoA activity, focal adhesion formation, and cell motility. J. Cell Biol. 180, 187–203.

Linder, S., 2007. The matrix corroded: podosomes and invadopodia in extracellular matrix degradation. Trends Cell Biol. 17, 107–117.

Linder, S., Aepfelbacher, M., 2003. Podosomes: adhesion hot-spots of invasive cells. Trends Cell Biol. 13, 376–385.

Linder, S., Nelson, D., Weiss, M., Aepfelbacher, M., 1999. Wiskott-Aldrich syndrome protein regulates podosomes in primary human macrophages. Proc. Natl. Acad. Sci. USA 96, 9648–9653.

Linder, S., Higgs, H., Hufner, K., Schwarz, K., Pannicke, U., Aepfelbacher, M., 2000. The polarization defect of Wiskott-Aldrich syndrome macrophages is linked to dislocalization of the Arp2/3 complex. J. Immunol. 165, 221–225.

Ling, K., Doughman, R.L., Iyer, V.V., Firestone, A.J., Bairstow, S.F., Mosher, D.F., et al., 2003. Tyrosine phosphorylation of type Igamma phosphatidylinositol phosphate kinase by Src regulates an integrin-talin switch. J. Cell Biol. 163, 1339–1349.

Liu, M., Horowitz, A., 2006. A PDZ-binding motif as a critical determinant of Rho guanine exchange factor function and cell phenotype. Mol. Biol. Cell 17, 1880–1887.

Liu, B.P., Chrzanowska-Wodnicka, M., Burridge, K., 1998. Microtubule depolymerization induces stress fibers, focal adhesions, and DNA synthesis via the GTP-binding protein Rho. Cell Adhes. Commun. 5, 249–255.

Liu, W.F., Nelson, C.M., Tan, J.L., Chen, C.S., 2007. Cadherins, RhoA, and Rac1 are differentially required for stretch-mediated proliferation in endothelial versus smooth muscle cells. Circ. Res. 101, e44–e52.

Lo, S., Lo, T., 2002. Cten, a COOH-terminal tensin-like protein with prostate restricted expression, is down-regulated in prostate cancer. Cancer Res. 62, 4217–4221.

Lo, S.H., Janmey, P.A., Hartwig, J.H., Chen, L.B., 1994. Interactions of tensin with actin and identification of its three distinct actin-binding domains. J. Cell Biol. 125, 1067–1075.

Lo, S.H., Yu, Q.C., Degenstein, L., Chen, L.B., Fuchs, E., 1997. Progressive kidney degeneration in mice lacking tensin. J. Cell Biol. 136, 1349–1361.

Lo, C.M., Wang, H.B., Dembo, M., Wang, Y.L., 2000. Cell movement is guided by the rigidity of the substrate. Biophys. J. 79, 144–152.

Lock, J.G., Wehrle-Haller, B., Stromblad, S., 2008. Cell–matrix adhesion complexes: master control machinery of cell migration. Semin. Cancer Biol. 18, 65–76.

Luxenburg, C., Parsons, J.T., Addadi, L., Geiger, B., 2006. Involvement of the Src-cortactin pathway in podosome formation and turnover during polarization of cultured osteoclasts. J. Cell Sci. 119, 4878–4888.

Lynch, D.K., Ellis, C.A., Edwards, P.A., Hiles, I.D., 1999. Integrin-linked kinase regulates phosphorylation of serine 473 of protein kinase B by an indirect mechanism. Oncogene 18, 8024–8032.

MacKenna, D.A., Dolfi, F., Vuori, K., Ruoslahti, E., 1998. Extracellular signal-regulated kinase and c-Jun NH2-terminal kinase activation by mechanical stretch is integrin-dependent and matrix-specific in rat cardiac fibroblasts. J. Clin. Invest. 101, 301–310.

Mackinnon, A.C., Qadota, H., Norman, K.R., Moerman, D.G., Williams, B.D., 2002. C. elegans PAT-4/ILK functions as an adaptor protein within integrin adhesion complexes. Curr. Biol. 12, 787–797.

Mahalingam, Y., Gallagher, J.T., Couchman, J.R., 2007. Cellular adhesion responses to the heparin-binding (HepII) domain of fibronectin require heparan sulfate with specific properties. J. Biol. Chem. 282, 3221–3230.

Maheshwari, G., Brown, G., Lauffenburger, D.A., Wells, A., Griffith, L.G., 2000. Cell adhesion and motility depend on nanoscale RGD clustering. J. Cell Sci. 113 (Pt. 10), 1677–1686.

Majumdar, M., Seasholtz, T.M., Buckmaster, C., Toksoz, D., Brown, J.H., 1999. A rho exchange factor mediates thrombin and Galpha(12)-induced cytoskeletal responses. J. Biol. Chem. 274, 26815–26821.

Marchisio, P.C., Cirillo, D., Naldini, L., Primavera, M.V., Teti, A., Zambonin-Zallone, A., 1984. Cell-substratum interaction of cultured avian osteoclasts is mediated by specific adhesion structures. J. Cell Biol. 99, 1696–1705.

Marchisio, P.C., D'Urso, N., Comoglio, P.M., Giancotti, F.G., Tarone, G., 1988. Vanadate-treated baby hamster kidney fibroblasts show cytoskeleton and adhesion patterns similar to their Rous sarcoma virus-transformed counterparts. J. Cell. Biochem. 37, 151–159.

Masiero, L., Lapidos, K.A., Ambudkar, I., Kohn, E.C., 1999. Regulation of the RhoA pathway in human endothelial cell spreading on type IV collagen: role of calcium influx. J. Cell Sci. 112 (Pt. 19), 3205–3213.

Massia, S.P., Hubbell, J.A., 1991. An RGD spacing of 440 nm is sufficient for integrin alpha V beta 3-mediated fibroblast spreading and 140 nm for focal contact and stress fiber formation. J. Cell Biol. 114, 1089–1100.

McClary, K.B., Grainger, D.W., 1999. RhoA-induced changes in fibroblasts cultured on organic monolayers. Biomaterials 20, 2435–2446.

McCleverty, C.J., Lin, D.C., Liddington, R.C., 2007. Structure of the PTB domain of tensin1 and a model for its recruitment to fibrillar adhesions. Protein Sci. 16, 1223–1229.

McQuade, K.J., Beauvais, D.M., Burbach, B.J., Rapraeger, A.C., 2006. Syndecan-1 regulates alphavbeta5 integrin activity in B82L fibroblasts. J. Cell Sci. 119, 2445–2456.

Meller, N., Merlot, S., Guda, C., 2005. CZH proteins: a new family of Rho-GEFs. J. Cell Sci. 118, 4937–4946.

Merkel, R., Nassoy, P., Leung, A., Ritchie, K., Evans, E., 1999. Energy landscapes of receptor-ligand bonds explored with dynamic force spectroscopy. Nature 397, 50–53.

Miao, H., Li, S., Hu, Y.L., Yuan, S., Zhao, Y., Chen, B.P., et al., 2002. Differential regulation of Rho GTPases by beta1 and beta3 integrins: the role of an extracellular domain of integrin in intracellular signaling. J. Cell Sci. 115, 2199–2206.

Mizutani, K., Miki, H., He, H., Maruta, H., Takenawa, T., 2002. Essential role of neural Wiskott-Aldrich syndrome protein in podosome formation and degradation of extracellular matrix in src-transformed fibroblasts. Cancer Res. 62, 669–674.

Mochitate, K., Pawelek, P., Grinnell, F., 1991. Stress relaxation of contracted collagen gels: disruption of actin filament bundles, release of cell surface fibronectin, and down-regulation of DNA and protein synthesis. Exp. Cell Res. 193, 198–207.

Moon, S.Y., Zheng, Y., 2003. Rho GTPase-activating proteins in cell regulation. Trends Cell Biol. 13, 13–22.

Moreau, V., Tatin, F., Varon, C., Genot, E., 2003. Actin can reorganize into podosomes in aortic endothelial cells, a process controlled by Cdc42 and RhoA. Mol. Cell Biol. 23, 6809–6822.

Morgan, M.R., Humphries, M.J., Bass, M.D., 2007. Synergistic control of cell adhesion by integrins and syndecans. Nat. Rev. Mol. Cell Biol. 8, 957–969.

Mostafavi-Pour, Z., Askari, J.A., Whittard, J.D., Humphries, M.J., 2001. Identification of a novel heparin-binding site in the alternatively spliced IIICS region of fibronectin: roles of integrins and proteoglycans in cell adhesion to fibronectin splice variants. Matrix Biol. 20, 63–73.

Mrksich, M., Whitesides, G.M., 1996. Using self-assembled monolayers to understand the interactions of man-made surfaces with proteins and cells. Annu. Rev. Biophys. Biomol. Struct. 25, 55–78.

Munevar, S., Wang, Y.L., Dembo, M., 2004. Regulation of mechanical interactions between fibroblasts and the substratum by stretch–activated Ca^{2+} entry. J. Cell Sci. 117, 85–92.

Narumiya, S., Ishizaki, T., Uehata, M., 2000. Use and properties of ROCK-specific inhibitor Y-27632. Methods Enzymol. 325, 273–284.

Nayal, A., Webb, D.J., Horwitz, A.F., 2004. Talin: an emerging focal point of adhesion dynamics. Curr. Opin. Cell Biol. 16, 94–98.

Nobes, C.D., Hall, A., 1995. Rho, rac, and cdc42 GTPases regulate the assembly of multimolecular focal complexes associated with actin stress fibers, lamellipodia, and filopodia. Cell 81, 53–62.

Oh, E.S., Woods, A., Couchman, J.R., 1997a. Multimerization of the cytoplasmic domain of syndecan-4 is required for its ability to activate protein kinase C. J. Biol. Chem. 272, 11805–11811.

Oh, E.S., Woods, A., Couchman, J.R., 1997b. Syndecan-4 proteoglycan regulates the distribution and activity of protein kinase C. J. Biol. Chem. 272, 8133–8136.

Oikawa, T., Itoh, T., Takenawa, T., 2008. Sequential signals toward podosome formation in NIH-src cells. J. Cell Biol. 182, 157–169.

Olski, T.M., Noegel, A.A., Korenbaum, E., 2001. Parvin, a 42 kDa focal adhesion protein, related to the alpha-actinin superfamily. J. Cell Sci. 114, 525–538.

Ory, S., Munari-Silem, Y., Fort, P., Jurdic, P., 2000. Rho and Rac exert antagonistic functions on spreading of macrophage-derived multinucleated cells and are not required for actin fiber formation. J. Cell Sci. 113 (Pt. 7), 1177–1188.

Osiak, A.E., Zenner, G., Linder, S., 2005. Subconfluent endothelial cells form podosomes downstream of cytokine and RhoGTPase signaling. Exp. Cell Res. 307, 342–353.

Palecek, S.P., Huttenlocher, A., Horwitz, A.F., Lauffenburger, D.A., 1998. Physical and biochemical regulation of integrin release during rear detachment of migrating cells. J. Cell Sci. 111 (Pt. 7), 929–940.

Pankov, R., Yamada, K.M., 2002. Fibronectin at a glance. J. Cell Sci. 115, 3861–3863.

Pankov, R., Cukierman, E., Katz, B.Z., Matsumoto, K., Lin, D.C., Lin, S., et al., 2000. Integrin dynamics and matrix assembly: tensin-dependent translocation of alpha(5)beta(1) integrins promotes early fibronectin fibrillogenesis. J. Cell Biol. 148, 1075–1090.

Paszek, M.J., Zahir, N., Johnson, K.R., Lakins, J.N., Rozenberg, G.I., Gefen, A., et al., 2005. Tensional homeostasis and the malignant phenotype. Cancer Cell 8, 241–254.

Paterson, H.F., Self, A.J., Garrett, M.D., Just, I., Aktories, K., Hall, A., 1990. Microinjection of recombinant p21rho induces rapid changes in cell morphology. J. Cell Biol. 111, 1001–1007.

Pelham Jr., R.J., Wang, Y., 1997. Cell locomotion and focal adhesions are regulated by substrate flexibility. Proc. Natl. Acad. Sci. USA 94, 13661–13665.

Pelham Jr., R.J., Wang, Y.L., 1998. Cell locomotion and focal adhesions are regulated by the mechanical properties of the substrate. Biol. Bull. 194, 348–349 discussion 349–350.

Pellegrin, S., Mellor, H., 2007. Actin stress fibres. J. Cell Sci. 120, 3491–3499.

Pertz, O., Hodgson, L., Klemke, R.L., Hahn, K.M., 2006. Spatiotemporal dynamics of RhoA activity in migrating cells. Nature 440, 1069–1072.

Petrie, T.A., Capadona, J.R., Reyes, C.D., Garcia, A.J., 2006. Integrin specificity and enhanced cellular activities associated with surfaces presenting a recombinant fibronectin fragment compared to RGD supports. Biomaterials 27, 5459–5470.

Pfaff, M., Jurdic, P., 2001. Podosomes in osteoclast-like cells: structural analysis and cooperative roles of paxillin, proline-rich tyrosine kinase 2 (Pyk2) and integrin alphaVbeta3. J. Cell Sci. 114, 2775–2786.

Pierschbacher, M.D., Ruoslahti, E., 1984. Cell attachment activity of fibronectin can be duplicated by small synthetic fragments of the molecule. Nature 309, 30–33.

Powelka, A.M., Sun, J., Li, J., Gao, M., Shaw, L.M., Sonnenberg, A., et al., 2004. Stimulation-dependent recycling of integrin beta1 regulated by ARF6 and Rab11. Traffic 5, 20–36.

Puklin-Faucher, E., Sheetz, M.P., 2009. The mechanical integrin cycle. J. Cell Sci. 122, 179–186.

Puklin-Faucher, E., Gao, M., Schulten, K., Vogel, V., 2006. How the headpiece hinge angle is opened: new insights into the dynamics of integrin activation. J. Cell Biol. 175, 349–360.

Qian, X., Li, G., Asmussen, H.K., Asnaghi, L., Vass, W.C., Braverman, R., et al., 2007. Oncogenic inhibition by a deleted in liver cancer gene requires cooperation between tensin binding and Rho-specific GTPase-activating protein activities. Proc. Natl. Acad. Sci. USA 104, 9012–9017.

Ren, X.D., Kiosses, W.B., Schwartz, M.A., 1999. Regulation of the small GTP-binding protein Rho by cell adhesion and the cytoskeleton. EMBO J. 18, 578–585.

Ren, X.D., Kiosses, W.B., Sieg, D.J., Otey, C.A., Schlaepfer, D.D., Schwartz, M.A., 2000. Focal adhesion kinase suppresses Rho activity to promote focal adhesion turnover. J. Cell Sci. 113 (Pt. 20), 3673–3678.

Ridley, A.J., Hall, A., 1992. The small GTP-binding protein rho regulates the assembly of focal adhesions and actin stress fibers in response to growth factors. Cell 70, 389–399.

Riveline, D., Zamir, E., Balaban, N.Q., Schwarz, U.S., Ishizaki, T., Narumiya, S., et al., 2001. Focal contacts as mechanosensors: externally applied local mechanical force induces growth of focal contacts by an mDia1-dependent and ROCK-independent mechanism. J. Cell Biol. 153, 1175–1186.

Romer, L.H., Birukov, K.G., Garcia, J.G., 2006. Focal adhesions: paradigm for a signaling nexus. Circ. Res. 98, 606–616.

Rosenberger, G., Kutsche, K., 2006. AlphaPIX and betaPIX and their role in focal adhesion formation. Eur. J. Cell Biol. 85, 265–274.

Rossman, K.L., Der, C.J., Sondek, J., 2005. GEF means go: turning on RHO GTPases with guanine nucleotide-exchange factors. Nat. Rev. Mol. Cell Biol. 6, 167–180.

Rubin, E.J., Gill, D.M., Boquet, P., Popoff, M.R., 1988. Functional modification of a 21-kilodalton G protein when ADP-ribosylated by exoenzyme C3 of Clostridium botulinum. Mol. Cell Biol. 8, 418–426.

Sai, X., Naruse, K., Sokabe, M., 1999. Activation of pp60(src) is critical for stretch-induced orienting response in fibroblasts. J. Cell Sci. 112 (Pt. 9), 1365–1373.

Sakai, T., Li, S., Docheva, D., Grashoff, C., Sakai, K., Kostka, G., et al., 2003. Integrin-linked kinase (ILK) is required for polarizing the epiblast, cell adhesion, and controlling actin accumulation. Genes Dev. 17, 926–940.

Samson, T., Will, C., Knoblauch, A., Sharek, L., von der Mark, K., Burridge, K., et al., 2007. Def-6, a guanine nucleotide exchange factor for Rac1, interacts with the skeletal muscle integrin chain alpha7A and influences myoblast differentiation. J. Biol. Chem. 282, 15730–15742.

Saoncella, S., Echtermeyer, F., Denhez, F., Nowlen, J.K., Mosher, D.F., Robinson, S.D., et al., 1999. Syndecan-4 signals cooperatively with integrins in a Rho-dependent manner in the assembly of focal adhesions and actin stress fibers. Proc. Natl. Acad. Sci. USA 96, 2805–2810.

Saoncella, S., Calautti, E., Neveu, W., Goetinck, P.F., 2004. Syndecan-4 regulates ATF-2 transcriptional activity in a Rac1-dependent manner. J. Biol. Chem. 279, 47172–47176.

Sawada, Y., Nakamura, K., Doi, K., Takeda, K., Tobiume, K., Saitoh, M., et al., 2001. Rap1 is involved in cell stretching modulation of p38 but not ERK or JNK MAP kinase. J. Cell Sci. 114, 1221–1227.

Sawada, Y., Tamada, M., Dubin-Thaler, B.J., Cherniavskaya, O., Sakai, R., Tanaka, S., et al., 2006. Force sensing by mechanical extension of the Src family kinase substrate p130Cas. Cell 127, 1015–1026.

Schramp, M., Ying, O., Kim, T.Y., Martin, G.S., 2008. ERK5 promotes Src-induced podosome formation by limiting Rho activation. J. Cell Biol. 181, 1195–1210.

Schwartz, M.A., DeSimone, D.W., 2008. Cell adhesion receptors in mechanotransduction. Curr. Opin. Cell Biol. 20, 551–556.

Schwartz, M.A., Schaller, M.D., Ginsberg, M.H., 1995. Integrins: emerging paradigms of signal transduction. Annu. Rev. Cell Dev. Biol. 11, 549–599.

Sechi, A.S., Wehland, J., 2000. The actin cytoskeleton and plasma membrane connection: PtdIns(4, 5)P(2) influences cytoskeletal protein activity at the plasma membrane. J. Cell Sci. 113 (Pt. 21), 3685–3695.

Shikata, Y., Rios, A., Kawkitinarong, K., DePaola, N., Garcia, J.G., Birukov, K.G., 2005. Differential effects of shear stress and cyclic stretch on focal adhesion remodeling, site-specific FAK phosphorylation, and small GTPases in human lung endothelial cells. Exp. Cell Res. 304, 40–49.

Shin, S.K., Yoon, H.J., Jung, Y.J., Park, J.W., 2006. Nanoscale controlled self-assembled monolayers and quantum dots. Curr. Opin. Chem. Biol. 10, 423–429.

Sieg, D.J., Hauck, C.R., Schlaepfer, D.D., 1999. Required role of focal adhesion kinase (FAK) for integrin-stimulated cell migration. J. Cell Sci. 112 (Pt. 16), 2677–2691.

Simons, M., Horowitz, A., 2001. Syndecan-4-mediated signalling. Cell. Signal. 13, 855–862.

Singer, I.I., 1979. The fibronexus: a transmembrane association of fibronectin-containing fibers and bundles of 5 nm microfilaments in hamster and human fibroblasts. Cell 16, 675–685.

Singer, I.I, Paradiso, P.R., 1981. A transmembrane relationship between fibronectin and vinculin (130 kd protein): serum modulation in normal and transformed hamster fibroblasts. Cell 24, 481–492.

Skalli, O., Ropraz, P., Trzeciak, A., Benzonana, G., Gillessen, D., Gabbiani, G., 1986. A monoclonal antibody against alpha-smooth muscle actin: a new probe for smooth muscle differentiation. J. Cell Biol. 103, 2787–2796.

Small, J.V., Rottner, R., Kaverina, I., Anderson, K.I., 1998. Assembling an actin cyto-skeleton for cell attachment and movement. Biochim. Biophys. Acta 1404, 271–281.

Soranno, T., Bell, E., 1982. Cytostructural dynamics of spreading and translocating cells. J. Cell Biol. 95, 127–136.

Spatz, J.P., Geiger, B., 2007. Molecular engineering of cellular environments: cell adhesion to nano-digital surfaces. Methods Cell Biol. 83, 89–111.

Spinardi, L., Rietdorf, J., Nitsch, L., Bono, M., Tacchetti, C., Way, M., et al., 2004. A dynamic podosome-like structure of epithelial cells. Exp. Cell Res. 295, 360–374.

Stanchi, F., Bordoy, R., Kudlacek, O., Braun, A., Pfeifer, A., Moser, M., et al., 2005. Consequences of loss of PINCH2 expression in mice. J. Cell Sci. 118, 5899–5910.

Steimle, P.A., Hoffert, J.D., Adey, N.B., Craig, S.W., 1999. Polyphosphoinositides inhibit the interaction of vinculin with actin filaments. J. Biol. Chem. 274, 18414–18420.

Stofega, M.R., Sanders, L.C., Gardiner, E.M., Bokoch, G.M., 2004. Constitutive p21-activated kinase (PAK) activation in breast cancer cells as a result of mislocalization of PAK to focal adhesions. Mol. Biol. Cell 15, 2965–2977.

Suzuki, N., Nakamura, S., Mano, H., Kozasa, T., 2003. Galpha 12 activates Rho GTPase through tyrosine-phosphorylated leukemia-associated RhoGEF. Proc. Natl. Acad. Sci. USA 100, 733–738.

Tadokoro, S., Shattil, S.J., Eto, K., Tai, V., Liddington, R.C., de Pereda, J.M., et al., 2003. Talin binding to integrin beta tails: a final common step in integrin activation. Science 302, 103–106.

Tague, S.E., Muralidharan, V., D'Souza-Schorey, C., 2004. ADP-ribosylation factor 6 regulates tumor cell invasion through the activation of the MEK/ERK signaling pathway. Proc. Natl. Acad. Sci. USA 101, 9671–9676.

Takagi, J., Petre, B.M., Walz, T., Springer, T.A., 2002. Global conformational rearrangements in integrin extracellular domains in outside-in and inside-out signaling. Cell 110, 599–611.

Tamada, M., Sheetz, M.P., Sawada, Y., 2004. Activation of a signaling cascade by cytoskeleton stretch. Dev. Cell 7, 709–718.

Tamariz, E., Grinnell, F., 2002. Modulation of fibroblast morphology and adhesion during collagen matrix remodeling. Mol. Biol. Cell 13, 3915–3929.

Tarone, G., Cirillo, D., Giancotti, F.G., Comoglio, P.M., Marchisio, P.C., 1985. Rous sarcoma virus-transformed fibroblasts adhere primarily at discrete protrusions of the ventral membrane called podosomes. Exp. Cell Res. 159, 141–157.

Tatin, F., Varon, C., Genot, E., Moreau, V., 2006. A signalling cascade involving PKC, Src and Cdc42 regulates podosome assembly in cultured endothelial cells in response to phorbol ester. J. Cell Sci. 119, 769–781.

Tehrani, S., Faccio, R., Chandrasekar, I., Ross, F.P., Cooper, J.A., 2006. Cortactin has an essential and specific role in osteoclast actin assembly. Mol. Biol. Cell 17, 2882–2895.

Terukina, S., Aoki, N., 1985. Fibronectin and deposits of fibrinolytic components in glomerular capillary walls. Am. J. Nephrol. 5, 248–254.

Thodeti, C.K., Albrechtsen, R., Grauslund, M., Asmar, M., Larsson, C., Takada, Y., et al., 2003. ADAM12/syndecan-4 signaling promotes beta 1 integrin-dependent cell spreading through protein kinase Calpha and RhoA. J. Biol. Chem. 278, 9576–9584.

Thoumine, O., Kocian, P., Kottelat, A., Meister, J.J., 2000. Short-term binding of fibroblasts to fibronectin: optical tweezers experiments and probabilistic analysis. Eur. Biophys. J. 29, 398–408.

Tkachenko, E., Lutgens, E., Stan, R.V., Simons, M., 2004. Fibroblast growth factor 2 endocytosis in endothelial cells proceed via syndecan-4-dependent activation of Rac1 and a Cdc42-dependent macropinocytic pathway. J. Cell Sci. 117, 3189–3199.

Tkachenko, E., Rhodes, J.M., Simons, M., 2005. Syndecans: new kids on the signaling block. Circ. Res. 96, 488–500.

Tkachenko, E., Elfenbein, A., Tirziu, D., Simons, M., 2006. Syndecan-4 clustering induces cell migration in a PDZ-dependent manner. Circ. Res. 98, 1398–1404.

Tomasek, J.J., Schultz, R.J., Episalla, C.W., Newman, S.A., 1986. The cytoskeleton and extracellular matrix of the Dupuytren's disease ''myofibroblast'': an immunofluorescence study of a nonmuscle cell type. J. Hand Surg. Am. 11, 365–371.

Tomasek, J.J., Haaksma, C.J., Eddy, R.J., Vaughan, M.B., 1992. Fibroblast contraction occurs on release of tension in attached collagen lattices: dependency on an organized actin cytoskeleton and serum. Anat. Rec. 232, 359–368.

Tomasek, J.J., Gabbiani, G., Hinz, B., Chaponnier, C., Brown, R.A., 2002. Myofibroblasts and mechano-regulation of connective tissue remodelling. Nat. Rev. Mol. Cell Biol. 3, 349–363.

Torgler, C.N., Narasimha, M., Knox, A.L., Zervas, C.G., Vernon, M.C., Brown, N.H., 2004. Tensin stabilizes integrin adhesive contacts in *Drosophila*. Dev. Cell 6, 357–369.

Tzima, E., del Pozo, M.A., Shattil, S.J., Chien, S., Schwartz, M.A., 2001. Activation of integrins in endothelial cells by fluid shear stress mediates Rho-dependent cytoskeletal alignment. EMBO J. 20, 4639–4647.

Varon, C., Tatin, F., Moreau, V., Van Obberghen-Schilling, E., Fernandez-Sauze, S., Reuzeau, E., et al., 2006. Transforming growth factor beta induces rosettes of podosomes in primary aortic endothelial cells. Mol. Cell Biol. 26, 3582–3594.

Vinogradova, O., Velyvis, A., Velyviene, A., Hu, B., Haas, T., Plow, E., et al., 2002. A structural mechanism of integrin alpha(IIb)beta(3) ''inside-out'' activation as regulated by its cytoplasmic face. Cell 110, 587–597.

Vogel, V., Sheetz, M., 2006. Local force and geometry sensing regulate cell functions. Nat. Rev. Mol. Cell Biol. 7, 265–275.

von Wichert, G., Jiang, G., Kostic, A., De Vos, K., Sap, J., Sheetz, M.P., 2003. RPTP-alpha acts as a transducer of mechanical force on alphav/beta3-integrin-cytoskeleton linkages. J. Cell Biol. 161, 143–153.

Voss, A.K., Gruss, P., Thomas, T., 2003. The guanine nucleotide exchange factor C3G is necessary for the formation of focal adhesions and vascular maturation. Development 130, 355–367.

Vouret-Craviari, V., Boulter, E., Grall, D., Matthews, C., Van Obberghen-Schilling, E., 2004. ILK is required for the assembly of matrix-forming adhesions and capillary morphogenesis in endothelial cells. J. Cell Sci. 117, 4559–4569.

Wang, F., Nobes, C.D., Hall, A., Spiegel, S., 1997. Sphingosine 1-phosphate stimulates rho-mediated tyrosine phosphorylation of focal adhesion kinase and paxillin in Swiss 3T3 fibroblasts. Biochem. J. 324 (Pt. 2), 481–488.

Wang, Q., Liu, M., Kozasa, T., Rothstein, J.D., Sternweis, P.C., Neubig, R.R., 2004. Thrombin and lysophosphatidic acid receptors utilize distinct rhoGEFs in prostate cancer cells. J. Biol. Chem. 279, 28831–28834.

Wang, R., Clark, R.A., Mosher, D.F., Ren, X.D., 2005. Fibronectin's central cell-binding domain supports focal adhesion formation and Rho signal transduction. J. Biol. Chem. 280, 28803–28810.

Watanabe, N., Madaule, P., Reid, T., Ishizaki, T., Watanabe, G., Kakizuka, A., et al., 1997. p140mDia, a mammalian homolog of *Drosophila diaphanous*, is a target protein for Rho small GTPase and is a ligand for profilin. EMBO J. 16, 3044–3056.

Wayner, E.A., Garcia-Pardo, A., Humphries, M.J., McDonald, J.A., Carter, W.G., 1989. Identification and characterization of the T lymphocyte adhesion receptor for an alternative cell attachment domain (CS-1) in plasma fibronectin. J. Cell Biol. 109, 1321–1330.

Weaver, A.M., 2006. Invadopodia: specialized cell structures for cancer invasion. Clin. Exp. Metastasis 23, 97–105.

Webb, D.J., Brown, C.M., Horwitz, A.F., 2003. Illuminating adhesion complexes in migrating cells: moving toward a bright future. Curr. Opin. Cell Biol. 15, 614–620.

Webb, D.J., Donais, K., Whitmore, L.A., Thomas, S.M., Turner, C.E., Parsons, J.T., et al., 2004. FAK–Src signalling through paxillin, ERK and MLCK regulates adhesion disassembly. Nat. Cell Biol. 6, 154–161.

Webb, B.A., Eves, R., Crawley, S.W., Zhou, S., Cote, G.P., Mak, A.S., 2005. PAK1 induces podosome formation in A7r5 vascular smooth muscle cells in a PAK–interacting exchange factor-dependent manner. Am. J. Physiol. Cell Physiol. 289, C898–C907.

Webb, B.A., Jia, L., Eves, R., Mak, A.S., 2007. Dissecting the functional domain requirements of cortactin in invadopodia formation. Eur. J. Cell Biol. 86, 189–206.

Wennerberg, K., Der, C.J., 2004. Rho-family GTPases: it's not only Rac and Rho (and I like it). J. Cell Sci. 117, 1301–1312.

Wennerberg, K., Rossman, K.L., Der, C.J., 2005. The Ras superfamily at a glance. J. Cell Sci. 118, 843–846.

White, D.P., Caswell, P.T., Norman, J.C., 2007. alpha v beta3 and alpha5beta1 integrin recycling pathways dictate downstream Rho kinase signaling to regulate persistent cell migration. J. Cell Biol. 177, 515–525.

Whiteford, J.R., Couchman, J.R., 2006. A conserved NXIP motif is required for cell adhesion properties of the syndecan-4 ectodomain. J. Biol. Chem. 281, 32156–32163.

Whiteford, J.R., Behrends, V., Kirby, H., Kusche-Gullberg, M., Muramatsu, T., Couchman, J.R., 2007. Syndecans promote integrin-mediated adhesion of mesenchymal cells in two distinct pathways. Exp. Cell Res. 313, 3902–3913.

Whitesides, G.M., Kriebel, J.K., Love, J.C., 2005. Molecular engineering of surfaces using self-assembled monolayers. Sci. Prog. 88, 17–48.

Wilcox-Adelman, S.A., Denhez, F., Goetinck, P.F., 2002a. Syndecan-4 modulates focal adhesion kinase phosphorylation. J. Biol. Chem. 277, 32970–32977.

Wilcox-Adelman, S.A., Denhez, F., Iwabuchi, T., Saoncella, S., Calautti, E., Goetinck, P.F., 2002b. Syndecan-4: dispensable or indispensable? Glycoconj. J. 19, 305–313.

Wilson, E., Mai, Q., Sudhir, K., Weiss, R.H., Ives, H.E., 1993. Mechanical strain induces growth of vascular smooth muscle cells via autocrine action of PDGF. J. Cell Biol. 123, 741–747.

Wilson, E., Sudhir, K., Ives, H.E., 1995. Mechanical strain of rat vascular smooth muscle cells is sensed by specific extracellular matrix/integrin interactions. J. Clin. Invest. 96, 2364–2372.

Wong, A.J., Pollard, T.D., Herman, I.M., 1983. Actin filament stress fibers in vascular endothelial cells *in vivo*. Science 219, 867–869.

Woods, A., Couchman, J.R., 1988. Focal adhesions and cell-matrix interactions. Coll. Relat. Res. 8, 155–182.

Woods, A., Couchman, J.R., 1992. Protein kinase C involvement in focal adhesion formation. J. Cell Sci. 101 (Pt. 2), 277–290.

Woods, A., Couchman, J.R., 1994. Syndecan 4 heparan sulfate proteoglycan is a selectively enriched and widespread focal adhesion component. Mol. Biol. Cell 5, 183–192.

Woods, A., Couchman, J.R., 1998. Syndecans: synergistic activators of cell adhesion. Trends Cell Biol. 8, 189–192.

Woods, A., Couchman, J.R., 2001. Syndecan-4 and focal adhesion function. Curr. Opin. Cell Biol. 13, 578–583.

Woods, A., Couchman, J.R., Johansson, S., Hook, M., 1986. Adhesion and cytoskeletal organisation of fibroblasts in response to fibronectin fragments. EMBO J. 5, 665–670.

Woods, A., Longley, R.L., Tumova, S., Couchman, J.R., 2000. Syndecan-4 binding to the high affinity heparin-binding domain of fibronectin drives focal adhesion formation in fibroblasts. Arch. Biochem. Biophys. 374, 66–72.

Yamaguchi, H., Lorenz, M., Kempiak, S., Sarmiento, C., Coniglio, S., Symons, M., et al., 2005. Molecular mechanisms of invadopodium formation: the role of the N-WASP-Arp2/3 complex pathway and cofilin. J. Cell Biol. 168, 441–452.

Yamaguchi, H., Pixley, F., Condeelis, J., 2006. Invadopodia and podosomes in tumor invasion. Eur. J. Cell Biol. 85, 213–218.

Yano, Y., Geibel, J., Sumpio, B.E., 1996a. Tyrosine phosphorylation of pp 125FAK and paxillin in aortic endothelial cells induced by mechanical strain. Am. J. Physiol. 271, C635–C649.

Yano, Y., Saito, Y., Narumiya, S., Sumpio, B.E., 1996b. Involvement of rho p21 in cyclic strain-induced tyrosine phosphorylation of focal adhesion kinase (pp 125FAK), morphological changes and migration of endothelial cells. Biochem. Biophys. Res. Commun. 224, 508–515.

Yoneda, A., Ushakov, D., Multhaupt, H.A., Couchman, J.R., 2007. Fibronectin matrix assembly requires distinct contributions from Rho kinases I and -II. Mol. Biol. Cell 18, 66–75.

Zaidel-Bar, R., Cohen, M., Addadi, L., Geiger, B., 2004. Hierarchical assembly of cell-matrix adhesion complexes. Biochem. Soc. Trans. 32, 416–420.

Zaidel-Bar, R., Itzkovitz, S., Ma'ayan, A., Iyengar, R., Geiger, B., 2007a. Functional atlas of the integrin adhesome. Nat. Cell Biol. 9, 858–867.

Zaidel-Bar, R., Milo, R., Kam, Z., Geiger, B., 2007b. A paxillin tyrosine phosphorylation switch regulates the assembly and form of cell-matrix adhesions. J. Cell Sci. 120, 137–148.

Zamir, E., Geiger, B., 2001. Molecular complexity and dynamics of cell-matrix adhesions. J. Cell Sci. 114, 3583–3590.

Zamir, E., Katz, B.Z., Aota, S., Yamada, K.M., Geiger, B., Kam, Z., 1999. Molecular diversity of cell-matrix adhesions. J. Cell Sci. 112 (Pt. 11), 1655–1669.

Zamir, E., Katz, M., Posen, Y., Erez, N., Yamada, K.M., Katz, B.Z., et al., 2000. Dynamics and segregation of cell–matrix adhesions in cultured fibroblasts. Nat. Cell Biol. 2, 191–196.

Zamir, E., Geiger, B., Kam, Z., 2008. Quantitative multicolor compositional imaging resolves molecular domains in cell–matrix adhesions. PLoS ONE 3, e1901.

Zervas, C.G., Gregory, S.L., Brown, N.H., 2001. *Drosophila* integrin-linked kinase is required at sites of integrin adhesion to link the cytoskeleton to the plasma membrane. J. Cell Biol. 152, 1007–1018.

Zhai, J., Lin, H., Nie, Z., Wu, J., Canete-Soler, R., Schlaepfer, W.W., et al., 2003. Direct interaction of focal adhesion kinase with p190RhoGEF. J. Biol. Chem. 278, 24865–24873.

Zhang, D., Udagawa, N., Nakamura, I., Murakami, H., Saito, S., Yamasaki, K., et al., 1995. The small GTP-binding protein, rho p21, is involved in bone resorption by regulating cytoskeletal organization in osteoclasts. J. Cell Sci. 108 (Pt. 6), 2285–2292.

Zhong, C., Chrzanowska-Wodnicka, M., Brown, J., Shaub, A., Belkin, A.M., Burridge, K., 1998. Rho-mediated contractility exposes a cryptic site in fibronectin and induces fibronectin matrix assembly. J. Cell Biol. 141, 539–551.

Zhou, S., Webb, B.A., Eves, R., Mak, A.S., 2006. Effects of tyrosine phosphorylation of cortactin on podosome formation in A7r5 vascular smooth muscle cells. Am. J. Physiol. Cell Physiol. 290, C463–C471.

Ziegler, W.H., Liddington, R.C., Critchley, D.R., 2006. The structure and regulation of vinculin. Trends Cell Biol. 16, 453–460.

Zimerman, B., Volberg, T., Geiger, B., 2004. Early molecular events in the assembly of the focal adhesion-stress fiber complex during fibroblast spreading. Cell Motil. Cytoskeleton 58, 143–159.

Zrihan-Licht, S., Fu, Y., Settleman, J., Schinkmann, K., Shaw, L., Keydar, I., et al., 2000. RAFTK/Pyk2 tyrosine kinase mediates the association of p190 RhoGAP with RasGAP and is involved in breast cancer cell invasion. Oncogene 19, 1318–1328.

Calcineurin Signaling and the Slow Oxidative Skeletal Muscle Fiber Type

Joanne Mallinson,* Joachim Meissner,[†] and Kin-Chow Chang*

Contents

Abstract

Calcineurin, also known as protein phosphatase 2B (PP2B), is a calcium–calmodulin-dependent phosphatase. It couples intracellular calcium to dephosphorylate selected substrates resulting in diverse biological consequences

* School of Veterinary Medicine and Science, University of Nottingham, Sutton Bonington LE12 5RD, United Kingdom
† Department of Physiology, OE4220, Hannover Medical School, D–30623 Hannover, Germany

depending on cell type. In mammals, calcineurin's functions include neuronal growth, development of cardiac valves and hypertrophy, activation of lymphocytes, and the regulation of ion channels and enzymes. This chapter focuses on the key roles of calcineurin in skeletal muscle differentiation, regeneration, and fiber type conversion to an oxidative state, all of which are crucial to muscle development, metabolism, and functional adaptations. It seeks to integrate the current knowledge of calcineurin signaling in skeletal muscle and its interactions with other prominent regulatory pathways and their signaling intermediates to form a molecular overview that could provide directions for possible future exploitations in human metabolic health.

Key Words: Calcineurin, Skeletal muscle, Oxidative fiber, Differentiation, Regeneration, Fiber type.   © 2009 Elsevier Inc.

1. INTRODUCTION

Skeletal muscle is remarkably able to adapt to its working conditions by changing its physical, contractile, and metabolic properties to accommodate alterations in functional demands. This tissue plasticity is manifested as changes in fiber size, as well as in coordinated changes in structural proteins and metabolic enzymes resulting in changes in fiber type (Schiaffino and Reggiani, 1996).

Of the different fiber types that are found in muscle, oxidative fibers, in particular, stand out as an important fiber type for human health and for animal production. Individuals with muscles that are rich in oxidative type I fibers tend to confer favorable metabolic health, and are less likely to predispose to obesity and insulin resistance (Fig. 2.1). In age-related muscle atrophy, the relative preservation of high-efficiency slow-oxidative fibers appears to be a protective compensatory response to maintain muscular performance (Horowitz et al., 1994). Therefore, a sound understanding of the molecular regulation of oxidative fiber type conversion is vital to the development of intervention strategies, such as pharmacological modulation and, in the case of animal production, genetic selection, to promote the enhancement of oxidative fibers in muscles.

A key regulatory route responsible for the fast-to-slow fiber type conversion is the calcineurin signaling pathway. Calcineurin is an enzyme complex that comprises calcineurin A (CnA) catalytic subunit, calcineurin B (CnB) regulatory subunit, and calcium–binding protein calmodulin (Schulz and Yutzey, 2004) (Fig. 2.2A). There are three major isoforms of CnA (α, β, and γ) (three genes) and two isoforms (two genes) of CnB (1 and 2). Only CnAα, CnAβ (CnAα more abundant than CnAβ), and CnB1 are expressed in skeletal muscle (Parsons et al., 2003, 2004).
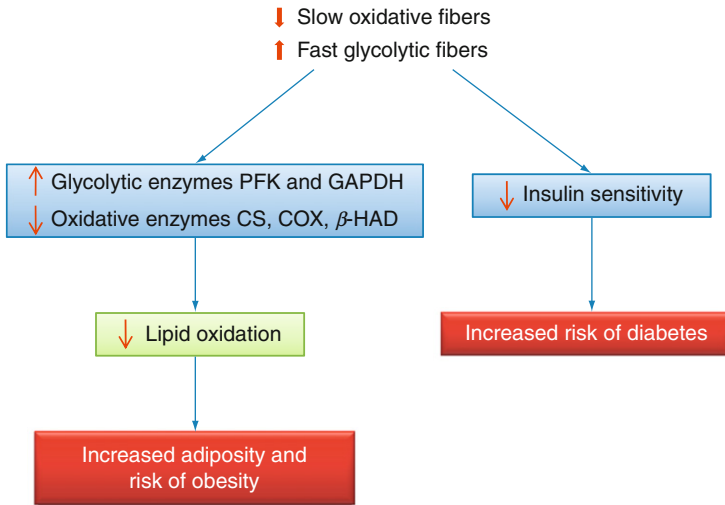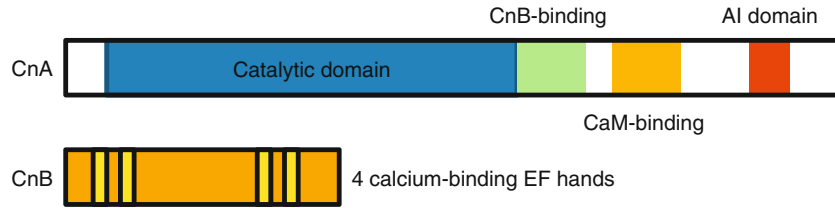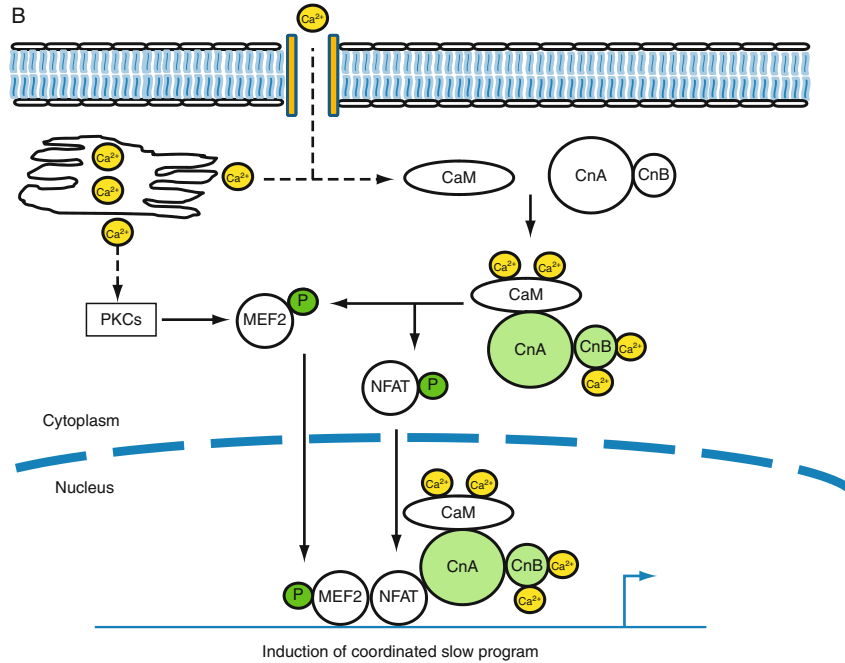
Figure 2.1 Consequences of reduced slow oxidative muscle fiber type. Skeletal muscle is a major contributor to a variety of metabolic conditions. Muscle groups with decreased slow oxidative fibers and increased fast glycolytic fibers have been shown to have altered glycolytic enzyme levels (PFK, phosphofructokinase; GAPDH, glyceraldehydephosphate dehydrogenase) and oxidative enzyme levels (CS, citrate synthase; COX, cytochrome oxidase *c*; β-HAD, beta-hydroxyacyl CoA dehydrogenase) (Simoneau et al., 1999), which reduce lipid oxidation capacity (Wade et al., 1990) and increase adiposity (Lillioja et al., 1987; Marin et al., 1992). A fast glycolytic fiber phenotype is also associated with decreased insulin sensitivity (He et al., 2001) resulting in an increased risk of developing diabetes (Nyholm et al., 1997).

Calcineurin is a calcium-dependent serine–threonine phosphatase (protein phosphatase 2B/PP2B) that is widely distributed throughout the body. It has been implicated in a wide variety of biological processes, including T-lymphocyte activation, vascular, neuronal, and cardiac development and growth, and, more recently, skeletal muscle development (Bueno et al., 2002a; Crabtree, 2001; Horsley and Pavlath, 2002). In cardiac muscle, calcineurin signaling is necessary for cardiomyocyte maturation, heart chamber formation, and cardiac hypertrophy (Schulz and Yutzey, 2004). In skeletal muscle, calcineurin is required in a number of key developmental processes, namely enhanced muscle cell differentiation, and in the fiber type context, conversion to a slow (oxidative) muscle phenotype (Bigard et al., 2000; Delling et al., 2000; Musarò et al., 1999; Semsarian et al., 1999). This chapter focuses on the key roles of calcineurin in skeletal muscle differentiation, regeneration, and fiber type conversion to an oxidative state, all of which are crucial to muscle development and oxidative functional adaptations.

A

CnA — Catalytic domain | CnB-binding | CaM-binding | AI domain

CnB — 4 calcium-binding EF hands

B

Ca²⁺

Ca²⁺ Ca²⁺ Ca²⁺ Ca²⁺

CaM

CnA CnB

Ca²⁺ Ca²⁺

CaM

PKCs → MEF2 P ← P

CnA CnB Ca²⁺

Ca²⁺

NFAT P

Cytoplasm

Nucleus

Ca²⁺ Ca²⁺

CaM

P MEF2 NFAT

CnA CnB Ca²⁺

Ca²⁺

Induction of coordinated slow program

2. Importance of Oxidative Skeletal Muscle Fiber Phenotype

2.1. Definition and properties of muscle fiber types

Traditionally, classification of muscle fiber types is based on differences in biochemical parameters between fibers (Gil et al., 2001; Zierath and Hawley, 2006). A commonly used histochemical method depends on the overall myosin adenosine triphosphatase (ATPase) activity in each fiber (Brooke and Kaiser, 1970; Neston and Bancroft, 2002). A more objective definition of fiber types is based on the identification of the primary myosin heavy chain (MyHC) isoform expressed in each fiber (Chang and Fernandes, 1997; Chang et al., 1993, 1995). MyHCs are encoded by a highly conserved multigene family, of which eight isoforms are known in mammals (*IIa*, *IIx*, *IIb*, *embryonic*, *perinatal*, *slow/I*, *extraocular,* and *α*), each with its own myosin ATPase activity and each encoded by a distinct gene (Weiss and Leinwand, 1996). Based on the MyHC approach, postnatal muscle fibers can be resolved by immunocytochemistry or *in situ* hybridization into three or four major types, depending on animal species. In postnatal muscles of pigs, dogs, and rodents, there are four major fiber types characterized by the expression of the *slow/I, IIa, IIx,* and *IIb* MyHC gene isoforms (Schiaffino and Reggiani, 1996; Wu et al., 2000b). On the other hand, in humans, cattle, and horses there are three main fiber types, MyHC slow, IIA, and IIX fibers as MyHC IIB fibers are effectively absent (Chikuni et al., 2004; Horton et al., 2001; Maccatrozzo et al., 2004).

Metabolic, biochemical, and biophysical characteristics, such as oxidative and glycolytic capacities, fiber size, color, and glycogen and lipid

---

Figure 2.2 Basic pathway of calcineurin activation in skeletal muscle. (A) In the absence or near absence of calcium, the carboxyl terminal autoinhibitory domain of the catalytic calcineurin A (CnA) subunit blocks its catalytic groove. Thus, the heterodimer CnA–calcineurin B regulatory subunit (CnA–CnB) is inactive. (B) Sustained elevation of intracellular calcium, from sarcoplasmic reticulum calcium store and from extracellular entry, through excitation–contraction coupling, and extracellular signaling resulting in 1,4,5-trisphosphate (IP3) and diacylglycerol (DG) induction, leads to calcium binding to calmodulin (CaM) and CnB. The association of calcium-CaM with the CnA–CnB dimer displaces the CnA autoinhibitory domain from its catalytic site, hence an activated phosphatase complex is formed. Activated calcineurin targets substrates, such as NFAT and MEF2 transcription factors, for dephosphorylation activation. Activated factors mediate the coordinated slow gene expression program. Note that raised intracellular calcium is also able to activate protein kinases C (PKCs). MEF2 is subjected to both differential phosphorylation by PKCs (D'Andrea et al., 2006) and dephosphorylation by activated calcineurin (Dunn et al., 2000). The intranuclear localization model of activated calcineurin complex is based on findings of NFATc3 (NFAT4) in nonmuscle cells (Zhu and McKeon, 1999, 2000).

contents, have been found to vary between MyHC fiber types (Karlsson et al., 1999; Klont et al., 1998; Schiaffino and Reggiani, 1996). The slow and fast IIB fibers, also known as slow oxidative (red) and fast glycolytic (white), respectively, represent two extreme metabolic profiles. Slow MyHC fibers are characterized by slow isoform contractile proteins, high levels of myoglobin, high volumes of mitochondria, high oxidative capacity, high lipid contents, and high capillary density. By contrast, fast MyHC IIB fibers are the largest of the four fiber types with fast isoform contractile proteins, low amounts of myoglobin and mitochondria, high glycolytic capacity (high glycogen store), low lipid contents, and low capillary density. The fast MyHC IIA and IIX fibers are intermediate fast oxidative-glycolytic fibers. Fast IIA fibers are more closely related to slow fibers, and fast IIX are more similar to fast IIB fibers.

2.2. Biomedical significance of oxidative muscle in relation to the metabolic syndrome and aging

Skeletal muscle is the most abundant human tissue comprising almost 50% of the total body mass, exhibiting major metabolic activity by contributing up to 40% of the resting metabolic rate in adults and serving as the largest body protein pool (Matsakas and Patel, 2009). In addition, skeletal muscle constitutes the largest insulin–sensitive tissue in the body and is the primary site for insulin–stimulated glucose utilization. Skeletal muscle resistance to insulin is fundamental to the metabolic dysregulation associated with obesity and physical inactivity, and contributes to the development of metabolic syndrome. Furthermore, it has been proposed that skeletal muscle fiber composition may contribute to insulin action *in vivo* (Lillioja et al., 1987; Marin et al., 1992) and muscle fiber phenotype has been shown to differ between lean healthy subjects and those presenting with insulin resistance and noninsulin–dependent diabetes mellitus (NIDDM) (Oberbach et al., 2006). Specifically, these studies show increased proportion of fast glycolytic fibers and a reduced number of oxidative type I fibers in NIDDM patients. In addition, the percentage of fast glycolytic fibers in the *vastus lateralis* was found to be inversely related to insulin sensitivity (Hickey et al., 1995b). Interestingly, healthy first-degree relatives of patients with NIDDM have a greater proportion of fast glycolytic fibers than control subjects, suggesting there could be a genetic predisposition to NIDDM through increased percentage of fast glycolytic fibers (Nyholm et al., 1997). Indeed, approximately 40% of NIDDM relatives are expected to develop overt diabetes (Kobberling and Tillil, 1982). A negative correlation was also found between the proportion of fast glycolytic fibers and insulin–stimulated glucose uptake, and a positive correlation between oxidative type I fibers and stimulated glucose uptake (Nyholm et al., 1997), supporting the notion of a strong association between muscle fiber composition and insulin

sensitivity (He et al., 2001). A similar association is found between muscle fiber type phenotype and obesity (Abou et al., 1992; Hickey et al., 1995a; Lillioja et al., 1987; Marin et al., 1992; Tanner et al., 2002). Early studies (Lillioja et al., 1987; Marin et al., 1992) have highlighted that abdominal adiposity, as assessed by either waist-to-thigh ratio or waist-to-hip ratio, was positively associated with the percentage of fast glycolytic fibers in the *vastus lateralis* and inversely related to insulin sensitivity. Loss of oxidative type I fibers in obese subjects results in reduced lipid oxidation capacity during submaximal exercise compared with lean subjects (Wade et al., 1990). Further studies highlighted that abdominal visceral adiposity is inversely related to citrate synthase activity, and a positive correlation exists between the percentage of fast glycolytic fibers and body mass index (Hickey et al., 1995a,b). The *vastus lateralis* of obese subjects also has higher activities for the two enzyme markers of glycolysis (phosphofructokinase and glyceraldehy-dephosphate dehydrogenase) and lower activities for enzymes of oxidative capacity (citrate synthase, cytochrome oxidase *c*, and beta-hydroxyacyl CoA dehydrogenase, β-HAD) (Simoneau et al., 1999). Collectively, these studies suggest that individuals with muscles that are abundant in oxidative type I fibers are associated with favorable metabolic health, and are less likely to predispose to obesity and insulin resistance (Fig. 2.1).

Advancing age leads to slow but progressive loss of muscle mass and is characterized by a deterioration of muscle quantity and quality, followed by a gradual slowing of movement and a decline in strength (Ryall et al., 2008). Sarcopenia is generally used to describe age-related changes that occur within skeletal muscle and thus encompasses the effects of altered central and peripheral nervous system innervation, altered hormonal status, inflammatory effects, and altered caloric and protein intake (Doherty, 2003). In humans, a gradual loss of muscle fibers begins at approximately 50 years of age and continues such that by 80 years of age, approximately 50% of the fibers are lost from the limb muscles that have been studied (Faulkner et al., 2007). However, many studies have highlighted that the age-related decrease in muscle mass is not due to a loss in fiber numbers, rather that muscle atrophy is the result of a reduction in fiber size (Coggan et al., 1992; Houmard et al., 1998; Larsson et al., 1978; Lexell et al., 1988). Age-related skeletal muscle atrophy has been shown to be fiber-type specific and is associated with diminishing fast glycolytic fiber size; however, the size of oxidative type I fibers is less affected (Larsson et al., 1978; Lexell et al., 1988). *MyHC slow* mRNA was found to be unchanged with age, whereas *MyHC IIa* and *IIx* mRNA declined by 14% and 10% per decade from 40 years of age, respectively (Short et al., 2005). However, others have found no age-related reduction in total *MyHC* mRNA abundance and suggest that the age-related decreases in MyHC and myofibrillar proteins are primarily through changes in the rate of translation (Toth and Tchernof, 2006; Toth et al., 2005; Welle et al., 1993). Interestingly, it was reported

that the mean number of satellite cells decreases in fast glycolytic fibers, but not in oxidative type I fibers of the *vastus lateralis* muscle of healthy elderly men which may help to explain the differential response of fast type II fibers compared with slow type I fibers with aging (Verdijk et al., 2007). Taken together, the relative preservation of high efficiency slow oxidative type I fibers in age-related atrophy appears to be a protective compensatory response to maintain muscular performance (Horowitz et al., 1994).

3. Calcium-Dependent Mediators of Oxidative Muscle Fiber Type Programing

3.1. Role of protein kinases C in the regulation of slow muscle genes

The mammalian protein kinase C family comprises at least 10 isoenzymes grouped into three classes. The conventional PKC isoforms (cPKCs: α, β, and γ isoforms) depend on calcium and diacylglycerol (DAG) for activation; the novel PKC isoforms (nPKCs: δ, ε, η, and θ) only depend on DAG, whereas the atypical PKC isoforms (aPKCs: λ and ξ) are activated independent of calcium and DAG (Newton, 2001). The nPKC subfamily member PKCθ is the predominant PKC isoenzyme expressed in skeletal muscle (Osada et al., 1992), with fast fibers exhibiting a higher level of expression than slow fibers in the rat (Donnelly et al., 1994). PKCs of all subfamilies are activated by exercise. Pharmacological inhibition of cPKCs and nPKCs blunts contraction induced glucose uptake in skeletal muscles (Rockl et al., 2008). The PKC isoform μ is presently considered as a distinct family called protein kinase D (PKD). The activation of PKD isoforms 1, 2, and 3 is calcium independent and is through PKC phosphorylation (Zugaza et al., 1996). In skeletal muscle, PKD1 is predominantly expressed in slow type I myofibers (Kim et al., 2008).

In accordance with its prominent expression in skeletal muscle, PKCθ was found to activate slow muscle genes by cooperating with calcineurin (D'Andrea et al., 2006). A constitutively active form of PKCθ coexpressed with a constitutively active calcineurin catalytic subunit A (CnA★) (Fig. 2.2A) increases slow MyHC and troponin I (TnI) protein expression in C2C12 muscle cells (D'Andrea et al., 2006). Primarily, PKCθ acts on myocyte enhancer factor 2 (MEF2), as demonstrated with a MEF2 reporter and mutation of its binding site on a *myoglobin* promoter (D'Andrea et al., 2006). Myoglobin is an oxygen-binding protein associated with oxidative energy metabolism, and is enriched in slow oxidative type I and in fast oxidative-glycolytic type IIA fibers. MEF2-dependent myoglobin promoter activation is also dependent on the cooperation of calcineurin and the transcriptional coactivator, peroxisome proliferator-activated receptor γ

coactivator–1α (PGC–1α) (Lin et al., 2002), a master regulator of energy metabolism. Thus PKCθ is required for calcineurin–PGC–1α–dependent myoglobin promoter activation (D'Andrea et al., 2006). In addition, PKCθ regulates the intracellular localization of class II histone deacetylase 5 (HDAC5) by promoting its nuclear export. Nuclear HDAC5 is known to act as a repressor of MEF2 transcriptional activity (McKinsey et al., 2001). PKD1 is also a highly effective class II HDAC kinase in skeletal muscle, thereby promoting MEF2 transcriptional activity (Kim et al., 2008). Moreover, PKD1 seems to be involved in slow fiber type transformation in synergy with calcineurin, as evident by increases of *TnI slow* and *myoglobin* mRNA expression in *extensor digitorum longus* (EDL) muscles in *PKD1-calcineurin* double transgenic animals (Kim et al., 2008). Hence, PKCθ and PKD1 are shown to play a key role in slow fiber type-specific gene expression in cooperation with calcineurin (Fig. 2.2B).

Further evidence for a role of PKC in oxidative energy metabolism was provided in a model of calcium ionophore-induced upregulation of the cytochrome *c* promoter in the L6E9 muscle cell line (Freyssenet et al., 1999). The effect of calcium ionophore on the cytochrome *c* promoter was significantly reduced, but not abolished by staurosporine, a nonspecific PKC inhibitor. It was further shown that the calcium-dependent upregulation of the cytochrome *c* promoter was mediated by cPKC isoforms α and β2, but not by the calcium–independent nPKC isoform δ. Taken together, these findings point to a role of cPKC isoforms in slow oxidative fiber type-specific gene expression.

Evidence for a role of PKC in the regulation of fast oxidative-glycolytic fiber type IIA is scarce and equivocal. An investigation into a possible role of PKC in the regulation of the *MyHCIIa* promoter in C2C12 myotubes found that staurosporine (2 nm) reduced the *MyHCIIa* promoter activity, but not with a more selective PKC inhibitor chelerythrine; however, a chelerythrine dose response was not performed (Allen and Leinwand, 2002).

PKC signaling has also been demonstrated to be involved in the expression of avian slow *MyHC2* expression in slow lineage skeletal muscle fibers (DiMario and Funk, 1999). Surprisingly, a completely different picture on the role of PKC in the regulation of the slow *MyHC* is seen in primary avian myoblast cultures. Avian secondary muscle fibers formed from myoblasts of slow muscle origin only express the slow *MyHC2* gene (DiMario and Stockdale, 1997). PKC activity is higher in fast *pectoralis major* (PM) compared with slow *medial adductor* (MA) muscle fibers *in vitro* (DiMario and Funk, 1999). Inhibition of PKC with staurosporine induces slow MyHC2 expression in slow but not in fast muscle fibers. Moreover, it was found that denervation of slow MA led to an increase in PKC activity which was associated with a lack of slow *MyHC2* expression. Overexpression of wild-type PKC isoforms α and θ *in vitro* resulted in the repression of slow *MyHC2*

expression in MA muscle fibers, but dominant negative mutants did not repress *MγHC2* expression in the nerve–muscle cocultures (DiMario, 2001). The results indicate that the downregulation of PKC isoforms in MA is required for slow *MγHC2* expression. Repression of *MγHC2* expression in the fast PM has been shown to be mediated by signaling involving PKC and the subunit α of the heterotrimeric guanine nucleotide-binding G-protein q as well as the muscarinic acetylcholine receptor (Jordan et al., 2003). PKC activity is regulated by phospholipase C (PLC), which in turn is activated from cell surface receptors via $G_{\alpha q}$. An indirect link of PKC signaling to the calcineurin–NFAT (nuclear factor of activated T cells) pathway in the regulation of *MγHC2* expression could be demonstrated by studies investigating the role of the ryanodine receptor 1 (RyR1) (Jordan et al., 2003). Use of high concentrations of ryanodine (100 μM) to inhibit RyR1 activity demonstrated that RyR1 activity enhanced PKC activity and repressed *MγHC2* expression in innervated fast PM (Jordan et al., 2003). RyR1 activity also inhibited the transcriptional activity of *NFAT* and *MEF2* sensor constructs and the binding of both transcription factors to binding sites in the slow *MγHC2* promoter in innervated PM. The experiments led to the hypothesis that increased calcium transients in fast PM muscles elicited by RyR1 activity can activate signaling compounds like PKC to repress slow *MγHC2* gene expression. In summary, data on the role of PKC in repressing slow fiber type gene expression in avian models are in contrast to mammalian models, which may indicate a fundamentally different regulation of slow *MγHC* expression between birds and mammals.

3.2. Role of calcium–calmodulin kinases in oxidative fiber determination

Adult skeletal muscle displays plasticity that allows conversion of different fiber types in response to chronic change in contractile demands. For instance, repeated mechanical overload and endurance training increase the percentage of slow type I fibers (Putman et al., 2004; Short et al., 2005; Thayer et al., 2000; Willoughby and Nelson, 2002) and these effects can be mimicked by electrical stimulation of motor nerves or cross–reinnervation of muscles with nerves supplying slow-twitch fibers (Jarvis et al., 1996; Maier et al., 1988; Pette et al., 2002; Schuler and Pette, 1996). Studies of pathways downstream of neural activity have implicated calcium signaling through calcium/calmodulin-dependent protein kinases (CaMKs) (Antipenko et al., 1999), specifically CaMKII and CaMKIV (Rose et al., 2007; Wu et al., 2002) and calcineurin, a calcium–calmodulin (CaM)-dependent protein phosphatase (Bigard et al., 2000; Chin et al., 1998; Naya et al., 2000) in the control of slow type I fiber-specific contractile protein expression.

Increases in intracellular calcium concentrations allow binding of calcium to the calcium receptor protein calmodulin, which subsequently undergoes conformational change and allosterically modify several proteins (Hook and Means, 2001), among which include CaMKs. CaMKs are a family of serine/threonine protein kinases, which are activated via binding of calcium/calmodulin to its calmodulin-binding domain (Wayman et al., 2008). This association also catalyzes the autophosphorylation of CaMKs (Miller and Kennedy, 1986) resulting in autonomous (i.e., Ca^{2+} independent) kinase activity. The multifunctional kinases CaMKII and CaMKIV have been described to play a functional role in skeletal muscle (Fluck et al., 2000b; Michel et al., 2004; Rose et al., 2007).

CaMKII is significantly enriched in skeletal muscle nuclei suggesting a role in the regulation of nuclear proteins. Its activity is strongly upregulated in stretch overloaded rooster muscle (Fluck et al., 2000b), and in humans subjected to short-term endurance training, with a concomitant increase in mitochondrial enzymes such as citrate synthase and β-HAD (Rose et al., 2007). The similarity in response of CaMKII to stretch overload and endurance training suggests that this pathway is upstream of the specific adaptations to these contractile demands (Chin, 2004). CaMKII has further been shown to be involved in muscle fiber type switching from a fast-to-slow phenotype (Mu et al., 2007). A specific inhibitor of CaMKII, KN62, strongly attenuates the ionophore-induced activation of the fast oxidative *MyHC IIa* promoter in C2C12 myotubes in a dose-dependent manner, suggesting a role of CaMKII in fiber type plasticity (Allen and Leinwand, 2002). Similarly, inhibition of CaMKII in cultured adult rodent fast twitch muscle fibers by another CaMKII-specific inhibitor KN93, resulted in a faster gene expression profile (Mu et al., 2007). In addition, KN93 in L6 myotubes blocks the calcium-induced increases in the mitochondrial enzymes cytochrome oxidase and citrate synthase (Ojuka et al., 2003). Taken together, these studies suggest that CaMKII upregulates slow gene expression and downregulates fast gene expression, thereby mediating fast-to-slow fiber type transformation (Fig. 2.4).

To date, several substrates of CaMKII have been identified. CaMKII activation results in the downstream activation of serum response factor and its binding to serum response elements on muscle promoters (Fluck et al., 2000a). Increased CaMKII activity has also been shown to indirectly activate the transcription factor MEF2 by negative regulation of HDAC 4 and 5 (Liu et al., 2005; McKinsey et al., 2002b; Miska et al., 1999). Slow fiber stimulation patterns in adult mouse skeletal muscle fibers activate CaMKII which in turn phosphorylates HDAC4, releasing MEF2 repression (Liu et al., 2005). It is also suggested that CaMKII coordinates with calcineurin to fully activate MEF2 (Wu et al., 2000a).

Another CaMK that is involved in the oxidative muscle phenotype is CaMKIV. Transgenic mice expressing a constitutively active form of

CaMKIV exhibited increased mitochondrial density and slow type I fiber number in the predominantly fast twitch *plantaris* muscle (Wu et al., 2002). These phenotypic changes were associated with increased expression of PGC-1α, a key regulator of mitochondrial biogenesis (Puigserver and Spiegelman, 2003; Wu et al., 1999) and an activator of the mitochondrial fatty acid oxidation pathway (Vega et al., 2000). PGC-1α transgenic mice have been shown to have increased type I fibers in the *plantaris* muscle (Lin et al., 2002). However, the physiological relevance of CaMKIV has been called into question, as recent findings have shown that CaMKIV protein is not significantly expressed in mouse (Akimoto et al., 2004) or human (Rose and Hargreaves, 2003; Rose et al., 2006) skeletal muscle. Furthermore, CaMKIV knockout mice have normal fiber type composition and respond to long-term voluntary running with increased expression of *MyHC IIa*, myoglobin, and PGC-1α in a manner similar to wild-type mice (Akimoto et al., 2005). Future studies will be needed to investigate the potential relevance of other CaMK family members in skeletal muscle fiber type adaptations in response to increased intracellular calcium.

4. BIOLOGICAL FUNCTIONS OF THE CALCINEURIN SIGNALING PATHWAY

4.1. Calcineurin induces cardiac hypertrophy

Although this chapter is focused on skeletal muscle, it is of comparative value to highlight a key influence of calcineurin signaling on the heart that is not found in skeletal muscle: induction of cardiac hypertrophy. Cardiac hypertrophy is an adaptive response to physiological or pathological stimuli (Clerk et al., 2007). It is defined as an increase in muscle mass, as opposed to an increase in the number of muscle cells, leading to enlarged cellular diameter and cross-sectional area, and muscle weight per body weight. Cardiac hypertrophy is associated with profound changes in gene expression with adult cardiomyocytes starting to reexpress a fetal gene program, including α-skeletal actin and MyHCb/slow expression in mice (Molkentin et al., 1998).

Several approaches have clearly defined the calcineurin–NFAT pathway as a mediator of cardiac hypertrophy. For example, transgenic mice over-expressing CnA* or constitutively active NFATc4 developed a profound hypertrophic response and heart failure that mimicked human heart disease (Molkentin et al., 1998). Recently, the deleterious effects of calcineurin overexpression in the heart were found to associate with the local production of nitric oxide (NO) activated via inducible NO synthase (iNOS)

(Somers et al., 2008). However, the precise role of each NFAT isoform on cardiac hypertrophy is not completely clear. NFATc4 was shown to interact with the cardiac–restricted zinc finger transcription factor GATA4. GATA4 can activate hypertrophic–responsive genes in cardiomyocytes, for example, by participating in pressure overload-induced cardiac hypertrophy (Herzig et al., 1997). Targeted disruption of NFATc4, however, did not compromise the ability of the myocardium to undergo hypertrophic growth. In contrast, hypertrophy induced by calcineurin was attenuated in NFATc3 null mice (Wilkins et al., 2002). Interestingly, significant expression of NFATc4 but not c3 mRNA was reported in the human heart (Hoey et al., 1995). Furthermore, transgenic mouse models have demonstrated a crucial role for NFATc2 in pathological but not physiological cardiac remodeling (Bourajjaj et al., 2008). Although the relative importance of individual NFAT isoforms is not completely clear, these data clearly demonstrate the important role of the calcineurin–NFAT signaling pathway for cardiac hypertrophic response (Heinke and Molkentin, 2006). With regard to the specific effect of physiological hypertrophy, the role of the calcineurin–NFAT pathway remains to be determined. It could be demonstrated by the use of a NFAT–luciferase reporter construct, that NFAT is not upregulated during physiological hypertrophy, induced by exercise or stimulation with insulin-like growth factor-1 (IGF-1) (Wilkins et al., 2004). The finding that calcineurin Aβ null mice showed a reduced basal heart size (Bueno et al., 2002b) indicates a possible role of calcineurin for physiological growth of the heart.

The two other major signaling pathways which are important for the mediation of physiological cardiac hypertrophy are the Ras–extracellular signal-regulated kinase-mitogen activated protein kinase (Erk-MAPK) and the phosphatidylinositol 3′-kinase (PI3K)–Akt1 pathways (Heinke and Molkentin, 2006). Cross talk between the calcineurin–NFAT and the Erk-MAPK pathway has been demonstrated. Targeted inhibition of Erk-MAPK signaling attenuates the hypertrophic growth response elicited by activated calcineurin (Sanna et al., 2005). Specific activation of Erk in the heart leads to stable compensated (physiological) hypertrophy (Bueno et al., 2000). Erk1/2-mediated phosphorylation increases the transcriptional activity of NFATc3 by augmenting its DNA-binding activity. Moreover, the hypertrophic effect of a MKK1 (mitogen–activated protein kinase kinase 1 or MEK1) transgene is reduced by genetic deletion of the calcineurin Aβ gene. Evidence of cross talk between calcineurin and PI3K–Akt1 signaling is explained in Section 5.2. To summarize, the calcineurin–NFAT signaling pathway is a major mediator of cardiac hypertrophy, based mainly on pathological remodeling studies. It remains a mystery why this major effect on cardiac muscle is not seen in skeletal muscle.

4.2. Calcineurin in muscle differentiation and regeneration

An important role of calcineurin signaling in skeletal muscle is in muscle differentiation. Constitutively active catalytic subunit calcineurin A (CnA★) enhances differentiation in muscle C2C12 cells (Delling et al., 2000; Friday et al., 2003). There is, however, no clear agreement on the role of NFATs in the mediation of muscle differentiation. Delling et al. showed the involvement of nuclear translocation of NFATc3, but not NFATc1 and NFATc4, in the differentiation of muscle C2C12 cells (Delling et al., 2000). Friday et al., on the other hand, demonstrated with the use of NFAT inhibitor (GFP-VIVIT) that calcineurin–dependent differentiation is NFAT independent (Friday et al., 2000). They also showed that CnA★–induced differentiation is dependent on the requirement of extracellular calcium (Friday et al., 2000), which indicates that other calcium-mediated downstream targets, in addition to CnA★ signaling, are required for differentiation.

Consistent with the role of calcineurin in muscle differentiation is the finding, by immunoprecipitation, that calcineurin and activated NFATc1 are markedly raised in regenerating rat muscles, which is also a feature of proliferating, but not quiescent, muscle satellite cells (Sakuma et al., 2003), which points to a role of calcineurin in muscle regeneration. It appears that reduced calcineurin activity is associated with the inhibition of muscle differentiation and/or regeneration. In summary, calcineurin is a key player in skeletal muscle differentiation and regeneration although the precise contributions of NFATs are unclear.

4.3. Calcineurin induces an oxidative skeletal muscle phenotype

Calcineurin signaling is a major pathway responsible for converting fast-to-slow muscle fibers. It was reported that activated calcineurin also mediates the hypertrophic effect of IGF-1 (Musarò et al., 1999; Semsarian et al., 1999). However, there is compelling evidence, including calcineurin transgenic and knockout data, to show that calcineurin has no significant impact on skeletal muscle hypertrophy but that the hypertrophic effect of IGF–1 is mediated by the PI3K pathway (Bodine et al., 2001b; Naya et al., 2000; Pallafacchina et al., 2002; Parsons et al., 2003, 2004; Rommel et al., 2001). The conversion of fast muscle fibers to and maintenance of slow oxidative fibers require a coordinated upregulation of structural and metabolic genes associated with the oxidative phenotype and the corresponding downregulation of fast muscle genes (Oh et al., 2005) (Fig. 2.2B). Slow-twitch fibers are characterized by a high sustained intracellular calcium concentration which is permissive to calcineurin activation, whereas short transient calcium elevation found in fast twitch fibers does not lead to calcineurin stimulation (Bassel–Duby and Olson, 2003; Fraysse et al., 2003; Kubis et al., 2003; Liu et al., 2001). However, as in other pathways, the effect of

calcineurin activation is not absolute in that it does not activate all slow genes in all muscles. Some fast muscle genes, like *MyHC IIb* and *SERCA1*, can be upregulated in activated calcineurin–transfected C2C12 cells (Swoap et al., 2000). Transgenic mice overexpressing CnA* in skeletal muscle showed substantial slow fiber switch but only in certain muscles (Naya et al., 2000). The MyHC IIA and IIX proteins in the transgenic mice can be up or downregulated depending on muscle type (Naya et al., 2000; Talmadge et al., 2004). Conversely, CnAα null or CnAβ null results in reduced oxidative capacity of all muscles examined, with the notable exception of the *soleus* muscle where oxidative capacity is unaffected (Parsons et al., 2003).

At present, it is not clear how calcineurin signaling actually leads to an oxidative fiber outcome. As in muscle differentiation, the role of NFATs in mediating oxidative fiber conversion is far from clear. NFATc1 appears to be important in the upregulation of *MyHC slow* in the context of regenerating muscles (McCullagh et al., 2004). NFATc3 null mice show reduced muscle mass and primary fiber number (Kegley et al., 2001), and NFATc2 null mice display reduced fiber size and nuclear number (Horsley et al., 2001). Neither NFATc3 nor NFATc2 knockout, however, has any apparent effect on fiber type. Likewise, NFATc3 overexpression alone does not upregulate *MyHC slow* (Delling et al., 2000). CnAβ null mice show no change in NFAT nuclear translocation which suggests that reduction of oxidative/slow fibers in such mice is independent of NFAT (Parsons et al., 2003).

At the gene level, CnA* expression activates the murine *MyHC IIa* promoter (Allen et al., 2001) and increases endogenous MyHC IIA protein expression (Allen and Leinwand, 2002). The expression of calcineurin inhibitor cain/cabin–1 (by electroporation) in fibers of normal adult rat *soleus* upregulates the expression of *MyHC IIx* and *IIb* but not *MyHC slow* and *IIa*, suggesting interestingly that calcineurin represses the *MyHC IIx* and *IIb* genes (Serrano et al., 2001). Indeed, we recently found that in C2C12 cells calcineurin differentially regulates *MyHC* genes; it upregulates *embryonic, perinatal,* and fast *IIa MyHCs* but downregulates fast *IIx* and *IIb MyHC* genes (da Costa et al., 2007). Furthermore, the upregulation of *MyHC slow* gene by calcineurin is not an immediate effect but is a time-dependent process (da Costa et al., 2007).

5. DOWNSTREAM EFFECTOR TARGETS OF CALCINEURIN IN SKELETAL MUSCLE

5.1. Known effector targets of calcineurin

Only a limited number of known direct effector targets of calcineurin and, in turn, genes regulated by these effectors are known in skeletal muscle. The best characterized targets of calcineurin are members of the NFAT and MEF2 transcription factor families. A less reported target of calcineurin is

the transcriptional coactivator PGC-1α, a master regulator of energy homeostasis, especially of oxidative energy metabolism (Puigserver and Spiegelman, 2003).

Genes regulated through calcineurin–NFAT and/or -MEF2 signaling include slow fiber-specific isoforms of genes of the contractile apparatus, *myoglobin*, and *utrophin A* which encodes a cytoskeletal protein. *Utrophin A* mRNA levels are most abundant in oxidative slow/I and IIA fibers. Calcineurin-NFAT signaling can activate the promoters of both *MyHC I* and *IIa* isoforms (Allen and Leinwand, 2002; Meissner et al., 2007b) as well as the *utrophin A* promoter (Chakkalakal et al., 2003). Another downstream target of calcineurin–NFAT signaling is the regulator of skeletal muscle growth, myostatin (Michel et al., 2007).

Calcineurin can dephosphorylate (activate) NFAT, which otherwise remains inactivated in a multiphosphorylated form in the cytoplasm (Hogan et al., 2003; Masuda et al., 1998). Dephosphorylated NFAT translocates in a complex with calcineurin into the nucleus, where it activates gene expression (Fig. 2.2B) (Zhu and McKeon, 1999). During calcium signaling, calcineurin remains in a complex with NFAT to prevent rapid rephosphorylation by kinases (Zhu and McKeon, 2000). Casein kinase 1/2 and glycogen synthase kinase 3β appear to be the main NFAT kinases *in vivo* (Shen et al., 2007). NFAT comprises a family of five different isoforms (Im and Rao, 2004), with NFATc1 and c3 being the main isoforms at least in human skeletal muscle at the level of mRNA expression (Hoey et al., 1995). Consistent with its role in oxidative phenotype determination, *in vivo* studies using an NFATc1-GFP (green fluorescent protein) fusion protein indicated that NFATc1 is predominantly localized in the cytoplasm of the fast *tibialis anterior* muscle, but is predominantly nuclear in the slow *soleus* (Tothova et al., 2006). In addition, nearly complete cytoplasmic localization of endogenous NFATc1 in fast fiber-like primary skeletal and C2C12 myotubes has been described (Meissner et al., 2001, 2007b).

Several lines of evidence indicate that NFAT is a target of calcineurin in slow fiber type-specific gene expression. In adult *soleus* muscle, an injected 1.1 kb *MyHC slow*-promoter-luciferase construct was inhibited by coinjection of a plasmid coding for VIVIT (McCullagh et al., 2004). Furthermore, VIVIT blocked endogenous *MyHC slow* mRNA expression in regenerating and adult *soleus* muscle. Constitutively active NFATc1 increased the activity of a cotransfected *MyHC slow* promoter construct in the fast EDL muscle, and of endogenous *MyHC slow* promoter mRNA in regenerating, but not in adult EDL. Coinjection of the calcineurin inhibitor cain/cabin-1 blocked nuclear translocation of NFATc1-GFP in soleus muscle (Tothova et al., 2006). In C2C12 myotubes, overexpression of a constitutively nuclear mutant of NFATc1 activated a 2.4 kb *MyHC slow* promoter reporter construct. Moreover, the calcineurin inhibitor cyclosporine A (CsA) blocked calcium ionophore-induced nuclear import and

binding of NFATc1 to an NFAT consensus-binding site in the *MyHC slow* promoter, demonstrating the importance of calcineurin–NFATc1 signaling in the upregulation of the *slow* promoter (Meissner et al., 2007b). In addition, NFATc1 recruits the transcriptional coactivator p300. NFATc1 can also interact with p300 in cardiac myocytes (Kawamura et al., 2004). The transactivation function of transcription factors is often mediated by coactivators, like p300, with histone acetyltransferase (HAT) activity (Kalkhoven, 2004); coactivators themselves are controlled by various covalent modifications (Gamble and Freedman, 2002). Inhibition of calcineurin by CsA also blocked electrostimulation–induced nuclear translocation of endogenous NFATc1 in rabbit primary skeletal muscle cells. Nuclear import of NFATc1 only occurred with a stimulation that mimicked slow motor neuron activity, leading also to the upregulation of *MyHC slow* mRNA expression (Kubis et al., 2002, 2003). Additionally, electrical stimulation–induced nuclear translocation of NFATc1-GFP and NFATc3-mRFP (monomeric red fluorescent protein) constructs in single fibers from adult *flexor digitorum brevis* (FDB) muscle was shown to be calcineurin dependent (Shen et al., 2006). Taken together, these data demonstrate that NFAT isoforms c1 and c3 are targets of calcineurin in skeletal muscle.

Although NFATs are targets of calcineurin–NFAT activation alone may not be sufficient to activate transcription of slow genes. For instance, a synthetic promoter containing the putative NFAT-binding site from the *myoglobin* promoter was not activated by constitutively active calcineurin, but the addition of MEF2-and Sp1-binding sites to the promoter construct led to a robustly strong response to calcineurin (Chin et al., 1998). It was reported that a slow *myosin light chain 2* (MLC2) promoter construct was not activated by coinjection with an *NFATc1* expression plasmid in rat *soleus* muscle (Swoap et al., 2000); this finding, however, might be related to the use of a relatively short promoter fragment (270 bp). Furthermore, as highlighted in Section 4.3, experiments with calcineurin catalytic Aβ subunit null mice showed no change in NFAT nuclear translocation which suggests that reduction of oxidative/slow fibers in such mice is independent of NFAT (Parsons et al., 2003). Clearly, there is a need to investigate the regulation of a larger number of slow type genes to determine the relative contribution of calcineurin and NFATs to their expression.

Calcineurin is involved in the regulation of MEF2 activity in skeletal muscle. MEF2 belongs to the family of MADS (MCM1, agamas, deficient, serum response factor) box transcription factors (McKinsey et al., 2002a). The MEF2 isoforms A, B, C, and D are expressed in distinct but overlapping patterns during muscle differentiation and in adult muscle. MEF2 activity is dependent on the phosphorylation state of its multiple phosphorylation sites (Cox et al., 2003). *In vivo*, calcineurin activates MEF2A and D by dephosphorylation in the *plantaris* muscle of transgenic mice carrying CnA$\star$ (Dunn et al., 2000). Slow pattern type electrical stimulation led to

calcineurin-dependent dephosphorylation of MEF2D in the fast *medial gastrocnemius*, and expression of a MEF2 promoter–reporter construct in fast glycolytic MyHC IIB fibers of the *plantaris* muscle (Dunn et al., 2001). Calcineurin increases MEF2A transactivation function *in vitro* by dephosphorylation of the transactivation domain (Wu et al., 2001). DNA binding of MEF2A can also be enhanced via phosphorylation of the DNA-binding domain by CaMKIV, demonstrating that the regulation of MEF2A transcriptional function is complex with different phosphorylation sites and signaling molecules involved. Indeed, calcineurin and CaMKIV can synergistically enhance a MEF2 reporter in C2C12 myotubes (Wu et al., 2000a). Moreover, MEF2-dependent reporter gene stimulation by sustained periods of endurance exercise or electrical pacing was ablated by CsA or an endogenous inhibitor of calcineurin, MCIP1 (myocyte-enriched calcineurin interacting protein 1). This finding suggests that calcineurin–MEF2 signaling is important for gene expression of the slow fiber type program in response to nerve activity. Targets for MEF2 in slow fibers comprise *MyHC slow*, *slow TnI*, and *myoglobin*. CnA★ transgenic mice show expression of slow TnI in the fast white *vastus lateralis* muscle (Wu et al., 2001). All four MEF2 isoforms can activate the SURE (slow upstream regulatory element) enhancer in the *slow TnI* promoter in a calcineurin-dependent manner (Wu et al., 2000a). In addition, CnA★ can activate a synthetic promoter containing a MEF2-binding site from the myoglobin promoter (Chin et al., 1998). In summary, there is a growing body of evidence to show that calcineurin–MEF2 signaling is crucial to slow fiber type-specific gene expression.

Few data exist that demonstrate an interaction between the two calcineurin target families NFAT and MEF2 in slow fiber type-specific gene expression. NFATc1 and MEF2D have been shown to interact with MyoD and the transcriptional coactivator p300 in the calcium ionophore-induced upregulation of the rabbit *MyHC slow*-promoter in a calcineurin–dependent manner in C2C12 myotubes (Meissner et al., 2007b) (Fig. 2.3). All four factors are detected as a multimeric complex at an NFAT-binding site with an adjacent E-box in the *MyHC slow* promoter after ionophore treatment of myotubes, as demonstrated by chromatin immunoprecipitation and gel shift assays (Meissner et al., 2007b). It was also shown that MEF2 and NFAT are required for innervation-induced slow avian *MyHC2* expression (Jiang et al., 2004). Moreover, there is collaborative interaction of the respective proteins at the NFAT-, MEF2-, and Sp1-binding sites of the myoglobin promoter in response to calcineurin (Chin et al., 1998). It is likely that coordinated slow fiber program is mediated through site-specific regulatory elements by specific temporal and spatial assembly of multimeric complexes of transcription and regulatory cofactors (Fig. 2.3).

Although NFATc1 and MEF2 interact in the activation of slow fiber type-specific gene expression, their roles are not confined to slow gene activation. NFATc1 is involved in the repression of fast *MyHC* isoforms *IIb*
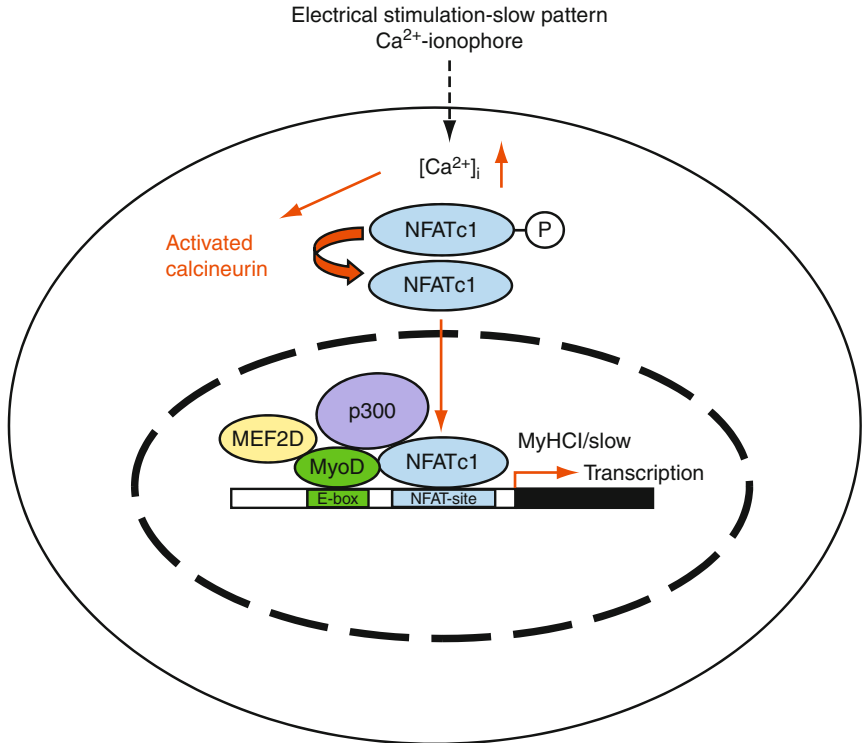
Figure 2.3   A model of transcription factor and coactivator assembly on the MyHC slow/I promoter in response to increased intracellular calcium concentration. The model shown is deduced from work in primary skeletal myotubes (Kubis et al., 1997; Meissner et al., 2001) and in C2C12 myotubes (Kubis et al., 2003; Meissner et al., 2007b). The calcineurin-NFATc1 signaling pathway is activated *in vitro* by Ca^{2+}-ionophore A23187 or electrostimulation with a pattern mimicking slow fiber nerve activity, resulting in raised intracellular calcium concentration. NFATc1 dephosphory-lated by activated calcineurin translocates to the nuclei of myotubes, where it binds to a proximal NFAT-binding site (-457/-439) in the rabbit *MyHC slow* promoter. NFATc1 interacts with MyoD bound to an E-box (-462/-457) adjacent to the NFATc1 site. The transcriptional coactivator p300, and MEF2D were recruited to the complex in a calcineurin-dependent manner. All three transcription factors as well as p300 transacti-vate the MyHC slow promoter in response to increased intracellular calcium. The model proposes a mechanism of MyHC slow upregulation during fast-to-slow fiber type transformation. The diagram is not drawn to scale.

and *IIx* (McCullagh et al., 2004; Meissner et al., 2007b), possibly by recruitment of the transcriptional corepressor HDAC as seen in NFATc2-mediated repression of *cyclin-dependent kinase 4* (*cdk4*) gene expression in T cells (Baksh et al., 2002). In addition, binding sites for MEF2 are commonly found in muscle–specific genes (Blake et al., 2002). MEF2 has been demon-strated to confer transcriptional activity on *MyHCIIb* and *IIx* promoters

which shows that MEF2 actions are not restricted to slow genes (Allen et al., 2005; Meissner et al., 2007a).

The transcriptional coactivator PGC-1α was shown to be involved in slow fiber type-specific gene expression in cooperation with calcineurin (Lin et al., 2002). PGC-1α transgenic mice, driven by a muscle creatine kinase (MCK) promoter, show an increase in slow and a decrease in fast TnI protein expression. Along with the upregulation of mitochondrial genes like cytochrome *c* oxidase (COX) II and IV, the data concluded that PGC-1α can drive the formation of slow type muscle fibers. PGC-1α activates transcription in cooperation with calcineurin and MEF2. Coexpression of PGC-1α in C2C12 cells with calcineurin increases the activating effect of calcineurin on *myoglobin* and *slow TnI* promoter activities. Overexpression of PGC-1α alone has only a minor effect. The *slow TnI* promoter was coactivated by MEF2 isoforms and PGC-1α, and coactivation of the *myoglobin* promoter required a proximal MEF2 site (Lin et al., 2002). Whether PGC-1α can serve as a direct target of calcineurin or directly interacts and activates MEF2 proteins remains to be fully elucidated.

A target of calcineurin–NFAT signaling, utrophin A, is an analog of the cytoskeletal protein dystrophin. Dystrophin is associated with the sarcolemma, as part of a large complex of transmembrane proteins named the dystrophin-associated protein complex (Blake et al., 2002). Utrophin A is expressed in patients with Duchenne muscular dystrophy (DMD) instead of dystrophin (Miura and Jasmin, 2006). DMD patients are characterized by a lack of dystrophin associated with severe muscle weakness, eventually leading to death. Overexpression of utrophin A has been considered to be a therapeutic approach for treating DMD (Miura and Jasmin, 2006). Using transgenic mice expressing CnA⋆, it has been shown that utrophin expression is dependent on calcineurin and its effector NFATc1 (Chakkalakal et al., 2003). Indeed, crossbreeding experiments demonstrated an attenuated pathological phenotype in dystrophin-deficient mdx mice overexpressing constitutively active calcineurin (Chakkalakal et al., 2004). Recently, a posttranscriptional mechanism has been implicated in conferring the higher levels of utrophin A mRNA found in slower fibers. Decay of mRNA in fast fibers was shown to be mediated by an AU-rich element (ARE) in the 3′-untranslated region (3′-UTR), with the stability of the mRNA depending on calcineurin *in vivo* and *in vitro* (Chakkalakal et al., 2008).

Myostatin is a member of transforming growth factor-beta (TGF-*β*) family of signaling proteins, acting as a negative regulator of skeletal muscle growth (McPherron et al., 1997). Calcineurin has also been implicated in the regulation of myostatin expression by *in vivo* experiments using genetic and pharmacological approaches (Michel et al., 2007). Accordingly, *myostatin* knockout leads to faster and more glycolytic phenotype (Girgenrath et al., 2005). Surprisingly, myostatin is able to downregulate the calcineurin–NFAT pathway in a negative regulatory control loop (Michel

et al., 2007). The *myostatin* promoter harbors three potential NFAT-binding sites, but the precise mechanism of myostatin regulation by calcineurin has not yet emerged.

From the collective calcineurin data on skeletal muscle, a picture is emerging to show a dual effect of calcineurin signaling that culminates in the activation of target genes in slow and oxidative fibers, and repression of genes in fast fiber types, both correlated with the recruitment of appropriate transcription factors and cofactors (Fig. 2.4).

5.2. Calcineurin interactions with other signaling pathways

As a signaling pathway, it is no surprise that calcineurin does not operate in isolation. Besides the involvement of the aforementioned calcium-dependent protein kinases C and calmodulin kinases pathways in slow fiber conversion, the activities of calcineurin is closely interconnected to other key signaling pathways through interactions with factors and cofactors associated with other networks.

Besides calcium, the activation of calcineurin is, at least in part, under the regulation of binding cofactors known as modulatory calcineurin-interacting proteins (MCIPs or RCANs) of which there are three corresponding gene members (Rothermel et al., 2003). MCIP1 (RCAN1 or DSCR1) and MCIP2 (RCAN2, ZAKI-4, or DSCR1L1) are highly expressed in striated muscles and brain (Rothermel et al., 2001; Yang et al., 2000). At high concentrations they act as inhibitors of calcineurin as were originally reported. MCIP1 is induced by calcineurin, thus forming a negative feedback loop to limit calcineurin activation (Yang et al., 2000); its overexpression in transgenic mice prevented cardiac hypertrophy (Rothermel et al., 2001; van Rooij et al., 2004). The role of MCIP2 is particularly relevant in the context of skeletal muscle as, unlike MCIP1, it is responsive to thyroid hormone stimulation (Cao et al., 2002). However, as subsequently discovered, endogenous (low) MCIP levels are also potent activators of calcineurin in the heart (Sanna et al., 2006; Vega et al., 2003). Therefore, the modulating influence of MCIPs on calcineurin is dose dependent.

Diverse extracellular ligands, such as interleukin (IL)-1, IL-18, and tumor necrosis factor-α (TNFα), signal through the intermediate complex of TAK1–TAB1–TAB2 (TGFβ-activated kinase 1–TAK1-binding protein 1–TAK1-binding protein 2) (Fig. 2.4). It was recently shown in neonatal cardiomyocytes that this complex physically binds and phosphorylates (via TAK1) MCIP1 at ser94 and ser136 which converts MCIP1 into a calcineurin activator, leading to NFAT activation and subsequent cardiac hypertrophy (Liu et al., 2009). In turn, activated calcineurin dephosphorylates (inactivates) TAK1 and TAB1 in a negative feedback manner. TAK1 and TAB1 are thus substrates of calcineurin dephosphorylation. Therefore, TAK1 is a positive regulator of calcineurin–NFAT activity in
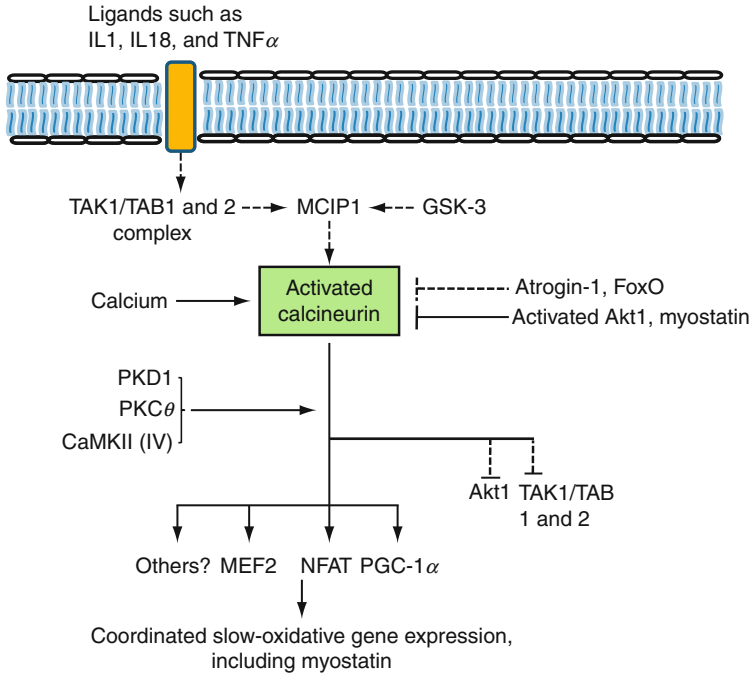
Figure 2.4 Summary of calcineurin signaling interactions. High-sustained intracellular calcium concentration is the primary driver that activates calcineurin (Bassel-Duby and Olson, 2003; Fraysse et al., 2003; Kubis et al., 2003; Liu et al., 2001), which dephosphorylates a range of transcription factors (including MEF2 and NFAT), cofactors (including PGC-1α), and kinases (including Akt1 and TAK1/TAB1 and 2). Activated calcineurin synergistically cooperates with PKD1 and members of PKC family, in particular PKCθ, and CaMKs to strongly induce a coordinated slow oxidative fiber phenotype (solid lines refer to findings based on skeletal muscle). Studies from cardiac muscle or nonmammalian species (indicated by broken lines) showed that activated TAK1/TAB1 and 2 complex (Liu et al., 2009) or GSK-3 (Hilioti et al., 2004) mediates the phosphorylation of endogenous MCIP1, which in turn activates calcineurin. Note that high levels of MCIPs, through overexpression, were first reported to inhibit calcineurin (Rothermel et al., 2001). A wide range of ligands (such as IL1, IL18, and TNFα) can activate TAK1 which indicate that various cytokines could have modulatory roles on calcineurin activation. In turn, calcineurin is inhibited (indicated by blunt ''T'' endings) by transcription factors like FoxO (Ni et al., 2006), factors such as atrogin-1 (Li et al., 2004) and myostatin (Michel et al., 2007), and by kinases including activated Akt1 (Rommel et al., 2001). Note that arrows indicate stimulation or activation. Given the complexity of coordinated oxidative fiber regulation, it is plausible that there are as yet unidentified effector factors (designated as ''others?'') downstream of calcineurin that collaborate with well-known factors, such as MEF2 and NFATs, to establish the slow program.

cardiomyocytes through MCIP1 facilitation (phosphorylation). It remains to be seen if TAK1 plays a functional role in calcineurin-mediated changes in skeletal muscle.

In yeast, RCN1 (homolog of MCIP1) is a target of phosphorylation at ser113 by MCK1, a member of GSK-3 (glycogen synthase kinase-3) family of kinases (Hilioti et al., 2004), which in turn stimulates calcineurin signaling. Conversely, dephosphorylation of RCN1 inhibits calcineurin activation. This finding further highlights MCIPs as key controls of calcineurin activity.

The interactive outcomes of FoxO (O subfamily of Forkhead/winged helix) transcription factors with the insulin/IGF1 signaling pathway (PI3K-Akt1 signaling) are not always clear-cut. There are both positive and negative effects. In neonatal cardiomyocytes, overexpression of FoxO increases Akt phosphorylation and kinase activity, which, unexpectedly, results in decreased insulin response with reduced glucose uptake. In turn, direct and multiple phosphorylation by Akt on FoxO factors leads to their displacement from the nucleus to the cytoplasm and to the inhibition of their transcriptional activities (Burgering and Medema, 2004). In cardiomyocytes, calcineurin directly binds and dephosphorylates (inactivates) Akt; FoxO indirectly activates Akt by inhibiting calcineurin phosphatase activity (Ni et al., 2006, 2007). In murine C2C12 myotubes, Akt was shown to antagonize calcineurin signaling by causing hyperphosphorylation of NFATc1 (Rommel et al., 2001). Thus, there are clear antagonistic interactions between Akt-calcineurin in cardiomyocytes and skeletal myotubes (Fig. 2.4).

Atrogin-1, also known as muscle atrophy F-box (MAFbx), is an E3 ubiquitin ligase that mediates skeletal muscle atrophy (Bodine et al., 2001a; Dehoux et al., 2003). In cardiomyocytes, atrogin-1 functions as an adaptor protein that targets calcineurin at the Z-line for ubiquitin-dependent proteasome degradation (Li et al., 2004). Overexpression of atrogin-1 *in vivo* blunts cardiac hypertrophy induced by aorta banding. It would be interesting to determine if atrogin-1 can also specifically target calcineurin breakdown in skeletal muscle (Fig. 2.4).

6. EXPLOITING THE BENEFICIAL EFFECTS OF CALCINEURIN SIGNALING IN SKELETAL MUSCLE

The potential to alter muscle fiber type composition through calcineurin signaling has many implications in human metabolic conditions. The identification of downstream targets of calcineurin is, however, needed to minimize the undesirable effects of activating the entire calcineurin signaling network, especially in nonskeletal muscle, such as cardiac muscle. Identification of effector protein or gene targets that are preferentially expressed in skeletal muscle will provide an opportunity for achieving tissue-restricted modulation of calcineurin signaling. This chapter highlights some

differences in expression of specific NFAT, MEF2, and GATA isoforms in response to calcineurin signaling in cardiac and skeletal muscle. Although these transcription factors may not represent the most ideal targets for pharmaceutical manipulation, they nevertheless illustrate the strategic relevance of identifying downstream calcineurin effector targets with restricted tissue expression as candidate drug targets. Indeed, as indicated in Sections 4.2 and 5.1, the artificial peptide VIVIT, an NFAT inhibitor, has been shown to be a potent inhibitor of cardiac hypertrophy (Aramburu et al., 1999; Yu et al., 2007). Drug-induced activation or inhibition of calcineurin effector targets in skeletal muscle can have important medical applications, including increased muscle mass or alteration of metabolic properties of skeletal muscle for therapeutic benefit in several modes of human disease.

Given the complexity of coordinated oxidative fiber regulation, it is plausible that there are as yet unidentified downstream effector factors of calcineurin that collaborate with known factors, such as MEF2 and NFATs, to establish the slow program. The use of microarray gene expression analysis to study oxidative fiber type conversion is helpful in highlighting a list of candidate genes that could mediate the fast-to-slow fiber type transformation. However, it is difficult to distinguish between a primary and a secondary response to calcineurin signaling based on differential gene expression alone. A powerful complement to expression profiling is to perform ChIP-on-chip assays, based on chromatin binding of calcineurin–transcription factor complexes (Cao et al., 2006; Hawkins and Ren, 2006) (Fig. 2.2B). Through this combined approach, differentially expressed genes that are under the primary transcriptional control of activated calcineurin can be more readily identified. In this context, it is worth to mention that the role of calcineurin in the regulation of metabolic adaption, for example, during fast-to-slow fiber type transformation, needs further investigation. So far, it has been demonstrated that calcineurin can coregulate contractile and metabolic components of slow muscle phenotype (Bigard et al., 2000). In contrast to the contractile apparatus, much less is known about the calcineurin effector targets in the regulation of energy metabolism or in the regulation of calcium handling. The identification and understanding of the regulation of such genes at the level of promoters might point to valuable targets for therapeutic intervention.

7. Concluding Remarks

A thorough understanding of the molecular mechanisms that govern the coordinated regulation of slow oxidative fibers is important because of the vital roles of oxidative fibers in skeletal muscle in the promotion of metabolic health. An overall picture has emerged on the central role of calcineurin in collaboration with other key signaling pathways and their

intermediates (such as PKD1, PKCθ, CaMKII, Akt1, and PGC-1α) in the direction of a slow oxidative gene expression program. While a few transcription factor families (namely NFAT and MEF2) have been well documented to play pivotal roles in the calcineurin mediation of slow genes expression, it is likely that there remain to be discovered additional positive or even negative transcription factors or cofactors that act in concert with NFAT and MEF2 factors. Hence, a future challenge is to understand the regulatory patterns of interactions between specific transcription factors and cofactors at chromatin sites of slow gene isoforms. Already it has been shown that MEF2 activation is dependent in part on the phosphorylation of class II HDACs by PKD1 (Section 3.1) and CaMKII (Section 3.2). It is anticipated that more will be known about the effects of calcineurin signaling at the level of chromatin interactions. A further relevant issue in calcineurin-mediated oxidative fiber type conversion relates to the observation that fast *MyHC IIx* and *IIb* genes appear to be actively downregulated by activated calcineurin. This finding suggests the possibility that calcineurin can actively repress fast muscle genes, in addition to promoting the expression of slow genes. At present, virtually nothing is known about how calcineurin may repress the fast muscle program.

ACKNOWLEDGMENT

REFERENCES

Abou, M.J., Yakubu, F., Lin, D., Peters, J.C., Atkinson, J.B., Hill, J.O., 1992. Skeletal muscle composition in dietary obesity-susceptible and dietary obesity-resistant rats. Am. J. Physiol. Regul. Integr. Comp. Physiol. 262, R684–R688.

Akimoto, T., Ribar, T.J., Williams, R.S., Yan, Z., 2004. Skeletal muscle adaptation in response to voluntary running in Ca^{2+}/calmodulin-dependent protein kinase IV-deficient mice. Am. J. Physiol. Cell Physiol. 287, C1311–C1319.

Akimoto, T., Pohnert, S.C., Li, P., Zhang, M., Gumbs, C., Rosenberg, P.B., et al., 2005. Exercise stimulates *Pgc-1α* transcription in skeletal muscle through activation of the p38 MAPK pathway. J. Biol. Chem. 280, 19587–19593.

Allen, D.L., Leinwand, L.A., 2002. Intracellular calcium and myosin isoform transitions. Calcineurin and calcium-calmodulin kinase pathways regulate preferential activation of the IIa myosin heavy chain promoter. J. Biol. Chem. 277, 45323–45330.

Allen, D.L., Sartorius, C.A., Sycuro, L.K., Leinwand, L.A., 2001. Different pathways regulate expression of the skeletal myosin heavy chain genes. J. Biol. Chem. 276, 43524–43533.

Allen, D.L., Weber, J.N., Sycuro, L.K., Leinwand, L.A., 2005. Myocyte enhancer factor-2 and serum response factor binding elements regulate fast myosin heavy chain transcription *in vivo*. J. Biol. Chem. 280, 17126–17134.

Antipenko, A., Frias, J.A., Parra, J., Cadefau, J.A., Cusso, R., 1999. Effect of chronic electrostimulation of rabbit skeletal muscle on calmodulin level and protein kinase activity. Int. J. Biochem. Cell Biol. 31, 303–310.

Aramburu, J., Yaffe, M.B., López-Rodriguez, C., Cantley, L.C., Hogan, P.G., Rao, A., 1999. Affinity-driven peptide selection of an NFAT inhibitor more selective than cyclosporin A. Science 285, 2129–2133.

Baksh, S., Widlund, H.R., Frazer-Abel, A.A., Du, J., Fosmire, S., Fisher, D.E., et al., 2002. NFATc2-mediated repression of cyclin-dependent kinase 4 expression. Mol. Cell 10, 1071–1081.

Bassel-Duby, R., Olson, E.N., 2003. Role of calcineurin in striated muscle: development, adaptation, and disease. Biochem. Biophys. Res. Commun. 311, 1133–1141.

Bigard, X., Sanchez, H., Zoll, J., Mateo, P., Rousseau, V., Veksler, V., et al., 2000. Calcineurin co-regulates contractile and metabolic components of slow muscle pheno-type. J. Biol. Chem. 275, 19653–19660.

Blake, D.J., Weir, A., Newey, S.E., Davies, K.E., 2002. Function and genetics of dystrophin and dystrophin-related proteins in muscle. Physiol. Rev. 82, 291–329.

Bodine, S.C., Latres, E., Baumhueter, S., Lai, V.K.M., Nunez, L., Clarke, B.A., et al., 2001a. Identification of ubiquitin ligases required for skeletal muscle atrophy. Science 294, 1704–1708.

Bodine, S.C., Stitt, T.N., Gonzalez, M., Kline, W.O., Stover, G.L., Bauerlein, R., et al., 2001b. Akt/mTOR pathway is a crucial regulator of skeletal muscle hypertrophy and can prevent muscle atrophy in vivo. Nat. Cell Biol. 3, 1014–1019.

Bourajjaj, M., Armand, A.S., Costa Martins, P.A., Weijts, B., van der Nagel, R., Heeneman, S., et al., 2008. NFATc2 is a necessary mediator of calcineurin-dependent cardiac hypertrophy and heart failure. J. Biol. Chem. 283, 22295–22303.

Brooke, M.H., Kaiser, K.K., 1970. Muscle fiber types: how many and what kind? Arch. Neurol. 23, 369–379.

Bueno, O.F., De Windt, L.J., Tymitz, K.M., Witt, S.A., Kimball, T.R., Klevitsky, R., et al., 2000. The MEK1-ERK1/2 signaling pathway promotes compensated cardiac hypertro-phy in transgenic mice. EMBO J. 19, 6341–6350.

Bueno, O.F., van Rooij, E., Molkentin, J.D., Doevendans, P.A., De Windt, L.J., 2002a. Calcium and hypertrophic heart disease: novel insights and remaining questions. Cardi-ovasc. Res. 53, 806–821.

Bueno, O.F., Wilkins, B.J., Tymitz, K.M., Glascock, B.J., Kimball, T.F., Lorenz, J.N., 2002b. Impaired cardiac hypertrophic response in calcineurin Aβ-deficient mice. Proc. Natl. Acad. Sci. USA 99, 4586–4591.

Burgering, B.M.T., Medema, R.H., 2004. Decisions on life and death: FOXO forkhead transcription factors are in command when PKB/Akt is off duty. J. Leukoc. Biol. 73, 689–701.

Cao, X., Kambe, F., Miyazaki, T., Sarkar, D., Ohmori, S., Seo, H., 2002. Novel human ZAKI-4 isoforms: hormonal and tissue-specific regulation and function as calcineurin inhibitors. Biochem. J. 367, 459–466.

Cao, Y., Kumar, R.M., Penn, B.H., Berkes, C.A., Kooperberg, C., Boyer, L.A., et al., 2006. Global and gene-specific analyses show distinct roles for Myod and Myog at a common set of promoters. EMBO J. 25, 502–511.

Chakkalakal, J.V., Stocksley, M.A., Harrison, M.A., Angus, L.M., Deschenes-Furry, J., St Pierre, S., et al., 2003. Expression of utrophin A mRNA correlates with the oxidative capacity of skeletal muscle fiber types and is regulated by calcineurin–NFAT signaling. Proc. Natl. Acad. Sci. USA 100, 7791–7796.

Chakkalakal, J.V., Harrison, M.A., Carbonetto, S., Chin, E., Michel, R.N., Jasmin, B.J., 2004. Stimulation of calcineurin signaling attenuates the dystrophic pathology in mdx mice. Hum. Mol. Genet. 13, 379–388.

Chakkalakal, J.V., Miura, P., Belanger, G., Michel, R.N., Jasmin, B.J., 2008. Modulation of utrophin A mRNA stability in fast versus slow muscles via an AU-rich element and calcineurin signaling. Nucleic Acids Res. 36, 826–838.

Chang, K.C., Fernandes, K., 1997. Developmental expression and 5′ end cDNA cloning of the porcine 2x and 2b myosin heavy chain genes. DNA Cell Biol. 16, 1429–1437.

Chang, K.C., Fernandes, K., Goldspink, G., 1993. In vivo expression and molecular characterization of the porcine slow-myosin heavy chain. J. Cell Sci. 106, 331–341.

Chang, K.C., Fernandes, K., Dauncey, M.J., 1995. Molecular characterization of a developmentally regulated porcine skeletal myosin heavy chain gene and its 5′ regulatory region. J. Cell Sci. 108, 1779–1789.

Chikuni, K., Muroya, S., Nakajima, I., 2004. Absence of the functional myosin heavy chain 2b isoform in equine skeletal muscles. Zool. Sci. 21, 589–596.

Chin, E.R., 2004. The role of calcium and calcium/calmodulin-dependent kinases in skeletal muscle plasticity and mitochondrial biogenesis. Proc. Nutr. Soc. 63, 279–286.

Chin, E.R., Olson, E.N., Richardson, J.A., Yang, Q., Humphries, C., Shelton, J.M., et al., 1998. A calcineurin-dependent transcriptional pathway controls skeletal muscle fiber type. Genes Dev. 12, 2499–2509.

Clerk, A., Cullingford, T.E., Fuller, S.J., Giraldo, A., Markou, T., Pikkarainen, S., et al., 2007. Signaling pathways mediating cardiac myocyte gene expression in physiological and stress responses. J. Cell. Physiol. 212, 311–322.

Coggan, A.R., Spina, R.J., King, D.S., Rogers, M.A., Brown, M., Nemeth, P.M., et al., 1992. Histochemical and enzymatic comparison of the gastrocnemius muscle of young and elderly men and women. J. Gerontol. 47, B71–B76.

Cox, D.M., Du, M., Marback, M., Yang, E.C., Chan, J., Siu, K.W., et al., 2003. Phosphorylation motifs regulating the stability and function of myocyte enhancer factor 2A. J. Biol. Chem. 278, 15297–15303.

Crabtree, G.R., 2001. Calcium, calcineurin, and the control of transcription. J. Biol. Chem. 276, 2313–2316.

da Costa, N., Edgar, J., Ooi, P.T., Su, Y., Meissner, J.D., Chang, K.C., 2007. Calcineurin differentially regulates fast myosin heavy chain genes in oxidative muscle fibre type conversion. Cell Tissue Res. 329, 515–527.

D'Andrea, M., Pisaniello, A., Serra, C., Senni, M.I., Castaldi, L., Molinaro, M., et al., 2006. Protein kinase C theta co-operates with calcineurin in the activation of slow muscle genes in cultured myogenic cells. J. Cell. Physiol. 207, 379–388.

Dehoux, M.J.M., van Beneden, R.P., Fernandez-Celemin, L., Lause, P.L., Thissen, J.P., 2003. Induction of MafBx and Murf ubiquitin ligase mRNAs in rat skeletal muscle after LPS injection. FEBS Lett. 544, 214–217.

Delling, U., Tureckova, J., Lim, H.W., De Windt, L.J., Rotwein, P., Molkentin, J.D., 2000. A calcineurin–NFATc3-dependent pathway regulates skeletal muscle differentiation and slow myosin heavy-chain expression. Mol. Cell. Biol. 20, 6600–6611.

DiMario, J.X., 2001. Protein kinase C signaling controls skeletal muscle fiber types. Exp. Cell Res. 263, 23–32.

DiMario, J.X., Funk, P.E., 1999. Protein kinase C activity regulates slow myosin heavy chain 2 gene expression in slow lineage skeletal muscle fibers. Dev. Dyn. 216, 177–189.

DiMario, J.X., Stockdale, F.E., 1997. Both myoblast lineage and innervation determine fiber type and are required for expression of the slow myosin heavy chain 2. Dev. Biol. 188, 167–180.

Doherty, T.J., 2003. Invited review: aging and sarcopenia. J. Appl. Physiol. 95, 1717–1727.

Donnelly, R., Reed, M.J., Azhar, S., Reaven, G.M., 1994. Expression of the major isoenzyme of protein kinase-C in skeletal muscle, nPKC theta, varies with muscle type and in response to fructose-induced insulin resistance. Endocrinology 135, 2369–2374.

Dunn, S.E., Chin, E.R., Michel, R.N., 2000. Matching of calcineurin activity to upstream effectors is critical for skeletal muscle fiber growth. J. Cell Biol. 151, 663–672.

Dunn, S.E., Simard, A.R., Bassel-Duby, R., Williams, R.S., Michel, R.N., 2001. Nerve activity-dependent modulation of calcineurin signaling in adult fast and slow skeletal muscle fibers. J. Biol. Chem. 276, 45243–45254.

Faulkner, J.A., Larkin, L.M., Claflin, D.R., Brooks, S.V., 2007. Age-related changes in the structure and function of skeletal muscles. Clin. Exp. Pharmacol. Physiol. 34, 1091–1096.

Fluck, M., Booth, F.W., Waxham, M.N., 2000a. Skeletal muscle CaMKII enriches in nuclei and phosphorylates myogenic factor SRF at multiple sites. Biochem. Biophys. Res. Commun. 270, 488–494.

Fluck, M., Waxham, M.N., Hamilton, M.T., Booth, F.W., 2000b. Skeletal muscle Ca^{2+}-independent kinase activity increases during either hypertrophy or running. J. Appl. Physiol. 88, 352–358.

Fraysse, B., Desaphy, J.F., Pierno, S., De Luca, A., Liantonio, A., Mitolo, C.I., et al., 2003. Decrease in resting calcium and calcium entry associated with slow-to-fast transition in unloaded rat soleus muscle. FASEB J. 17, 1916–1918.

Freyssenet, D., Di Carlo, M., Hood, D.A., 1999. Calcium-dependent regulation of cytochrome *c* gene expression in skeletal muscle cells. Identification of a protein kinase c-dependent pathway. J. Biol. Chem. 274, 9305–9311.

Friday, B.B., Horsley, V., Pavlath, G.K., 2000. Calcineurin activity is required for the initiation of skeletal muscle differentiation. J. Cell Biol. 149, 657–665.

Friday, B.B., Mitchell, P.O., Kegley, K.M., Pavlath, G.K., 2003. Calcineurin initiates skeletal muscle differentiation by activating MEF2 and MyoD. Differentiation 71, 217–227.

Gamble, M.J., Freedman, L.P., 2002. A coactivator code for transcription. Trends Biochem. Sci. 27, 165–167.

Gil, F., Lopez-Albors, O., Vazquez, J.M., Latorre, R., Ramirez-Zarzosa, G., Moreno, F., 2001. The histochemical profiles of fibre types in porcine skeletal muscle. Histol. Histopathol. 16, 439–442.

Girgenrath, S., Song, K., Whittemore, L.A., 2005. Loss of myostatin expression alters fiber-type distribution and expression of myosin heavy chain isoforms in slow- and fast-type skeletal muscle. Muscle Nerve 31, 34–40.

Hawkins, R.D., Ren, B., 2006. Genome-wide location analysis: insights on transcriptional regulation. Hum. Mol. Genet. 15, R1–R7.

He, J., Watkins, S., Kelley, D.E., 2001. Skeletal muscle lipid content and oxidative enzyme activity in relation to muscle fiber type in type 2 diabetes and obesity. Diabetes 50, 817–823.

Heinke, J., Molkentin, J.D., 2006. Regulation of cardiac hypertrophy by intracellular signalling pathways. Nat. Rev. Mol. Cell Biol. 7, 589–600.

Herzig, T.C., Jobe, S.M., Aoki, H., Molkentin, J.D., Cowley Jr., A.W., Izumo, S., et al., 1997. Angiotensin II type1a receptor gene expression in the heart: AP-1 and GATA-4 participate in the response to pressure overload. Proc. Natl. Acad. Sci. USA 94, 7543–7548.

Hickey, M.S., Carey, J.O., Azevedo, J.L., Houmard, J.A., Pories, W.J., Israel, R.G., et al., 1995a. Skeletal muscle fiber composition is related to adiposity and *in vitro* glucose transport rate in humans. Am. J. Physiol. Endocrinol. Metab. 268, E453–E457.

Hickey, M.S., Weidner, M.D., Gavigan, K.E., Zheng, D., Tyndall, G.L., Houmard, J.A., 1995b. The insulin action-fiber type relationship in humans is muscle group specific. Am. J. Physiol. Endocrinol. Metab. 269, E150–E154.

Hilioti, Z., Gallagher, D.A., Low-Nam, S.T., Ramaswamy, P., Gajer, P., Kingsbury, T.J., et al., 2004. GSK-3 kinases enhance calcineurin signaling by phosphorylation of RCNs. Genes Dev. 18, 35–47.

Hoey, T., Sun, Y.L., Williamson, K., Xu, X., 1995. Isolation of two new members of the NF-AT gene family and functional characterization of the NF-AT proteins. Immunity 2, 461–471.

Hogan, P.G., Chen, L., Nardone, J., Rao, A., 2003. Transcriptional regulation by calcium, calcineurin and NFAT. Genes Dev. 17, 2205–2232.

Hook, S.S., Means, A.R., 2001. Ca^{2+}/CaM-dependent kinases: from activation to function. Annu. Rev. Pharmacol. Toxicol. 41, 471–505.

Horowitz, J.F., Sidossis, L.S., Coyle, E.F., 1994. High efficiency of type I muscle fibers improves performance. Int. J. Sports Med. 15, 152–157.

Horsley, V., Pavlath, G.K., 2002. NFAT: ubiquitous regulator of cell differentiation and adaptation. J. Cell Biol. 156, 771–774.

Horsley, V., Friday, B.B., Matteson, S., Kegley, K.M., Gephart, J., Pavlath, G.K., 2001. Regulation of the growth of multinucleated muscle cells by an NFATC2-dependent pathway. J. Cell Biol. 153, 329–338.

Horton, M.J., Brandon, C.A., Morris, T.J., Braun, T.W., Yaw, K.M., Sciote, J.J., 2001. Abundant expression of myosin heavy-chain IIB RNA in a subset of human masseter muscle fibres. Arch. Oral Biol. 46, 1039–1050.

Houmard, J.A., Weidner, M.L., Gavigan, K.E., Tyndall, G.L., Hickey, M.S., Alshami, A., 1998. Fiber type and citrate synthase activity in the human gastrocnemius and vastus lateralis with aging. J. Appl. Physiol. 85, 1337–1341.

Im, S.H., Rao, A., 2004. Activation and deactivation of gene expression by Ca^{2+}/calcineurin–NFAT-mediated signaling. Mol. Cells 18, 1–9.

Jarvis, J.C., Mokrusch, T., Kwende, M.M., Sutherland, H., Salmons, S., 1996. Fast-to-slow transformation in stimulated rat muscle. Muscle Nerve 19, 1469–1475.

Jiang, H., Jordan, T., Li, J., Li, H., DiMario, J.X., 2004. Innervation-dependent and fiber type-specific transcriptional regulation of the slow myosin heavy chain 2 promoter in avian skeletal muscle fibers. Dev. Dyn. 231, 292–302.

Jordan, T., Li, J., Jiang, H., DiMario, J.X., 2003. Repression of slow myosin heavy chain 2 gene expression in fast skeletal muscle fibers by muscarinic acetylcholine receptor and Gαq signaling. J. Cell Biol. 162, 843–850.

Kalkhoven, E., 2004. CBP and p300: HATs for different occasions. Biochem. Pharmacol. 68, 1145–1155.

Karlsson, A.H., Klont, R.E., Fernandez, X., 1999. Skeletal muscle fibres as factors for pork quality. Livestock Production Science 60, 225–269.

Kawamura, T., Ono, K., Morimoto, T., Akao, M., Iwai-Kanai, E., Wada, H., et al., 2004. Endothelin-1-dependent nuclear factor of activated T-lymphocytes signaling associates with transcriptional coactivator p300 in the activation of the B cell leukemia-2 promoter in cardiac myocytes. Circ. Res. 94, 1492–1499.

Kegley, K.M., Gephart, J., Warren, G.L., Pavlath, G.K., 2001. Altered primary myogenesis in NFATC3-/- mice leads to decreased muscle size in the adult. Dev. Biol. 232, 115–126.

Kim, M.S., Fielitz, J., McAnally, J., Shelton, J.M., Lemon, D.D., McKinsey, T.A., et al., 2008. Protein kinase D1 stimulates MEF2 activity in skeletal muscle and enhances muscle performance. Mol. Cell. Biol. 28, 3600–3609.

Klont, R.E., Brocks, L., Eikelenboom, G., 1998. Muscle fibre type and meat quality. Meat Science 49, S219–S229.

Kobberling, J., Tillil, H., 1982. Empirical risk figures for first degree relatives of non insulin dependant diabetes. In: Kobberling, J., Tattersal, R. (Eds.), The Genetics of Diabetes Mellitus. Academic Press, San Diego, pp. 201–209.

Kubis, H.P., Haller, E.-A., Wetzel, P., Gros, G., 1997. Adult fast myosin pattern and Ca^{2+}-induced slow myosin pattern in primary skeletal muscle cell culture. Proc. Natl. Acad. Sci. USA 94, 4205–4210.

Kubis, H.P., Scheibe, R.J., Meissner, J.D., Hornung, G., Gros, G., 2002. Fast-to-slow transformation and nuclear import/export kinetics of the transcription factor NFATc1 during electrostimulation of rabbit muscle cells in culture. J. Physiol. 541, 835–847.

Kubis, H.P., Hanke, N., Scheibe, R.J., Meissner, J.D., Gros, G., 2003. Ca^{2+} transients activate calcineurin/NFATc1 and initiate fast-to-slow transformation in a primary skeletal muscle culture. Am. J. Physiol. Cell Physiol. 285, C56–C63.

Larsson, L., Sjodin, B., Karlsson, J., 1978. Histochemical and biochemical changes in human skeletal muscle with age in sedentary males, age 22–65 years. Acta Physiol. Scand. 103, 31–39.

Lexell, J., Taylor, C.C., Sjostrom, M., 1988. What is the cause of the ageing atrophy? Total number, size and proportion of different fiber types studied in whole vastus lateralis muscle from 15- to 83-year-old men. J. Neurol. Sci. 84, 275–294.

Li, H.H., Kedar, V., Zhang, C., McDonough, H., Arya, R., Wang, D.Z., et al., 2004. Atrogin-1/muscle atrophy F-box inhibits calcineurin-dependent cardiac hypertrophy by participating in SCF ubqiquitin ligase complex. J. Clin. Invest. 114, 1058–1071.

Lillioja, S., Young, A.A., Culter, C.L., Ivy, J.L., Abbott, W.G., Zawadzki, J.K., et al., 1987. Skeletal muscle capillary density and fiber type are possible determinants of *in vivo* insulin resistance in man. J. Clin. Invest. 80, 415–424.

Lin, J., Wu, H., Tarr, P.T., Zhang, C.Y., Wu, Z., Boss, O., et al., 2002. Transcriptional co-activator PGC-1α drives the formation of slow-twitch muscle fibres. Nature 418, 797–801.

Liu, Y., Cseresnyés, Z., Randall, W.R., Schneider, M.F., 2001. Activity-dependent nuclear translocation and intranuclear distribution of NFATc in adult skeletal muscle fibers. J. Cell Biol. 155, 27–40.

Liu, Y., Randall, W.R., Schneider, M.F., 2005. Activity-dependent and -independent nuclear fluxes of HDAC4 mediated by different kinases in adult skeletal muscle. J. Cell Biol. 168, 887–897.

Liu, Q., Busby, J.C., Molkentin, J.D., 2009. Interaction between TAK1-RAB1-TAB2 and RCAN1-calcineurin defines a signalling nodal control point. Nat. Cell Biol. 11, 154–161.

Maccatrozzo, L., Patruno, M., Toniolo, L., Reggiani, C., Mascarello, F., 2004. Myosin heavy chain 2B isoform is expressed in specialized eye muscles but not in trunk and limb muscles of cattle. Eur. J. Histochem. 48, 357–366.

Maier, A., Gorza, L., Schiaffino, S., Pette, D., 1988. A combined histochemical and immunohistochemical study on the dynamics of fast-to-slow fiber transformation in chronically stimulated rabbit muscle. Cell Tissue Res. 254, 59–68.

Marin, P., Hogh-Kristiansen, I., Jansson, S., Krotkiewski, M., Holm, G., Bjorntorp, P., 1992. Uptake of glucose carbon in muscle glycogen and adipose tissue triglycerides *in vivo* in humans. Am. J. Physiol. Endocrinol. Metab. 263, E473–E480.

Masuda, E.S., Imamura, R., Amasaki, Y., Arai, K., Arai, N., 1998. Signalling into the T-cell nucleus: NFAT regulation. Cell. Signal. 10, 599–611.

Matsakas, A., Patel, K., 2009. Skeletal muscle fibre plasticity in response to selected environmental and physiological stimuli. Histol. Histopathol. 24, 611–629.

McCullagh, K.J.A., Calabria, E., Pallafacchina, G., Ciciliot, S., Serrano, A.L., Argentini, C., et al., 2004. NFAT is a nerve activity sensor in skeletal muscle and controls activity-dependent myosin switching. Proc. Natl. Acad. Sci. USA 101, 10590–10595.

McKinsey, T.A., Zhang, C.L., Olson, E.N., 2001. Identification of a signal-responsive nuclear export sequence in class II histone deacetylases. Mol. Cell. Biol. 21, 6312–6321.

McKinsey, T.A., Zhang, C.L., Olson, E.N., 2002a. MEF2: a calcium-dependent regulator of cell division, differentiation and death. Trends Biochem. Sci. 27, 40–47.

McKinsey, T.A., Zhang, C.L., Olson, E.N., 2002b. Signaling chromatin to make muscle. Curr. Opin. Cell Biol. 14, 763–772.

McPherron, A.C., Lawler, A.M., Lee, S.J., 1997. Regulation of skeletal muscle mass in mice by new TGF-β superfamily member. Nature 387, 83–90.

Meissner, J.D., Gros, G., Scheibe, R.J., Scholz, M., Kubis, H.P., 2001. Calcineurin regulates slow myosin, but not fast myosin or metabolic enzymes, during fast-to-slow transformation in rabbit skeletal muscle cell culture. J. Physiol. 533, 215–226.

Meissner, J.D., Chang, K.C., Kubis, H.P., Nebreda, A.R., Gros, G., Scheibe, R.J., 2007a. The p38alpha /beta MAP kinases mediate recruitment of CBP to preserve fast myosin heavy chain IId/x gene activity in myotubes. J. Biol. Chem. 282, 7265–7275.

Meissner, J.D., Umeda, P.K., Chang, K.C., Gros, G., Scheibe, R.J., 2007b. Activation of the β myosin heavy chain promoter by MEF-2D, MyoD, p300, and the calcineurin/ NFATc1 pathway. J. Cell. Physiol. 211, 138–148.

Michel, R.N., Dunn, S.E., Chin, E.R., 2004. Calcineurin and skeletal muscle growth. Proc. Nutr. Soc. 63, 341–349.

Michel, R.N., Chin, E.R., Chakkalakal, J.V., Eibl, J.K., Jasmin, B.J.J., 2007. Ca^{2+}/calmodulin-based signalling in the regulation of the muscle fibre phenotype and its therapeutic potential via modulation of utrophin and myostatin expression. Appl. Physiol. Nutr. Metab. 32, 921–929.

Miller, S.G., Kennedy, M.B., 1986. Regulation of brain type II Ca^{2+}/calmodulin-dependent protein kinase by autophosphorylation: a Ca^{2+}-triggered molecular switch. Cell 44, 861–870.

Miska, E.A., Karlsson, C., Langley, E., Nielsen, S.J., Pines, J., Kouzarides, T., 1999. HDAC4 deacetylase associates with and represses the MEF2 transcription factor. EMBO J. 18, 5099–5107.

Miura, P., Jasmin, B.J., 2006. Utrophin upregulation for treating Duchenne or Becker muscular dystrophy: how close are we? Trends Mol. Med. 12, 122–129.

Molkentin, J.D., Lu, J.R., Antos, C.L., Markham, B., Richardson, J., Robbins, J., et al., 1998. A calcineurin-dependent transcriptional pathway for cardiac hypertrophy. Cell 93, 215–228.

Mu, X., Brown, L.D., Liu, Y., Schneider, M.F., 2007. Roles of calcineurin and CaMK signaling pathways in fast-to-slow fiber type transformation of cultured mouse skeletal muscle fibers. Physiol. Genomics 30, 300–312.

Musarò, A., McCullagh, J.A., Naya, F.J., Olson, E.N., Rosenthal, N., 1999. IGF-1 induces skeletal myocyte hypertrophy through calcineurin in association with GATA-2 and NF-ATc1. Nature 400, 581–585.

Naya, F.J., Mercer, B., Shelton, J., Richardson, J.A., Williams, R.S., Olson, E.N., 2000. Stimulation of slow skeletal muscle fiber gene expression by calcineurin *in vivo*. J. Biol. Chem. 275, 4545–4548.

Neston, S.L., Bancroft, J.D., 2002. Enzyme histochemistry and diagnostic applications. In: Bancroft, J.D., Gamble, M. (Eds.), Theory and Practice of Histological Techniques. Churchill Livingston, London.

Newton, A.C., 2001. Protein kinase C: structural and spatial regulation by phosphorylation, cofactors and macromolecular interactions. Chem. Rev. 101, 2353–2364.

Ni, Y.G., Berenji, K., Wang, N., Oh, M., Sachan, N., Dey, A., et al., 2006. FoxO transcription factors blunt cardiac hypertrophy by inhibiting calcineurin signaling. Circulation 114, 1159–1168.

Ni, Y.G., Wang, N., Cao, D.J., Sachan, N., Morris, D.J., Gerard, R.D., et al., 2007. FoxO transcription factors activate Akt and attenuate insulin signaling in heart by inhibiting protein phosphatases. Proc. Natl. Acad. Sci. USA 104, 20517–20522.

Nyholm, B., Qu, Z., Kaal, A., Pedersen, S.B., Gravholt, C.H., Andersen, J.L., et al., 1997. Evidence of an increased number of type IIb muscle fibers in insulin-resistant first-degree relatives of patients with NIDDM. Diabetes 46, 1822–1828.

Oberbach, A., Bossenz, Y., Lehmann, S., Niebauer, J., Adams, V., Paschke, R., et al., 2006. Altered fiber distribution and fiber-specific glycolytic and oxidative enzyme activity in skeletal muscle of patients with type 2 diabetes. Diabetes Care 29, 895–900.

Oh, M., Rybkin, I.I., Copeland, V., Czubryt, M.P., Shelton, J.M., van Rooij, E., et al., 2005. Calcineurin is necessary for the maintenance but not embryonic development of slow muscle fibers. Mol. Cell. Biol. 25, 6629–6638.

Ojuka, E., Jones, T., Han, D., Chen, M., Holloszy, J.O., 2003. Raising Ca^{2+} in L6 myotubes mimics effects of exercise on mitochondrial biogenesis in muscle. FASEB J. 17, 675–681.

Osada, S., Mizuno, K., Saido, T.C., Suzuki, K., Kuroki, T., Ohno, S., 1992. A new member of the protein kinase C family, nPKC theta, predominantly expressed in skeletal muscle. Mol. Cell. Biol. 12, 3930–3938.

Pallafacchina, G., Calabria, E., Serrano, A.L., Kalhovde, J.M., Schiaffino, S., 2002. A protein kinase B-dependent and rapamycin-sensitive pathway controls skeletal muscle growth but not fiber type specification. Proc. Natl. Acad. Sci. USA 99, 9213–9218.

Parsons, S.A., Wilkins, B.J., Bueno, O.F., Molkentin, J.D., 2003. Altered skeletal muscle phenotypes in calcineurin Aα and Aβ gene-targeted mice. Mol. Cell. Biol. 23, 4331–4343.

Parsons, S.A., Millay, D.P., Wilkins, B.J., Bueno, O.F., Tsika, G.L., Neilson, J.R., et al., 2004. Genetic loss of calcineurin blocks mechanical over-load induced skeletal fiber type switching but not hypertrophy. J. Biol. Chem. 279, 26192–26200.

Pette, D., Sketelj, J., Šákorjanc, D., Leisner, E., Traub, I., Bajrovic, F., 2002. Partial fast-to-slow conversion of regenerating rat fast-twitch muscle by chronic low-frequency stimulation. J. Muscle Res. Cell Motil. 23, 215–221.

Puigserver, P., Spiegelman, B.M., 2003. Peroxisome proliferator-activated receptor-gamma coactivator 1 alpha (PGC-1 alpha): transcriptional coactivator and metabolic regulator. Endocr. Rev. 24, 78–90.

Putman, C.T., Xu, X., Gillies, E., MacLean, I.M., Bell, G.J., 2004. Effects of strength, endurance and combined training on myosin heavy chain content and fibre-type distribution in humans. Eur. J. Appl. Physiol. 92, 376–384.

Rockl, K.S., Witczak, C.A., Goodyear, L.J., 2008. Signaling mechanisms in skeletal muscle: acute responses and chronic adaptations to exercise. IUBMB Life 60, 145–153.

Rommel, C., Bodine, S.C., Clarke, B.A., Rossman, R., Nunez, L., Stitt, T.N., et al., 2001. Mediation of IGF-1-induced skeletal myotube hypertrophy by PI(3)K/Akt/mTOR and PI(3)K/Akt/GSK3 pathways. Nat. Cell Biol. 3, 1009–1013.

Rose, A.J., Hargreaves, M., 2003. Exercise increases Ca^{2+}-calmodulin-dependent protein kinase II activity in human skeletal muscle. J. Physiol. 553, 303–309.

Rose, A.J., Kiens, B., Richter, E.A., 2006. Ca^{2+}-calmodulin-dependent protein kinase expression and signalling in skeletal muscle during exercise. J. Physiol. 574, 889–903.

Rose, A.J., Frosig, C., Kiens, B., Wojtaszewski, J.F.P., Richter, E.A., 2007. Effect of endurance exercise training on Ca^{2+} calmodulin-dependent protein kinase II expression and signalling in skeletal muscle of humans. J. Physiol. 583, 785–795.

Rothermel, B.A., McKinsey, T.A., Vega, R.B., Nicol, R.L., Mammen, P., Yang, J., et al., 2001. Myocyte-enriched calcineurin-interacting protein, MCIP1, inhibits cardiac hypertrophy in vivo. Proc. Natl. Acad. Sci. USA 98, 3328–3333.

Rothermel, B.A., Vega, R.B., Williams, R.S., 2003. The role of modulatory calcineurin-interacting proteins in calcineurin signaling. Trends Cardiovasc. Med. 13, 15–21.

Ryall, J.G., Schertzer, J.D., Lynch, G.S., 2008. Cellular and molecular mechanisms underlying age-related skeletal muscle wasting and weakness. Biogerontology 9, 213–228.

Sakuma, K., Nishikawa, J., Nakao, R., Watanabe, K., Totsuka, T., Nakano, H., et al., 2003. Calcineurin is a potent regulator for skeletal muscle regeneration by association with NFATc1 and GATA-2. Acta Neuropathol. 105, 271–280.

Sanna, B., Bueno, O.F., Dai, Y.S., Wilkins, B.J., Molkentin, J.D., 2005. Direct and indirect interactions between calcineurin–NFAT and MEK1-extracellular signal-regulated kinase 1/2 signaling pathways regulate cardiac gene expression and cellular growth. Mol. Cell. Biol. 25, 865–878.

Sanna, B., Brandt, E.B., Kaiser, R.A., Pfluger, P., Witt, S.A., Kimball, T.R., et al., 2006. Modulatory calcineurin-interacting proteins 1 and 2 function as calcineurin facilitators *in vivo*. Proc. Natl. Acad. Sci. USA 103, 7327–7332.

Schiaffino, S., Reggiani, C., 1996. Molecular diversity of myofibrillar proteins: gene regulation and functional significance. Physiol. Rev. 76, 371–423.

Schuler, M., Pette, D., 1996. Fiber transformation and replacement in low-frequency stimulated rabbit fast-twitch muscles. Cell Tissue Res. 285, 297–303.

Schulz, R.A., Yutzey, K.E., 2004. Calcineurin signaling and NFAT activation in cardiovascular and skeletal muscle development. Dev. Biol. 266, 1–16.

Semsarian, C., Wu, M.J., Ju, Y.K., Marcinec, T., Yeoh, T., Allen, D.G., et al., 1999. Skeletal muscle hypertrophy is mediated by a Ca^{2+}-dependent calcineurin signalling pathway. Nature 400, 576–581.

Serrano, A.L., Murgia, M., Pallafacchina, G., Calabria, E., Coniglio, P., Lomo, T., et al., 2001. Calcineurin controls nerve activity-dependent specification of slow muscle fibers but not muscle growth. Proc. Natl. Acad. Sci. USA 98, 13108–13113.

Shen, T., Liu, Y., Cseresnyes, Z., Hawkins, A., Randall, W.R., Schneider, M.F., 2006. Activity- and calcineurin-independent nuclear shuttling of NFATc1, but not NFATc3, in adult skeletal muscle fibers. Mol. Biol. Cell 17, 1570–1582.

Shen, T., Cseresnyes, Z., Liu, Y., Randall, W.R., Schneider, M.F., 2007. Regulation of the nuclear export of the transcription factor NFATc1 by protein kinases after slow fibre type electrical stimulation of adult mouse skeletal muscle fibres. J. Physiol. 579, 535–551.

Short, K.R., Vittone, J.L., Bigelow, M.L., Proctor, D.N., Coenen-Schimke, J.M., Rys, P., et al., 2005. Changes in myosin heavy chain mRNA and protein expression in human skeletal muscle with age and endurance exercise training. J. Appl. Physiol. 99, 95–102.

Simoneau, J.A., Veerkamp, J.H., Turcotte, L.P., Kelley, D.E., 1999. Markers of capacity to utilize fatty acids in human skeletal muscle: relation to insulin resistance and obesity and effects of weight loss. FASEB J. 13, 2051–2060.

Somers, J.R., Beck, P.L., Lees-Miller, J.P., Roach, D., Li, Y., Guo, J., et al., 2008. iNOS in cardiac myocytes plays a critical role in death in a murine model of hypertrophy induced by calcineurin. Am. J. Physiol. Heart Circ. Physiol. 295, H1122–H1131.

Swoap, S.J., Hunter, R.B., Stevenson, E.J., Felton, H.M., Kansagra, N.V., Lang, J.M., et al., 2000. The calcineurin–NFAT pathway and muscle fiber-type gene expression. Am. J. Physiol. Cell Physiol. 279, C915–C924.

Talmadge, R.J., Otis, J.S., Rittler, M.R., Garcia, N.D., Spencer, S.R., Lees, S.J., et al., 2004. Calcineurin activation influences muscle phenotype in a muscle-specific fashion. BMC Cell Biol. 5, 28.

Tanner, C.J., Barakat, H.A., Dohm, G.L., Pories, W.J., MacDonald, K.G., Cunningham, P.R.G., et al., 2002. Muscle fiber type is associated with obesity and weight loss. Am. J. Physiol. Endocrinol. Metab. 282, E1191–E1196.

Thayer, R., Collins, J., Noble, E.G., Taylor, A.W., 2000. A decade of aerobic endurance training: histological evidence for fibre type transformation. J. Sports Med. Phys. Fitness 40, 284–289.

Toth, M.J., Tchernof, A., 2006. Effect of age on skeletal muscle myofibrillar mRNA abundance: relationship to myosin heavy chain protein synthesis rate. Exp. Gerontol. 41, 1195–1200.

Toth, M.J., Matthews, D.E., Tracy, R.P., Previs, M.J., 2005. Age-related differences in skeletal muscle protein synthesis: relation to markers of immune activation. Am. J. Physiol. Endocrinol. Metab. 288, E883–E891.

Tothova, J., Blaauw, B., Pallafacchina, G., Rudolf, R., Argentini, C., Reggiani, C., et al., 2006. NFATc1 nucleocytoplasmic shuttling is controlled by nerve activity in skeletal muscle. J. Cell Sci. 119, 1604–1611.

van Rooij, E., Doevendans, P.A., Crijns, H.J.G.M., Heeneman, S., Lips, D.J., van Bilsen, M., et al., 2004. MCIP1 overexpression suppresses left ventricular remodeling and sustains cardiac function after myocardial infarction. Circ. Res. 94, 18e–26e.

Vega, R.B., Huss, J.M., Kelly, D.P., 2000. The coactivator PGC-1 cooperates with peroxisome proliferator-activated receptor alpha in transcriptional control of nuclear genes encoding mitochondrial fatty acid oxidation enzymes. Mol. Cell. Biol. 20, 1868–1876.

Vega, R.B., Rothermel, B.A., Weinheimer, C.J., Kovacs, A., Naseem, R.H., Bassel-Duby, R., et al., 2003. Dual roles of modulatory calcineurin-interacting protein 1 in cardiac hypertrophy. Proc. Nat. Acad. Sci. USA 100, 669–674.

Verdijk, L.B., Koopman, R., Schaart, G., Meijer, K., Savelberg, H.H., van Loon, L.J., 2007. Satellite cell content is specifically reduced in type II skeletal muscle fibers in the elderly. Am. J. Physiol. Endocrinol. Metab. 292, E151–E157.

Wade, A.J., Marbut, M.M., Round, J.M., 1990. Muscle fibre type and aetiology of obesity. Lancet 335, 805–808.

Wayman, G.A., Lee, Y.S., Tokumitsu, H., Silva, A., Soderling, T.R., 2008. Calmodulin-kinases: modulators of neuronal development and plasticity. Neuron 59, 914–931.

Weiss, A., Leinwand, L.A., 1996. The mammalian myosin heavy chain gene family. Annu. Rev. Cell Dev. Biol. 12, 417–439.

Welle, S., Thornton, C., Jozefowicz, R., Statt, M., 1993. Myofibrillar protein synthesis in young and old men. Am. J. Physiol. Endocrinol. Metab. 264, E693–E698.

Wilkins, B.J., De Windt, L.J., Bueno, O.F., Braz, J.C., Glascock, B.J., Kimball, T.F., et al., 2002. Targeted disruption of NFATc3, but not NFATc4, reveals an intrinsic defect in calcineurin-mediated cardiac hypertrophic growth. Mol. Cell. Biol. 22, 7603–7613.

Wilkins, B.J., Dai, Y.S., Bueno, O.F., Parsons, S.A., Xu, J., Plank, D.M., et al., 2004. Calcineurin–NFAT coupling participates in pathological, but not physiological, cardiac hypertrophy. Circ. Res. 94, 110–118.

Willoughby, D.S., Nelson, M.J., 2002. Myosin heavy-chain mRNA expression after a single session of heavy-resistance exercise. Med. Sci. Sports Exerc. 34, 1262–1269.

Wu, P., Inskeep, K., Bowker-Kinley, M.M., Popov, K.M., Harris, R.A., 1999. Mechanism responsible for inactivation of skeletal muscle pyruvate dehydrogenase complex in starvation and diabetes. Diabetes 48, 1593–1599.

Wu, H., Naya, F.J., McKinsey, T.A., Mercer, B., Shelton, J.M., Chin, E.R., et al., 2000a. MEF2 responds to multiple calcium-regulated signals in the control of skeletal muscle fiber type. EMBO J. 19, 1963–1973.

Wu, Y.Z., Crumley, R.L., Caiozzo, V.J., 2000b. Are hybrid fibers a common motif of canine laryngeal muscles?: single-fiber analyses of myosin heavy-chain isoform composition. Arch. Otolaryngol. Head Neck Surg. 126, 865–873.

Wu, H., Rothermel, B., Kanatous, S., Rosenberg, P., Naya, F.J., Shelton, J.M., et al., 2001. Activation of MEF2 by muscle activity is mediated through a calcineurin-dependent pathway. EMBO J. 20, 6414–6423.

Wu, H., Kanatous, S.B., Thurmond, F.A., Gallardo, T., Isotani, E., Bassel-Duby, R., et al., 2002. Regulation of mitochondrial biogenesis in skeletal muscle by CaMK. Science 296, 349–352.

Yang, J., Rothermel, B., Vega, R.B., Frey, N., McKinsey, T.A., Olson, E.N., et al., 2000. Independent signals control expression of the calcineurin inhibitory proteins MCIP1 and MCIP2 in striated muscles. Circ. Res. 87, 61–68.

Yu, H., van Berkel, T.J., Biessen, E.A., 2007. Therapeutic potential of VIVIT, a selective peptide inhibitor of nuclear factor of activated T cells, in cardiovascular disorders. Cardiovasc. Drug Rev. 25, 175–187.

Zhu, J., McKeon, F., 1999. NF-AT activation requires supression of Crm1-dependent export by calcineurin. Nature 398, 256–260.

Zhu, J., McKeon, F., 2000. Nucleocytoplasmic shuttling and the control of NF-AT signaling. Cell. Mol. Life Sci. 57, 411–420.

Zierath, J.R., Hawley, J.A., 2006. Skeletal muscle fiber type: influence on contractile and metabolic properties. PLoS Biol. 2, 1523–1527.

Zugaza, J.L., Sinnett-Smith, J., Van Lint, J., Rozengurt, E., 1996. Protein kinase D (PKD) activation in intact cells through a protein kinase C-dependent signal transduction pathway. EMBO J. 15, 6220–6230.

New Insights into Plant Vacuolar Structure and Dynamics

Yoshihisa Oda,[*] Takumi Higaki,[†,‡] Seiichiro Hasezawa,[†,‡] and Natsumaro Kutsuna[†,‡]

Contents

Abstract

The plant vacuole is a multifunctional organelle and is essential for plant development and growth. The most distinctive feature of the plant vacuole is its size, which usually occupies over 80–90% of the cell volume in well-developed somatic cells, and is therefore highly involved in cell growth and plant body size. Recent progress in the visualization of the vacuole, together with

* Department of Biological Sciences, Graduate School of Science, The University of Tokyo, Tokyo 113-0033, Japan
† Department of Integrated Biosciences, Graduate School of Frontier Sciences, The University of Tokyo, Chiba 277-8562, Japan
‡ Institute for Bioinformatics Research and Development (BIRD), Japan Science and Technology Agency (JST), Tokyo 102-8666, Japan

developments in image analysis, has revealed the highly organized and complex morphology of the vacuole, as well as its dynamics. The plant vacuolar membrane (VM) forms not only a typically large vacuole but also other structures, such as tubular structures, transvacuolar strands, bulbs, and sheets. In higher plant cells, actin microfilaments are mainly located near the VM and are involved in vacuolar shape changes with the actin–myosin systems. Most recently, microtubule-dependent regulation of vacuolar structures in moss plant cells was reported, suggesting a diversity of mechanisms regulating vacuolar morphogenesis.

Key Words: Actin microfilaments, Cytoskeleton, Image analysis, Membrane, Microtubule, Tonoplast, Vacuole. © 2009 Elsevier Inc.

ABBREVIATIONS

BCECF	2′,7′-bis-(2-carboxyethyl)-5-(and-6)-carboxyfluorescein
BDM	2,3-butanedion monoxime
ER	endoplasmic reticulum
FM4-64	*N*-(3-triethylammoniumpropyl)-4-(4-diethylamino-phenylhexatrienyl) pyridinium dibromide
GFP	green fluorescent protein
LV	lytic vacuole
MIP	maximum intensity projection
PSV	protein storage vacuole
PVC	prevacuolar compartment
TGN	*trans*-Golgi network
TIP	tonoplast intrinsic protein
TVM	tubular structure of vacuolar membrane
TVS	transvacuolar strand
VM	vacuolar membrane

1. INTRODUCTION

The vacuole is a multifunctional organelle and is essential for plant development and life maintenance (Marty, 1999; Rojo et al., 2001). It functions in various cellular processes, such as the storage of proteins, ions, and secondary metabolites, including pigments and toxic compounds, as well as in protein degradation, autophagy, defense responses,

programmed cell death, the adjustment of osmotic pressure, and the maintenance of turgor pressure. A single plant cell may sometimes possess several different types of vacuoles simultaneously (Paris et al., 1996). Generally, plant vacuoles can be divided into lytic vacuoles (LVs) or protein storage vacuoles (PSVs). LVs are acidic compartments that contain hydrolases, whereas PSVs develop mainly in seeds and can store large amounts of proteins. In this review, we focus on the structure and dynamics of LVs.

The vacuole is not a separate organelle but rather a compartment of membrane traffic, and is located at the endpoint of the secretory pathway. The pathway begins at the endoplasmic reticulum (ER), proceeds through the Golgi body and *trans*-Golgi network (TGN), and finally reaches the LVs via the prevacuolar compartments (PVCs) or PSVs via dense vesicles or precursor-accumulating vesicles (Hara–Nishimura et al., 1998; Hohl et al., 1996; Mo et al., 2006). The endocytotic pathway from the plasma membrane to the vacuole also exists for the internalization of a variety of molecules, and is thus important for labeling the vacuolar membrane (VM) with fluorescent dyes (Section 2).

The most distinctive feature of the plant vacuole is its large size, which usually occupies over 80–90% of the cell volume in well-developed somatic cells (Wink, 1993), and which therefore plays a major role in cell growth and plant body size. Recent technical advances in the visualization of vacuoles and in image analysis of living cells by fluorescent dyes and fluorescent proteins have revealed the highly organized and complex morphology and dynamics of vacuoles (Section 2). Plant vacuoles exhibit not only simple inflated balloons but also other structures, such as tubular structures, transvacuolar strands (TVS), bulbs, and sheets (Section 3). Some of these vacuolar structures are found to be regulated by the cytoskeleton (Section 4).

In this chapter, we summarize the techniques that allow visualization and analysis of vacuoles, the structure and dynamics of vacuoles, and also the mechanisms that regulate vacuolar structures by the cytoskeleton. Finally, we discuss the implication and perspectives of this area of research.

2. Methods to Reveal Vacuolar Structure and Dynamics

Plant vacuoles occupy a considerable proportion of the cellular volume in many plant tissues (Marty, 1999). In addition, the large vacuoles appear as ''cavities'' that possess no noticeable structures in their lumen, in contrast to the cytoplasm that contains a variety of organelles and vesicles. The large vacuoles can, therefore, be easily detected as large transparent regions in the plant cell by light microscopy. More detailed views of vacuoles, and a greater

understanding of their structure and dynamics, have been recently obtained from the developments in cell biology observation techniques. In this section, we will first introduce the major approaches for analyzing the vacuolar morphology and dynamics of LVs, and will then describe how three-dimensional (3-D) and time-sequential imaging of vacuoles have been used to clarify their detailed structures and dynamics.

2.1. Electron and immunofluorescence microscopy for imaging vacuoles

2.1.1. Ultrastructure and chemical composition of vacuolar compartments

The detailed morphology of vacuolar structures has been established mainly through transelectron microscopy (Marty, 1997). Moreover, electron microscopy has been an important tool in the discovery and description of some vacuole-related endomembrane systems, including provacuoles (Marty, 1978), autophagosomes (Aubert et al., 1996; Moriyasu and Ohsumi, 1996), dense vesicles (Hohl et al., 1996), and precursor-accumu- lating vesicles (Hara-Nishimura et al., 1998), which play important roles in the biogenesis and differentiation of vacuoles. In addition, ultrastructural analysis by electron microscopy has been indispensable to the study of intravacuolar compartments (Gaffal et al., 2007; Gao et al., 2005; Morita et al., 2002; Saito et al., 2002), since their dimensions are sometimes below the diffraction limits of light microscopy. However, as the vacuolar lumen is filled with aqueous solutions that complicate chemical fixation, the intra- vacuolar compartments tend to be very delicate and easily deformed by conventional electron microscopy. This limitation was recently resolved by the use of physical fixation methods, such as high-pressure freezing and freeze-substitution techniques (Iwano et al., 2007; Saito et al., 2002).

For the localization of vacuolar proteins, immunoelectron microscopy has been used with fluorescent proteins, as well as fluorescent immunostain- ing and Western-blotting analyses. Indeed, the localization of proteins on the VM (Saito et al., 2002) and within the vacuolar lumen (Avci et al., 2008) has been demonstrated by immunoelectron microscopy. Compared with fluorescent protein tagging, immunostaining has been able to clarify the existence of native proteins with high spatial resolution. This characteristic has, therefore, been used to analyze the localization of tonoplast intrinsic proteins (TIPs), especially in studying the relationship between vacuolar species and expressed TIPs in single cells in testing the multiple-vacuole hypothesis (Frigerio et al., 2008; Olbrich et al., 2007).

In addition to the study of vacuolar proteins, electron microscopy has been used to estimate the vacuolar localization of ionic and inorganic compounds by X-ray microanalysis, leading to the identification and quan- tization of the ionic composition and inorganic crystals within the vacuolar

lumen. Vacuolar differentiation for calcium accumulation has been studied using a strontium tracer (Storey and Leigh, 2004).

2.1.2. Immunofluorescence microscopy for mapping of vacuolar protein

With recent advances in the molecular and physiological characterization of vacuoles, many proteins have been identified as vacuolar localized, and immunofluorescence labeling has been a major tool in the verification of their expression at the tissue and cellular level. For example, multiple vacuoles have been found within a single cell by simultaneous observation of different vacuolar proteins by immunofluorescence microscopy (Jauh et al., 1999; Paris et al., 1996). Typically, each of these multiple vacuoles within a plant cell contains different TIPs on its membrane, whereas multiple TIPs may also colocalize to the same VM (Olbrich et al., 2007). The generality of the multiple-vacuole hypothesis will certainly be the subject of further study in various species and tissues using immunoelectron and immunofluorescence microscopy.

2.2. Dyes and fluorescent proteins used for live imaging of vacuoles

The approximate shape of large vacuoles has been clarified without labeling procedures in light microscopy such as bright-field optics. Using phase-contrast or Nomarski optics (DIC, differential interference contrast), more comprehensive images of vacuoles have been obtained. For example, TVSs (Section 3.3) in the vacuolar lumen have been distinguished by the contrast between the cytoplasm and vacuoles (Hoffman and Nebenführ, 2004). In addition to the TVS, the vacuolar lumen sometimes contains crystallized structures that can be observed by polarized light microscopy (Prychid et al., 2008). To determine the structure and dynamics of vacuoles in more detail, numerous vacuolar markers, with specific absorbance and/or fluorescence spectra, are now being utilized.

2.2.1. Endogenic vacuolar dyes

Plant cells may accumulate endogenous organic dyes, such as anthocyanins, flavonoids, and betaine, in their vacuolar lumen (Wink, 1993). Endogenic dyes can, therefore, be used as vacuolar markers because they absorb or emit specific light spectra. To study the movement and morphogenesis of vacuoles in stomatal and mother stomatal cells, autofluorescence of the vacuolar lumen was utilized together with video-enhanced optics (Palevitz and O'Kane, 1981; Palevitz et al., 1981). The fluorescence of anthocyanin (Poustka et al., 2007) and autofluorescence of PSVs (Fuji et al., 2007; Hunter et al., 2007; Li et al., 2006; Shimada et al., 2003) have also been used as markers of the vacuolar lumen. As endogenic-labeled vacuoles

are limited to particular species and tissues, a variety of synthetic dyes and chimeric fluorescent proteins have been developed to specifically visualize vacuoles.

2.2.2. Dyes for vacuolar lumen

Neutral red is the most frequently used dye for staining the vacuolar lumen (Di Sansebastiano et al., 1998; Ehara et al., 1996; Guillermond, 1929; Kawai et al., 1998; Ngo et al., 2005; Nishimura, 1982; Nobel et al., 1998; Smith and Raven, 1979; Timmers et al., 1995; Wilson et al., 1998). Neutral red is rapidly incorporated into cells and stains acidic compartments red–brown. In addition, it has a visible fluorescence spectrum that combined with fluorescence microscopy can be used to visualize plant vacuoles (Dubrovsky et al., 2006). However, as neutral red may stain various other cellular structures and may also alter vacuolar morphology, considerable care must be taken in selecting neutral red as a vacuolar marker. Fortunately, numerous dyes are available for fluorescently labeling the vacuolar lumen, including Lucifer yellow CH (Hillmer et al., 1989; Park et al., 2009; Yano et al., 2004), BCECF (2′,7′-bis-(2-carboxyethyl)-5-(and-6)-carboxyfluorescein) (Higaki et al., 2007; Kutsuna and Hasezawa, 2002; Mitsuhashi et al., 2000; Swanson et al., 1998; Toyooka et al., 2006), Alexa hydrazide (Emans et al., 2002; Kutsuna et al., 2003), CDCFDA (5-(and-6)-carboxy-2′,7′-dichlorodihydrofluorescein diacetate) (Lovy-Wheeler et al., 2007; Park et al., 2009), lysotracker (Gao et al., 2005; Moriyasu et al., 2003; Park et al., 2009), acridine orange (Gao et al., 2005; Timmers et al., 1995), and quinacrine (Toyooka et al., 2006). Figure 3.1A shows the vacuolar lumen of tobacco BY-2 cells labeled with BCECF. Generally, these dyes are applied in the medium and are incorporated into the vacuolar lumen. Although various dyes can be incorporated into the lumen, their mechanisms of incorporation are thought to differ. However, little is currently known about the molecular mechanisms through which these dyes are incorporated.

These dyes have also enabled a study of the connectivity between vacuolar structures. While vacuoles may have complicated configurations, in some cases, single vacuoles can be observed as multiple vacuoles in two–dimensional (2-D) images. The connectivity between such complicated vacuoles has been clarified by photobleaching (Gao et al., 2005; Kutsuna et al., 2003; Tanaka et al., 2007) or the injection (Park et al., 2009) of lumenal dyes.

In addition to just visualizing the vacuolar lumen, some dyes have been used to measure the content and enzymatic activity of the vacuolar lumen. By utilizing the pH dependency of the absorbance or fluorescence spectrum, vacuolar pH has been estimated by neutral red (Timmers et al., 1995; Wilson et al., 1998), BCECF (Swanson et al., 1998), carboxy-SNARE (Leshem et al., 2006), and Lysosensor Yellow/Blue DND-160 (Otegui et al., 2005). The enzymatic activity of the vacuolar lumen could be estimated by using conjugated dyes. Swanson et al. (1998) studied the
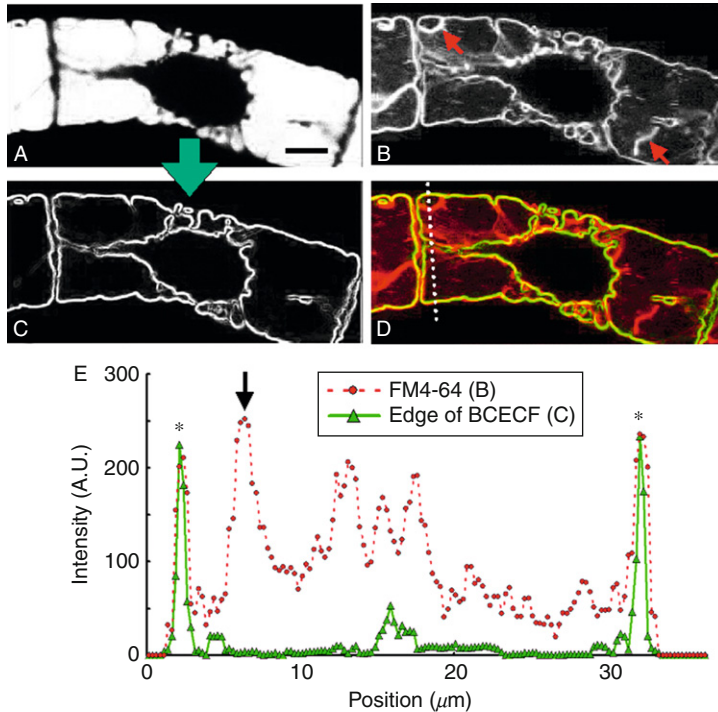
Figure 3.1 Double staining of vacuolar structures in a living tobacco BY-2 cell. (A) Vacuolar lumen labeled with BCECF. (B) VM labeled with FM4-64. (C) Vacuolar edges extracted from (A) by image processing. (D) Merged image of (B) and (C). (E) Intensity profiles measured along the dashed line in (D). Arrows represent thin TVSs. Asterisks represent outer borders of vacuole. Bar represents 10 μm.

vacuolar incorporation of fluorescent indicators to determine protease activity and glutathione S-transferase activity.

2.2.3. Dyes for VM

Specific dyes for the VM were not known until recently, and these are still presently limited. The amphiphilic styryl dyes, FM1-43 (N-(3-triethylam-moniumpropyl)-4-(4-(dibutylamino)styryl) pyridinium dibromide) and FM4-64 (N-(3-triethylammoniumpropyl)-4-(4-diethylaminophenylhexa-trienyl) pyridinium dibromide), are valuable and frequently used tools for vital staining of the VM (Emans et al., 2002; Higaki et al., 2006; Kim et al., 2001; Kutsuna and Hasezawa, 2002; Kutsuna et al., 2003; Leshem et al., 2006; Okubo-Kurihara et al., 2009; Ovecka et al., 2005, 2008; Parton et al., 2001; Silady et al., 2008; Tanaka et al., 2007; Ueda et al., 2001). FM dyes are incorporated from the medium, transported through the endocytosis pathway, and finally targeted to the VM (Fig. 3.1B). FM dyes directly injected into cytoplasm do not label the VM (Parton et al., 2001; van

Gisbergen et al., 2008). Therefore, to label the VM with FM dyes, cells are commonly pulse labeled for several minutes and then chased for several hours in fresh medium. The optimum duration of the chase period appears to differ depending on the trafficking activities of the cells. In the early stage of the chase period, the dyes simultaneously label the VM and other endomembrane components, including endosomal organelles and developing cell plates (Higaki et al., 2008; Kutsuna and Hasezawa, 2002; Ovecka et al., 2005; Parton et al., 2001; Tanaka et al., 2007; Ueda et al., 2001; Vermeer et al., 2006). A longer period of chase is required to only visualize the VM (Emans et al., 2002; Kutsuna and Hasezawa, 2002; Ueda et al., 2001). Vesicle trafficking of FM dyes in plant cells has been reviewed (Aniento and Robinson, 2005; Bolte et al., 2004; Geldner, 2004).

For detailed morphological analysis of vacuoles, VM is a better choice for visualization than the vacuolar lumen. In contrast to lumen markers, the FM dyes can clearly demarcate the border between vacuoles and the cytoplasm. This is particularly advantageous for detecting intravacuolar structures, since these structures tend to be masked by the surrounding fluorescence of the lumen and may be overlooked when lumen markers are used. Double staining of the vacuolar lumen and VM has shown that the outer border of vacuoles can be similarly observed (Fig. 3.1). Using a Sobel edge detector (Russ, 2002), the vacuolar edges (Fig. 3.1C) could be extracted from vacuolar lumen images stained with BCECF (Fig. 3.1A). When the VM of the same cell was labeled with FM4-64 (Fig. 3.1B), the edge image overlapped well with the outer membranes of the VM image (Fig. 3.1D). Intensity profiles showed that the edge of the vacuolar lumen could predict the outer border of the vacuoles with submicrometer accuracy (Fig. 3.1E asterisks). On the other hand, thin TVSs were overlooked in the lumen image (Fig. 3.1A and C), but could be visualized with the VM marker (Fig. 3.1B and E, arrows).

2.2.4. Fluorescent proteins

Fluorescent protein applications enable the visualization of vacuolar proteins in living cells (Berg and Beachy, 2008; Brandizzi et al., 2004). Using fluorescent proteins, many proteins have been found to localize to the vacuolar lumen and VMs. The mechanism of vacuolar protein trafficking has also been studied using fluorescent proteins. Recent advances in our understanding of transporter proteins on VMs were summarized (Martinoia et al., 2007; Neuhaus, 2007), and of protein dynamics and proteolysis in vacuoles were also reviewed (Mo et al., 2006; Muntz, 2007). Localization studies using fluorescent proteins as markers have been frequently conducted and some of these are listed below.

Vacuolar lumen: sorting signal of chitinase (Di Sansebastiano et al., 1998; Flucktiger et al., 2003; Poustka et al., 2007; Tamura et al., 2003); sorting signal of aleuline (Flucktiger et al., 2003; Poustka et al., 2007; Tamura et al., 2003); sorting signal of phaseolin (Frigerio et al., 1998, 2008; Hunter et al.,

2007); Aggulutinin (Fouquaert et al., 2007); sorting signal of β–conglycinin (Fuji et al., 2007); amaranth 11S globulin (Petruccelli et al., 2007); aspartic proteinases (Terauchi et al., 2006); calmodulin-like protein (Yamaguchi et al., 2005); sporamin (Kim et al., 2001; Mitsuhashi et al., 2000); and the sorting signal of pumpkin 2S–albumin (Tamura et al., 2003).

VM: nitrate transporter (Angeli et al., 2006); TIPs (Boursiac et al., 2005; Hicks et al., 2004; Hunter et al., 2007; Jaquinod et al., 2007; Okubo-Kurihara et al., 2009; Poustka et al., 2007; Saito et al., 2002); carbohydrate transporter (Endler et al., 2006; Jaquinod et al., 2007; Wormit et al., 2006); phosphate transporter (Escobar et al., 2003); small G protein (Saito et al., 2002); syntaxin (Uemura et al., 2002); metal transporter (Jaquinod et al., 2007; Thomine et al., 2003); lipocalin (Jaquinod et al., 2007); CCD1 (Jaquinod et al., 2007); Ca^{2+} transporter (Kamiya et al., 2006; Peiter et al., 2005); Zn^{2+} transporter (Kobae et al., 2004); malate transporter (Kovermann et al., 2007); organic cation transporter (Kufner and Koch, 2008); phospholipase–like protein (Morita et al., 2002); AtIREG2 (Schaaf et al., 2006); K^{+} transporter (Voelker et al., 2006); and cytochrome P450 (Xu et al., 2006).

It is noteworthy that the fluorescence of some vacuolar proteins is also detected in other organelles, including the ER, Golgi body, and PVC. Such multiple localizations of fluorescently tagged proteins may result from over–expression of the chimeric proteins which, during transport through the endomembrane pathway, may overload the trafficking pathway. Using marker genes under the control of their own promoters may reduce the risk of overexpression and thus misinterpretation of the data. In addition to difficulties arising from overexpression, the acidic and proteolytic environment of the vacuolar lumen may also affect the fluorescence proteins by irreversibly damaging their fluorophores (Tamura et al., 2003). Ratiometric assays of fluorescence intensity could contribute to the quantitative evaluation of vacuolar targeting (Samalova et al., 2006).

Fluorescent proteins are also useful for visualizing vacuoles (Yoneda et al., 2007). To obtain detailed images of vacuoles, fluorescent proteins have been attached to VM proteins, including TIPs (Hicks et al., 2004; Higaki et al., 2006; Reisen et al., 2005; Saito et al., 2002, 2005; Sheahan et al., 2007; Silady et al., 2008; Toyooka et al., 2006; Yano et al., 2004), small G proteins (Saito et al., 2002), and AtVAM3/AtSYP22 (Higaki et al., 2006, 2007; Kutsuna and Hasezawa, 2002; Kutsuna et al., 2003; Tanaka et al., 2007; Uemura et al., 2002; Yano et al., 2004).

2.3. High-dimensional image analysis of vacuolar structure and dynamics

2.3.1. Reconstruction of 3-D structures

Vacuoles are usually spread throughout the whole cell and occupy most of the cell volume. Therefore, 3-D reconstructions are necessary to capture the entire vacuole. To date, 3-D images of vacuoles have been constructed from

series of confocal images, stacks of electron micrographs (Saito et al., 2002; Segui–Simarro and Staehelin, 2006), and electron tomographic slices (Iwano et al., 2007; Otegui et al., 2006). The vacuole 3–D reconstruction methods can be classified into two groups depending on their approach: intensity projection and surface modeling.

The intensity projection method is convenient for obtaining 3–D images from fluorescent images in combination with confocal microscopy, particularly when maximum intensity projection (MIP) is employed (Emans et al., 2002; Reisen et al., 2005; Ruthardt et al., 2005; Sheahan et al., 2007; Silady et al., 2008). When viewed at the same angle as observations under a microscope, MIP is found to preserve the quality and resolution of the original images. However, rotated MIP images tend to be blurred and degraded because of low resolution along the optical axis. In particular, VM intensities are severely biased by the angle of the membranes. Depending on the membrane angle, the intensity bias is about threefold that of usual confocal microscope settings (Sano et al., 2008), and results in MIP unequally emphasizing a portion of the VMs. Thus, considerable caution is required in interpreting vacuolar 3–D structures from MIP images. Image processing prior to MIP may be effective in reducing the intensity bias. For example, blind deconvolution of confocal images was performed to preprocess MIP images (Ruthardt et al., 2005).

Another approach for 3–D reconstruction of vacuoles is surface modeling, which is superior to MIP for determining the 3–D shape from different angles and views. To reconstruct the 3–D surface of vacuoles, the vacuolar region is segmented by some methods from microscopic images. In the case of fluorescent images, the fluorescence intensity has been mainly used as a threshold for segmentation (Reisen et al., 2005; Uemura et al., 2002). Similar to MIP, intensity thresholding was initially affected by an optic-derived intensity bias. This problem was overcome by replacing the intensity threshold with more stable segmentation methods, such as contour extraction (Kutsuna and Hasezawa, 2005). Moreover, the development of robust algorithms for interpolation between slices enabled 3–D reconstruction of complicated vacuoles (Higaki et al., 2006, 2007; Kutsuna and Hasezawa, 2005; Kutsuna et al., 2003; Oda et al., 2009; Tanaka et al., 2007). From these detailed vacuolar models, the vacuole volumes and surface areas could be determined (Kutsuna and Hasezawa, 2005; Tanaka et al., 2007). On the other hand, surface modeling of vacuolar structures is a popular method for transelectron microscopy, including electron tomography. The 3–D models of intravacuolar structures (Saito et al., 2002), multivesicular bodies (Otegui et al., 2006), and vacuoles in meristematic cells (Segui–Simarro and Staehelin, 2006) have been reconstructed with ultrastructural detail.

A comparison of intensity projection and surface modeling is shown in Fig. 3.2. MIP (Fig. 3.2B) generated acceptable images when viewed along
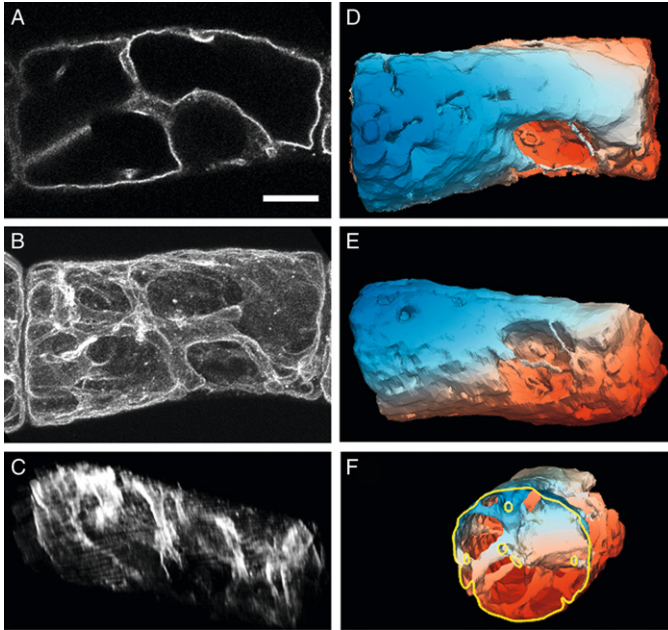
Figure 3.2 The 3-D images of VMs in a BY–2 cell. VMs were visualized by GFP-AtVAM3 and serial optical sections then obtained at 1.0 μm intervals. (A) One of the confocal sections in the midplane of the cell. (B) Maximum intensity projection (MIP) viewed along the optical axis. (C) A rotated view of (B). (D) Surface model reconstructed by contour connection. (E) A rotated view of (D). (F) Split view of (D). Colors of the surface model (D–F) represent the distance from the top of the cell along the Z-axis. Bar represents 10 μm.

the optical axis. However, artificial lines and severe blurring appeared in rotated views (Fig. 3.2C). In contrast, by surface modeling, performed by contour connection using our developed software, REANT (Fig. 3.2D), the images could be rotated (Fig. 3.2E) and cut (Fig. 3.2F) without artificial lines and blurring.

2.3.2. Evaluation of vacuolar movement

Visualization of vacuoles has revealed the movement and deformation of vacuoles, similar to other plant organelles. Improvements in the temporal resolution of confocal microscopy have enabled the rapid movement of intravacuolar structures, including the TVS, to be captured. As a result, the dynamics of vacuolar structures could be studied in various physiological processes, such as the movements and deformation of TVS (Higaki et al., 2006; Hoffman and Nebenführ, 2004; Ruthardt et al., 2005; Sheahan et al., 2007), deformation of the intra–VM (Uemura et al., 2002), deformation and separation of vacuoles in mitosis (Kutsuna and Hasezawa, 2002; Kutsuna

et al., 2003), invagination of the VM during plasmolysis (Kutsuna and Hasezawa, 2005), continuous movements of the TVS in endodermal cells (Saito et al., 2005), vacuolar movements in pollen tubes (Ovecka et al., 2005), the fusion of autophagosomes to vacuoles (Toyooka et al., 2006), and the disappearance of intravacuolar structures during pathogenic elicitor–induced programmed cell death (Higaki et al., 2007). Currently, time-sequential images are mainly presented as movies and measurements have rarely been performed. In order to understand the physical and molecular
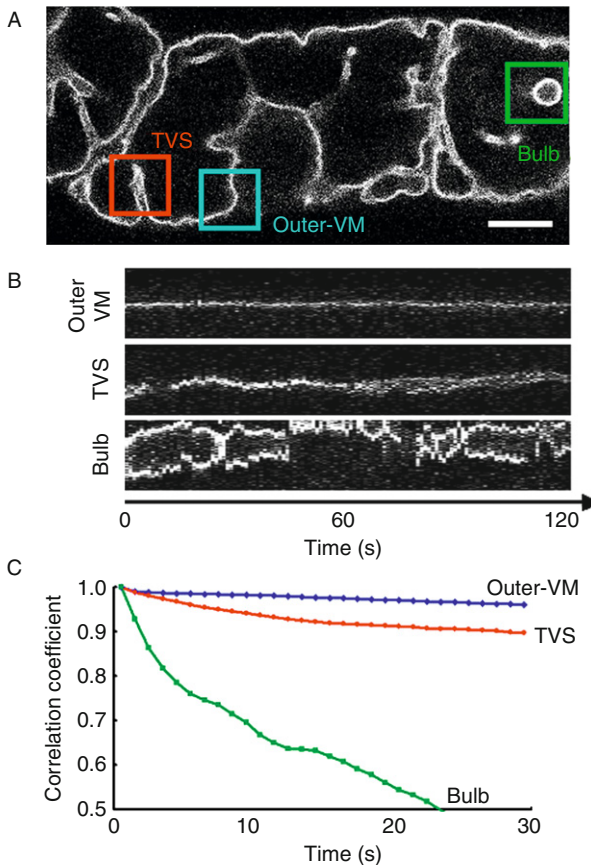
Figure 3.3 Movements of VM in BY-2 cells. VMs were visualized by GFP–AtVAM3 and time-sequential images were obtained at 1.0 s intervals. (A) One of the time-sequential images. Movements within the three boxed regions were analyzed. (B) Kymograph analysis along diagonal lines (upper left corner to lower right corner) in the regions. Intravacuolar membranes undergoing dynamic fluctuations, with prominent VM fluctuations in the bulb region. (C) Correlation analysis of the three regions. After noise reduction, the cross-correlation coefficients were calculated between time-sequential frames of the regions. Bar represents 10 μm.

mechanisms of vacuolar dynamics, quantitative evaluation of vacuolar movements is essential. To measure the velocity of intracellular structures from time-sequential images, particle tracking and kymography were used as comprehensive tools, and these were found suitable for determining the directional movements of small organelles and cytoskeletons. However, it has been difficult to measure vacuolar movements using these methods as the vacuolar structures could not be approximated to particles and the VMs usually showed fluctuations (Fig. 3.3B).

Digital image correlation is an alternative and preferable method to quantify vacuolar movements and deformation. As correlation coefficients between images represent the similarity of images, any movement and deformation lower the coefficients. An estimation of the magnitude and direction of velocity could be performed using image correlation without the setting for particles or regions of interest. In plant sciences, correlation-based velocimetry has been performed to measure the elongation of root tissues (Bengough et al., 2006) and also vesicle trafficking in pollen tubes (Bove et al., 2008). To evaluate vacuolar movements quantitatively, the cross-correlation coefficients between frames were measured from time-sequential images of VMs (Higaki et al., 2006). The slope of the coefficients reflected the fluctuation in VMs and corresponded well with the qualitative observations. Using these coefficients as measure of vacuolar movements, the effects of some inhibitors on vacuolar dynamics could be evaluated. Figure 3.3 demonstrates the cross-correlation coefficients of time-sequential images visualizing VMs. The intravacuolar structures were moving more rapidly than the outer-VMs (Fig. 3.3C).

3. Vacuolar Structure and Functions

As described earlier, technical advances in visualization and image analysis have given us a deeper understanding of plant vacuolar structures and dynamics. The vacuoles show diverse structures that are continuously undergoing transformation. It is, therefore, rather difficult to classify vacuolar structures and formulate clear definitions. In this section, however, we roughly categorize vacuolar structures into the four major types of large vacuoles, tubular vacuoles, TVSs, and also bulb and sheets, and describe their structural features and possible biological significance.

3.1. Large vacuoles

The plant cell is distinguished by its large vacuoles that may occupy over 80–90% of the cell volume in mature plant cells (Wink, 1993), as shown in elongated *Arabidopsis* root cells (Fig. 3.4A). Indeed, 3-D measurements of
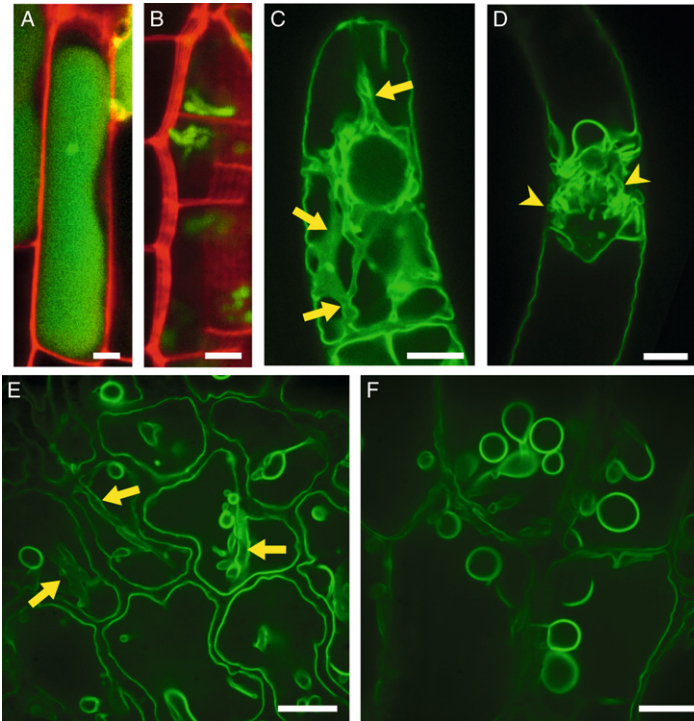
Figure 3.4 Examples of vacuolar structures. (A, B) *Arabidopsis* root cells in the elongation (A) and meristematic (B) zones. The vacuolar lumen and cell wall are stained with BCECF (green) and propidium iodide (red), respectively. (C, D) Tobacco BY-2 cells expressing GFP-AtVAM3, which is mainly localized to the VM, in inter-phase (C) and mitotic phase (D). Yellow arrows and arrowheads indicate transvacuolar strands (TVSs) and the tubular structure of the vacuolar membrane (TVM), respectively. (E) Leaf epidermal cells in 1-week-old *Arabidopsis* expressing GFP-AtVAM3. Yellow arrows indicate TVSs. (F) Hypocotyl cells in 1-week-old *Arabidopsis* expressing GFP-AtVAM3. Spherical VM structures are bulbs. Scale bars indicate 2 μm (A and B) and 10 μm (C–F).

cell and vacuolar volumes have also shown that vacuoles occupy about 90% of the tobacco BY-2 cell volume (Kutsuna and Hasezawa, 2005). Large vacuoles are not just simple in shape, like an inflated balloon, but are far more complicated and similar to a cave with an undulating surface (Hillmer et al., 1989; Verbelen and Tao, 1998), with specialized structures such as TVSs and bulbs as detailed further below. The space-filling properties and solute contents of vacuoles play important roles in the growth of plants. During rapid growth, increased vacuolar volumes can promote cell expansion without the need for cell division (Dolan and Davies, 2004). The large size also favors more rapid cell volume changes during environmental adaptation in stomatal guard cells (Fricker and White, 1990) and pulvinar

motor cells (Fleurat-Lessard et al., 1997; Kanzawa et al., 2006). Gao et al. (2005) reported that small vacuoles fuse with each other or with bigger vacuoles to generate large vacuoles during stomatal opening in *Vicia fava*. In *Arabidopsis* guard cells, internal VM stores increase with expansion of the large vacuole during stomatal closure (Tanaka et al., 2007).

The large size of the vacuoles is also useful for storage of various materials, including ions, sugars, amino acids, and secondary metabolites, as well as flower pigments and defense chemicals (Marty, 1999; Raven, 1997; Wink, 1993). Cytoplasmic toxic metals are chelated and sequestered into the large vacuoles (Tong et al., 2004). In addition, large vacuoles contain many hydrolytic enzymes for digestive processes, such as lysosomes in animal cells. Therefore, various discarded cytoplasmic constituents are taken up into the large vacuoles for degradation through the process of autophagy (Bassham, 2007). Furthermore, the breakdown of large vacuoles has been proposed to be a crucial event in plant programmed cell death during development and in disease resistance (Jones, 2001). During tracheary element differentiation, vacuolar collapse and nuclear DNA degradation has been directly observed (Obara et al., 2001). Vacuolar collapse has also been observed in tobacco mosaic virus–induced cell death (Hatsugai et al., 2004) and pathogenic elicitor–induced programmed cell death (Higaki et al., 2007). Although the molecular mechanisms of vacuolar collapse have not yet been described in detail, the above observations imply that the large plant vacuoles are involved in rapid self-degradation and in defense against pathogenic invaders.

3.2. Tubular vacuoles

Tubular vacuoles have been observed in meristematic cells by several visualization methods. Using high-voltage electron microscopy, the tubular and webbed structures of provacuoles were identified in *Euphorbia characias* meristematic cells (Marty, 1978). Immunofluorescent labeling has also demonstrated the tubular and spherical structures of vacuoles in pea root tip cells (Paris et al., 1996). More recently, 3-D reconstructions of shoot apical meristem cells of *Arabidopsis*, established from serial transelectron microscopy sections (Segui-Simarro and Staehelin, 2006), have shown that the tubular and globular vacuoles are interconnected. Similar tubular structures are observed by BCECF staining in *Arabidopsis* root meristematic cells (Fig. 3.4B). In dividing *Allium* mother guard cells, the tubular vacuoles appeared transiently (Palevitz and O'Kane, 1981). In mitotic BY-2 cells, tubular vacuoles, named TVM, developed from a part of the large vacuole and became localized around the mitotic apparatus and cell plate (Kutsuna and Hasezawa, 2002; Fig. 3.4D, arrowheads). TVMs were localized between the cell plate and nucleus, and then expanded to the large vacuole at the early G_1 phase (Kutsuna et al., 2003). Although experimental evidence for the exact roles of TVMs is still lacking, it

has been suggested that they could be the destination of removed lipid membranes from the cell plate during cell plate maturation (Kutsuna et al., 2003).

In *Vicia faba* guard cells, the tubular vacuoles became transformed into spherical vacuoles during stomatal opening (Gao et al., 2005). Such tubular vacuoles were also observed in the pollen tubes of *Arabidopsis* (Hicks et al., 2004), and these expanded to form larger vacuoles in mature pollen tubes. In tobacco BY-2 miniprotoplasts, which are protoplasts evacuolated by centrifugation, the tubular vacuoles appeared during expansion of the large vacuole (Okubo-Kurihara et al., 2009). These results suggest that the tubular structures are not only involved in the storage of excess VMs but also in the preparation for vacuolar enlargement.

3.3. Transvacuolar strand (cytoplasmic strand)

The TVS is one of several cytoplasmic tunnels within the large vacuoles that serves as a route for material/organelle transport. Indeed, it was observed that Golgi bodies (Nebenführ et al., 1999), mitochondria (van Gestel et al., 2002), endosomes (Ovecka et al., 2005; Ruthardt et al., 2005), and amyloplasts (Saito et al., 2005) dynamically move through the TVSs. In a tip-growing root hair cell of *Hydrocharis*, a single thick TVS was found that runs toward the apex. The cells showed fountain cytoplasmic streaming through the TVS, which suggested that it may be required for transport of materials toward the growing tip (Shimmen et al., 1995). TVSs are also required for gravisensing via regulation of amyloplast movement that has statolith functions in endodermal cells (Saito et al., 2005). In dividing cells, TVSs that connect between nuclei and the cell surface are suggested to be involved in determining the cell division site (Flanders et al., 1990; Panteris et al., 2004). Furthermore, breakdown of TVSs by laser microsurgery was found to induce relocation of the premitotic nuclei (Goodbody et al., 1991), suggesting important roles of TVSs in nuclear positioning. However, as detailed in Section 4, cytoskeletons, which always run through the TVSs, are required for maintenance of the TVSs, implying that the possible functions of TVSs and cytoskeletons are inseparable. In this context, TVS appear to be structures that allow the cytoskeletons to move freely in vacuolated plant cells.

In tobacco BY-2 culture cells, many of the complicated TVSs are found to undergo rapid changes by displacement, branching, and fusion (Hoffman and Nebenführ, 2004; Ruthardt et al., 2005; Fig. 3.4C, arrows). Although TVSs can be observed in various materials (e.g., *Arabidopsis* leaf epidermal cells as shown in Fig. 3.4E, arrows), the most detailed TVS dynamics have been described in tobacco BY-2 cells. Ruthardt et al. (2005) performed four-dimensional imaging of TVSs in FM dye-labeled BY-2 cells. Their high-quality observations showed that new TVSs are formed by fission of intravacuolar sheet-like VMs within several minutes (Ruthardt et al., 2005). Similar results have been found during the conversion of sheet-like VM

structures to TVSs (Higaki et al., 2006; Sheahan et al., 2007). Alternatively, as VM groove structures appear on the large vacuolar surface during TVS formation in BY-2 cells, it has been suggested that TVSs are also created by invagination of the VM groove (Higaki et al., 2006).

3.4. Bulbs and sheets

In rapidly expanding cells, spherical structures designated as ''bulbs'' within the lumen of vacuoles have been shown by electron microscopy to be basic projections of the cytoplasm, and often consisting of two VMs (Saito et al., 2002; Fig. 3.4E and F). The term bulb was derived from their spherical shapes and the brightness of the VM fluorescence (Saito et al., 2002), which implies that bulbs are formed from a double VM that sandwiches a thin cytoplasm (Reisen et al., 2005; Saito et al., 2002; Uemura et al., 2002). Indeed, electron microscope studies have demonstrated a thin cytoplasm invagination surrounding the VMs in large vacuoles (Saito et al., 2002), whereas cytoskeletons have not yet been detected in these invagination. The existence of bulbs has been demonstrated using various VM markers; GFP-AtVAM3 (Kutsuna and Hasezawa, 2005; Uemura et al., 2002), AtTIP1;1-GFP (Boursiac et al., 2005), GFP-δTIP (Sheahan et al., 2007), BobTIP26-1-GFP (Reisen et al., 2005), phosphate transporter homolog-GFP (Escobar et al., 2003), and YFP-2xFYVE, a phosphatidylinositol 3-phosphate probe (Vermeer et al., 2006). Furthermore, similar spherical vesicles in the vacuolar lumen have been observed by GFP fusions to the endosome-binding domain that specifically binds phosphatidylinositol 3-phosphate (Kim et al., 2001) and γTIP (Hawes et al., 2001).

Many bulbs are observed in young leaf and hypocotyls cells (Saito et al., 2002; Fig. 3.4E and F). They also appear in cells under hyperosmotic conditions (Kutsuna and Hasezawa, 2005; Uemura et al., 2002) and in guard cells of closed stomata (Gao et al., 2005; Tanaka et al., 2007). As bulbs disappear in old expanded cells, it has been suggested that they may serve as VM reservoirs for rapid cell expansion during water absorption in vacuoles (Saito et al., 2002). The bulbs move continuously like a bubble (Fig. 3.3, bulb), and although are normally spherical they could be distorted in shape and converted to sheet-like VM invagination (Uemura et al., 2002). In addition, bulbs often connect with sheet-like VM invagination and TVSs (Kutsuna and Hasezawa, 2005; Reisen et al., 2005; Saito et al., 2002; Uemura et al., 2002; Fig. 3.4E), suggesting that these structures have similar functions. Interestingly, γTIP-GFP is found to be concentrated in bulb VMs, whereas GFP-AtRAB7c is depleted (Saito et al., 2002). Although this latter report suggests the heterogeneity of VM proteins between the bulb and large vacuolar surface, future studies are needed to clarify their distinct localization mechanisms and significance.

In summary, vacuoles undergo dynamic changes in shape, according to the developmental stage, in order to adapt to environmental changes, maintain intracellular homeostasis and prepare for rapid cell growth. Recent studies have shown the importance of cytoskeletons in vacuolar morphogenesis, and we describe these in the following section.

4. REGULATION OF VACUOLAR STRUCTURE AND DYNAMICS

Plant cells have two types of cytoskeleton: actin microfilaments and microtubules. In higher plant cells, actin microfilaments appear to be mainly used for positioning and morphogenesis of organelles (Wada and Suetsugu, 2004), such as Golgi bodies (Boevink et al., 1998; Nebenführ et al., 1999), the ER (Runions et al., 2006; Sheahan et al., 2004a,b), mitochondria (van Gestel et al., 2002), peroxisomes (Collings et al., 2002; Jedd and Chua, 2002; Mano et al., 2002; Mathur et al., 2002), and chloroplasts (Takagi, 2003; Wada et al., 2003). In contrast, microtubules are involved in the regulation of cell wall deposition, especially the alignment of cellulose microfibrils along the cortical microtubule array in both primary cell walls (Paredez et al., 2006a,b) and secondary cell walls (Oda and Hasezawa, 2006; Oda et al., 2005; Wightman and Turner, 2008). Although evidence to date has suggested that actin microfilaments regulate vacuolar morphogenesis and dynamics, the recent demonstration in moss plants of microtubule, rather than actin microfilament, involvement in vacuolar morphogenesis suggests a diversity of mechanisms in the plant kingdom. In this section, we summarize the findings of studies on the relationship between vacuolar morphogenesis and the cytoskeleton.

4.1. Actin-dependent regulation

Because of the difficulties in visualizing both actin microfilaments and VMs, early evidence for the involvement of actin microfilaments in vacuolar morphogenesis were based on pharmacological experiments using cytochalasin D, latrunculin B, and bistheonellide A, all of which induce depolymerization of actin microfilaments. Vacuolar dynamics in *Allium* stomatal cells require actin microfilaments (Palevitz and O'Kane, 1981). In *Arabidopsis* leaf epidermal cells, cytochalasin D was found to block VM dynamics (Uemura et al., 2002). In *Arabidopsis* trichomes, latrunculin B induced fragmentation of the large vacuole into small compartments. Similar vacuolar deformation was observed in the *arp2* mutant (Mathur et al., 2003). In *Arabidopsis* root hair cells, latrunculin B induced deformation of the fine vacuolar protrusions (Ovecka et al., 2005). In lily pollen tubes, latrunculin B treatment significantly affected vacuolar motion and morphology whereas oryzalin,

which inhibits microtubule polymerization, had no effect on the vacuole (Lovy-Wheeler et al., 2007). Similar results were also obtained using tobacco BY-2 cells. Bistheonellide A, which inhibits polymerization of G-actin (Saito et al., 1998), prevented the structural rearrangement of vacuoles during mitosis and disrupted the TVMs (Kutsuna et al., 2003) and in addition deformed the vacuolar structures and induced fragmentation of small vacuoles whereas depolymerization of the microtubules by propy-zamide treatment did not (Higaki et al., 2006). Furthermore, bistheonellide A treatment reduced VM movement and prevented reorganization of TVSs during the early G_1 phase. The general myosin ATPase inhibitor, 2,3-butanedion monoxime (BDM), also inhibited both events and suggested the involvement of an actin–myosin system in vacuolar morphogenesis (Higaki et al., 2006). During programmed cell death induced by a pathogenic elicitor, bistheonellide A modified vacuolar rearrangements and the timing of vacuolar rupture (Higaki et al., 2007).

Despite various lines of evidence suggesting actin microfilament-dependent regulation of vacuolar morphogenesis, there were no reports directly showing the colocalization of actin microfilaments and VM until recently. This was largely due to the difficulties of visualizing actin micro-filaments in plant cells. For example, visualization of actin microfilaments by fluorescently labeled phallotoxins caused cytoplasmic disorganization during detergent treatment of the staining procedure. To overcome such technical difficulties, Kutsuna et al. (2003) visualized actin microfilaments in living tobacco BY-2 cells using the weak detergent, saponin, and demonstrated the colocalization of TVM and actin microfilaments. More recently, the visualization of actin microfilaments in living cells has progressed through the use of fluorescent proteins fused to the actin-binding domain 2 (ABD2) of the *Arabidopsis* fimbrin AtFIM1 protein (Sano et al., 2005; Sheahan et al., 2004a,b; Voigt et al., 2005; Wang et al., 2004). By using GFP-ABD2, Higaki et al. (2006) succeeded in dual labeling of the VM and actin microfilaments in BY-2 cells and revealed the colocalization of actin microfilaments with VM of the TVS and large vacuole (Fig. 3.5). They also observed the concomitant appearance of bundles of actin microfilaments and grooves of VM, which would represent the initial state of a TVS in the early G_1 phase. These observations are in accord with previous pharmacological reports on vacuolar morphology and suggest an active role of actin microfilaments in regulating vacuolar structures, such as TVSs.

These reports strongly imply a direct connection between the VM and actin microfilaments. Inhibition of vacuolar dynamics by BDM suggested the involvement of the actin–myosin system (Higaki et al., 2006). In fact, a proteome approach revealed that cytoskeletal motor proteins, such as myosin–related proteins and dynamin–related proteins, are included in vacuolar proteins (Carter et al., 2004). The involvement of myosins in other plant
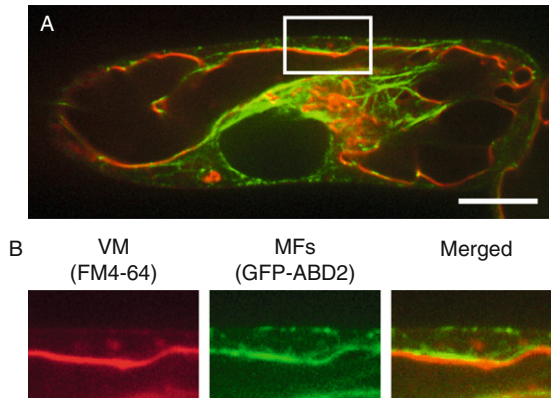
Figure 3.5 Interaction between vacuoles and actin microfilaments in tobacco BY-2 cells. (A) Dual visualization of VM and actin microfilaments by staining with FM4-64 (red) and by expression of GFP–ABD2 (green), respectively. Scale bar indicates 10 μm. (B) Magnified images of boxed region in (A). Note the dense localization of actin microfilaments on the vacuolar surface.

organelle positioning systems has also been suggested (Avisar et al., 2008; Li and Nebenführ, 2007; Peremyslov et al., 2008; Reisen and Hanson, 2007; Sattarzadeh et al., 2008; Sparkes et al., 2008). However, the linker protein connecting the VM and actin microfilaments has not yet been identified. In budding yeast, the vacuole is transported to the budding site along the actin cable for vacuolar inheritance. This movement is mediated by a myosin V heavy chain, Myo2, that is connected to the VM via its receptor, Vac17p (Ishikawa et al., 2003; Tang et al., 2003). In plants, several anchors between organelle membrane and the actin microfilaments have been identified. KAM1/MUR3 is a linkage component between Golgi bodies and actin microfilaments that was identified in an *Arabidopsis* mutant with an aberrant endomembrane structure (Tamura et al., 2005). In an *Arabidopsis* mutant with defects in chloroplast movement, CHUP1 was identified as a component connecting the chloroplast envelope and actin microfilaments (Oikawa et al., 2003, 2008). Screening of mutants with abnormal vacuolar morphogenesis, as well as proteome analysis and a reverse genetics approach will be important strategies in the identification of molecule(s) connecting the VM and actin microfilaments.

4.2. Microtubule-dependent regulation

Although actin microfilaments appear to spatially regulate vacuoles and other endomembrane systems in higher plant cells, several contradictions, mainly in bryophytes, have been reported. The association of microtubules with various organelles, including plastids, mitochondria, ERs, and

vacuole-like vesicles, was observed by transparent electron microscopy of inner parenchyma cells of bryoid mosses (Ligrone and Duckett, 1994, 1996), leafy stem cells of *Sphagnum* mosses (Ligrone and Duckett, 1998), and moss protonema cells (Pressel et al., 2008). Depolymerization of microtubules by oryzalin induced aberrant positioning of these organelles and disorganization of cytoplasmic distribution, whereas they were largely unaffected by disruption of actin microfilaments with cytochalasin D (Ligrone and Duckett, 1996; Pressel et al., 2008). In leafy stem cells of *Sphagnum* mosses, the close association between small vacuoles and microtubules was observed by electron microscopy (Ligrone and Duckett, 1998). Recently, Oda et al. (2009) reported the detailed analysis of vacuolar structures and dynamics in living protonema and rhizoid cells of the moss *Physcomitrella patens* using the VM marker, AtVAM3-GFP. In protonema cells of *P. patens*, tubular vacuoles were observed around the cortex of the cell around the large vacuoles and in the apical region of rhizoid cells where they exhibited dynamic motion, such as rapid elongation and shrinkage, fusion, and separation. Microtubule depolymerization by oryzalin caused a dramatic deformation of vacuoles (Fig. 3.6), swelling of tubular vacuoles around the cell cortex, the complete loss of tubular vacuoles in rhizoid cells, and the complete cessation of the dynamic motions of vacuoles. Furthermore, dual labeling of VM and microtubules revealed their colocalization and concomitant movements. These studies are indicative of the involvement of microtubules in vacuolar morphogenesis.

There appear to be three possibilities that could explain the discrepancies in cytoskeleton dependency in vacuolar morphogenesis. One possibility, in view of the fact that the moss cells in which the vacuolar structures appear regulated by microtubules are mainly tip-growing protonema and rhizoid cells, is that tip-growing cells and diffusely growing cells employ different regulatory systems. However, this possibility may be low because in root hair cells, that are typical tip-growing cells in higher plants, vacuolar morphogenesis is also dependent on actin microfilaments (Ovecka et al., 2005). The second possibility is that gametophytic and sporophytic cells use different cytoskeleton systems for vacuolar morphogenesis. In pollen tubes, the movement of small organelles along microtubules and the involvement of kinesins have been reported (Cai et al., 2000; Romagnoli et al., 2003, 2007). However, in regard to the vacuole and cytoskeleton, this possibility also seems unlikely as oryzalin-induced microtubule depolymerization had no effect on vacuoles in lily pollen tubes (Lovy-Wheeler et al., 2007). The other possibility is that plants developed different regulatory systems for the endomembranes and cytoskeletons during evolution. This possibility is supported by the fact that microtubule dependency on endomembrane organization, including vacuoles, is mainly observed in lower species like moss cells. In fungi, vacuolar distribution is regulated by microtubules (Ashford, 1998), and in animal cells the distribution of endomembranes,
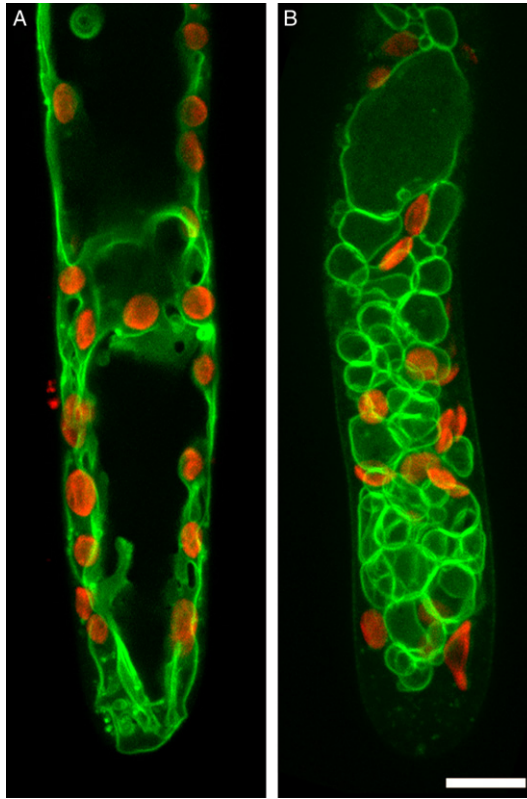
Figure 3.6 Effects of microtubule depolymerization on vacuole structure in proto-
nema cells of the moss, *P. patens*. Green signals represent fluorescence of the VM
marker, GFP-AtVAM3. Red signals represent the autofluorescence of chloroplasts.
(A) Normal vacuolar structure and chloroplast distribution. (B) VM and chloroplasts
of an oryzalin-treated protonema cell. Compared with the normal vacuole shown in
panel A, the vacuole is highly disorganized due to depolymerization of microtubules.
Scale bar indicates 10 μm.

such as the ER and Golgi bodies, are mainly regulated by microtubules
(Allan et al., 2002; Rios and Bornens, 2003; Shorter and Warren, 2002;
Thyberg and Moskalewski, 1999; Vedrenne and Hauri, 2006), whereas
higher plant cells utilize actin microfilaments to regulate these organelles.
It is, therefore, possible that moss plants (and other lower plants) developed
different cytoskeleton–endomembrane systems, including vacuoles and
microtubules, than those of higher plants. In moss plants, microtubules
may have developed to regulate endomembranes rather than cell wall
deposition, which is largely dependent on highly organized cortical micro-
tubule arrays in higher plant cells. Further investigation of various species
and cell types is needed to confirm this possibility.

5. Concluding Remarks

Numerous studies have revealed vacuolar morphologies and dynamics of plant cells, and are indicative of the uniqueness of the plant vacuole in its remarkable structural diversity and flexibility in comparison with other organelles. Some of these studies focused on the regulatory system of vacuolar morphology and somehow succeeded in gaining deeper insight into the relationship between vacuolar morphology and the cytoskeletons. Figure 3.7 shows a summary of these vacuolar structures and the possible regulatory mechanisms and functions. However, the molecular mechanism underlying vacuolar morphogenesis and functions remain obscure. In
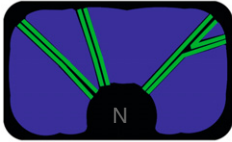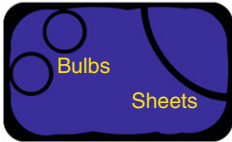
Types	Regulatory factors	Possible functions
A Large vacuole	(Higher plants) Actin microfilaments (Moss plants) Microtubules?	Space-filling and rapid cell expansion Storage of materials Trigger of programmed cell death
B Tubular vacuole	(Higher plants) Actin microfilaments (Moss plants) Microtubules	Destination of membrane from cell plate Preparation of vacuolar enlargement
C TVSs	(Higher plants) Actin microfilaments (Moss plants) Microtubules	Routes for materials and organelles Nuclear positioning Gravity sensing
D Bulbs and sheets	Independent of cytoskeletons	VM reservoir

Figure 3.7 Summary of plant vacuolar structures, their regulatory mechanisms, and possible functions. (A) Large vacuole. (B) Tubular vacuoles in a meristematic cell. The white line represents a developing cell plate. (C) TVSs in a diffusely growing cell. N represents the nucleus. (D) Bulbs and sheets. Although the schematic models are only for cases of diffusely growing (or grown) cells, tubular vacuoles, and TVSs are also conspicuous in tip-growing cells, such as root hairs, pollen tubes, protonema cells, and rhizoid cells. Bulbs and sheets are observed in various cells.

budding yeast, the molecular complex that transports vacuoles along the actin microfilaments was identified by screening mutants defective in vacuolar inheritance. Although none of the factors related to vacuolar morphogenesis have yet been identified in plants, concerted effort and focus on identifying such mutants should reveal the molecular mechanisms of vacuolar morphogenesis.

Another important finding regarding vacuolar morphogenesis is the diversity of its regulatory systems in the plant kingdom. Although the mechanisms regulating vacuolar structures may differ between plant lineages, all plants essentially use vacuoles in their development. A detailed investigation into the various types of cells and species should contribute to this issue. Furthermore, the use of recently available model plants, such as the liverwort, *Marchantia polymorpha*, and the lycophyte, *Selaginella moellendorffii*, may bring further important insights into the evolutionary aspects of vacuolar morphogenesis in the plant kingdom.

Finally, the most important issue should be to clarify the function of each vacuolar structure. As there appears to be a clear relationship between vacuolar structure and cellular type, these structures may have specific roles in each cell. When mutants in vacuolar morphogenesis become more readily available, they will certainly contribute to significant breakthroughs in this area. The goal of this research should therefore be to integrate insights about vacuolar morphology, its regulatory mechanisms, and its cellular functions in order to understand the role of the vacuole, as an active and dynamic organelle, in plant development.

REFERENCES

Allan, V.J., Thompson, H.M., McNiven, M.A., 2002. Motoring around the Golgi. Nat. Cell Biol. 4, 236–242.

Angeli, A.D., Monachello, D., Ephritikhine, G., Frachisse, J.M., Thomine, S., Gambale, F., et al., 2006. The nitrate/proton antiporter AtCLCa mediates nitrate accumulation in plant vacuoles. Nature 442, 939–942.

Aniento, F., Robinson, D.G., 2005. Testing for endocytosis in plants. Protoplasma 226, 3–11.

Ashford, A.E., 1998. Dynamic pleiomorphic vacuole systems: are they endosomes and transport compartments in fungal hyphae? Adv. Bot. Res. 28, 119–159.

Aubert, S., Gout, E., Bligny, R., Marty-Mazars, D., Barrieu, F., Alabouvette, J., et al., 1996. Ultrastructural and biochemical characterization of autophagy in higher plant cells subjected to carbon deprivation: control by the supply of mitochondria with respiratory substrates. J. Cell Biol. 133, 1251–1263.

Avci, U., Petzold, H.E., Ismail, I.O., Beers, E.P., Haigler, C.H., 2008. Cysteine proteases XCP1 and XCP2 aid micro-autolysis within the intact central vacuole during xylogenesis in *Arabidopsis* roots. Plant J. 56, 303–315.

Avisar, D., Prokhnevsky, A.I., Makarova, K.S., Koonin, E.V., Dolja, V.V., 2008. Myosin XI-K is required for rapid trafficking of Golgi stacks, peroxisomes, and mitochondria in leaf cells of *Nicotiana benthamiana*. Plant Physiol. 146, 1098–1108.

Bassham, D.C., 2007. Plant autophagy—more than a starvation response. Curr. Opin. Plant Biol. 10, 587–593.

Bengough, A.G., Bransby, M.F., Hans, J., McKenna, S.J., Roberts, T.J., Valentine, T.A., 2006. Root responses to soil physical conditions; growth dynamics from field to cell. J. Exp. Bot. 57, 437–447.

Berg, R.H., Beachy, R.N., 2008. Fluorescent protein applications in plants. Methods Cell Biol. 85, 153–177.

Boevink, P., Oparka, K., Santa Cruz, S., Martin, B., Betteridge, A., Hawes, C., 1998. Stacks on tracks: the plant Golgi apparatus traffics on an actin/ER network. Plant J. 15, 441–447.

Bolte, S., Talbot, C., Boutte, Y., Catrice, O., Read, N.D., Satiat-Jeunemaitre, B., 2004. FM-dyes as experimental probes for dissecting vesicle trafficking in living plant cells. J. Microsc. 214, 159–173.

Boursiac, Y., Chen, S., Luu, D.T., Sorieul, M., van der Dries, N., Maurel, C., 2005. Early effect of salinity on water transport in *Arabidopsis* roots. Molecular and cellular features of aquaporin expression. Plant Physiol. 139, 790–805.

Bove, J., Vaillancourt, B., Kroeger, J., Hepler, P.K., Wiseman, P.W., Geitmann, A., 2008. Magnitude and direction of vesicle dynamics in growing pollen tubes using spatiotemporal image correlation spectroscopy and fluorescence recovery after photobleaching. Plant Physiol. 147, 1646–1658.

Brandizzi, F., Irons, S.L., Johansen, J., Kotzer, A., Neumann, U., 2004. GFP is the way to glow: bioimaging of the plant endomembrane system. J. Microsc. 214, 138–158.

Cai, G., Romagnoli, S., Moscatelli, A., Ovidi, E., Gambellini, G., Tiezzi, A., et al., 2000. Identification and characterization of a novel microtubule-based motor associated with membranous organelles in tobacco pollen tubes. Plant Cell 12, 1719–1736.

Carter, C., Pan, S., Zouhar, J., Avila, E.L., Girke, T., Raikhel, N.V., 2004. The vegetative vacuole proteome of *Arabidopsis thaliana* reveals predicted and unexpected proteins. Plant Cell 16, 3285–3303.

Collings, D.A., Harper, J.D.I., Marc, J., Overall, R.L., Mullen, R.T., 2002. Life in the fast lane: actin-based motility of plant peroxisomes. Can. J. Bot. 80, 430–441.

Di Sansebastiano, G.P., Paris, N., Marc-Martin, S., Neuhaus, J.M., 1998. Specific accumulation of GFP in a non-acidic vacuolar compartment via a C-terminal propeptide-mediated sorting pathway. Plant J. 15, 449–457.

Dolan, L., Davies, J., 2004. Cell expansion in roots. Curr. Opin. Plant Biol. 7, 33–39.

Dubrovsky, J.G., Guttenberger, M., Saralegui, A., Napsucialy-Mendivil, S., Voigvt, B., Baluska, F., et al., 2006. Neutral red as a probe for confocal laser scanning microscopy studies of plant roots. Ann. Bot. 97, 1127–1138.

Ehara, M., Noguchi, T., Ueda, K., 1996. Uptake of neutral red by the vacuoles of a green alga, *Micrasterias pinnatifida*. Plant Cell Physiol. 37, 734–741.

Emans, N., Zimmermann, S., Fischer, R., 2002. Uptake of a fluorescent marker in plant cells is sensitive to brefeldin A and wortmannin. Plant Cell 14, 71–86.

Endler, A., Meyer, S., Schelbert, S., Schneider, T., Weschke, W., Peters, S.W., et al., 2006. Identification of a vacuolar sucrose transporter in barley and *Arabidopsis* mesophyll cells by a tonoplast proteomic approach. Plant Physiol. 141, 196–207.

Escobar, N.M., Haupt, S., Thow, G., Boevink, P., Chapman, S., Oparka, K., 2003. High-throughput vital expression of cDNA-green fluorescent protein fusions reveals novel subcellular addresses and identifies unique proteins that interact with plasmodesmata. Plant Cell 15, 1507–1523.

Flanders, D.J., Rawlins, D.J., Shaw, P.J., Lloyd, C.W., 1990. Nucleus-associated microtubules help determine the division plane of plant epidermal cells: avoidance of four-way junctions and the role of cell geometry. J. Cell Biol. 110, 1111–1122.

Fleurat-Lessard, P., Frangne, N., Maeshima, M., Ratajczak, R., Bonnemain, J.L., Martinoia, E., 1997. Increased expression of vacuolar aquaporin and H^+-ATPase related to motor cell function in *Mimosa pudica* L. Plant Physiol. 114, 827–834.

Flucktiger, R., De Caroli, M., Piro, G., Dalessandro, G., Neuhaus, J.M., Di Sansebastiano, G.P., 2003. Vacuolar system distribution in *Arabidopsis* tissues, visualized using GFP fusion proteins. J. Exp. Bot. 54, 1577–1584.

Fouquaert, E., Hanton, S.L., Brandizzi, F., Peumans, W.J., Van Damme, E.J.M., 2007. Localization and topogenesis studies of cytoplasmic and vacuolar homologs of the *Galanthus nivalis* Aggulutinin. Plant Cell Physiol. 48, 1010–1021.

Fricker, M.D., White, N., 1990. Volume measurements of guard cell vacuoles during stomatal movements using confocal microscopy. Trans. R. Microsc. Soc. 1, 345–348.

Frigerio, L., de Virgilio, M., Prada, A., Faoro, F., Vitale, A., 1998. Sorting of phaseolin to the vacuole is saturable and requires a short C-terminal peptide. Plant Cell 10, 1031–1042.

Frigerio, L., Hinz, G., Robinson, D.G., 2008. Multiple vacuoles in plant cells: rule or exception? Traffic 9, 1564–1570.

Fuji, K., Shimada, T., Takahashi, H., Tamura, K., Koumoto, Y., Utsumi, S., et al., 2007. *Arabidopsis* vacuolar sorting mutants (*green fluorescent seed*) can be identified efficiently by secretion of vacuole-targeted green fluorescent protein in their seeds. Plant Cell 19, 597–609.

Gaffal, K.P., Friedrichs, G.J., El-Gammal, S., 2007. Ultrastructural evidence for a dual function of the phloem and programmed cell death in the floral nectary of *Digitalis purpurea*. Ann. Bot. 99, 593–607.

Gao, X.Q., Li, C.H., Wei, P.C., Zhang, X.Y., Chen, J., Wang, X.C., 2005. The dynamic changes of tonoplasts in guard cells are important for stomatal movement in *Vicia faba*. Plant Physiol. 139, 1207–1216.

Geldner, N., 2004. The plant endosomal system—its structure and role in signal transduction and plant development. Planta 219, 547–560.

Goodbody, K.C., Venverloo, C.J., Lloyd, C.W., 1991. Laser microsurgery demonstrates that cytoplasmic strands anchoring the nucleus across the vacuole of premitotic plant cells are under tension. Implications for division plane alignment. Development 113, 931–939.

Guillermond, A., 1929. The recent development of our idea of the vacuole of plant cells. Am. J. Bot. 16, 1–22.

Hara-Nishimura, I., Shimada, T., Hatano, K., Takeuchi, Y., Nishimura, M., 1998. Transport of storage proteins to protein storage vacuoles is mediated by large precursor-accumulating vesicles. Plant Cell 10, 825–836.

Hatsugai, N., Kuroyanagi, M., Yamada, K., Meshi, T., Tsuda, S., Kondo, M., et al., 2004. A plant vacuolar protease, VPE, mediates virus-induced hypersensitive cell death. Science 305, 855–858.

Hawes, C., Saint-Jore, C.M., Brandizzi, F., Zheng, H., Andreeva, A.V., Boevink, P., 2001. Cytoplasmic illuminations: in planta targeting of fluorescent proteins to cellular organelles. Protoplasma 215, 77–88.

Hicks, G.R., Rojo, E., Hong, S., Carter, D.G., Reikhel, N.V., 2004. Germinating pollen has tubular vacuoles, displays highly dynamic vacuole biogenesis, and requires VACUOLESS1 for proper function. Plant Physiol. 134, 1227–1239.

Higaki, T., Kutsuna, N., Okubo, E., Sano, T., Hasezawa, S., 2006. Actin microfilaments regulate vacuolar structures and dynamics: dual observation of actin microfilaments and vacuolar membrane in living tobacco BY-2 cells. Plant Cell Physiol. 46, 2005–2018.

Higaki, T., Goh, T., Hayashi, T., Kutsuna, N., Kadota, Y., Hasezawa, S., et al., 2007. Elicitor-induced cytoskeletal rearrangement relates to vacuolar dynamics and execution of cell death: *in vivo* imaging of hypersensitive cell death in tobacco BY-2 cells. Plant Cell Physiol. 48, 1414–1425.

Higaki, T., Kutsuna, N., Sano, T., Hasezawa, S., 2008. Quantitative analysis of changes in actin microfilament contribution to cell plate development in plant cytokinesis. BMC Plant Biol. 8, 80.

Hillmer, S., Quader, H., Robert-Nicound, M., Robinson, D.G., 1989. Lucifer yellow uptake in cells and protoplasts of *Daucas carota* visualized by laser scanning microscopy. J. Exp. Bot. 40, 417–423.

Hoffman, A., Nebenführ, A., 2004. Dynamic rearrangements of transvacuolar strands in BY-2 cells imply a role of myosin in remodelling of the plant actin cytoskeletons. Protoplasma 24, 201–210.

Hohl, I., Robinson, D.G., Chrispeels, M.J., Hinz, G., 1996. Transport of storage proteins to the vacuole is mediated by vesicles without a clathrin coat. J. Cell Sci. 109, 2539–2550.

Hunter, P.R., Craddock, C.P., Benedetto, S.D., Roberts, L.M., Frigerio, L., 2007. Fluorescent reporter proteins for the tonoplast and the vacuolar lumen identify a single vacuolar compartment in *Arabidopsis* cells. Plant Physiol. 145, 1371–1382.

Ishikawa, K., Catlett, N.L., Novak, J.L., Tang, F., Nau, J.J., Weisman, L.S., 2003. Identification of an organelle-specific myosin V receptor. J. Cell Biol. 160, 887–897.

Iwano, M., Shiba, H., Matoba, K., Miwa, T., Funato, M., Entani, T., et al., 2007. Actin dynamics in papilla cells of *Brassica rapa* during self- and cross-pollination. Plant Physiol. 144, 72–81.

Jaquinod, M., Villers, F., Kieffer-Jaquinod, S., Hugouvieux, V., Bruley, C., Garin, J., et al., 2007. A proteomics dissection of *Arabidopsis thaliana* vacuoles isolated from cell culture. Mol. Cell. Proteomics 6, 394–412.

Jauh, G.Y., Philips, T.E., Rogers, J.C., 1999. Tonoplast intrinsic protein isoforms as markers for vacuolar functions. Plant Cell 11, 1867–1882.

Jedd, G., Chua, N.H., 2002. Visualization of peroxisomes in living plant cells reveals acto-myosin-dependent cytoplasmic streaming and peroxisome budding. Plant Cell Physiol. 43, 384–392.

Jones, A.M., 2001. Programmed cell death in development and defense. Plant Physiol. 125, 94–97.

Kamiya, T., Akahori, T., Ashikari, M., Maeshima, M., 2006. Expression of the vacuolar Ca^{2+}/H^+ exchanger, OsCAX1a, in rice: cell and age specificity of expression, and enhancement by Ca^{2+}. Plant Cell Physiol. 47, 96–106.

Kanzawa, N., Hoshino, Y., Chiba, M., Hoshino, D., Kobayashi, H., Kamasawa, N., et al., 2006. Changes in the actin cytoskeleton during seismonastic movement of *Mimosa pudica*. Plant Cell Physiol. 47, 531–539.

Kawai, M., Samarajeewa, P.K., Barrero, R.A., Nishiguchi, M., Uchimiya, H., 1998. Cellular dissection of the degradation pattern of cortical cell death during aerenchyma formation of rice roots. Planta 204, 277–287.

Kim, D.H., Eu, Y.J., Yoo, C.M., Kim, Y.W., Pih, K.T., Jin, J.B., et al., 2001. Trafficking of phosphatidylinositol 3-phosphate from the *trans*-Golgi network to the central vacuole in plant cells. Plant Cell 13, 287–301.

Kobae, Y., Uemura, T., Sato, M.H., Ohnishi, M., Mumura, T., Nakagawa, T., et al., 2004. Zinc transporter of *Arabidopsis thaliana* AtMTP1 is localized to vacuolar membranes and implicated in zinc homeostasis. Plant Cell Physiol. 45, 1749–1758.

Kovermann, P., Meyer, S., Hortensteiner, S., Picco, C., Scholz-Starke, J., Ravera, S., et al., 2007. The *Arabidopsis* vacuolar malate channel is a member of the ALMT family. Plant J. 52, 1169–1180.

Kufner, I., Koch, W., 2008. Stress regulated members of the plant organic cation transporter family are localized to the vacuolar membrane. BMC Res. Notes 1, 43.

Kutsuna, N., Hasezawa, S., 2002. Dynamic organization of vacuolar and microtubule structures during cell cycle progression in synchronized tobacco BY-2 cells. Plant Cell Physiol. 43, 965–973.

Kutsuna, N., Hasezawa, S., 2005. Morphometrical study of plant vacuolar dynamics in living cells using three-dimensional reconstruction from optical sections. Microsc. Res. Tech. 68, 296–306.

Kutsuna, N., Kumagai, F., Sato, M.H., Hasezawa, S., 2003. Three-dimensional reconstruction of tubular structure of vacuolar membrane throughout mitosis in living tobacco cells. Plant Cell Physiol. 44, 1045–1054.

Leshem, Y., Melamed-Bock, N., Cagnac, O., Ronen, G., Nishri, Y., Solomon, M., et al., 2006. Suppression of *Arabidopsis* vesicle-SNARE expression inhibited fusion of H_2O_2-containing vesicles with tonoplast and increased salt tolerance. Proc. Natl. Acad. Sci. USA 103, 18008–18013.

Li, J.F., Nebenführ, A., 2007. Inter-dependence of dimerization and organelle binding in myosin XI. Plant J. 55, 478–490.

Li, L., Shimada, T., Takahashi, H., Ueda, H., Fukao, Y., Kondo, M., et al., 2006. MAIGO2 is involved in exit of seed storage proteins from the endoplasmic reticulum in *Arabidopsis thaliana*. Plant Cell 18, 3535–3547.

Ligrone, R., Duckett, J.G., 1994. Cytoplasmic polarity and endoplasmic microtubules associated with the nucleus and organelles are ubiquitous features of food-conducting cells in bryoid mosses (Bryophyta). New Phytol. 127, 601–614.

Ligrone, R., Duckett, J.G., 1996. Polarity and endoplasmic microtubules in food-conducting cells of mosses: an experimental study. New Phytol. 134, 503–516.

Ligrone, R., Duckett, J.G., 1998. The leafy stems of Sphagnum (Bryophyta) contain highly differentiated polarized cells with axial arrays of endoplasmic microtubules. New Phytol. 140, 567–579.

Lovy-Wheeler, A., Cardenas, L., Kunkel, J.G., Hepler, P.K., 2007. Differential organelle movement on the actin cytoskeleton in lily pollen tubes. Cell Motil. Cytoskeleton 64, 217–232.

Mano, S., Nakamori, C., Hayashi, M., Kato, A., Kondo, M., Nishimura, M., 2002. Distribution and characterization of peroxisomes in *Arabidopsis* by visualization with GFP: dynamic morphology and actin-dependent movement. Plant Cell Physiol. 43, 331–341.

Martinoia, E., Maeshima, M., Neuhaus, H.E., 2007. Vacuolar transporters and their essential role in plant metabolism. J. Exp. Bot. 58, 83–102.

Marty, F., 1978. Cytochemical studies on GERL, provacuoles, and vacuoles in root meristematic cells of *Euphobia*. Proc. Natl. Acad. Sci. USA 75, 852–856.

Marty, F., 1997. The biogenesis of vacuoles: insights from microscopy. Adv. Bot. Res. 25, 1–42.

Marty, F., 1999. Plant vacuoles. Plant Cell 11, 587–599.

Mathur, J., Mathur, N., Hülskamp, M., 2002. Simultaneous visualization of peroxisomes and cytoskeletal elements reveals actin and not microtubule-based peroxisome motility in plants. Plant Physiol. 128, 1031–1045.

Mathur, J., Mathur, N., Kernebeck, B., Hulskamp, M., 2003. Mutations in actin-related proteins 2 and 3 affect cell shape development in *Arabidopsis*. Plant Cell 15, 1632–1645.

Mitsuhashi, N., Shimada, T., Mano, S., Nishimura, M., Hara-Nishimura, I., 2000. Characterization of organelles in the vacuolar-sorting pathway by visualization with GFP in tobacco BY-2 cells. Plant Cell Physiol. 41, 993–1001.

Mo, B., Tse, Y.C., Jiang, L., 2006. Plant prevacuolar/endosomal compartments. Int. Rev. Cytol. 253, 95–129.

Morita, M.T., Kato, T., Nagafusa, K., Saito, C., Ueda, T., Nakano, A., et al., 2002. Involvement of the vacuoles of the endodermis in the early process of shoot gravitropism in *Arabidopsis*. Plant Cell 14, 47–56.

Moriyasu, Y., Ohsumi, Y., 1996. Autophagy in tobacco suspension-cultured cells in response to sucrose starvation. Plant Physiol. 111, 1233–1241.

Moriyasu, Y., Hattori, M., Jauh, G.Y., Rogers, J.C., 2003. Alpha tonoplast intrinsic protein is specifically associated with vacuole membrane involved in an autophagic process. Plant Cell Physiol. 44, 795–802.

Muntz, K., 2007. Protein dynamics and proteolysis in plant vacuoles. J. Exp. Bot. 58, 2391–2407.

Nebenführ, A., Gallagher, L.A., Dunahay, T.G., Frohlick, J.A., Mazurkiewicz, A.M., Meehl, J.B., et al., 1999. Stop-and-go movements of plant Golgi stacks are mediated by the acto-myosin system. Plant Physiol. 121, 1127–1142.

Neuhaus, H.E., 2007. Transport of primary metabolites across the plant vacuolar membrane. FEBS Lett. 581, 2223–2226.

Ngo, D.A., Garland, P.A., Mandoli, D.F., 2005. Development and organization of the central vacuole of *Acetabularia acetabulum*. New Phytol. 165, 731–746.

Nishimura, M., 1982. pH in vacuoles isolated from castor bean endosperm. Plant Physiol. 70, 742–746.

Nobel, P.A., Castaneda, M., North, G., Pimienta-Barrios, E., Ruiz, A., 1998. Temperature influences on leaf CO_2 exchange, cell viability and cultivation range for *Agave tequilana*. J. Arid Environ. 39, 1–9.

Obara, K., Kuriyama, K., Fukuda, H., 2001. Direct evidence of active and rapid nuclear degradation triggered by vacuole rupture during programmed cell death in Zinnia. Plant Physiol. 125, 615–626.

Oda, Y., Hasezawa, S., 2006. Cytoskeletal organization during xylem cell differentiation. J. Plant Res. 119, 167–177.

Oda, Y., Mimura, T., Hasezawa, S., 2005. Regulation of secondary cell wall development by microtubules during tracheary element differentiation in *Arabidopsis* suspensions. Plant Physiol. 137, 1027–1036.

Oda, Y., Hirata, A., Sano, T., Fujita, T., Hiwatashi, Y., Sato, Y., et al., 2009. Microtubules regulate dynamic organization of vacuoles in *Physcomitrella patens*. Plant Cell Physiol. 50, 855–868.

Oikawa, K., Kasahara, M., Kiyosue, T., Kagawa, T., Suetsugu, N., Takahashi, F., et al., 2003. Chloroplast unusual positioning1 is essential for proper chloroplast positioning. Plant Cell 15, 2805–2815.

Oikawa, K., Yamasato, A., Kong, S.G., Kasahara, M., Nakai, M., Takahashi, F., et al., 2008. Chloroplast outer envelope protein CHUP1 is essential for chloroplast anchorage to the plasma membrane and chloroplast movement. Plant Physiol. 148, 829–842.

Okubo-Kurihara, E., Sano, T., Higaki, T., Kutsuna, N., Hasezawa, S., 2009. Acceleration of vacuolar regeneration and cell growth by overexpression of an aquaporin NtTIP1;1 in tobacco BY-2 cells. Plant Cell Physiol. 50, 151–160.

Olbrich, A., Hillmer, S., Hinz, G., Oliviusson, P., Robinson, D.G., 2007. Newly formed vacuoles in root meristems of barley and pea seedlings have characteristics of both protein storage and lytic vacuoles. Plant Physiol. 145, 1383–1394.

Otegui, M.S., Noh, Y.S., Martinez, D.E., Vila Petroff, M.G., Staehelin, L.A., Amasino, R.M., et al., 2005. Senescence-associated vacuoles with intense proteolytic activity develop in leaves of *Arabidopsis* and soybean. Plant J. 41, 831–844.

Otegui, M.S., Herder, R., Schulze, J., Jung, R., Staehelin, L.A., 2006. The proteolytic processing of seed storage proteins in *Arabidopsis* embryo cells starts in the multivesicular bodies. Plant Cell 18, 2567–2581.

Ovecka, M., Lang, I., Baluska, F., Ismail, A., Illes, P., Lichtscheidl, I.K., 2005. Endocytosis and vesicle trafficking during tip growth of root hairs. Protoplasma 226, 39–54.

Ovecka, M., Baluska, F., Lichtscheidl, I., 2008. Non-invasive microscopy of tip-growing root hairs as a tool for study of dynamic and cytoskeleton-based vesicle trafficking. Cell Biol. Int. 32, 549–553.

Palevitz, B.A., O'Kane, D.J., 1981. Epifluorescence and video analysis of vacuole motility and development in stomatal cells of *Allium*. Science 214, 443–445.

Palevitz, B.A., O'Kane, D.J., Kobres, R.E., Raikhel, N.V., 1981. The vacuole system in stomatal cells of *Allium*. Vacuole movements and changes in morphology in differentiating cells as revealed by epifluorescence, video and electron microscopy. Protoplasma 109, 23–55.

Panteris, E., Apostolakos, P., Quader, H., Galatis, B., 2004. A cortical cytoplasmic ring predicts the division plane in vacuolated cells of Coleus: the role of actomyosin and microtubules in the establishment and function of the division site. New Phytol. 163, 271–286.

Paredez, A.R., Somerville, C.R., Ehrhardt, D.W., 2006a. Visualization of cellulose synthase demonstrates functional association with microtubules. Science 312, 1491–1495.

Paredez, A., Wright, A., Ehrhardt, D.W., 2006b. Microtubule cortical array organization and plant cell morphogenesis. Curr. Opin. Plant Biol. 9, 571–578.

Paris, N., Stanley, C.M., Jones, R.L., Rogers, J.C., 1996. Plant cells contain two functionally distinct vacuolar compartments. Cell 85, 563–572.

Park, J., Knoblauch, M., Okita, T.W., Edwards, G.E., 2009. Structural changes in the vacuole and cytoskeleton are key to development of the two cytoplasmic domains supporting single-cell C_4 photosynthesis in *Bienertia sinuspersici*. Planta 229, 369–382.

Parton, R.M., Fischer-Parton, S., Watahiki, M.K., Trewavas, A.J., 2001. Dynamics of the apical vesicle accumulation and the rate of growth are related in individual pollen tubes. J. Cell Sci. 114, 2685–2695.

Peiter, E., Maathuis, F.J.M., Mills, L.N., Knight, H., Pelloux, J., Hetherington, A.M., et al., 2005. The vacuolar Ca^{2+}-activated channel TPC1 regulates germination and stomatal movement. Nature 434, 404–408.

Peremyslov, V.V., Prokhnevsky, A.I., Avisar, D., Dolja, V.V., 2008. Two class XI myosins function in organelle trafficking and root hair development in *Arabidopsis*. Plant Physiol. 146, 1109–1116.

Petruccelli, S., Molina, M.I., Lareu, F.J., Circosta, A., 2007. Two short sequences from amaranth 11S globulin are sufficient to target green fluorescent protein and beta-glucuronidase to vacuoles in *Arabidopsis* cells. Plant Physiol. Biochem. 45, 400–409.

Poustka, F., Irani, N.G., Feller, A., Lu, Y., Pourcel, L., Frame, K., et al., 2007. A trafficking pathway for anthocyanins overlaps with the endoplasmic reticulum-to-vacuole protein-sorting route in *Arabidopsis* and contributes to the formation of vacuolar inclusions. Plant Physiol. 145, 1323–1335.

Pressel, S., Ligrone, R., Duckett, J.G., 2008. Cellular differentiation in moss protonemata: a morphological and experimental study. Ann. Bot. (Lond.) 102, 227–245.

Prychid, C.J., Jabaily, R.S., Rudall, P.J., 2008. Cellular ultrastructure and crystal development in *Amorphophallus* (Araceae). Ann. Bot. 101, 985–995.

Raven, J.A., 1997. The vacuole: a cost-benefit analysis. Adv. Bot. Res. 25, 59–86.

Reisen, D., Hanson, M.R., 2007. Association of six YFP-myosin XI-tail fusions with mobile plant cell organelles. BMC Plant Biol. 7, 6.

Reisen, D., Marty, F., Leborgne-Castel, N., 2005. New insights into the tonoplast architecture of plant vacuoles and vacuolar dynamics during osmotic stress. BMC Plant Biol. 5, 13.

Rios, R.M., Bornens, M., 2003. The Golgi apparatus at the cell centre. Curr. Opin. Cell Biol. 15, 60–66.

Rojo, E., Gllimor, C.S., Kovaleva, V., Somerville, C.R., Raikhel, N.V., 2001. VACUO-LESS 1 is an essential gene required for vacuole formation and morphogenesis in *Arabidopsis*. Dev. Cell 1, 303–310.

Romagnoli, S., Cai, G., Cresti, M., 2003. *In vitro* assays demonstrate that pollen tube organelles use kinesin-related motor proteins to move along microtubules. Plant Cell 15, 251–269.

Romagnoli, S., Cai, G., Faleri, C., Yokota, E., Shimmen, T., Cresti, M., 2007. Microtubule- and actin filament-dependent motors are distributed on pollen tube

mitochondria and contribute differently to their movement. Plant Cell Physiol. 48, 345–361.

Runions, J., Brach, T., Kühner, S., Hawes, C., 2006. Photoactivation of GFP reveals protein dynamics within the endoplasmic reticulum membrane. J. Exp. Bot. 57, 43–50.

Russ, J.C., 2002. The Image Processing Handbook, fourth ed. CRC Press, Boca Raton, FL.

Ruthardt, N., Gulde, N., Spiegel, H., Fischer, R., Emans, N., 2005. Four-dimensional imaging of transvacuolar strand dynamics in tobacco BY-2 cells. Protoplasma 225, 205–215.

Saito, S.Y., Watabe, S., Ozaki, H., Kobayashi, M., Suzuki, T., Kobayashi, H., et al., 1998. Actin-depolymerizing effect of dimeric macrolides, bistheonellide A and swinholide A. J. Biochem. 123, 571–578.

Saito, C., Ueda, T., Abe, H., Wada, Y., Kuroiwa, T., Hisada, A., et al., 2002. A complex and mobile structure forms a distinct subregion within the continuous vacuolar membrane in young cotyledons of *Arabidopsis*. Plant J. 29, 245–255.

Saito, C., Morita, M.T., Kato, T., Tasaka, M., 2005. Amyloplasts and vacuolar membrane dynamics in the living graviperceptive cell of the *Arabidopsis* influorescence stem. Plant Cell 17, 548–558.

Samalova, M., Fricker, M., Moore, I., 2006. Ratiometric fluorescence-imagin assays of plant membrane traffic using polyproteins. Traffic 7, 1701–1723.

Sano, T., Higaki, T., Oda, Y., Hayashi, T., Hasezawa, S., 2005. Appearance of actin microfilament 'twin peaks' in mitosis and their function in cell plate formation, as visualized in tobacco BY-2 cells expressing GFP-fimbrin. Plant J. 44, 595–605.

Sano, T., Kutsuna, N., Hasezawa, S., Tanaka, Y., 2008. Membrane trafficking in guard cells during stomatal movement: application of an image processing technique. Plant Signal. Behav. 3, 233–235.

Sattarzadeh, A., Franzen, R., Schmelzer, E., 2008. The *Arabidopsis* class VIII myosin ATM2 is involved in endocytosis. Cell Motil. Cytoskeleton 65, 457–468.

Schaaf, G., Honsbein, A., Meda, A.R., Kirchner, S., Wipf, D., von Wiren, N., 2006. AtIREG2 encodes a tonoplast transport protein involved in iron-dependent nickel detoxification in *Arabidopsis thaliana* roots. J. Biol. Chem. 281, 25532–25540.

Segui-Simarro, J.M., Staehelin, L.A., 2006. Cell cycle-dependent changes in Golgi stacks, vacuoles, clathrin-coated vesicles and multivesicular bodies in meristematic cells of *Arabidopsis thaliana*: a quantitative and spatial analysis. Planta 223, 223–236.

Sheahan, M.B., Rose, R.J., McCurdy, D.W., 2004a. Organelle inheritance in plant cell division: the actin cytoskeleton is required for unbiased inheritance of chloroplasts, mitochondria and endoplasmic reticulum in dividing protoplasts. Plant J. 37, 379–390.

Sheahan, M.B., Staiger, C.J., Rose, R.J., McCurdy, D.W., 2004b. A green fluorescent protein fusion to actin-binding domain 2 of *Arabidopsis* fimbrin highlights new features of a dynamic actin cytoskeleton in live plant cells. Plant Physiol. 136, 3968–3978.

Sheahan, M.B., Rose, R.J., McCurdy, D.W., 2007. Actin-filament–dependent remodeling of the vacuole in cultured mesophyll protoplasts. Protoplasma 230, 141–152.

Shimada, T., Fuji, K., Tamura, K., Kondo, M., Nishimura, M., Hara-Nishimura, I., 2003. Vacuolar sorting receptor for seed storage proteins in *Arabidopsis thaliana*. Proc. Natl. Acad. Sci. USA 100, 16095–16100.

Shimmen, T., Hamatani, M., Saito, S., Yokota, E., Mimura, T., Fusetani, N., Karaki, H., 1995. Roles of actin filaments in cytoplasmic streaming and organization of transvacuolar strands in root hair cells of Hydrocharis. Protoplasma 185, 188–193.

Shorter, J., Warren, G., 2002. Golgi architecture and inheritance. Annu. Rev. Cell Dev. Biol. 18, 379–420.

Silady, R.A., Ehrhardt, D.W., Jackson, K., Faulkner, C., Oparka, K., Somerville, C.R., 2008. The GRV2/RME-8 protein of *Arabidopsis* functions in the late endocytic pathway and is required for vacuolar membrane flow. Plant J. 53, 29–41.

Smith, F.A., Raven, J.A., 1979. Intracellular pH and its regulation. Ann. Rev. Plant Physiol. 30, 289–311.

Sparkes, I.A., Teanby, N.A., Hawes, C., 2008. Truncated myosin XI tail fusions inhibit peroxisome, Golgi, and mitochondrial movement in tobacco leaf epidermal cells: a genetic tool for the next generation. J. Exp. Bot. 59, 2499–2512.

Storey, R., Leigh, R.A., 2004. Process modulating calcium distribution in citrus leaves. An investigation using X-ray microanalysis with strontium as a tracer. Plant Physiol. 136, 3838–3848.

Swanson, S.J., Bethke, P.C., Jones, R.L., 1998. Barley aleurone cells contain two types of vacuoles: characterization of lytic organelles by use of fluorescent probes. Plant Cell 10, 685–698.

Takagi, S., 2003. Actin-based photo-orientation movement of chloroplasts in plant cells. J. Exp. Biol. 206, 1963–1969.

Tamura, K., Shimada, T., Ono, E., Tanaka, Y., Nagatani, A., Higashi, S., et al., 2003. Why green fluorescent fusion proteins have not been observed in the vacuoles of higher plants. Plant J. 35, 545–555.

Tamura, K., Shimada, T., Kondo, M., Nishimura, M., Hara-Nishimura, I., 2005. KATA-MARI1/MURUS3 is a novel Golgi membrane protein that is required for endomembrane organization in *Arabidopsis*. Plant Cell 17, 1764–1776.

Tanaka, Y., Kutsuna, N., Kanazawa, Y., Kondo, N., Hasezawa, S., Sano, T., 2007. Intravacuolar reserves of membranes during stomatal closure: the possible role of guard cell vacuoles estimated by 3-D reconstruction. Plant Cell Physiol. 48, 1159–1169.

Tang, F., Kauffman, E.J., Novak, J.L., Nau, J.J., Catlett, N.L., Weisman, L.S., 2003. Regulated degradation of a class V myosin receptor directs movement of the yeast vacuole. Nature 422, 87–92.

Terauchi, K., Asakura, T., Ueda, H., Tamura, T., Tamura, K., Matsumoto, I., et al., 2006. Plant-specific insertions in the soybean aspartic proteinases, soyAP1 and soyAP2, perform different functions of vacuolar targeting. J. Plant Physiol. 163, 856–862.

Thomine, S., Lelievre, F., Debarbieux, E., Schroeder, J.I., Barbier Brygoo, H., 2003. AtNRAMP3, a multispecific vacuolar metal transporter involved in plant responses to iron deficiency. Plant J. 34, 685–695.

Thyberg, J., Moskalewski, S., 1999. Role of microtubules in the organization of the Golgi complex. Exp. Cell Res. 246, 263–279.

Timmers, A.C.J., Tirlapur, U.K., Schel, J.H.N., 1995. Vacuolar accumulation of acridine orange and neutral red in zygotic and somatic embryos of carrot (*Daucus carota* L.). Protoplasma 188, 236–244.

Tong, Y.P., Kneer, R., Zhu, Y.G., 2004. Vacuolar compartmentalization: a second-generation approach to engineering plants for phytoremediation. Trends Plant Sci. 9, 7–9.

Toyooka, K., Moriyasu, Y., Goto, Y., Takeuchi, M., Fukuda, H., Matsuoka, K., 2006. Protein aggregates are transported to vacuoles by a macroautophagic mechanism in nutrient-starved plant cells. Autophagy 2, 96–106.

Ueda, T., Yamaguchi, M., Uchimiya, H., Nakano, A., 2001. Ara6, a plant-unique novel type Rab GTPase, functions in the endocytic pathway of *Arabidopsis thaliana*. EMBO J. 20, 4730–4741.

Uemura, T., Yoshimura, S.H., Takeyasu, K., Sato, M.H., 2002. Vacuolar membrane dynamics revealed by GFP-AtVam3p fusion protein. Genes Cells 7, 743–753.

Van Gestel, K., Kohler, R.H., Verbelen, J.P., 2002. Plant mitochondria move on F-actin, but their positioning in the cortical cytoplasm depends on both F-actin and microtubules. J. Exp. Bot. 53, 659–667.

Van Gisbergen, P.A.C., Esseling-Ozdoba, A., Vos, J.W., 2008. Microinjecting FM4-64 validates it as a marker of the endocytic pathway in plants. J. Microsc. 231, 284–290.

Vedrenne, C., Hauri, H.P., 2006. Morphogenesis of the endoplasmic reticulum: beyond active membrane expansion. Traffic 7, 639–646.

Verbelen, J.P., Tao, W., 1998. Mobile arrays of vacuole ripples are common in plant cells. Plant Cell Rep. 17, 917–920.

Vermeer, J.E.M., van Leeuwen, W., Tobena-Santamaria, R., Laxalt, A.M., Jones, D.R., Divecha, N., et al., 2006. Visualization of PtdIns3*P* dynamics in living plant cells. Plant J. 47, 687–700.

Voelker, C., Schmidt, D., Mueller-Roeber, B., Czempinski, K., 2006. Members of the *Arabidopsis* AtTPK/KCO family form homomeric vacuolar channels in *planta*. Plant J. 48, 296–306.

Voigt, B., Timmers, A.C., Samaj, J., Muller, J., Baluska, F., Menzel, D., 2005. GFP–FABD2 fusion construct allows *in vivo* visualization of the dynamic actin cytoskeleton in all cells of *Arabidopsis* seedlings. Eur. J. Cell Biol. 84, 595–608.

Wada, M., Suetsugu, N., 2004. Plant organelle positioning. Curr. Opin. Plant Biol. 7, 626–631.

Wada, M., Kagawa, T., Sato, Y., 2003. Chloroplast movement. Annu. Rev. Plant Biol. 54, 455–468.

Wang, Y.S., Motes, C.M., Mohamalawari, D.R., Blancaflor, E.B., 2004. Green fluorescent protein fusions to *Arabidopsis* fimbrin 1 for spatio-temporal imaging of F-actin dynamics in roots. Cell Motil. Cytoskeleton 59, 79–93.

Wightman, R., Turner, S.R., 2008. The roles of the cytoskeleton during cellulose deposition at the secondary cell wall. Plant J. 54, 794–805.

Wilson, G.H., Grolig, F., Kosegarten, H., 1998. Differential pH restoration after ammonia-elicited vacuolar alkalization in rice maize root hairs as measured by fluorescence ratio. Planta 206, 154–161.

Wink, M., 1993. The plant vacuole: a multifunctional compartment. J. Exp. Bot. 44, 231–246.

Wormit, A., Trentmann, O., Feifer, I., Lohr, C., Tjaden, J., Meyer, C., et al., 2006. Molecular identification and physiological characterization of a novel monosaccharide transporter from *Arabidopsis* involved in vacuolar sugar transport. Plant Cell 18, 3476–3490.

Xu, Y., Ishida, H., Reisen, D., Hanson, M.R., 2006. Upregulation of a tonoplast-localized cytochrome P450 during petal senescence in *Petunia inflata*. BMC Plant Biol. 6, 8.

Yamaguchi, T., Aharon, G.S., Sottosanto, J.B., Blumwald, E., 2005. Vacuolar Na^+/H^+ antiporter cation selectivity is regulated by calmodulin from within the vacuole in a Ca^{2+}- and pH-dependent manner. Proc. Natl. Acad. Sci. USA 102, 16107–16112.

Yano, K., Matsui, S., Tsuchiya, T., Maeshima, M., Kutsuna, N., Hasezawa, S., et al., 2004. Contribution of the plasma membrane and central vacuole in the formation of autolysosomes in cultured tobacco cells. Plant Cell Physiol. 45, 951–957.

Yoneda, A., Kutsuna, N., Higaki, T., Oda, Y., Sano, T., Hasezawa, S., 2007. Recent progress in living cell imaging of plant cytoskeleton and vacuole using fluorescent-protein transgenic lines and three-dimensional imaging. Protoplasma 230, 129–139.

CYTOMECHANICS OF HAIR: BASICS OF THE MECHANICAL STABILITY

Crisan Popescu[*,†] *and* Hartwig Höcker[*]

Contents

Abstract

Hair is a complex "cornified" multicellular tissue composed of cuticle and cortex cells mechanically acting as a whole. The cuticle cells overlap and cortex cells interdigitate, all cells being composed of different morphological elements and separated by the cell membrane complex (CMC). The CMC and the morphological elements of the cortex cells, the macrofibrils, composed of microfibrils or intermediate filaments (IFs), and the intermacrofibrillar and intermicrofibrillar cement or the amorphous matrix material determine the mechanical properties of hair. The IFs consist of α-keratin molecules being arranged in a sophisticated way of two parallel monomers and antiparallel and shifted dimers rationalized by the amino acid composition and sequence. The mechanical properties of hair result from mechanical interlocking effects, hydrophobic effects, hydrogen bridges, Coulombic interactions, and (covalent) isodipeptide and, in particular, disulfide bridges on a molecular level. The mechanical models applied to hair are based on a simple two-component system, the microfibril/matrix structure. An important regime of the stress–strain curve is the transition of the molecules of the microfibrils from the α-helical to the β-sheet structure.

[*] DWI an der RWTH Aachen e.V. Pauwelsstrasse 8, D-52056 Aachen, Germany
[†] University "Aurel Vlaicu," Bd. Revolutiei 77, RO-310130 Arad, Romania

Due to the longitudinal orientation of the IF molecules the longitudinal swelling of the fibers in water is negligible, the radial swelling, however, is substantial.

1. Introduction

There are no fundamental differences between the hair of different human beings and between the hair of humans and animals. However, DNA from nuclear remnants in hair allows even the identification of individuals. Human hair is incontestably one of the most important attributes of people in all cultures. It has been of particular importance for human beings from their earliest times, as a symbol of strength, power, and beauty, accompanying human development for these qualities since the dawn of civilization until today (Popescu and Höcker, 2007). Style, length, and color changes are influenced by fashion trends. The hair reflects feelings of health and beauty, and thus its properties are of great importance. It has fundamental social and cultural significance for the individual. From a physiological point of view, hair provides mechanical protection, insulation, and a wick effect for the dispersal of lubricating sebum and sweat over the adjacent skin.

Hair is made out of two parts: the follicle, located below the surface of the skin, which produces the hair material, and the shaft, which grows from the follicle and is composed mainly of α-keratin, a fibrous protein (Fig. 4.1). While the follicle is a living cell, producing continuously substance, the hair shaft (hair) is a complex ''cornified'' multicellular tissue which mechanically acts as a whole. Cytomechanics is the application of the principles of mechanics to cytology, in other words it is the mechanics at the level of the cell or of an ensemble of cells or—which will be particularly important for hair—of their components. As a result, cytomechanics of hair describes the mechanics of the hair fiber.

2. Morphology of the Hair Fiber

The hair fiber is a multicellular tissue comprising several morphological components, each with a specific chemical composition (Popescu and Höcker, 2007; Zahn et al., 1980). The hair shaft (the fiber) is a two-component assembly consisting of the cortex, the core of the shaft, and of
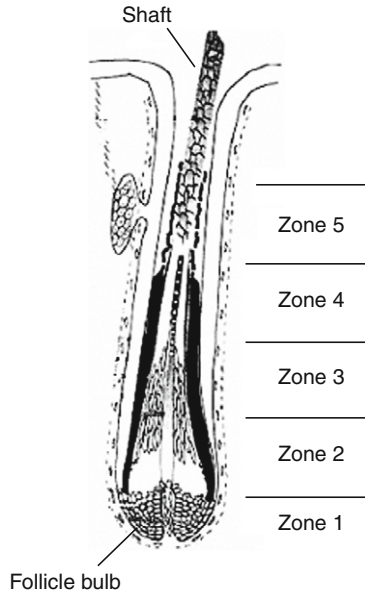
Figure 4.1   The follicle and the shaft of a hair (Zahn et al., 2003a). Zone 1, bulb zone (proliferation and differentiation); zone 2, elongation (fibril formation); zone 3, prekeratinization (lateral aggregation); zone 4, hardening (keratinization); zone 5, post-hardening (hard keratin).

the cuticle, the shell that wraps the cortex. Each of the two components is formed of various components (Popescu and Höcker, 2007).

   The cuticle is made up by flat, overlapping, tile-like cells. The cortex which constitutes the larger portion of the hair mass is composed of spindle-shaped cells which mutually penetrate each other or are interdigitating. Thicker hair often shows a tube-like structure with more or less hollow medulla cells in the center. Cuticle cells, as well as cortical cells, are separated by the cell membrane complex (CMC) which consists of lipids and proteins. The overall morphology of a hair fiber, at various scales, is illustrated in Fig. 4.2.

2.1. The cuticle

The cuticle is the outer protective layer of the hair and consists of plate-shaped cells that overlap longitudinally and peripherally, with up to 1 μm thick edges of the scales pointing to the tip of the fiber. Each cuticle cell consists of four layers with different content of disulfide and isodipeptide bonds: the epicuticle at the very surface, which is an approximately 5 nm thick hydrophobic-resistant membrane, the A-layer, a resistant layer with a
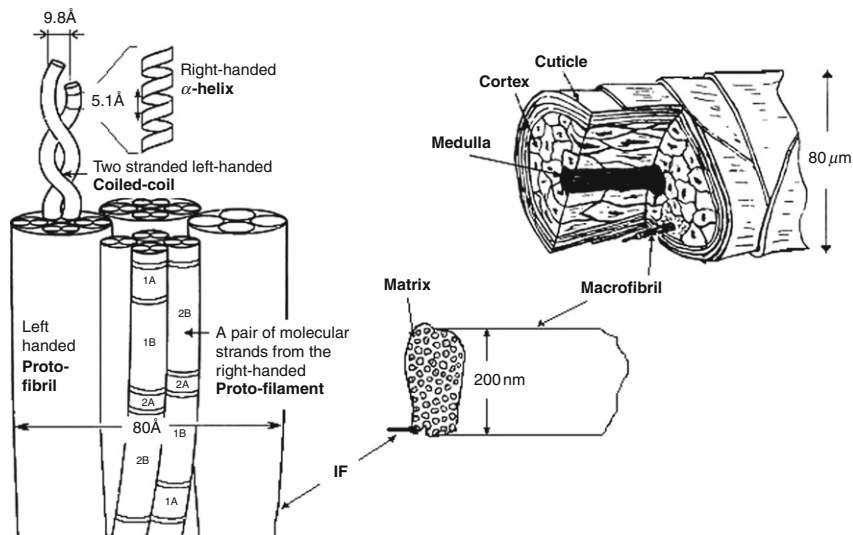
Figure 4.2 The morphology of the hair fiber (Popescu and Höcker, 2007). Reproduced with permission from The Royal Society of Chemistry.

high cystine content (>30 mol% as half–cystine), the exocuticle, also rich in cystine (~15 mol%), and the endocuticle, low in cystine content (~3 mol%) (Fig. 4.3).

The CMC which glues overlapping cuticle cells, cuticle and cortex cells, and neighboring cortex cells together (Dobb et al., 1961; Popescu and Höcker, 2007) consists of cell membrane and adhesive proteinic material. The CMC contains a rather low portion of sulfur. A number of sublayers of the CMC were identified. The most important one is the central δ-layer (Swift and Holmes, 1965), which is the "intercellular cement." Its proteins are low in cystine (<2%) and high in polar sulfur-containing amino acids (cysteine, thio-cysteine). This layer is sandwiched between two layers, sometimes called the inert β-layers, made up by lipids like squalene and fatty acids rich in palmitic, stearic, and oleic acid. The proteins of the cuticle are present in predominantly amorphous state (Bradbury et al., 1966).

2.2. The cortex

The cortex constitutes the major part of the fiber and is composed of spindle-shaped cells, which are 1–6 μm thick and approximately 100 μm long (Robbins, 2002). The cells are separated by the CMC. *Ortho-*, *para-*, and more rarely *meso*-cortical cells are distinguished, according to their cystine content and consequently their staining behavior. Each cortical cell is composed of macrofibrils and intermacrofibrillar material. The macrofibrils consist of 500–800 microfibrils (Popescu and Höcker, 2007),
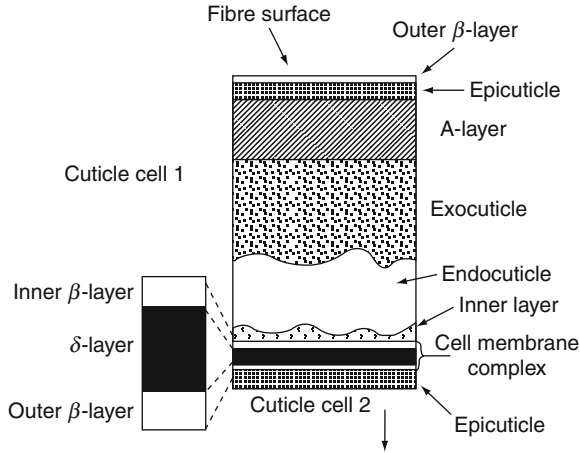
Figure 4.3 The sublamellar structure of the human hair cuticle, with the cuticle cells separated by the CMC layers (Swift and Smith, 2001). Reproduced with permission from Wiley-Blackwell.

which represent the α-keratin and an intermicrofibrillar material. The intermacrofibrillar and the intermicrofibrillar material is called "matrix." As a result of chemical and X-ray diffraction analysis, the structure of microfibrils is known in great detail. In physical, chemical, and biological studies of proteins, the microfibrils are called intermediate filaments (IFs) because of their diameter of ca. 10 nm as opposed to microfilaments or actin filaments with a diameter of ca. 5 nm and microtubuli with a diameter of ca. 20 nm. The precise sequences of amino acid residues of some members of the two α-keratin families (type 1 and type 2, acid and neutral, respectively) in the IFs of human hair and sheep's wool are known, together with the way in which they are packed in a staggered array with a substructure of coiled coils (Hearle, 2003). The basic shape of an IF monomer consists mainly of a central α-helical rod with nonhelical C- and N-terminal regions. It was suggested that the N- and C-terminal domains are likely to play a crucial role in directing molecular and filament aggregation (Parry and Fraser, 1985).

The central rod domain largely consists of four α-helical segments (lA, lB, 2A, and 2B) separated by three, supposedly amorphous linker sequences (Ll, L12, and L2) (Steinert et al., 1988). The repeating heptades in the α-helical segments favor the formation of both the α-helical structure of the segments and the parallel, super helical dimer structure of two IF monomers (Fig. 4.4).

One notes that parts of the final domains from the protofilaments stand out laterally, the same situation being valid also for the IFs surface (Popescu and Höcker, 2007).
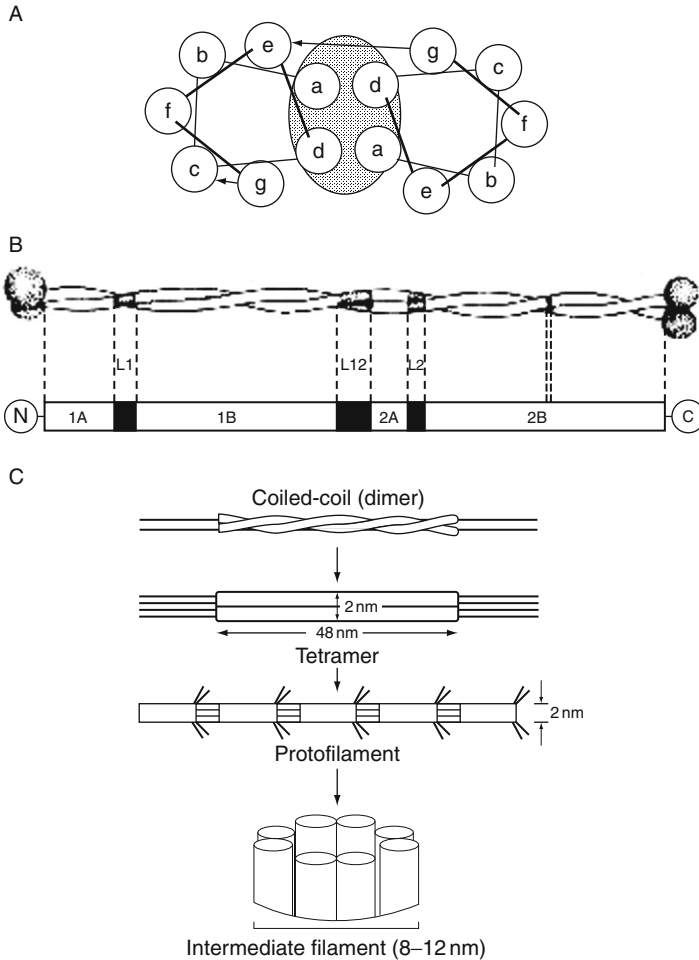
Figure 4.4   (A) The cross-section of a dimer indicating the heptades with the apolar residues a and d in neighboring positions (Zahn et al., 2003a). (B) Structure of an IF dimer. A and B: helical domains; L: nonhelical linker sequences; N, C: N and C termini, respectively (Parry and Fraser, 1985). (C) Structure of the IFs. A and B: helical domains; L: nonhelical linkers; N, C: N and C termini, respectively. Hierarchy ''from dimer to filament'' (Zahn, 1989).

Figure 4.4 shows the association of two right–handed α–helical chains (IF monomers) to form a left–handed coiled coil structure, realized by the hydrophobic effect due to the apolar residues in positions a and d and by electrostatic interactions between the residues in positions e and g. The formed dimers then aggregate in an antiparallel and shifted arrangement to form structural units of higher order and eventually the IF (Fig. 4.4).

The matrix forms the largest structural unit of the cortex of human hair fibers being of less organized structure, which is often referred to as the amorphous region. Paradoxically, the chemical composition and the chemical fine structure of the matrix is much less well known than that of the IFs. The proteins that form the matrix between the IFs are the α-keratin or IFs-associated proteins (KAP or IFAP) (Powell and Rogers, 1997) and are classified into three groups, that is, "high-sulfur," "ultra–high-sulfur," and "glycine/tyrosine-rich" proteins. A major component of the matrix consists of globular, high-sulfur proteins (25 wt% of the total protein), with about 20 wt% of cysteine, which can form cystine bridges and hence cross-links within the globules, between pairs of globules, and between globules and the terminal domains of the IF proteins (Hearle, 2003). High glycine and tyrosine (HGT) proteins, ca. 10 wt% of the total protein, are also part of the amorphous matrix. Ultra–high-sulfur proteins were only found in the paracortex.

The medulla in coarser hair fibers consists of hollow cells with a skeleton of amorphous proteins and fine filaments (Popescu and Höcker, 2007). The medulla is variable in the extent to which it is found in normal hair and occupies a minor portion of the cross-sectional area along the hair's axis. Medulla cells are loosely packed and during formation they shrivel up, leaving a series of vacuoles along the fiber axis (Swift, 1997a).

The color of human hair ranges from shades of yellow and red to black and is entirely due to the melanin granules, ellipsoidal particles of about 0.6 μm in length which are synthesized within specialized cells of the hair follicle, the melanocytes. After synthesis, the particles are passed on so that they are distributed mainly inside the cortical cells of the fully formed hair shaft. The melanin granules contain small amounts of protein and varying portions of two types of highly heterogeneous polymeric pigments, eumelanin and phaeomelanin, which are bio-elaborated within the melanocyte from tyrosine. Eumelanin is responsible of black and brown hair colors, is insoluble in solvents and chemically intractable to all but powerful oxidizing agents such as hydrogen peroxide. Phaeomelanin is responsible of yellow and brownish–red hair coloring, contains significant amounts of sulfur and is soluble in strong alkali (Castanet and Ortonne, 1997). Hair deficient in melanins is unpigmented or white. The melanin granules are mainly found in the macrofibrils and in the matrix.

3. Chemical Composition of Human Hair

Human hair is predominantly proteinaceous, consisting of approximately 65–95 wt% proteins, the remaining being water, lipids (sterols, free fatty acids, and polar lipids), sugars, pigment (melanins), nucleic acids, and

trace elements (Swift, 1997b). The elemental analysis of hair shows around 50 wt% carbon, 7 wt% hydrogen, 22 wt% oxygen, 16 wt% nitrogen, and 5 wt% sulfur. The unusually high sulfur value results from the high cystine content. This is the characteristic feature of α-keratin fibers and distinguishes them from other protein fibers such as silk and collagen (Popescu and Höcker, 2007). In addition, trace elements are detected that may be components of pigments. The total ash content of hair ranges from 0.3 to 0.9 wt%. The most frequent trace metals found are Ca, Cd, Cr, Cu, Hg, Zn, Pb, Fe, As, and Si. Most of them are incorporated in hair from extraneous sources but are probably integrated into the fiber structure via salt linkages or as coordination complexes with side chains of pigments and/or proteins.

Total hydrolysis of the peptide bonds in human hair proteins reveals 24 different amino acids, which are classified in five groups: acidic amino acids, basic amino acids, amino acids with hydroxyl groups, sulfur–containing amino acids, and amino acids with no reactive groups in the side chains (Zahn et al., 2003b). The side groups which account for a considerable portion (50 wt%) of the molecular mass of the proteins interact with each other, thereby stabilizing the protein structure by forming links between chains and rings within a chain (Popescu and Höcker, 2007). Possible interactions between phenyl rings, hydrogen bonds, salt bridges, disulfide bridges between two cysteine residues, and isodipeptide bridges between segments of two hypothetical peptide chains are schematically represented in Fig. 4.5.
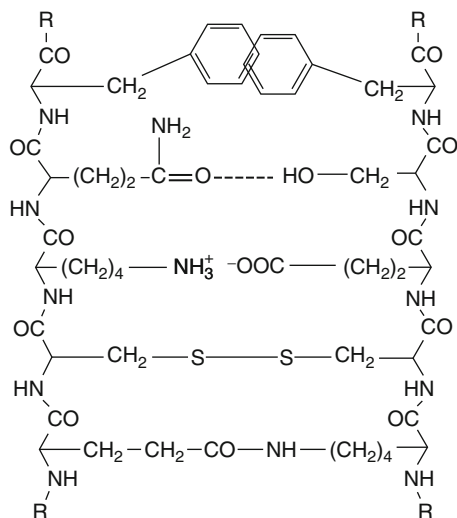
Figure 4.5 Schematic representation of covalent and noncovalent interactions between segments of two hypothetical peptide chains (Popescu and Höcker, 2007).

The cystine content of virgin human hair, expressed in mol% of half-cystine, ranges from about 13% to 18%. Cystine residues provide stability of the hair as long as it is not exposed to reducing, oxidizing, and/or hydrolytic agents or to weathering. In general, the cuticle cells contain a higher percentage of cystine, cysteic acid, proline, serine, threonine, isoleucine, methionine, leucine, tyrosine, phenylalanine, and arginine than does the whole fiber (Robbins, 2002). Beside the highly cross-linked structure, the cuticle contains a low but important amount of fatty acids, in particular of 18-methyl eicosanoic acid (18-MEA) which is responsible of the water repellent behavior of the very surface.

However, because the cortex comprises the major part of the fiber mass, results of whole-fiber analysis may be considered to be a good approximation to the composition of the cortex. The two components of the cortex—the IFs and the matrix—are very different in chemical composition. The matrix is rich in cystine (21 mol%), calculated from the sulfur content of γ-keratose of human hair (Robbins, 2002), HGT proteins, proline, and other amino acids that resist helix formation.

The IFs are rich in leucine, glutamic acid, and those amino acids that are generally found in α-helical proteins, although small quantities of cystine ($\sim$6%), lysine, and tyrosine are regularly arranged in the IFs. The cystine content of the low-sulfur IF region is not uniformly dispersed between domains of an IF chain. Eight N-terminal amino acids have been determined: cystine (11 mol% half-cystine) (Fraser et al., 1988), glycine, threonine, valine, alanine, serine, glutamic, and aspartic acids. Other N-terminal amino acids are present in N-acetylated form. The rod domain contain only 3 mol% half-cystine (Fraser et al., 1988) while the C-terminal unit, beside threonine, glycine, alanine, serine, glutamic acid, aspartic acid, contains about 17 mol% half-cystine (Fraser et al., 1988).

4. INTERACTIONS OF KERATIN PROTEINS

Interactions of the main morphological components of human hair will be considered here as far as they are specifically related to the various aspects of the stability or mechanical properties of hair. Physical and/or chemical interaction between IFs, IFs–IFAPs, or IFAPs has been of a great interest, leading to academic debates. These interactions are believed to control the stabilization of the whole keratin fiber structure. Many of the cysteine residues of the hair proteins participate in disulfide cross-links and thus play a major role in the interactions of the proteins.

The fundamental unit of the IFs is formed by the pairing of two protein types, known as type I (acidic) and type II (basic) keratins, and the keratin pairs are expressed in complex tissue- and differentiation-specific patterns

(Powell and Rogers, 1997). Characteristically, the end domains of the hair IF lack the extended runs of glycine residues found in epidermal IF and contain many cysteine residues that enable them to participate in extensive disulfide bond formation, that is, cross–linking with the abundant cysteine-rich proteins of the hair matrix (Hearle, 2003; Powell and Rogers, 1997; Robbins, 2002; Zahn, 1991) (Fig. 4.6).

The disulfide linkages are responsible of the chemical inertness of hair and of many of its characteristic mechanical properties (Fraser et al., 1988). A classification of possible disulfide linkages in α-keratins, based on structural features, was given by Fraser et al., 1988 (Fig. 4.7). He also concluded that while IFAP–IFAP, IF–IF, and IF–IFAP disulfide linkages are highly probable to exist, intracoil disulfide bridges (i.e., within a single α-helix) can
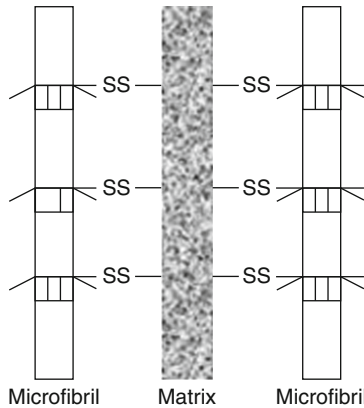
Figure 4.6 Model proposed for wool keratin structure: one microfibrillar component and two matrix components (Spei, 1973).
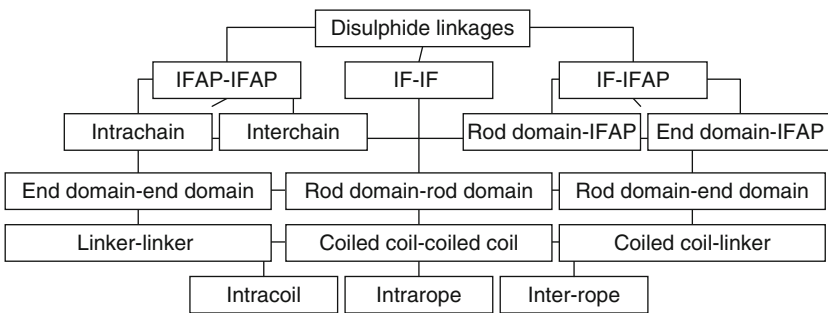
Figure 4.7 Classification of disulfide linkages in α-keratin based on structural features. IF, intermediate filament chains; IFAP, intermediate filament associated proteins or matrix chains; linker, rod domain segments L1, L2, or L12, coiled coil refers to a component chain of the two–strand rope (Fraser et al., 1988).

be excluded and intrarope disulfide bonds (i.e., between two α-helices in the same rope) are unlikely to be present for sterical constraints.

Using X-ray diffraction and cross-link data, as well as homology information, the axial structure of IFs was formulated by Parry (1995, 1996, 1999). He showed that the stability of the IF axial assembly of this hard α-keratin is due to covalent interactions provided by disulfide bonds formed between the rod domains of neighboring molecules or between an IF protein and the matrix proteins in which the IFs are embedded *in vivo* (Parry and Steinert, 1999). Low-angle X-ray scattering investigations (Spei, 1972; Spei and Zahn, 1971; Spei et al., 1970) of chemically modified and extended α-keratins showed that along the fiber axis there are at least two ordered regions: one the microfibrillar region and the other one the matrix. Furthermore, the cross-links between the matrix and the microfibrils were indexed as disulfide bonds, although experimental evidence for acid labile bonds is also available (Crewther, 1956).

At the junctions of all types of cells lies the intercellular material, the CMC. The integrity of the hair and its mechanical properties depend as much on the cellular adhesion provided by this intercellular layer as it does on the intracellular IFs and the matrix, that is, the intracellular components, in particular the molecules of the cytoskeleton (Powell and Rogers, 1997). The CMC of α-keratin fibers is reported to consist mainly of fatty acids and sterols, cholesterol, and desmosterol (Herrling and Zahn, 1985). In the epidermis there was found a link between the IF and the desmosomal component of the cell membrane (Kouklis et al., 1994). However, in the epidermis there is evidence for molecular interactions between desmoplakin and a conserved 18 amino acid region in the N-terminal domains of the type II keratin IF. Part of this region is also conserved in hair type II keratins, indicating that hair IFs may also interact with desmoplakins (Powell and Rogers, 1997).

The potential interactions of so many proteins could attain a bewildering complexity (Powell and Rogers, 1997). The glycine/tyrosine-rich proteins are believed to be the first proteins of the matrix that interact with the nascent filaments, helping to establish their orderly spacing prior to the influx of the cysteine-rich proteins (Fraser and MacRae, 1980). Interactions between the hair type II keratin IF and the glycine/tyrosine-rich proteins might be promoted by glycine loops, analogous to the predicted interaction of the epidermal keratin IF and the cell envelope protein loricrin (Powell and Rogers, 1997; Steinert and Freedberg, 1991). Glycine loops have been already predicted to occur in the small glycine/tyrosine-rich hair proteins (Fratini et al., 1993) and might be important in providing some noncovalent interactions.

The head and tail domains in keratin molecules generally contain a multitude of sites that allow keratin IFs to covalently bind with other proteins. Lysine to glutamine cross-links (isodipeptide bonds) were

obtained between the head and the tail domains in both type I and type II chains (Parry, 2005). A large body of literature follows the way in which IFs interact and aggregate to form what is termed as macrofibrils (Fraser and MacRae, 1982; Fraser and Parry, 2003; Wang et al., 2000). Micro X–ray investigations show that the α–helix molecules form an amorphous structure when produced in the bulb; however, along the first 1400 μm (which is the distance to the zone 5, Fig. 4.1), they organize to form the crystalline α–helical phase (Er Rafik et al., 2006). At the time of disulfide bond formation, the cysteine residues present in aligned regions may form cross–links and stabilize the interactions.

   The process of ordering IFs while fiber material is produced in the follicle looks like a lyotropic phase transition. However, in the case of hair one should take also into account that the follicle pushes out the produced protein material at a rate of about 3.5 nm/s (hair growths with about 1 cm per month). Assuming an ideal behavior of the protein flow in the follicle (no friction, incompressible fluid), the expulsion rate requires a dynamic pressure of about 8000 N/nm^2 (calculated for a material with specific weight of 1.3); this helps to orient the 40 nm $\times$ 2 nm (Fig. 4.4) IFs before cross–linking and hence stabilizes the structure. The role of the interactions mentioned and the location of disulfide bonds (IFs or matrix/IFs) are, however, at the origin of the divergence of the structural mechanical models.

5. MECHANICAL MODELS

   The physical models for describing the mechanical behavior of keratin fibers use a general microfibril/matrix structure. The most important attempts to consistently interpret the shape of the stress–strain curve in relation to fiber structure have been made by Hearle (Hearle, 1967, 1969, 2000; Hearle and Chapman 1968a,b; Hearle and Susutoglu, 1985) and by Feughelman (Feughelman, 1959, 1979, 1994; Feughelman and Hally, 1960; Bendit and Feughelman, 1968). Both authors regard the fiber as made of a crystalline region, that is, the highly oriented, relatively parallel, α–helices, which is embedded in an amorphous matrix. While Feughelman's (1994) model does not take into consideration any interaction between the two main components, the Chapman and Hearle model proposes a link between them (Chapman, 1969; Chapman and Hearle, 1970; Hearle, 1969). A variant of the Chapman and Hearle model was developed by Wortmann and Zahn (1994) by considering that six sulfur bonds between the 2B segments of different dimers stabilize the protofilament structure. As a consequence, α–helical blocks are formed across the tetramer by the 1A, 2A, and the 1B segments, respectively. Recent experiments on the thermal

behavior of keratin fibers point to the role of the interface between the crystalline and amorphous phases which protects the α-helices (Baias et al., 2009; Istrate et al., 2009).

The stress–strain curve of a keratin fiber has the specific shape shown in Fig. 4.8. It may be separated into three different regions, R1–R3, according to the profile of the curve, and certain physical phenomena are assigned to each of them. The first region, going up to about 2% strain, illustrates a linear growing of stress with strain as requested by Hooke's law. This region is known as the elastic one and it is considered that it reflects the elastic stretching of the α-helices. The second region, R2, the yielding, looks like a plateau and covers a large part of the curve. Quite a lot of analytical evidence suggests that in the system—after having reached an activated state at the end of R1—the polymorphic transformation from α-helix into β-sheet takes place over this region (Hearle, 2000). Interestingly enough, X-ray diffraction analysis indicates that the α–β transformation takes place when a minimum amount of moisture (relative humidity higher than 30–45%) is present; for a relative humidity below this limit it appears that the yielding region reflects mainly the sliding of IFs (Paquin and Colomban, 2007). Yet, the change of relative humidity from 0% to 100% does not change the shape, but enlarges the plateau of the region R2 from extension values of below 30% at 0% RH to 40% at 100% RH.

Of special importance is also the fact that a keratin fiber stretched up to almost the end of the region R2 relaxes back to the original form after the stress is removed. The process, as documented by X-ray investigations,
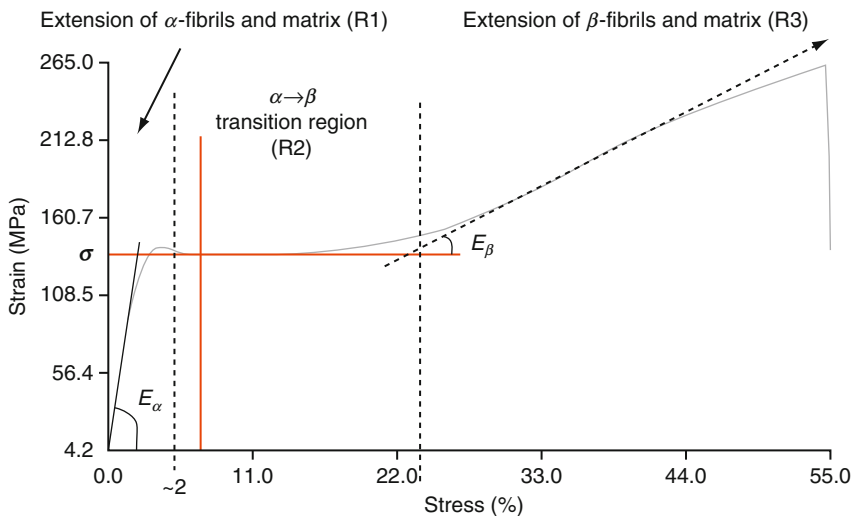
Figure 4.8   Model of the three-region stress–strain curve of hair fiber.

encompasses the returning of the β-sheet to the α-helix structure and is also assisted by moisture. As it appears, the matrix plays a significant role for the processes occurring within the R2 region (Hearle, 2000). The third region, R3, the region of postyielding, is supposed to represent the elastic behavior of the β-sheet structures, which are the stretched supporting elements at that stress. The slopes of the three regions are in the approximate ratio of 100:1:10 and this ratio is fairly well preserved when the relative humidity changes (Zahn et al., 2003).

The humidity plays an important role for the mechanical values of the keratin fiber. As it has been already mentioned the values of stress diminish with increasing humidity; this is understood as the effect of breaking hydrogen bonds in the matrix, which leads to the weakening of its contribution to the total load (Nissan, 1976). Therefore, chemically speaking, the mechanics of keratin fibers are based on the interplay of disulfide and hydrogen bonds. Moreover, the moisture sorption by the keratin fiber leads to changes of its geometry. Figure 4.9 shows how the fiber grows laterally and longitudinally with moisture uptake.

Summing up, over the first region, R1, the IFs behave elastically upon stretching, and the matrix has the characteristics of a viscoelastic material. Accordingly, the elastic modules of the IFs and of matrix differ with the moisture uptake and this is reflected in the overall elastic modulus of the fiber which is decreasing with increasing relative humidity. Young's modulus of IFs is in the range of 8–9 GPa, independent of the humidity, while
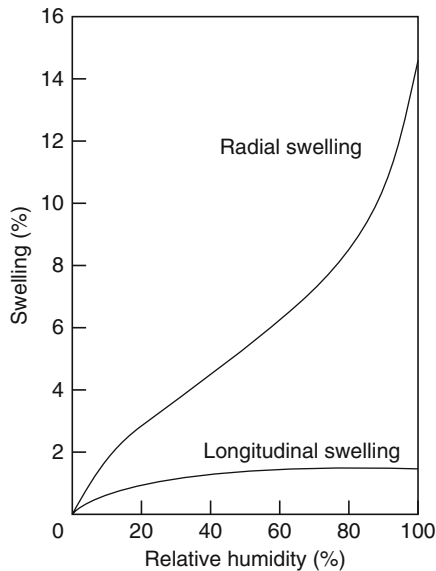
Figure 4.9   Directional swelling of keratin fibers.

that of the matrix is considered to be 6–7 GPa for the dry and of 0.5 GPa for the wet (100% relative humidity) matrix (Zahn et al., 2003b).

Recent investigations of the keratin modifications under stress, carried out by means of Raman spectroscopy, indicate that some irreversible transformations (breaking of disulfide bonds) take place within regions R1 and R2 (Paquin and Colomban, 2007). This means that in spite of the hypothesised complete recovery of the fiber structure when small to medium strain (up to 30%) is applied, the process is not totally reversible. Astbury and Street (1931) and Speakman (1936) suggested that the disulfide bonds of stretched wool are more reactive than those of unstretched wool. The experimental proof was acquired recently. Dealing with a single protein molecule stretched by means of an AFM and reduced with dithiothreitol (DTT), it was observed that the reactivity of the protein disulfide bond increases exponentially with the force applied, by a factor of 10 over a range of 300 pN (Wiita et al., 2006).

In line with describing the mechanics of the fiber as being based on disulfide and hydrogen bonds, one may speculate on the role of water as more than only hydrogen bond breaker (platisizer of the matrix). The anisotropic swelling of the fiber increases the stretching force on radially oriented S–S bonds and, accordingly, increases the reactivity of these bonds. As it was found (Wiita et al., 2006), at the transition state of a thiol/disulfide exchange reaction the S–S bond lengthens by 34 pm, which is about 16% of the unstretched disulfide length (of ∼206 pm). This, according to Fig. 4.9, corresponds to the effect of 100% relative humidity on the fiber, which suggests that at high humidity the radially oriented S–S bonds are in the activated state. As a consequence, this reduces the energy barrier to the activated state of the phase transition from α-helix into β-sheet, and hence lowers the stress required.

Water may also react with S–S bonds and break the disulfide bridge by a β-elimination mechanism for which the pH value plays a significant role (Florence, 1980). The fiber may be not only stretched, but also bent, or twisted, and both actions depend on the moisture amount of the fiber. The bending of keratin fiber results in a bending modulus of 3–5 GPa and is approximately equal to the elastic modulus for a large range of relative humidity values. The FESEM image in Fig. 4.10 shows how the scales of the external side of the fiber open without sliding during the bending. This may indicate that cuticle cells and the CMC contribute also to the bending modulus. Since the IFs bend less because of their size, the measured values reflect the performance of the other components of the fiber.

The torsion, on the other side, with values of the torsion modulus ranging from 2 (for dry) to 0.2 (for wet) GPa, seems to be more affected by moisture uptake of the fiber than the other two mechanical motions (Bogaty, 1967). This, as well as the fact that the chemical treatments which break the disulfide bonds have a larger effect on torsion modulus than on
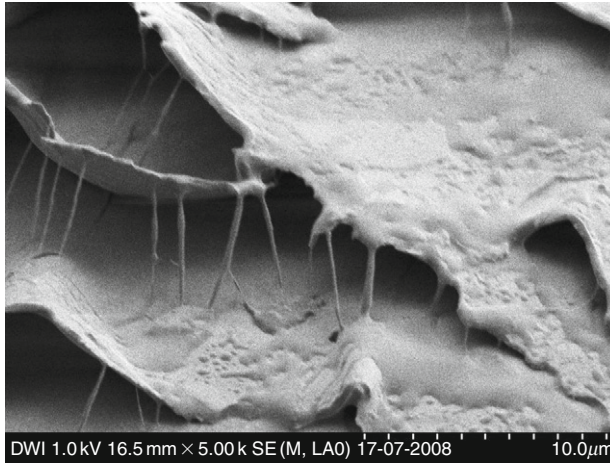
Figure 4.10   Scales of hair in a knot. The fiber was previously covered with a polymer which allows observing the straight opening movement of the scales.

elastic or bending ones (Wolfram and Albrecht, 1985), suggests that the torsion reflects mostly the mechanical properties of the amorphous matrix. Because of transmitting the shear forces to the matrix the cuticle may also play a role (Swift, 1995).

The CMC seems to be less important to the mechanical properties of the keratin fiber, provided the continuity of the adhesion of the cortical cells is maintained (Feughelman, 1997). The same author remarks that our understanding of the role of the CMC in mechanical properties is still limited by a lack of information on CMC components and their arrangement (Feughelman, 1997).

In all, the keratin fiber is regarded as semicrystalline polymeric material and this view is supported by the existence of the viscoelastic transitions usually found at polymers: a glass transition (Wortmann et al., 1984) and a low temperature γ-transition (Druhala and Feughelman, 1971, 1974). Both transitions are related to the mobility of the polymer chains, which means that they occur in the amorphous matrix: the glass transition is considered to be the moment when the system changes from a viscoelastic into a glassy state, that is, when the movement of the backbone of polymer chains is frozen in and the γ-transition indicates the moment when even the movement of protein side chains is frozen in.

The transitions are influenced by temperature and low-molecular-weight plasticizers (here, e.g., water). The relation between temperature at which the two transitions occurs, T_{tr}, and the amount of the plasticizer was studied in detail for the case of water (Druhala and Feughelman, 1971, 1974; Huson, 1991; Kure et al., 1997; Phillips, 1985; Wortmann et al., 1984) and was demonstrated to follow Fox's (1956) law:

$$\frac{1}{T_{tr}} = \frac{w_1}{T_{tr1}} + \frac{w_2}{T_{tr2}}$$

where w is the weight fraction and the subscripts 1 and 2 refer to dry keratin fiber and pure water, respectively.

The glass transition temperature of dry keratin fibers varies with the source of the fiber, being around 175 °C for wool and around 145 °C for human hair (Wortmann et al., 2006). The differences are speculated to be due to the various amounts of high glycine–tyrosine proteins in these keratin fibers which have a potential plasticizer effect (Wortmann et al., 2006). The glass transition temperature of hair at usual values of relative humidity of 60–70% when the moisture content of the fiber is 16–18% is around 45 °C, obtained from the equation above with the glass transition temperature of water being taken at −135 °C (Kalichevsky et al., 1992). This means that under normal circumstances the hair shaft on the head (at 37 °C) is in a glassy state and falls into the plastic state when humidity increases, or when it is sun exposed. Although it plays a role in understanding the phenomenon of physical aging, which relates to shape retention of the fiber, the γ-transition is, so far, less investigated.

6. CONCLUDING REMARKS

Summing up, the follicle, producing the hair shaft, pushes out of the living cell the protein material at a rate of 3.5 nm/s and orients by this the IF proteins which form the crystalline phase of the fiber. Further on, the external application of mechanical stress, that is, the stretching of a keratin fiber in the presence of water (moisture sorption) is a sequence of activating S–S bonds, followed by breaking and reforming of some disulfide bonds and irreversible breaking of others, as a result of a mechanochemical effect.

Since hair is composed of "cornified" cells, cytomechanics, that is, the mechanics between cells rather play a marginal role; clearly more substantial are the mechanics provided by the components of the cells, in particular the cytoskeleton mechanics or the mechanics of the IFs in conjunction with the matrix.

REFERENCES

Astbury, W.T., Street, A., 1931. X-ray studies of the structure of hair, wool, and related fibres. I General. Phil. Trans. Roy. Soc. A 230, 75–101.
Baias, M., Demco, D.E., Popescu, C., Fechete, R., Melian, C., Blümich, B., et al., 2009. Thermal denaturation of hydrated wool keratin by 1H solid-state NMR. J. Phys. Chem. B 113, 2184–2192.

Bendit, E.G., Feughelman, M., 1968. Keratin. In: Encyclopedia of Polymer Science and Technology, vol. 8. pp. 1–44.

Bogaty, H., 1967. Torsional properties of hair in relation to permanent waving and setting. J. Soc. Cosmet. Chem. 18, 575–580.

Bradbury, J.H., Chapman, G.V., Hambly, A.N., King, N.L.R., 1966. Separation of chemically unmodified histological components of keratin fibres and analyses of cuticles. Nature 210, 1333–1334.

Castanet, J., Ortonne, J.-P., 1997. Hair melanin and hair color. In: Jolles, P., Zahn, H., Höcker, H. (Eds.), Formation and Structure of Human Hair. Birkhauser Verlag, Basel, pp. 209–226.

Chapman, B.M., 1969. A mechanical model for wool and other keratin fibers. Text. Res. J. 39, 1102–1109.

Chapman, B.M., Hearle, J.W.S., 1970. On polymeric materials containing fibrils with a phase transition. Part III. The effect of slip at the fibril matrix interface. J. Macromol. Sci. Phys. B 4, 127–151.

Crewther, W.G., 1956. The stress–strain characteristics of animal fibers after reduction and alkylation. Text. Res. J. 35, 867–877.

Dobb, M.G., Johnston, F.R., Nott, J.A., Oster, L., Sikorski, J., Simpson, W.S., 1961. Morphology of the cuticle layer in wool fibres and other animal hairs. J. Text. Inst. Trans. 52, T153–T171.

Druhala, M., Feughelman, M., 1971. Mechanical properties of keratin fibres between − 196 °C and 20 °C. Kolloid. ZZ Polym. 248, 1032–1033.

Druhala, M., Feughelman, M., 1974. Dynamic mechanical loss in keratin at low temperatures. Colloid. Polym. Sci. 252, 381–391.

Er Rafik, M., Briki, F., Burghammer, M., Doucet, J., 2006. *In vivo* formation steps of the hard α-keratin intermediate filament along a hair follicle: evidence for structural polymorphism. J. Struct. Biol. 154, 79–88.

Feughelman, M., 1959. A two-phase structure for keratin fibers. Text. Res. J. 29, 223–228.

Feughelman, M., 1979. A note on the role of the microfibrils in the mechanical properties of α-keratins. J. Macromol. Sci. Phys. B 16, 155–162.

Feughelman, M., Hally, A.R., 1960. The mechanical properties of wool keratin and its molecular configuration. Kolloid Z. 168, 107–115.

Feughelman, M., 1994. A model for the mechanical properties of the α-keratin cortex. Text. Res. J. 64, 236–239.

Feughelman, M., 1997. Mechanical Properties and Structure of Alpha-Keratin Fibres. University of New South Wales Press, Sydney, pp. 17–147.

Florence, T.M., 1980. Degradation of protein disulphide bonds in dilute alkali. Biochem. J. 189, 507–520.

Fox, T.G., 1956. Influence of diluent and of copolymer composition on the glass temperature of a polymer system. Bull. Am. Phys. Soc. 1, 123.

Fraser, R.D.B., MacRae, T.P., 1980. Molecular structure and mechanical properties of keratins. Symp. Soc. Exp. Biol. 34, 211–246.

Fraser, R.D.B., MacRae, T.P., 1982. The fine structure of keratin fibres. In: Breuer, M.M. (Ed.), Milton Harris: Chemist, Innovator and Entrepreneur. American Chemical Society, USA, pp. 119–137.

Fraser, R.D.B., Parry, D.A.D., 2003. Macrofibril assembly in trichocyte (hard α-) keratins. J. Struct. Biol. 142, 319–325.

Fraser, R.D.B., MacRae, T.P., Sparrow, L.G., Parry, D.A.D., 1988. Disulphide bonding in α-keratin. Int. J. Biol. Macromol. 10, 106–112.

Fratini, A., Powell, B.C., Rogers, G.E., 1993. Sequence, expression, and evolutionary conservation of a gene encoding a glycine/tyrosine-rich keratin-associated protein of hair. J. Biol. Chem. 268, 4511–4518.

Hearle, J.W.S., 1967. The structural mechanics of fibers. J. Polym. Sci. C 20, 215–251.

Hearle, J.W.S., 1969. The Chapman mechanical model for wool and other keratin fibres. Text. Res. J. 39, 1109.

Hearle, J.W.S., 2000. A critical review of the structural mechanics of wool and hair fibres. Int. J. Biol. Macromol. 27, 123–138.

Hearle, J.W.S., 2003. A total model for the structural mechanics of wool. Wool Tech. Sheep Breed 5, 95–117.

Hearle, J.W.S., Chapman, B.M., 1968a. On polymeric materials containing fibrils with a phase transition I. General discussion of mechanics applied particularly to wool fibers. J. Macromol. Sci. Phys. B 2, 663–695.

Hearle, J.W.S., Chapman, B.M., 1968b. On polymeric materials containing fibrils with a phase transition. II. The mechanical consequences of matrix shear. J. Macromol. Sci. Phys. B 2, 697–741.

Hearle, J.W.S., Susutoglu, M., 1985. Interpretation of the mechanical properties of wool fibres. Proc. 7th Int. Wool Text. Res. Conf., Tokyo 1, 214.

Herrling, J., Zahn, H., 1985. Investigations of the cell membrane complex and its modifications during industrial processing of wool. Proc. 7th Int. Wool Text. Res. Conf., Tokio 1, 181–193.

Huson, M.G., 1991. DSC investigation of the physical ageing and deageing of wool. Polym. Int. 26, 157–161.

Istrate, D., Popescu, C., Möller, M., 2009. Nonisothermal kinetics of hard α-keratin thermal denaturation. Macromol. Biosci. doi:10.1002/mabi.200800344.

Kalichevsky, M.T., Jaroszkiewics, E.M., Blanchard, J.M.V., 1992. Glass transition of gluten. 1. Gluten and gluten-sugar mixtures. Int. J. Biol. Macromol. 14, 257–266.

Kouklis, P.D., Hutton, E., Fuchs, E., 1994. Making a connection: direct binding between keratin intermediate filaments and desmosomal proteins. J. Cell Biol. 127, 1049–1060.

Kure, J.M., Pierlot, A.P., Russell, I.M., Shanks, R.A., 1997. The glass transition of wool: an improved determination using DSC. Text. Res. J. 67, 18–22.

Nissan, A.H., 1976. H-bond dissociation in hydrogen bond dominated solids. Macromolecules 9, 840–850.

Paquin, R., Colomban, P., 2007. Nanomechanics of single keratin fibres: a Raman study of the α-helix$\rightarrow\beta$-sheet transition and the effect of water. J. Raman Spectrosc. 38, 504–514.

Parry, D.A.D., 1995. Hard-keratin IF: a structural model lacking a head-to-tail molecular overlap but having hybrid features characteristic of both epidermal keratin and vimentin IF. Proteins 22, 267–272.

Parry, D.A.D., 1996. Hard α-keratin intermediate filaments: an alternative interpretation of the low-angle equatorial X-ray diffraction pattern and the axial disposition of putative disulphide bonds in the intra- and inter-protofilamentous networks. Int. J. Biol. Macromol. 19, 45–50.

Parry, D.A.D., 2005. Microdissection of the sequence and structure of intermediate filament chains. Adv. Protein Chem. 70, 113–142.

Parry, D.A.D., Fraser, R.D.B., 1985. Intermediate filament structure. 1. Analysis of IF protein sequence data. Int. J. Biol. Macromol. 7, 203–213.

Parry, D.A.D., Steinert, P.M., 1999. Intermediate filaments: molecular architecture, assembly, dynamics and polymorphism. Q. Rev. Biophys. 32, 99–187.

Phillips, D.G., 1985. Detecting a glass transition in wool by differential scanning calorimetry. Text. Res. J. 55, 171–174.

Popescu, C., Höcker, H., 2007. Hair-the most sophisticated biological composite material. Chem. Soc. Rev. 36, 1282–1291.

Powell, B.C., Rogers, G.E., 1997. The role of keratin proteins and their genes in the growth, structure and properties of hair. In: Jolles, P., Zahn, H., Höcker, H. (Eds.), Formation and Structure of Human Hair. Birkhauser Verlag, Basel, pp. 59–149.

Robbins, C.R., 2002. Chemical and Pyhsical Behavior of Human Hair, fourth ed. Springer Verlag, New York.

Speakman, J.B., 1936. The reactivity of the sulphur linkage in animal fibres—Part I. The chemical mechanism of permanent set. J. Soc. Dyers Colourists 52, 335–341.

Spei, M., 1972. Small-angle X-ray scattering investigations of the matrix in α-keratin (in German). Kolloid Z.u.Z, Polymere 250, 214–221.

Spei, M., 1973. Structure of α-keratin. Text. Res. J. 43, 692–693.

Spei, M., Zahn, H., 1971. Small-angle X-ray scattering of the stretched keratin fibre (in German). Monatsh. Chem. 102, 1163.

Spei, M., Stein, W., Zahn, H., 1970. The influence of anionic tensides on the XRD spectrum of fibrous keratins (in German). Kolloid Z.u.Z. Polymere 238, 447–454.

Steinert, P.M., Freedberg, I.M., 1991. Molecular and cellular biology of keratins. In: Goldsmith, L.A. (Ed.), Physiology, Biochemistry, and Molecular Biology of the Skin, vol. I. Oxford University Press, New York, pp. 113–147.

Steinert, P.M., Torchia, D.R., Mack, J.W., 1988. In: Rogers, G.E. et al. (Ed.), The Biology of Wool and Hair. Chapman & Hall, London, p. 157.

Swift, J.A., 1995. Some simple theoretical considerations on the bending stiffness of human hair. Int. J. Cosmetic Sci. 17, 245–253.

Swift, J.A., 1997a. Morphology and histochemistry of human hair. In: Jolles, P., Zahn, H., Höcker, H. (Eds.), Formation and Structure of Human hair. Birkhauser Verlag, Basel, pp. 149–176.

Swift, J.A., 1997b. Fundamentals of Hair Science. Micelle Press, Weymouth, Dorset, UK.

Swift, J.A., Holmes, A.W., 1965. Degradation of human hair by papain. Part III. Some electron microscope observations. Text. Res. J. 35, 1014–1019.

Swift, J.A., Smith, J.R., 2001. Microscopical investigations on the epicuticle of mammalian keratin fibres. J. Microscopy 204, 203–211.

Wang, H., Parry, D.A.D., Jones, L.N., Idler, W.W., Marekov, L.N., Steinert, P.M., 2000. In vitro assembly and structure of trichocyte keratin intermediate filaments: a novel role for stabilization by disulfide bonding. J. Cell Biol. 151, 1459–1468.

Wiita, A.P., Ainavarapu, S.R.K., Huang, H.H., Fernandez, J.M., 2006. Force-dependent chemical kinetics of disulfide bond reduction observed with single-molecule techniques. PNAS 103, 7222–7227.

Wolfram, L.J., Albrecht, L., 1985. Torsional behavior of human hair. J. Soc. Cosmet. Chem. 36, 87–99.

Wortmann, F.-J., Zahn, H., 1994. The stress/strain curve of α-keratin fibers and the structure of the intermediate filament. Text. Res. J. 64, 737–743.

Wortmann, F.-J., Rigby, B.J., Phillips, D.G., 1984. Glass transition temperature of wool as a function of regain. Text. Res. J. 54, 6–8.

Wortmann, F.-J., Stapels, M., Elliott, R., Chandra, L., 2006. The effect of water on the glass transition of human hair. Biopolymers 81, 371–375.

Zahn, H., 1989. The hair from the chemists' point of view (in German). Chemie in unserer Zeit 23, 141–150.

Zahn, H., 1991. On the role of Mohair for the research of keratine (in German). Melliand-Textilber. 72, 926–931.

Zahn, H., Föhles, J., Nienhaus, M., Schwan, A., Spei, M., 1980. Wool as a biological composite structure. Ind. Eng. Chem. Prod. Res. Dev. 19, 496–501.

Zahn, H., Schaefer, K., Popescu, C., 2003a. Wool from animal sources. In: Steinbüchel, A., Fahnestock, S.R. (Eds.), Biopolymers. Polyamides and Complex Proteinaceous Materials II, vol. 8. Wiley-VCH Verlag GmbH & Co., Germany, pp. 155–202.

Zahn, H., Wortmann, F.-J., Wortmann, G., Schäfer, K., Hoffmann, R., Finch, R., 2003b. Wool. In: Ullmann's Encyclopedia of Industrial Chemistry, A28, pp. 395–421.

NUCLEAR ACTIN-RELATED PROTEINS IN EPIGENETIC CONTROL

Richard B. Meagher, Muthugapatti K. Kandasamy, Elizabeth C. McKinney, *and* Eileen Roy

Contents

Department of Genetics, Davison Life Sciences Building, University of Georgia, Athens, Georgia 30602

Abstract

The nuclear actin-related proteins (ARPs) share overall structure and low-level sequence homology with conventional actin. They are indispensable subunits of macromolecular machines that control chromatin remodeling and modification leading to dynamic changes in DNA structure, transcription, and DNA repair. Cellular, genetic, and biochemical studies suggest that the nuclear ARPs are essential to the epigenetic control of the cell cycle and cell proliferation in all eukaryotes, while in plants and animals they also exert epigenetic controls over most stages of multicellular development including organ initiation, the switch to reproductive development, and senescence and programmed cell death. A theme emerging from plants and animals is that in addition to their role in controlling the general compaction of DNA and gene silencing, isoforms of nuclear ARP-containing chromatin complexes have evolved to exert dynamic epigenetic control over gene expression and different phases of multicellular development. Herein, we explore this theme by examining nuclear ARP phylogeny, activities of ARP-containing chromatin remodeling complexes that lead to epigenetic control, expanding developmental roles assigned to several animal and plant ARP-containing complexes, the evidence that thousands of ARP complex isoforms may have evolved in concert with multicellular development, and ARPs in human disease.

Key Words: ARPs, Nucleosome, Epigenetic control, Chromatin remodeling, Histone variant, Multicellular development, SWI/SNF, SWR1, INO8o.

1. Introduction

The nuclear actin–related proteins (ARPs) were first discovered in the early 1990s, but their central role as components of chromatin remodeling and modifying machines has emerged only recently. Various studies in yeast, animals, and plants reveal that nuclear ARPs are essential to the epigenetic control of chromatin structure. Nuclear ARP–dependent

epigenetic controls participate in DNA repair, chromosome segregation, and gene expression, which in turn regulate the cell cycle and cell proliferation, phase transitions in development, and senescence and programmed cell death (PCD). In plants and animals, these processes are at the heart of multicellular tissue and organ development. Due to the combinatorial complexity of the numerous subunits of these chromatin complexes, the nuclear ARPs may participate in hundreds if not thousands of different complex isoforms, with the potential to evolve novel activities essential to the macroevolution of new tissues and organs. Nuclear ARP-containing machines are involved in an organism's responses to environment, diet, and age, which are known to be key factors in the onset of numerous human diseases. In this broad context, we have attempted to review the evolution and functions of the nuclear ARPs in regulating cell and organismal development.

2. NUCLEAR ARPs AS EPIGENETIC FACTORS

2.1. Structural and sequence identity

The ARPs share limited sequence identity with conventional actins, but they appear to maintain the actin–fold, a potential nucleotide-binding pocket and hinged structure that enables a conformational change in actin family members. Eight to ten ancient classes of ARPs are found in most eukaryotes that have been examined, and all appear to participate in protein complexes (Chen and Shen, 2007; Muller et al., 2005). A subset of the more divergent ARPs can be identified in most eukaryotes as homologues of yeast Arp4, Arp5, Arp6, and Arp8, which are found primarily in the nucleus (Harata et al., 2000; Kandasamy et al., 2003; Shen et al., 2003b). The predominantly nuclear localization distinguishes them from actin or Arp2 and Arp3, which are detected in the nucleus, but are primarily concentrated in the cytoplasm and participate in cytoskeletal functions (Harries et al., 2005). None of the nuclear ARPs are known to form polymers such as F–actin microfilaments or the short filaments formed from ARP1 and ARP10 in the centractin complex (Eckley and Schroer, 2003). Instead, nuclear ARPs act as essential subunits of macromolecular machines controlling chromatin dynamics with subsequent effects on transcription and DNA repair.

2.2. Exclusive function in chromatin remodeling and modifying machines

The only functions demonstrated for nuclear ARPs are as subunits of chromatin remodeling and modifying complexes (Chen and Shen, 2007). Specifically, ARP-containing remodeling complexes are responsible for nucleosome phasing and movement and exchange of histone subunit isovariants within nucleosomes (nucleosome remodeling (NR) complexes).

ARP-containing chromatin modification complexes direct posttranscriptional modifications to histone amino acid residues such as the acetylation or methylation of lysine residues. The dynamic activities of chromatin remodeling and modifying complexes serve a basal regulatory function by reinforcing or alleviating the nucleosomal suppression of transcription that affects most genes due to the extreme compaction of DNA in nuclei or nucleoids (Yuan et al., 2005). Conversely, because there is only room for a small fraction of any genome to be in an open chromatin conformation and transcriptionally active at any one time, chromatin remodeling is a dynamic process necessary to unfold and refold various loci throughout the cell and developmental cycles of the organism. Although most of these chromatin activities appear global in nature, the nuclear ARPs may also exert more precise epigenetic control over the activities of particular regulatory genes that have an overriding influence on cell and organ ontogeny or on the response to environmental stress (Jonsson et al., 2004; Meagher et al., 2007; Oma et al., 2003; Wu et al., 2007).

2.3. Distinguishing genetic from epigenetic controls

For most of the last century, it was presumed that only genetic mutation provided the variation acted on by natural selection and neutral drift, thus leading to the evolution of new organisms and new structures within organisms. After the 1960s, with the knowledge that regulatory genes encode transcription factors that act on specific DNA-binding motifs, a more defined molecular genetic model emerged. Such interactions between transcription factors and *cis*-DNA elements produce linear or branched information cascades that directly control a few to dozens of genes and subsequently development. Mutations in these sequences are then acted on during evolution. However, as the gene compositions of multicellular plants and animals were determined, it became increasingly difficult to explain the significant physical differences among organisms and their rapid rates of morphological change from common ancestors as resulting only from gene duplications and mutant alleles affecting linear pathways of developmental control.

There were problems with this simple gene and *cis*-element mutation model for morphological evolution. If chimpanzees have the same genes and nearly identical protein sequences as humans (Kehrer-Sawatzki and Cooper, 2007; Wilson and Sarich, 1969) and if the Tetraodontoid fish, *Fugu rubripes*, has a similar gene composition as mammals (Aparicio et al., 2002), how do we account for the remarkable diversity of organisms and organ structures that evolved within chordates and vertebrates over the last 650 million years? Similar questions are asked about plant genomes and the rates of plant morphological evolution for the last 600 million years, since vascular plants evolved from common ancestors with moss. Again, the rapid rates of morphological evolution and macroevolution in higher plants and

animals far out strips the observed rates of gene duplication, mutation, and evolution of new protein sequences. Regulatory genes and DNA motifs may accumulate mutations at slightly faster rates than structural genes (Elango et al., 2008), but probably not fast enough to fully explain these rapid changes in morphology. This dilemma is at least partially addressed by the view that natural selection may be acting on mutations in epigenetic control systems that network chromatin structure and gene expression. Mutations in a single epigenetic factor can alter the expression of thousands of genes in multiple gene networks and can have widely varied and pleiotropic consequences on phenotype in yeast, plants, or animals (Meagher et al., 2005; Morgan et al., 1999; Roux-Rouquie, 2000; True et al., 2004). Epigenetic control adds a level of complexity to the inter regulation of gene activities that is now widely recognized as essential to multicellular development and macroevolution.

2.4. The nuclear ARPs are epigenetic factors

The majority of epigenetic controls are exerted by changes to chromatin structure leading to alterations in gene expression. As mentioned earlier, the nuclear ARP-dependent modifications of chromatin include histone modifications and NR. These activities contribute to "epigenetic control" of cell development, a phrase that David Nanney used to define "inherited differences between two cells that are not due to changes in DNA sequence" (Haig, 2004; Nanney, 1958). Nanney's definition of *epigenetic control* and the roles we infer for nuclear ARPs applys to two differentiating yeast or protozoan cells that have divided, just as well as it does to two differentiating cells within a mammalian limb bud, insect imaginal disk, or plant organ primordia. Nuclear ARPs also function in the epigenetic control of chromosome segregation and DNA repair (Minoda et al., 2005). Therefore, most of the direct functions of nuclear ARPs fit within this definition making them fundamental if not essential factors in epigenetic control.

However, the indirect roles of nuclear ARPs in the regulation of pathways of multicellular development also fit a slightly older definition of epigenetics as "the interactions among cells and cell products that lead to morphogenesis and differentiation" (Haig, 2004; Waddington, 1957). Waddington focused on defining the inherited differences and interactions among cells of a differentiating multicellular organ. This definition of epigenetics particularly takes into account the interactions and networking of information that results from diffusible signaling molecules moving between subsets of cells in an organ primordia. While nuclear ARPs do not diffuse between cells or act as receptors themselves, their chromatin activities are associated with the differential expression of many genes in receptor-mediated intracellular signaling pathways directing plant and animal organ development (Mehler, 2008b; Walley et al., 2008; Williams and

Fletcher, 2005). Furthermore, most scientists today do not include this concept of signals diffusing between cells as part of modern epigenetics. Waddington's definition of epigenetics also does not encompass the role of nuclear ARPs in chromosome segregation or DNA repair, in generational epigenetic inheritance, or in inheritance of epigenetic differences between dividing single cell fungi or protists.

While Nanny and Waddington had intimate familiarity with particular protist and mammalian models of development, yeast emerged early as model genetic system to dissect mechanisms of epigenetic control (Pillus and Rine, 1989). Shortly after the discovery of the nuclear ARPs, mutants in yeast ARP4 (originally Act3b) were isolated as suppressors of an epigenetic reporter *his4δ–ADE2* (Jiang and Stillman, 1996). ARP4–defective yeast containing this reporter in an *ade2⁻* background show reversible and stochastic changes in the morphology of colored sectors of cells within single yeast colonies, red to white and back to red as shown in Fig. 5.1. The *his4δ* promoter contains an insertion δ (Fig. 5.1C) separating the *HIS4* gene's transcriptional enhancers from its TATA box (Fig. 5.1B) rendering the *his4δ-ADE2* gene inactive "Off" in a wild-type yeast background. The cells produce red pigment when the reporter is inactive because they are still *ade2⁻*. In ARP4–defective yeast cells, the variegated colony color results from stochastic reversible modifications to the chromatin structure of the *his4δ-ADE2* promoter turning the gene "On" (white cells) and "Off" again. By the model shown in Fig. 5.1C, in the *arp4⁻* background, changes occur to chromatin structure that allow the *HIS4-enhancer* to interact with the *HIS4-TATA* sequence turning "On" *ADE2*. The results of this study demonstrate that ARP4's activities are involved in epigenetic control and not classical genetic control. In another more widely known example of loss of normal epigenetic control, stochastic changes to *Drosophila* eye color result from position effect variegation of white gene expression (Csink and Henikoff, 1996; Henikoff, 1979). The yeast colony color and eye color phenotypes highlight the stochastic changes in gene expression often associated with epigenetic defects. All the activities discovered so far for nuclear ARPs and their constituent remodeling complexes involve making transient changes to chromatin structure and are consistent with ARPs being defined as factors in epigenetic control.

3. Evolutionary Origin and Phylogeny of Nuclear ARPs

3.1. A class of nuclear proteins

3.1.1. ARP localization to the nucleus

Considering the decades of research on conventional actin as a cytoplasmic cytoskeletal protein, it was at first surprising to find a class of ARPs had evolved activity in the nucleus. Yeast ARP4 (ACT3b) was the first ARP to
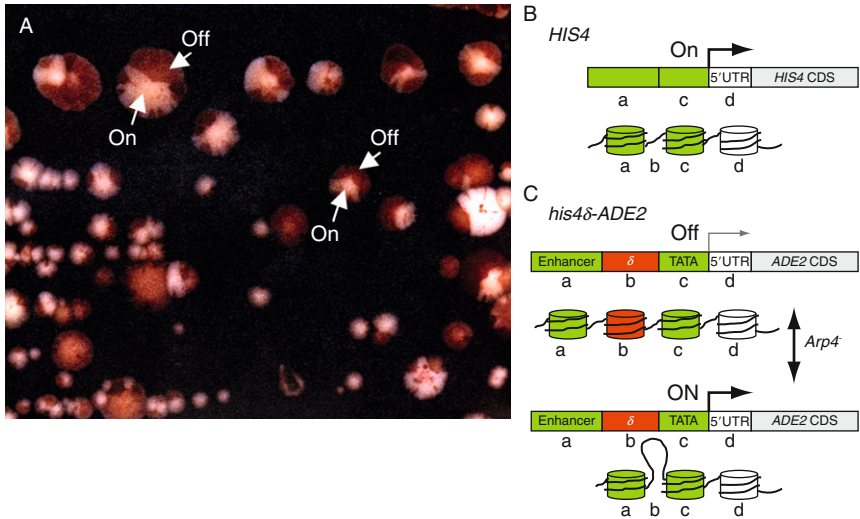
Figure 5.1 Sectored colony color morphology of ARP4–defective yeast results from an epigenetic defect. (A) Sectored colony color phenotype resulting from the loss of ARP4 function in an *ade2⁻* yeast strain containing the epigenetic reporter *his4δ–ADE2* (Jiang and Stillman, 1996). Portions of two colonies where the *his4δ-ADE2* reporter gene is "Off" (red) or "On" (white) are indicated with arrows. This reporter with a dysfunctional promoter is normally "Off" producing red colonies in *ade2⁻* yeast cells. The reporter is turned "On" stochastically in *arp4⁻* yeast cells. Photo, courtesy of David Stillman. (B) Normal *HIS4* promoter and gene structure. (C) A model showing the structure of the *his4δ-ADE2* epigenetic reporter gene in relation to possible changes in chromatin structure that render the gene transcriptionally "On" or "Off".

be found localized to the nucleus (Weber et al., 1995), followed closely by *Drosophila* ARP4 (Frankel et al., 1997), two isovariants of human ARP4 (Baf53A and Baf53B) (Harata et al., 1999a), and *Drosophila* and vertebrate ARP6 (Kato et al., 2001; Ohfuchi et al., 2006). Harata et al. (2000) delineate and define the entire class of nuclear ARPs by showing that yeast Arp5, Arp6, Arp7, and Arp8, and Arp9 are also localized to the nucleus, while fungal Arp1, Arp2, Arp3, and Arp10 are predominantly in the cytoplasm (Eckley et al., 1999; Zhang et al., 2008). We have shown that *Arabidopsis* ARP4, ARP5, ARP6, ARP7, and ARP8 are also localized to the nucleus as illustrated in Fig. 5.2 (Deal et al., 2005; Kandasamy et al., 2003, 2008, 2009). *Arabidopsis* ARP8 is the first ARP found to be concentrated in the nucleolus and not in the nucleoplasm (Fig. 5.2).

Most published studies used immunofluorescence microscopy or fluorescently tagged proteins to show the nuclear ARPs are concentrated in the nucleus during interphase, though they are mostly dissociated from chromatin during cell division (e.g., metaphase). For example, during telophase, anaphase, and metaphase we found weak immunofluorescent staining
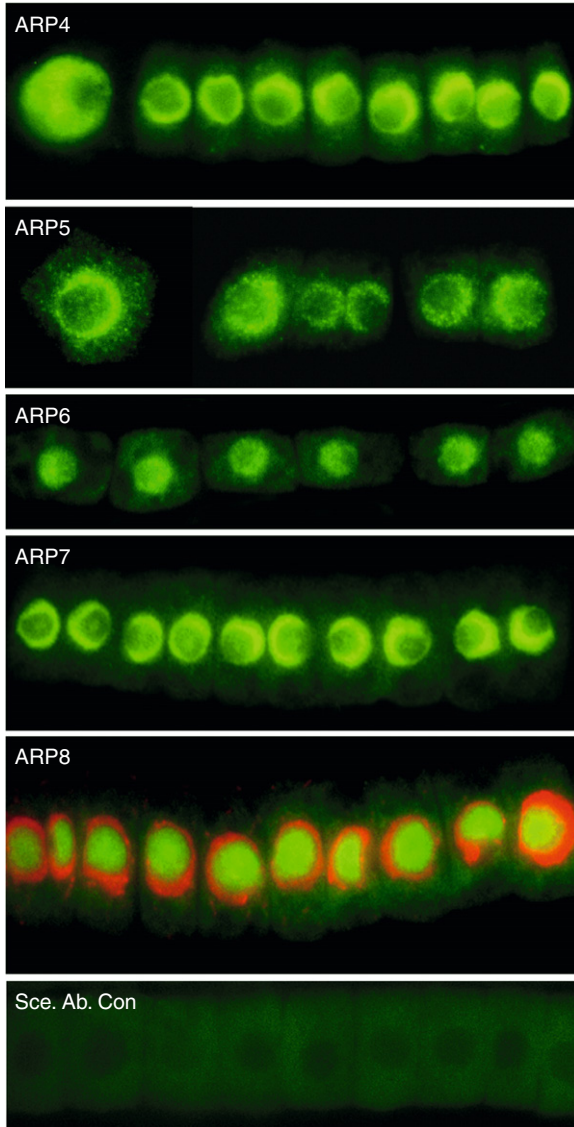
Figure 5.2 Nuclear localization of five plant ARPs. The nuclear localization of *Arabidopsis* ARP4, ARP5, ARP6, ARP7, and ARP8 were demonstrated using ARP-class-specific monoclonal antibodies prepared against the various recombinant plant proteins or synthetic peptides. ARP4, ARP5, ARP6, and ARP7 are concentrated in the nucleoplasm, while ARP8 is concentrated in the nucleolus. For the ARP8 image, DNA staining with DAPI (red) is merged with the ARP8-specific monoclonal antibody immunostaining (green). A control strip of root cells with secondary antibody labeling is shown in the bottom panel.

throughout most of the cell for *Arabidopsis* ARP4, ARP5, ARP6, ARP7, and ARP8 (Deal et al., 2005; Kandasamy et al., 2003, 2004, 2005a,b, 2008, 2009). Most of the nuclear ARPs appear to diffuse into the cytoplasm after the nuclear membrane breaks down during cell division and then are transported back and associated with chromatin before the nuclear membrane is reformed. This ebb and flow of ARP proteins is in contrast, for example, to the four core histones that stay concentrated on chromatin. The dissociation of the bulk of nuclear ARPs may be contrary to expectation, because chromatin is rapidly remodeled during all stages of the cell cycle.

Human ARP8 is the first among the nuclear ARPs to be identified as associating almost exclusively with mitotic chromatin in a dividing cell, and human ARP8 is essential to mitotic alignment of chromosomes (Aoyama et al., 2008). In addition, ARP4 was found weakly localized to the surface of mitotic chromatin in cultured mouse and human cells in more detailed immunofluorescence analyses of metaphase (Lee et al., 2007b). Genetic and biochemical studies also demonstrate that yeast ARP4 is associated with centromeric DNA during metaphase (Ogiwara et al., 2007b; Steinboeck et al., 2006). Its location here in previous studies may have been missed using standard microscopic techniques.

3.1.2. Nuclear transport

Nuclear ARPs are synthesized in the cytoplasm and transported into the nucleus, but the ratio of nuclear to cytoplasmic ARP4 concentration varies dramatically among mammalian cell types in culture (Lee et al., 2003). A bipartite nuclear localization signal (NLS) sequence (195KKALE199, 210KQRK213) was first identified in yeast ARP4 within the conserved insertion shared among all ARP4s (Fig. 5.3A) (Stefanov, 2000). The NLS is essential to yeast ARP4 nuclear localization and function. However, alignment of this region with homologous domains from *Arabidopsis*, human, and *Tetrahymena* ARP4 sequences reveals poor conservation of these particular NLS sequences across kingdoms. This same general region in each of the plant, animal, and protist ARP4 proteins does contain alternative Lys- and Arg–rich motifs with potential NLS activities. Thus, different NLSs may have evolved independently among distant members of the ARP4 class. Similarly, all ARP5 sequences contain potential NLSs that are not well conserved across kingdoms in the very large conserved insertion located after actin amino acid 246. Lee et al. (2003) have shown that the shuttling of human ARP4 (Baf53) between the nucleus and the cytoplasm is energy dependent. Again the location of independently evolved NLS motifs in ARP4- and ARP5-specific insertions argues that ARP4 and ARP5 evolved independently from an ancestral actin sequence, and that ARP5 did not evolve from ARP4.

Conventional actins contain two leucine–rich nuclear export signal sequences (NESs), located between residues 85 and 137 (Fig. 5.3B).

A

Potential and known NLS sequences among ARP4 polypeptides

```
ScARP4          193-LIKKALEPKE--IIPLFAIKQRK-------PEFIKKTFDYE
AtARP4          213-LLK-SLESKGIKIRPRYSFKRKEVRA----GEFQVEDVDIP
HsARP4(Baf53)202-QCRELFQEMAIDIIPPYMIAAKEPVREGAPPNWKKKEKLPQ
TtARP4          216-KILNNLQKEQNTRVYPRYCLQFAKEGP------KKIDKYLE
```

B

Potential NES sequences among actin and nuclear ARP polypeptides

```
                    NES1                NES2
        ScACT1  SLPHAILRIDLA    DIKEKL-CYVALD
        ScARP4  TLSKSTRRNFIA    ECKETL-CHICPK
        ScARP5  GILTDAKRINWG    MYKD-Y-CYVSRN
        ScARP6  PYYKAVKKLDIG    NIKEQC-LFVSPV
        ScARP7  VVKNAVVRSKFG    YYKEQADIYAKQQ
        ScARP8  VLEHSAITLDYG    RLKKNFTTFQDAD
        ScARP9  QLDHLVSSIPMG    SLKKSP-IFEVLS
        CON     L    V  L I     L    L    V L
                       I        I
                                Y
```

C

Potential N-terminal phosphorylation sites among ARP4 polypeptides

```
    ScACT1       1----------MDSEVAALVIDNGSGMCKAGFAGDDAP
    HsARP4(Baf53)1-MS-GG--VYGGDEVGALVFDIGSYTVRAGYAGEDCP
    ScARP4       1-MSNAALQVYGGDEVSAVVIDPGSYTTNIGYSGSDFP
    AtARP4       1-------MYGGDEVSAIVVDLGSHTCKAGYAGEDAP
    TtARP4       1---------MFTEDITAIVVDPGSLSIRAGYSGEDTP
    CON              S       Y          S       Y
```

Figure 5.3   Potential NLS, NES, and phosphorylation sites. (A) The proposed nuclear localization sequences (NLS) in various ARP4s are underlined and appear to be only moderately well conserved across the four eukaryotic kingdoms. The human (*Hs*), *Arabidopsis* (*At*), yeast (*Sc*), and protist (*Tetrahymena thermophila*, Tt) sequences are compared. (B) Proposed nuclear export sequences are compared among the yeast nuclear ARPs and actin and a consensus (CON) sequence is given. (C) Potential N-terminal phosphorylation sequences in ARP4 class members from the various kingdoms are compared to actin sequence. The conserved serine (S) and tyrosine (Y) residues that may be phosphorylated are underlined.

The first of these NESs is easily identifiable in the N-terminal region of all nuclear ARPs, while the second is less frequently conserved among the ARPs (Harata et al., 2000, 2001). NES sequences might mediate ATP-dependent ARP export. However, initial studies suggest that, at least for human ARP4, nuclear export is not inhibited by leptomycin B an inhibitor of the export receptor CRM1 that generally controls the export of leucine-rich NES proteins (Lee et al., 2003). At least two interesting questions remain: (1) To what purpose are the nuclear ARPs shuttled between the nucleus and the cytoplasm? (2) What regulates their concentrations in the two compartments? Perhaps their transport is essential for cytoplasmic–nuclear communication controlling the cell cycle and multicellular development.

3.2. Overall relationship to actin

The nuclear *ARP* sequences evolved from a common ancestral actin or actin–related gene prior to the divergence of the four eukaryotic kingdoms. They share only 17–35% amino acid sequence identity with conventional actin and are significantly more divergent from conventional actin than the cytoplasmic ARPs (Kandasamy et al., 2004; McKinney et al., 2002; Muller et al., 2005). For comparison, the cytoplasmic ARP1, ARP2, and ARP3 sequences average 38–52% identity with actin. Because the initial characterization of all the classes of ARPs was performed in yeast, most nuclear ARPs in other organisms are named relative to the yeast nuclear ARPs: Arp4, Arp5, Arp6, Arp7, Arp8, and Arp9 (Harata et al., 2000; Poch and Winsor, 1997). The larger numbers in this ARP nomenclature represent increasing divergence from conventional actin, with ARP4 being most closely related (approximately 35% amino acid identity to actin) and ARP8 and ARP9 the most divergent (an average of 18% identity to actin) (Goodson and Hawse, 2002; Kandasamy et al., 2004; McKinney et al., 2002; Muller et al., 2005). Protein sequence divergence within each nuclear ARP class is also relatively high. For example, ARP8 sequences from different kingdoms usually share less than 30% identity (Muller et al., 2005). These data demonstrate that nuclear ARP sequences evolve much more rapidly than conventional actin sequences.

3.3. Relationships among the nuclear ARPs

There are four classes of ARPs whose origins clearly predate the divergence of the four eukaryotic kingdoms. The yeast representatives of these four classes are ARP4, ARP5, ARP6, and ARP8. The phylogenetic relationships among the nuclear ARPs from humans, *Saccharomyces cerevisiae (Sc)*, *Arabidopsis thaliana (At)*, and *Dictyostelium discoideum* representing animal, plant, fungal, and protist kingdoms are illustrated in Fig. 5.4. Humans, *Arabidopsis*, and *Dictyostelium* contain clear homologs of yeast ARP4, ARP5, ARP6, and ARP8.

Relative to conventional actin, the nuclear ARPs contain numerous insertions, some very large, and a few small deletions. Figure 5.5 maps the location of 12 insertions that help define the four conserved nuclear ARP classes relative to the sequence of conventional mammalian β-actin (cytoplasmic actin) as first summarized by Muller et al. (2005). The insertion after the equivalent of mammalian β-actin amino acid 246 is found in all ARP5 and ARP6 sequences and the insertion results in a large increased in the size of all ARP5 proteins, however, ARP7 contains an insertion in this position in only a few species. All ARP4 sequences contain a small insertion after actin amino acid 203, but ARP4s in a few species contain insertions in three other locations (not shown). Numerous other kingdom and/or species-specific
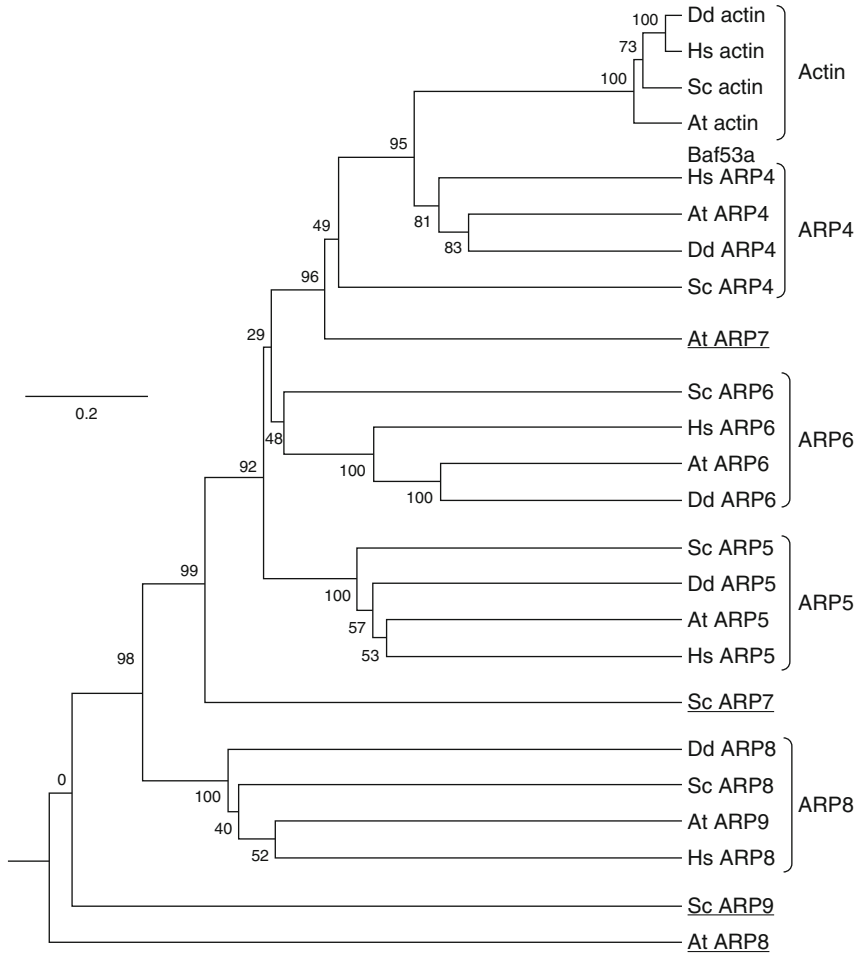
Figure 5.4 Phylogenetic relationships among nuclear ARPs from the four eukaryotic kingdoms. The phylogenetic relationships among the nuclear ARPs encoded by the animal (human, *Hs*), yeast (*Saccharomyces cerevisiae*, *Sc*), plant (*Arabidopsis thaliana*, *At*), and protist (*Dictyostelium discoideum*, Dd) genomes are illustrated. The four classes of nuclear ARPs—ARP4, ARP5, ARP6, and ARP8—that are generally conserved among animals, plants, fungi, and some protists are indicated. A few examples of orphaned ARPs are indicated by underlining. Clustal was used to align the sequences. The phylogram presented used the unweighted pair-group method with arithmetic means (UPGMA) to create the tree's topography based on sequence similarity (Tamura et al., 2007). The neighbor joining tree building method also yields a tree with very similar, but not identical, branching patterns. Human *β*-actin and *Arabidopsis* ACTIN2 were used as conventional actin gene representatives from within the divergent families of animal and plant actins.
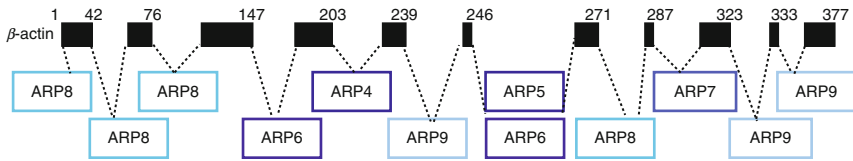
Figure 5.5 Coding sequence insertions in ARPs with respect to amino acid positions in conventional human β-actin. The locations of polypeptide insertions in the ARP4, ARP5, ARP6, and ARP8 classes that are conserved across all four eukaryotic kingdoms are shown. Numbered positions refer to amino acids in human β-actin. Insertions in yeast orphaned ARPs—ARP7 and ARP9—that are conserved in fungi are also shown for comparison.

insertions are also reported and the orphaned ARPs may share the insertions shown and other novel insertions (Muller et al., 2005). For example, the novel insertions found in yeast ARP7 and ARP9 are shown in Fig. 5.5. The resulting variation in amino acid length of the four conserved classes of nuclear ARPs is summarized in Table 5.1. Overall, the low level of sequence identity among the nuclear ARPs in a class and between classes and the variation in size and location of INDELs create difficulties in aligning, identifying, and naming them. In many genome databases, the nuclear ARPs are annotated simply as "actin-like" or "actin-related" sequences.

Considering the ancient common origin of four classes of nuclear ARPs, it seemed possible that intron–exon positions might reveal something about their evolutionary history. We compared the 19 intron positions in the *Arabidopsis ARP4* gene, to the 13 in the human *ARP4* (Baf53a) gene, and the 4 in the *Dictyostelium ARP4* gene as shown in Fig. 5.6. Like most yeast genes, yeast ARP4 lacks any introns. Overall, it is clear that intron–exon positions are poorly conserved even between plant and human *ARP4s* that each contains large number of introns. We observed seven intron locations (dotted lines, Fig. 5.6) that were conserved between pairs of *ARP4* genes in different kingdoms.

3.4. Inconsistent composition of the nuclear ARP classes in various protists

Considering that protist development was an early model of epigenetic control, we and others have looked for homologs of nuclear ARPs encoded in several representative and relatively complete protist genomes (Hedges et al., 2004; Muller et al., 2005). However, unlike the other eukaryotic kingdoms, the protists comprise an ancient, complex, and polyphyletic group of organisms (Adl et al., 2007). Hence, no single species or group can be considered as truly representative of the protist kingdom. We found clear homologs of ARP4 and ARP6 in representative species

Table 5.1 Across kingdom comparisons of the amino acid lengths of four ARP classes of known phylogenic origin

ARP	Species	length a.a.
ARP4 (isovariant)		
"	Sc	498
"	Dd	440
" (Baf53a)	Hs	429
" (Baf53b)	Hs	426
"	At	441
ARP5		
"	Sc	755
"	Dd	684
"	Hs	607–620
"	At	726
ARP6		
"	Sc	438
"	Dd	490
"	Hs	396
"	At	420
ARP8		
	Sc	881
	Dd	873
	Hs	624
(ARP9)	At	596

from diverse protist groups including *Tetrahymena thermophila* and *Toxoplasma gondii* representing the chromalveolates, *Entamoeba histolytica* representing the amoeba, *Trypanosoma brucei* representing the kinetoplastids (Gordon and Sibley, 2005), and *Chlamydomonas reinhardtii* representing the euglenids. The *T. thermophila* and *D. discoideum* genomes contained ARP5 and ARP8 homologs, while most protist species lacked them. *Dictyostelium* sequences were used in the nuclear ARP phylogeny (Fig. 5.4), because this protist had one of the most complete complements. Without inferring that the sequences were lost repeatedly, it is hard to reconcile the lack of ARP5 and ARP8 homologs in most protist genomes with the likely basal ancestry of protists to the other eukaryotic kingdoms. As might be expected, the extremely simple and possibly basal genomes of the parabasalids, *Giardia lamblia* and *Trichomonas vaginalis*, contained only an ARP4 homolog and no nuclear ARP homologs, respectively (Adam, 2000). We cannot yet say if this is a derived state representing loss of ARP sequences from an ancestral protist ancestor, or if this represents the early evolutionary state of chromatin remodeling systems, or some combination of both.
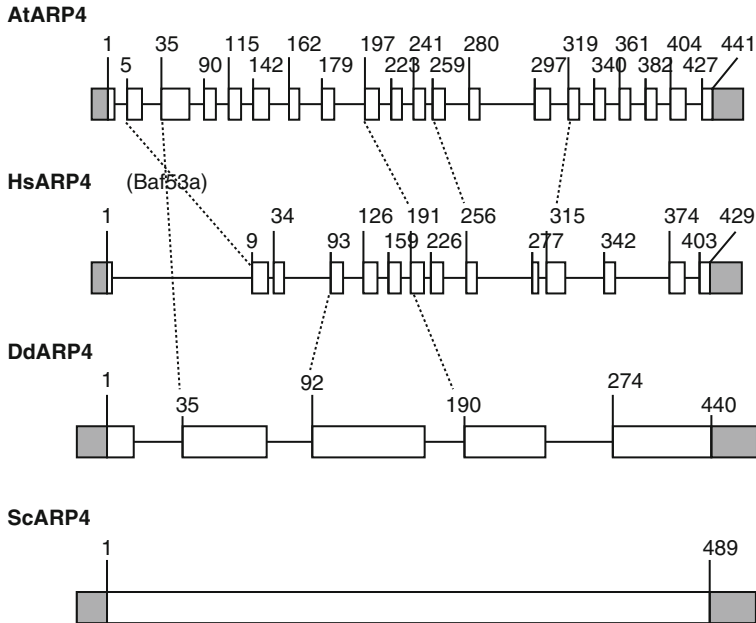
Figure 5.6 Comparison of intron–exon structures for ARP4 genes across the four eukaryotic kingdoms. The intron/exon structure of ARP4 genes from *Arabidopsis* (*At*), human (*Hs*, *Baf53a* gene), protist (*Dictyostelium discoideum*, *Dd*), and yeast (*Sc*) genomes are compared. Coding exons are shown as white boxes, introns as lines, and transcribed but untranslated flanking regions (UTRs) in light gray boxes. The accession numbers of the particular transcript sequence compared are AT1G18450.1, BAG51043, XP_640964, and NP_012454, respectively, distinguishing these data from other possible transcript variants that exist for the plant and animal sequences. Conserved intron–exon junction positions are indicated by dashed lines. To generate these data, the intron positions identified from transcript and gene sequence alignments were compared to the amino acid sequence alignment of the four ARP4 protein sequences.

3.5. Orphaned ARPs

The orphaned nuclear ARPs are so named, because their phylogenetic relationships across kingdoms are less clear. *Arabidopsis* ARP7 and ARP8, yeast ARP7 and ARP9, and human ARP7 and ARP11 are examples of orphaned ARPs. In particular, *Arabidopsis* ARP7 shares 39% amino acid identity with actin and the basal structure of a conventional actin, but is only 23–27% identical to yeast ARP4, ARP5, ARP6, ARP7, or ARP8. As a result of numerous small insertions and deletions and small sequence similarities, ARP7 is phylogenetically positioned among the nuclear ARPs (Blessing et al., 2004; Kandasamy et al., 2004), and yet not clearly allied with any one yeast or animal nuclear ARP. *Arabidopsis* ARP8 and other plant ARP8 homologs are distinct from any ARP found outside the plant

kingdom in that they combine a 40 amino acid long hydrophopic leader followed by a 50 amino acid long complete F-box domain and a complete 380 amino acid long C-terminal actin–related sequence (Kandasamy et al., 2008; McKinney et al., 2002). F-box domains target protein ubiquitination in other proteins, but how the F-box and the hydrophobic domain function together as part of any nuclear ARP is unknown. Moreover, this novel ARP is localized to the nucleolus. It seems possible that the N-terminal hydrophobic domain targets ARP8 to the nucleolus. Thus, plant ARP7 and ARP8 belong to plant-specific (Kandasamy et al., 2004; McKinney et al., 2002) or orphaned (Blessing et al., 2004) ARP classes. This does not mean that ARP7 and ARP8 do not share a common evolutionary origin with other specific nuclear ARPs (Fig. 5.4), but only that phylogenetic analysis has not unambiguously resolved these evolutionary relationships, if they exist. Similarly, yeast nuclear ARP7 and ARP9 also share no immediate homologs in other kingdoms and have an orphaned status (Blessing et al., 2004). Yeast and *Arabidopsis* ARP7 both appear more closely related in sequence to ARP4. Considering that yeast ARP7 is known to be part of SWI/SNF complexes, while ARP4 is a component in animal counterparts, it is reasonable to speculate that ARP7 evolved directly from ARP4. Many tree building programs place yeast and *Arabidopsis* ARP7 most closely allied to ARP4 and *Arabidopsis* ARP8 as most closely related to other ARP9s. Some protist genomes including *Tetrahymena* and *Disctyostelium* contained several other orphaned ARPs with questionable phylogenies and unknown functions.

3.6. Ancient origins of nuclear ARP sequences

The three-dimensional structures of the actins and ARPs reveal that they belong to a diverse and older family of proteins found in archaea, prokaryotes, and eukaryotes (Muller et al., 2005). This family includes glycerol kinases, hexokinases, and some chaperones like the 70 kDa heat shock protein, all of which share the actin-fold and the theoretical capacity for conformational change (Galkin et al., 2002). While the origin of conventional actin has been traced to a common ancestor of the bacterial structural protein MreB (van den Ent et al., 2001), a bacterial origin for an ARP with chromatin remodeling activity has not yet been identified. Some bacteria contain nucleosomal DNA and may remodel their chromatin, thus the bacterial origin of nuclear ARPs as part of chromatin remodeling machines remains a possibility (Bendich and Drlica, 2000; Champion and Higgins, 2007).

The topographies of the tree in Fig. 5.4 and other phylogenies comparing actins and nuclear ARP sequences (Kandasamy et al., 2004; Muller et al., 2005) generally position ARP4 closest to conventional actin and basal to the other nuclear ARPs. This topography not only reflects the rooting of the tree with conventional actin, and ARP4's relatively high level of

conservation and sequence identity with actin, but might also reflect the possibility that ARP4 was the first nuclear ARP to evolve. Supporting the view that ARP4 evolved first, ARP4 is found in more kinds of chromatin remodeling complexes (e.g., SWI/SNF, INO80, and SWR1) than any other nuclear ARP (Chen and Shen, 2007). Because ARP4 is involved in various kinds of complexes and perhaps is the most ancient, it may be the most indispensable nuclear ARP. Further, ARP4 homologs are the only nuclear ARPs present in a few simple protist genomes suggesting again that ARP4 may be the most ancestral (Gordon et al., 2008). It is reasonable to speculate that ARP5, ARP6, and ARP8 evolved from ARP4, but have become more subfunctionalized. ARP5 and ARP8 are part of the yeast and human INO80 NR complexes, while ARP6 is only found in SWR1-related histone variant exchange (HVE) complexes.

However, ARP4s contain an insertion after actin amino acid 203 that is conserved across all eukaryotes and not found in any other nuclear ARPs, except for a subset of ARP7 sequences in a few species. For ARP4 to be ancestral to the other nuclear ARPs, the founding ARP4 genes would need to have acquired this same insertion in multiple ancient phyla independently, after the evolution of ARP5, ARP6, and/or ARP8. The distinct insertions shared among each of these three ARP classes can be used to make similar arguments about the independent evolution of each classes from actin. Thus, it seems unlikely that the other nuclear ARPs are descended from ARP4 and, more likely, they evolved directly from conventional actin. The binding of conventional actins to Swi2- and Vid21-related ATPases and their role in chromatin remodeling and modification may have provided the target for natural selection of new nuclear ARPs (Szerlong et al., 2008). By this model, duplication of conventional actin genes followed by selective modification and subfunctionalization for nuclear chromatin activity would have independently produced ARP4, ARP5, ARP6, ARP8, and ARP9.

4. FUNCTION OF THE NUCLEAR ARPS IN CHROMATIN REMODELING AND MODIFYING COMPLEXES

4.1. Nuclear ARPs bind Swi2-related DNA-dependent ATPases in chromatin remodeling machines

The nuclear ARPs are multifunctional proteins and some appear to have their own distinct properties, but only recently has a single common activity emerged that may be conserved among all members of the family. The nuclear ARPs are constituents of ATP-dependent chromatin remodeling complexes (e.g., SWI/SNF, SWR1, RSC, INO80, p400) and/or chromatin modifying complexes (NuA4 HAT) (Chen and Shen, 2007; Krogan et al., 2003; Mizuguchi et al., 2004; Olave et al., 2002b). Indeed, all chromatin remodeling complexes that contain a Swi2-related DNA-

dependent ATPase subunit also include one or more nuclear ARPs, and if they contain only a single nuclear ARP subunit, this is in association with an actin subunit (Szerlong et al., 2008). Figure 5.7 models the assembly of one possible isoform of the mammalian Swi/Snf BRG chromatin remodeling complex containing approximately 13 subunits. It will be used as an example in the following discussion. Nucleosomal movement is powered by ATP hydrolysis mediated by the Swi2-related ATPase (Dang and Bartholomew, 2007). Swi2-related proteins share a rapidly evolving HSA (helicase SANT-associated) domain and an adjacent post–HSA domain of approximately 100 amino acid in length and located within a few hundred amino acid of the N-terminus of these very large proteins (Szerlong et al., 2008).

A number of early studies lent strong support to the particular binding of nuclear ARPs and Swi2-related ATPases. For example, the BAF complex of mutant human cells lacking the Swi2-related Brg1 subunit also were missing the ARP4 (Baf53) and actin subunits, while a BAF subcomplex lacking all
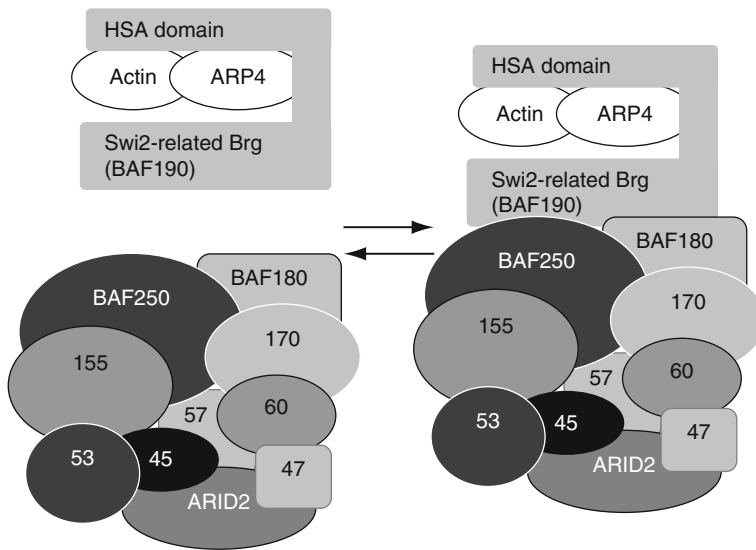
Figure 5.7 Nuclear ARP4 (Baf53) and actin bind the HSA domain of the Swi2–related Brg DNA–dependent ATPase in the mammalian Swi/Snf BRG chromatin remodeling complex. This model illustrates that β-actin and ARP4 bind Brg, and that the β-actin/ ARP4/Brg subcomplex binds to a second subcomplex containing several other Brg proteins to form an active chromatin-remodeling machine (Lessard et al., 2007; Szerlong et al., 2008). A related model may be proposed for a large number of chromatin-active complexes. Two nuclear ARPs or a nuclear ARP and actin bind as heterodimers to the helicase-SANT (HSA) domain of the large Swi2-related DNA-dependent ATPase subunit in chromatin remodeling complexes or the Vid21-related helicase subunit in chromatin modifying complexes. Again, the ARP-containing subcomplex then binds a second subcomplex with a larger number of subunits.

three of these components still formed (Zhao et al., 1998). Furthermore, the binding of ARP8 in the INO80 complex and the binding of actin and ARP4 in the SWR1 complex both require N-terminal regions of the Swi2-related Ino80 and Swr1 subunits, respectively (Shen et al., 2003b; Wu et al., 2005). INO80 complexes purified from yeast *arp5Δ* or *arp8Δ* strains still retain most other subunits, but are deficient in the Ino80 ATPase, ARP4, and actin, indicating that ARP5 and ARP8 may be needed to recruit these other subunits into the complex (Shen et al., 2003b). In *Arabidopsis*, the N-terminal half of Swi2-related SPLAYED retains activities necessary for normal meristem development and flowering (Su et al., 2006). Finally, yeast ARP7 and ARP9 were shown to both interact with Swi2-related Sth1 subunit to form a catalytic SWI/SNF subcomplex (Yang et al., 2007).

Isolation of yeast suppressor mutations of ARP deletions *Δarp7* and *Δarp9* provided genetic proof of the interaction between nuclear ARP and HSA domain of Swi2-related proteins. All 10 suppressors of these null mutants mapped as amino acid substitutions within the 83 amino acid HSA domain or an immediately adjacent 20 amino acid post-HSA domain of the Swi2-related Sth1 subunit of a SWI/SNF complex (Szerlong et al., 2008). Biochemical protein interaction assays suggest that ARP7 and ARP9 bind the HSA/post-HSA domain as a heterodimer similar to the interaction of actin and ARP4 in the BRG complex (Fig. 5.7). Yeast ARP7 and ARP9 also bind the HSA domain of yeast Swi2-related subunit Snf2 of the RSC complex. Similarly, human and yeast actin and ARP4 subunits of SWI/SNF complexes bind the HSA domains of Swi2-related human Brg1 and yeast Swr1, respectively. Furthermore, yeast actin, ARP4 and ARP8 subunits of the INO80 complex bind the HSA domain of the Ino80 subunit. Of particular note is the significant specificity within the various divergent HSA domains that directs binding of the correct nuclear ARP and actin partners to the corresponding Swi2-related sequence, and not to irrelevant HSA domain proteins. Szerlong et al. (2008) propose that ARPs bind as dimers to an HSA domain protein in all complexes in which they participate.

4.2. Nuclear ARPs bind Vid21-related helicase subunits in chromatin modifying machines

These data beg the question: why are nuclear ARP4 and actin found in large histone acetylation complexes that lack a Swi2-homolog like the various fungal NuA4 HAT and mammalian TIP60 complexes? Szerlong et al. (2008) show that the Eaf1 subunit of NuA4 and other Vid21-related subunits of fungal HAT complexes each contain a HSA domain and the HSA domain of Eaf1 binds ARP4 and actin as this domain binds Brg in the BRG complex (Fig. 5.7). Hence, an alternate HSA domain protein interacts with two actin-related sequences in these fungal HAT complexes. Sequence

conservation among the Vid21 sequences and their HSA domains is weak even among distant fungi and thus structural homologs in other kingdoms may be difficult to identify. Eaf1 has some weak and previously undetected homology of its HSA and SANT domains with a few Swi2-related proteins such as human p400/Domino (Auger et al., 2008). We observed that the human genome encodes a few other proteins similar in size to the 982 amino acid long yeast Eaf1 protein with low-complexity sequence matches to Eaf1's HSA domain (e.g., BAC04759) that are not yet identified as HSA-containing homologs. These and other HSA domain proteins have the potential to interact with nuclear ARPs and actins in novel chromatin modifying complexes. Finally, mammalian TIP60 complexes contain Ruvbl1 (RuvB-like 1, Tap54, Tip49) with both DNA helicase and ATPase domains (Ikura et al., 2000). Although human Ruvbl1 (456 amino acid) shows no statistically significant amino acid sequence homology with the larger Swi2-related proteins or Vid21-related sequences, it is reasonable to speculate that actin and ARP4 might interact via a poorly conserved and ancient HSA domain.

4.3. Other activities and interactions with chromatin

Most models for ARP and actin function in chromatin remodeling and modifying complexes center on the actin-fold and hinge region that impart the ability to shift between distinct conformational states upon nucleotide binding, ATP hydrolysis, and ATP/ADP exchange. Nuclear ARPs belong to the actin superfamily of proteins that include cytoskeletal actins, heat shock proteins, ATPases, and sugar kinases that all appear to retain the structural potential to bind a nucleotide and to change conformation (Boyer and Peterson, 2000; Sunada et al., 2005). Conventional actin, for example, is converted from an inactive ADP bound conformational state to an ATP bound active form via its interaction with profilin. ATP-actin is added to actin filaments, but subsequent ATP hydrolysis within monomers lowers filament stability, alters filament turnover rates, and changes the affinity for different actin-binding proteins. The ARP and actin subunits of chromatin remodeling machines may undergo similar nucleotide-dependent changes in the nucleus to act as molecular switches controlling the assembly, stability, and/or activity of these complexes. To date, only ARP4 has been shown to bind nucleotides, but it is possible that more evidence for nucleotide binding will follow for other nuclear ARP family members. Biochemical and genetic studies in yeast demonstrate that mutant ARP4 proteins defective in nucleotide binding are more concentrated in high-molecular-weight protein fractions containing remodeling complexes than wild-type ARP4 protein (Sunada et al., 2005). By contrast, mutant forms of ARP4 enhanced for ATP binding remain mostly as unbound monomers. Perhaps the nucleotide bound state of ARP4 and other

ARPs may affect their assembly and disassembly as ARP-ARP-HSA or ARP–actin–HSA trimer subcomplexes.

ARPs are required to associate some complexes with the nuclear matrix (Zhao et al., 1998). Yeast ARP4 and ARP8 bind histones directly, so ARPs may help recruit complexes directly to nucleosomes (Harata et al., 1999b; Shen et al., 2003b). In addition, ARPs and actins may connect one chromatin complex to another to create higher order chromatin complexes, acting similarly to conventional actin, only in the ''polymerization'' of higher order chromatin structures (Olave et al., 2002b). Silencing of mammalian ARP4 (Baf53) or conditional knockdown mutations of yeast ARP4 causes a loss of chromatin compaction, as revealed by increases in the nuclease sensitivity of nucleosomes (Georgieva et al., 2008; Lee et al., 2007a). Furthermore, higher order interactions of distinct chromatin remodeling complexes INO80, SRCAP, and TIP60 are supported by initial proteomic data. Analyses of the proteins bound to large numbers of individually epitope tagged subunits of these complexes revealed interactions between and among complexes (Sardiu et al., 2008), further supporting the idea that nuclear ARP complexes contribute to the formation and integrity of higher ordered chromatin structures.

4.4. Activities of particular ARPs

4.4.1. ARP4

ARP4 is an essential gene in yeast and appears to be essential in *Arabidopsis*, because severe knockdown plants with less than 15–20% of wild-type levels of ARP4 protein are extremely dwarfed and highly sterile (Kandasamy et al., 2005a). ARP4 is found in more diverse chromatin remodeling complexes than any other ARP in plants, animals, and fungi. Yeast ARP4 is found in the NUA4 HAT (histone acetyltransferase) nucleosome modifying complex, the INO80 NR complex and the SWR1 HVE and NR complex (Galarneau et al., 2000; Harata et al., 1994; Huang et al., 1996; Krogan et al., 2003; Minoda et al., 2005; Mizuguchi et al., 2004; Shen et al., 2000). The 1.3 MDa NUA4 complex contains 11 subunits, including ARP4 and conventional actin, and it is known to primarily acetylate histone H4. In temperature-sensitive yeast *arp4* mutants, the full NUA4 complex is absent at the restrictive temperature (Galarneau et al., 2000). These same mutants display increases or decreases in the transcription of a number of target genes at the restrictive temperature, coinciding with changes in the normal chromatin structure around those genes (Harata et al., 2002; Jiang and Stillman, 1996). ARP4 orthologs are also found in several different mammalian ATP-dependent NR and HVE complexes (Fuchs et al., 2001; Lee et al., 2005; Nie et al., 2000; Oma et al., 2003; Rando et al., 2002; Ruhl et al., 2006), in mammalian INO80 NR DNA repair complexes (Cai et al., 2006), in mammalian Tip60 NR HAT complexes (Feng et al., 2003; Ikura

et al., 2000), and in *Drosophila* NR complexes (Mohrmann and Verrijzer, 2005; Papoulas et al., 1998).

ARP4 binds all four core histones *in vitro* (Harata et al., 1999b) although yeast ARP4 shows some preference for H2A. The particular histone-binding preferences reported for ARP4 vary among the different species in which binding was measured. How histone modification may affect ARP4's preferential binding is only now being addressed. It has been well established that a phosphoserine residue in the C-terminal domain of H2A variant H2AX tags nucleosomes at sites of severely damaged DNA (e.g., double-strand breaks (DSBs) requiring recombination repair) (Kuo and Yang, 2008; Morrison et al., 2004; van Attikum et al., 2004). ARP4 binds this residue within nucleosomes and directs the binding of yeast ARP4-containing complexes, NUA1, INO80, and SWR1, to remodel chromatin at these damaged sites (Bird et al., 2002; Downs et al., 2004). Thus, another reason that ARP4 is such a widely conserved subunit of diverse complexes may be its ability to bind different core histones and histone modifications, and hence, target complexes to chromatin.

Molecular genetic evidence suggests that the N-terminal Ser2 and Tyr6 residues of human ARP4 (Baf53) may be phosphorylated for at least some ARP4 activities (Lee et al., 2005). A small N-terminal extension encodes Ser and/or Tyr residues in the human, *S. cerevisiae* and *A. thaliana* sequences, but not in *T. thermophila* ARP4 homologs as shown in Fig. 5.3C. Mammalian ARP4 sequences also contain Ser20 and Tyr27 residues in the first actin homology domain that are conserved among ARP4 homologs from all four eukaryotic kingdoms. The possible conservation of the phosphorylation of N-terminal Ser and Tyr residues and the significance of these modified residues on ARP4 activities outside of human cell culture have yet to be determined. Phosphoinositol (PIP2) addition to cultured mouse lymphocytes rapidly targets ARP4-containing BAF complexes to chromatin, but it is not known if PIP2 signaling affects phosphorylation of ARP4 or if this phosphorylation independently affects localization of the complex (Zhao et al., 1998). Surprisingly, expression of a truncated ARP4 (Baf53b) mutant protein lacking this short N-terminal domain has dominant negative effects and is lethal to human cells (Choi et al., 2001).

4.4.2. ARP5 and ARP8

ARP5 and ARP8 proteins are not essential to the viability of budding yeast (Shen et al., 2003b; van Attikum et al., 2004). Yeast, mammalian, plant, and protist ARP5 and ARP8 (*Arabidopsis* ARP9) are highly modified by insertions of protein sequences relative to actin (Fig. 5.5) making them the largest nuclear ARPs, typically 600–800 amino acids (Muller et al., 2005). In addition to ARP5 and ARP8, the yeast and mammalian INO80 NR complexes also contain ARP4, monomeric actin, a Swi2-related DNA-dependent ATPase Ino80, and several other subunits (Cai et al., 2006;

Jin et al., 2005). The *Arabidopsis* genome encodes homologous of all the subunits of the yeast INO80 complex (Fritsch et al., 2004; Meagher et al., 2005).

Because *ARP4*, *ARP5*, *ARP8*, and *Ino80* genes and most other subunits are conserved across the fungal, animal, and plant kingdoms, it appears that INO80 complexes will be relatively universal. Roles for INO80 complexes are reported in dynamic control of transcription, DNA repair, and DNA replication (Conaway and Conaway, 2009). Yeast loss-of-function mutations for the Ino80 Swi2-related subunit are defective in transcribing the genes needed for inositol biosynthesis (e.g., the *INO1* gene) and require inositol, signifying that the INO80 complex is involved in transcriptional control as expected for a NR complex. Ino80 defective cells are hypersensitive to several DNA damaging agents demonstrating INO80 is also involved in DNA damage repair (Ebbert et al., 1999; Shen et al., 2000). Deletion mutants lacking the *ARP5* and *ARP8* genes are defective in the DNA-dependent ATPase activity of the Ino80 subunit and require inositol. This undoubtedly occurs because these ARPs are critical to binding the HSA domain on Ino80 (Szerlong et al., 2008) and assembly of a subcomplex needed for the full activity of INO80 (Fig. 5.7). ARP8 is also required for the INO80 complex to bind the promoter of the *INO1* gene affording some mechanistic explanation for the phenotype of *Arp8* and *Ino80* defective mutants (Ford et al., 2008). The ATP-binding Rvb helicase proteins bind ARP5 and are essential for its assembly into INO80 complexes and for formation of a functional complex (Jonsson et al., 2004). ARP5- and ARP8-defective mutants in yeast are dramatically altered in DNA repair and the cell cycle (van Attikum et al., 2004, 2007).

In mammalian and yeast systems, extensive effort has gone into studying the role of INO80 in repairing radiation-induced double-strand breaks in DNA (Cairns, 2004; Morrison et al., 2004). Less is known about the particular roles of ARP5 and ARP8 in these processes. Cells with mutations in Arp8 are defective in end-processing of gamma radiation-induced DSBs (van Attikum et al., 2007) and in recombination repair of sister chromatids (Kawashima et al., 2007). The finding that ARP8 binds histones H3 and H4 *in vitro* suggests that along with ARP4, ARP8 may also serve as a point of contact between the complex and chromatin (Shen et al., 2003b). Human ARP8 was one of the first nuclear ARPs to be shown to accumulate on mitotic chromatin. The transient silencing of ARP8 or expression of truncated ARP8 variants causes misalignment of metaphase chromosomes, while the silencing of ARP5 or Ino80 homologs did not (Aoyama et al., 2008). These data suggest novel functions for ARP8 outside those known for INO80 complexes.

Despite the low level of homology, human ARP5 partially complements the loss of UV resistance of yeast *arp5Δ* strains (Kitayama et al., 2009). HeLa cells partially silenced for *ARP5* expression are significantly more sensitive to DSBs caused by bleomycin than control cells. Kitayama et al. (2009) also show that ARP5 appears to bind directly to both H2AX and

phosphorylated γH2AX after treatment with bleomycin. Finally, overexpression of ARP5 causes an increase in γH2AX levels. *Arabidopsis* plants defective in ARP5 are hypersensitive to DNA damaging agents HU, MMS, and bleomycin, and show dramatic defects in multicellular development (Kandasamy et al., 2009). Together these data suggest that ARP5 may interact directly with chromatin in regulating the activities of the INO80 complex in chromatin remodeling and DSB repair.

4.4.3. ARP6

ARP6 is not essential for the viability of budding or fission yeast or *Arabidopsis*, but it is essential for their normal growth and development (Deal et al., 2005; Kawashima et al., 2007; Ueno et al., 2004). ARP6 is a universally conserved subunit of HVE complexes found in fungi and plants (SWR1), *Drosophila* (dISWI), and mammals (SRCAP) (Cai et al., 2005; Ruhl et al., 2006). The *S. cerevisiae* SWR1 and human SRCAP complexes share a large part of their subunit composition with other ATP-dependent NR complexes including the ARP4 and actin subunit (Kobor et al., 2004). The biochemically characterized ARP6–HVE complexes from animals and yeast also contain a large and conserved Swi2-related Swr1 subunit that is distinct among the families of fungal and animal DNA–dependent ATPases (Mizuguchi et al., 2004). Genetic and biochemical evidence support the existence of the SWR1 complex in plants. The *Arabidopsis* genome encodes homologs of all the subunits of yeast SWR1 (Meagher et al., 2005). Null mutants in *ARP6* and the Swr1-related *PIE1* (*Snf2/Swr1*), and another conserved SWR1 subunit, *Swc6*, share most of the same suite of developmental phenotypes (Choi et al., 2005, 2007; Deal et al., 2005, 2007; Lazaro et al., 2008; March-Diaz et al., 2007; Noh and Amasino, 2003). We have shown that *ARP6-* and *PIE1-defective* mutants lack measurable levels of histone variant H2AZ deposition at a number of target loci, lending strong support for the presence of a plant SWR1-like complex (Deal et al., 2007).

Despite sharing many subunits with other NR complexes, SWR1 homologs have the unique ability to catalyze the replacement of histone H2A with the variant H2AZ at specific chromosomal locations (Krogan et al., 2003). In yeast and *Arabidopsis*, the H2AZ variant plays important roles in promoting transcription and probably in antagonizing the spread of heterochromatin into euchromatic regions (Adam et al., 2001; Deal et al., 2007; Larochelle and Gaudreau, 2003; Meneghini et al., 2003; Santisteban et al., 2000). In both yeast and *Arabidopsis*, ARP6 is essential for the activity of the complex depositing H2AZ into chromatin (Deal et al., 2007; Wu et al., 2005). Within the yeast SWR1 complex, ARP6 recruits other critical subunits, one of which, Swc2, interacts directly with the C-terminal end of H2AZ, and hence, ARP6 is indirectly required for binding of the complex to nucleosomes. There are numerous other histone variants (e.g., H2AX), but it is unknown if SWR1 controls their deposition into nucleosomes.

Work in animals shows an association of ARP6 activity and HETERO-CHROMATIN PROTEIN1 in hetrochromatic regions (Kato et al., 2001; Ohfuchi et al., 2006). The histone variant H2AZ exchange activity of ARP6-containing SWR1 complexes is interpreted as antagonizing the spread of inactive heterochromatin into active euchromatic regions of the genome and as maintaining gene silencing (Kato et al., 2001; Ohfuchi et al., 2006; Ueno et al., 2004). Contrary to this view, detailed mapping at individual loci in yeast and *Arabidopsis* shows H2AZ distributed at the 5′ ends of most genes, both active and inactive (Deal et al., 2007; Raisner and Madhani, 2006; Raisner et al., 2005), and is not particularly concentrated in heterochromatic regions (Dryhurst et al., 2004; Fan et al., 2004; Li et al., 2005; Meneghini et al., 2003). Thus, ARP6 appears to have multiple and contrasting functions that must be viewed as part of an integrated system of chromatin remodeling activities, with activities in heterochromatic regions that are not yet fully defined. Supporting the view that ARP6 can have opposing functions on different genes, we found that loss of ARP6 activity in *Arabidopsis* caused loss of H2AZ deposition at the 5′ and 3′ ends of three active MADS box loci that are generally active in nongametic tissues. Loss of ARP6 results in significant repression of their transcript levels (Deal et al., 2007). We have found other classes of transcription factors where the loss of 5′ H2AZ deposition in ARP6-deficient plants caused activation (unpublished data), fitting the original view of ARP6 and H2AZ as silencing gene activities. Perhaps ARP6-dependent H2AZ deposition can potentiate transcriptional activation serving an epigenetic memory function by marking the ends of active genes and preparing silenced genes for reactivation (Meagher et al., 2007).

4.4.4. Orphan ARPs

As discussed previously, a number of nuclear ARPs are classified as orphaned sequences, because they cannot be reliably grouped in phylogenies across the various eukaryotic kingdoms (Fig. 5.4, Section 3.5). Yeast orphaned ARPs, ARP7 and ARP9, are found among the 11–15 subunits of the SWI/SNF and RSC ATP-dependent NR complexes (Cairns et al., 1998; Peterson et al., 1998; Szerlong et al., 2003). It is unclear how human or *Arabidopsis* ARP7 and ARP8 sequences relate to these yeast sequences (Kandasamy et al., 2004, 2008). Unlike the complexes described here, neither yeast SWI/SNF nor RSC contain monomeric actin. The SWI/SNF complex was identified independently in genetic screens for genes involved in mating-type switching and sucrose fermentation, and the RSC complex was later isolated based on homology to SWI/SNF complex components. Strains lacking ARP7 or ARP9 show phenotypes typical of *swi/snf⁻* mutants, indicating that these proteins play an essential role in the function of SWI/SNF.

In addition to the *swi/snf⁻* phenotype, mutations in yeast *ARP7* or *ARP9* also lead to other transcriptional defects, indicating that RSC plays a role in general transcriptional regulation (Cairns et al., 1998). Surprisingly, RSC complexes isolated from *arp7Δ/arp9Δ* cells are otherwise fully intact and retain the ability to remodel nucleosomes *in vitro*. However, a screen for suppressors of *arp7* and *arp9* mutations identified the architectural transcription factor Nhp6, which interacts physically with RSC and enhances the activity of the complex *in vitro* (Szerlong et al., 2003). These data suggest that ARP7 and ARP9 serve to connect the RSC complex to interacting proteins or other complexes, allowing functionality *in vivo*. The characterized animal SWI/SNF (NR) complexes contain homologs of yeast ARP4 instead of homologs of the orphaned yeast ARP7 and ARP9 found in the yeast complex. This suggests at least a functional relationship exists between the orphaned ARPs and the reasonably well-conserved ARP4, if not an undetected closer phylogenetic relationship.

Arabidopsis ARP7 is an essential gene. Nearly normal heterozygous plants carrying a null allele produce homozygous *arp7-1/arp7-1* embryos that abort at the torpedo stage, and mutant seeds containing defective embryos arrest their development. It is possible that a small amount of residual ARP7 from the parental egg cell cytoplasm may support early embryonic development. Plants partially silenced for ARP7 expression display a wide variety of dramatic phenotypes (Table 5.2) some of which are discussed in the following sections. Even though the phylogenic origin of plant ARP7 is not clear, this ARP has important role(s) in multicellular development.

5. Isoforms of ARP Complexes

5.1. Defining isoforms of chromatin complexes

A theme emerging in plants and animals is that diverse isoforms of nuclear ARP-containing chromatin complexes exert epigenetic control over multicellular development (Brown et al., 2007; Dirscherl and Krebs, 2004; Meagher et al., 2005; Nie et al., 2000; Olave et al., 2002b). Furthermore, there are increasing combinatorial possibilities in the numbers of isoforms of nuclear ARP complexes, paralleling the macroevolution of organismal complexity from single-celled organisms like yeast and *Tetrahymena* to more complex eukaryotes like humans and *Arabidopsis* (Dirscherl and Krebs, 2004; Iyer et al., 2008). To illustrate what is meant by isoforms of chromatin complexes, consider the ARP-containing SWI/SNF (NR), INO80 (NR), and SWR1 (HVE) complexes. Based on their composition in yeast or mouse, these three complexes contain 12 or more different protein subunits. Small gene families frequently encode these individual

subunits. Thus, isoforms of a complex may be defined as those complexes containing altered isovariant subunit compositions, but composed of the same general subunit makeup. In our usage, protein ''isovariants'' or ''variants'' are closely related polypeptides with altered sequences encoded by different gene family members. Besides being derived from different members of gene families, protein isovariants also can be generated from single genes by alternate RNA splicing and poly(A) site selection, by alternate initiation and termination of translation, and by posttranslational protein modifications such as phosphorylation. In plants and animals, divergent gene families encode multiple isovariants of several subunits in each of these three types of complexes and perhaps even all major classes of complexes. Substituting one single subunit with a second different isovariant would generate a new isoform of a complex. A new isoform has the potential to recognize a new target gene based on local histone modification or nucleosome composition or bound protein factors. Alternatively, a new isoform may carry out a slightly different chromatin modifying reaction such as different phasing of nucleosomes, exchange of a different histone isovariant, or different histone modifications. For example, substituting two different isovariants of the large Swi2-related DNA-dependent ATPase subunit into a SWI/SNF complex will undoubtedly generate two isoforms of a complex with different activities on nucleosomes.

5.2. The numbers of isoforms increase with organismal complexity

Chromatin remodeling proteins in single-celled organisms like yeast ($\sim$ 6000 genes) are encoded by singlet genes and a few small gene families. Most of these genes were expanded into much larger gene families in complex multicellular organisms like humans encoding $\sim$ 37,000 genes and *A. thaliana* encoding $\sim$ 36,000 genes. Again, using the Swi2-related subunit as an example, there are 10 Swi2-related sequences in yeast, but more than 30 in the mouse and human genomes and 44 in *Arabidopsis*. Thus, by increasing the number of Swi2-related isovariants the number of isoforms of remodeling complexes was increased during the evolution of multicellular plants and animals. By extension, holding one of these Snf2-related subunits constant and substituting two isovariants of another subunit generates two other novel isoforms. Supporting the reality of this view are numerous papers on the importance of Swi2-related isovariants. For example, in embryonal cells, Swi2-related β-BRG1, but not α-BRG1, plays an essential role in basal processes involved in cell proliferation (Sumi-Ichinose et al., 1997). Finally, it should be mentioned that the tissue- or organ-specific expression of even one isovariant within a complex has the potential to refine epigenetic control by a complex.

In fact, several human and mouse chromatin remodeling complexes were isolated as mixtures of isoforms. For example, the purified mammalian BAF or SWI/SNF complex was shown to have a basic composition of about 9–12 proteins, but it existed in several isoforms. Isoforms purified from various organs varied in their Baf60 subunit and Swi2-related subunit compositions (Debril et al., 2004; Wang et al., 1996a,b). BAF60a is ubiquitously expressed, whereas the BAF60b and BAF60c isovariants are expressed in a subset of tissues and organs. The Baf60 isovariants appear to contribute to the target gene specificity of the complex. Furthermore, phosphorylation of BAF60 subunits creates additional isovariants that appear to target a subset of BAF complex isoforms to particular myogenic target genes (Simone et al., 2004).

Surprisingly, the nuclear ARP genes themselves are seldom found duplicated into gene families, with a notable exception. Mammalian isovariants of ARP4, Baf53a, and Baf53b, participate in SWI/SNF and TRAAP chromatin remodeling complexes and are differentially expressed. Baf53a expression is restricted primarily to brain and other neuronal tissues, while the Baf53b isovariant, which is the product of a separate gene, is more broadly expressed (Kuroda et al., 2002; Lessard et al., 2007; Olave et al., 2002a; Wu et al., 2007). Baf53a interacts specifically with a transcriptional corepressor CtPB, but Baf53b does not. The activity of SWI/SNF complex and its target genes are repressed in the presence of Baf53a, but not Baf53b (Oma et al., 2003). Baf53a isovariant cannot be replaced by Baf53b, because particular sequences in subdomain 2 of Baf53a add necessary and specific protein–protein interactions to chromatin remodeling in the nervous system. Baf53b is assembled into multiple PBAF complexes in postmitotic neurons (Choi et al., 2001; Lee et al., 2003; Ohfuchi et al., 2002; Olave et al., 2002a). In summary, remodeling complexes with the Baf53a isovariant are functionally distinct from those containing the Baf53b isovariant.

Analyses of mutants in the four *Arabidopsis* Swi3 isovariants suggest different developmental roles for four likely SWI/SNF complex isoforms, each with a different Swi3 isovariant (Sarnowski et al., 2005; Zhou et al., 2003). Each mutant with defects in *swi3a*, *swi3b*, *swi3c*, or *swi3d* displays a distinct set of phenotypes, including embryo lethality and vegetative and reproductive defects. The sum of the phenotypes described for these four mutants include most of the phenotypes we described for plants deficient in ARP7, which is likely to be a member of this SWI/SNF complex (Kandasamy et al., 2005b). For example, the *swi3a* and *swi3b* mutants display an embryo lethal phenotype similar to the homozygous null *arp7-1 Arabidopsis* mutant. In addition, the *swi3d* mutations cause severe dwarfism and complete male and female infertility like strong *ARP7* knockdown epialleles. Plants carrying *swi3c* mutations share retarded root and plant growth, curly leaf, and reduced fertility phenotypes with the moderate ARP7 epialleles.

We have shown previously that homologs of most subunit proteins within the yeast SWI/SNF, SWR1 and INO80 complexes are encoded by gene families in *Arabidopsis* (Meagher et al., 2005). There are 12 likely subunit isovariants in five gene families that may produce 64 SWI/SNF isoforms. There are 19 subunit isovariants in six gene families with the potential to produce 600 SWR1 isoforms. There are 13 isovariants in four gene families with the potential to produce 56 INO80 isoforms. These estimates exclude variations in the possible actin and Swi2-related subunit isovariant composition, each variation having the potential to add significantly to the complexity of isoforms. Each individual ARP complex isoform with a different isovariant composition may only control a small subset of all epigenetically controlled target genes with a specific impact on development. Using the same yeast query sequences (Meagher et al., 2005) to explore the mouse and human genomes reveals that a similar high level of combinatorial diversity exists among the subunits of these remodeling complexes in mammals (not shown). Hence, it is reasonable to propose that in plants and animals there are hundreds of functional isoforms of each type of basic remodeling or modifying complex and that each isoform of a complex may differ in some way in its activity.

5.3. Contingency, macroevolution, and the origin of new isoforms

One evolutionary view connecting ARP complexes to the macroevolution of multicellular development is that as plants and animals diversified from single-celled protist ancestors, there was a combinatorial expansion in the number of nuclear ARP complex isoforms following an expansion and diversification of the gene families encoding their various subunit isovariants. Besides normal gene endoduplication, a number of ancient genome wide duplications are identified in the ancient ancestry of higher plants and animals. Thus, gene duplication is not likely to have limited increases in the numbers of protein isovariants (Meagher et al., 1999b). An increase in chromatin complex isoforms allowed the natural selection of more specialized control over chromatin dynamics and target-gene transcription, which generated more specialized epigenetic control over multicellular development. Greater target gene specificity and more finely tuned epigenetic control should be a selective advantage to multicellular organisms. Contingency theory can be used to explain the seemingly improbable pathways of gene duplication, gene divergence, neutral drift, natural selection, and stepwise increases in the complexity of chromatin complex isoforms that lead to increasing complexity of tissue and organ development in animals and plants (Bak and Paczuski, 1995). Previous discussion linking the long pathways of genetic events to the evolution of protein–protein interactions and macroevolution of developmental pathways rely heavily

upon arguments of historical contingency (Meagher, 1995; Meagher et al., 1999a, 2008; Muller and Newman, 2005).

6. Role of Nuclear ARPs in the Epigenetic Control of Morphological Development

6.1. ARP complexes control development

The following section summarizes several functional studies demonstrating an essential role for nuclear ARPs in different pathways of yeast, animal, and plant development. In plants, for example, chromatin remodeling and epigenetic control are directly linked to numerous pathways of multicellular development (Bezhani et al., 2007; Chen, 2007; Cuzin et al., 2008; Henderson and Jacobsen, 2007; Kwon and Wagner, 2007; Saze et al., 2008). Analysis of mutants in Swi2-related family members likely to interact directly with ARPs via their HSA domains (Fig. 5.7) led the way in these studies, including defects in *SYD* (Wagner and Meyerowitz, 2002), *PIE1* (Swr1 homolog) (Noh and Amasino, 2003), *DDM1* (Bartee and Bender, 2001; Brzeski and Jerzmanowski, 2003; Jeddeloh et al., 1999; Johnson et al., 2002; Mittelsten Scheid and Paszkowski, 2000; Miura et al., 2001), *CR12* (Iswi) (Huanca-Mamani et al., 2005), *DRD1* (Kanno et al., 2004), Ino80 (Fritsch et al., 2004), and *Rad54* (Shaked et al., 2006). Considering that *Arabidopsis* has 44 predicted Swi2-like genes, but only six nuclear ARPs, it was not surprising to find that knocking down or knocking out individual *Arabidopsis* nuclear ARPs in whole plants resulted in even more severe and pleiotropic defects in more pathways of development than Swi2-related gene mutations (Choi et al., 2005; Deal et al., 2005, 2007; Kandasamy et al., 2005a,b; March–Diaz et al., 2007; Martin–Trillo et al., 2006; Meagher et al., 2005, 2007). A sampling of the cell proliferation and developmental abnormalities associated with *Arabidopsis* ARP4, ARP5, ARP6, and ARP7 deficiencies is summarized in Table 5.2. In animals, the majority of studies on nuclear ARPs are focused on conditional and knockdown mutants in cultured cells, where organismal viability is not compromised. It is possible that the plasticity of *Arabidopsis* development may allow individuals partially compromised for nuclear ARP-dependent epigenetic control to survive. New conditional knockdown technologies in the mouse should allow organismal- or organ-level gene silencing of nuclear ARPs to proceed.

A theme presented at the beginning of this chapter states that in addition to their role in controlling the compaction of DNA and associated gene silencing, *isoforms of nuclear ARP-containing chromatin complexes have evolved to exert dynamic epigenetic control over gene expression and different phases of multicellular development.* A general model for the position of the nuclear ARPs in

Table 5.2 Defects in *Arabidopsis* actin-related protein expression lead to numerous alterations in multicellular development

	Nuclear ARP defect			
Phenotype	ARP4	ARP5	ARP6	ARP7
Small leaves	Yes	Yes	Yes	Yes
Small leaf cells	Yes	Yes	No	Yes
Upward curled leaves	No	Yes	No	Yes
Excess stomata relative to other epidermal cells	No	Yes	No	No
Delayed stomatal development	No	Yes	No	No
Flower early with long days	Yes	No	Yes	No
Flower early with short days	No	No	Yes	No
Small flowers and floral organs	Yes	Yes	Yes	Yes
Delayed floral senescence	Yes	No	No	Yes
Excessive root hairs	ND	Yes	Yes	No
Shortened root apical zone	ND	No	Yes	Yes
HU hypersensitivity	Yes	Yes	ND	ND
MMS hypersensitivity	Yes	Yes	ND	ND
Bleomycin hypersensitivity	Yes	Yes	ND	ND

ND, no data.

various pathways of developmental control is outlined in Fig. 5.8E. Chromatin remodeling factors like the ARPs affect epigenetic controls over the regulation of transcriptional repressors and activators leading to the display of various morphological phenotypes. However, the epigenetic controls themselves appear to be influenced by environmental factors such as age and diet in animals and age, nutrients, temperature, and light in plants.

6.2. Developmental transitions

Epigenetic controls are essential to most major developmental phase transitions in animals and plants including the transitions from undifferentiated stem cells and primordia to organ development, from embryonic to vegetative growth, and from vegetative to reproductive development (Bezhani et al., 2007; Ooi and Henikoff, 2007; Vignon et al., 2002). Homeotic genes that act early to determine organ identity appear to be under particularly strong epigenetic control (O'Dor et al., 2006; Papoulas et al., 1998; Pien et al., 2008; Vasanthi and Mishra, 2008). While ARP-containing complexes are clearly required for these processes, the role of nuclear ARPs themselves has been demonstrated in only a limited number of cases.
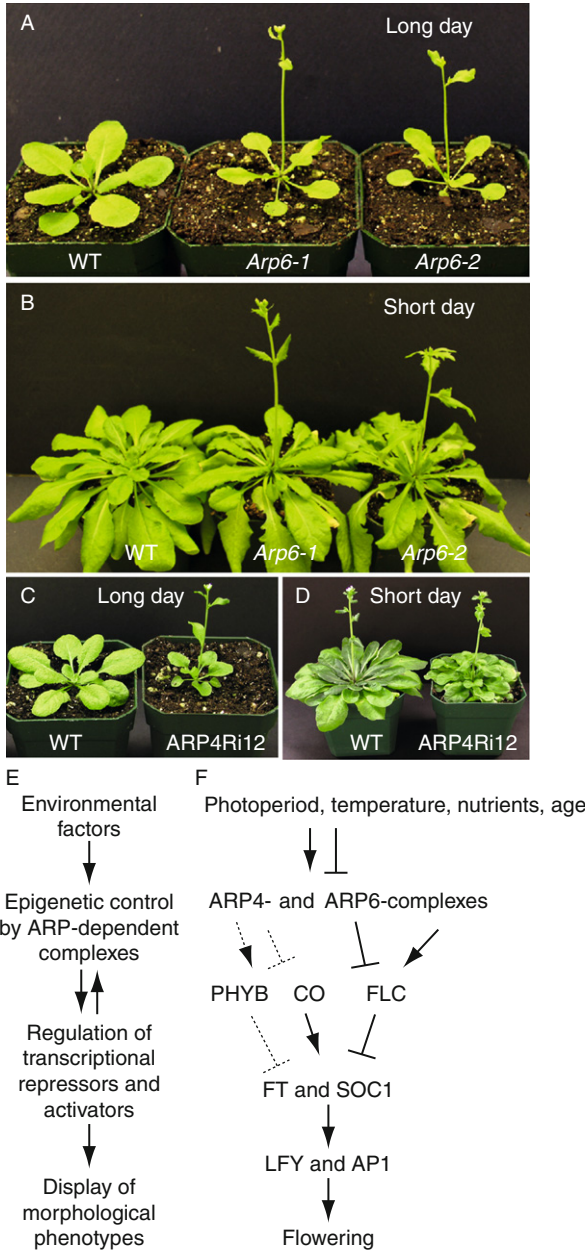
Figure 5.8 *ARP6–* and *ARP4–*defective *Arabidopsis* plants misregulate the phase tran-sition from vegetative to reproductive growth. *ARP6*-defective plants flower early when grown under long- or short-day growth conditions, while *ARP4*-defective plants flower early only when grown under long-day conditions. (A) Twenty-day-old WT and *arp6-1* (null) and *arp6-2* (strong knockdown allele) plants grown under long-day

The transition from vegetative growth to flowering is one of the most important and most highly regulated developmental phase change in the life of a plant and appears exquisitely sensitive to changes in chromatin remodeling and modification. The decision to make this transition is regulated by a variety of environmental and endogenous plant cues including day length (photoperiod), temperature, nutrient status, the age of the plant and for many plants even the number of hours of exposure to cold weather (Fig. 5.8F). Each of these stimuli is sensed by separate genetic pathways, which feed into a central regulatory module that controls the switch from vegetative growth to flowering. This central module consists of the flowering repressor gene *FLOWERING LOCUS C* (*FLC*), which acts to repress the floral promoting genes *FLOWERING LOCUS T* (*FT*) and *SUPRESSOR OF OVEREXPRESSION OF CONSTANS 1* (*SOC1*). When *FLC* levels are high, the *FT* and *SOC1* genes are repressed, and vegetative growth continues. However, when *FLC* is epigenetically silenced, the *FT* and *SOC1* genes are expressed and act to promote the expression of the floral meristem identity genes, resulting in flowering. Thus, these sensory pathways can promote flowering by repressing the expression of *FLC* or activating the expression of *FT* and *SOC1*, or they can repress flowering by activating *FLC* expression (Putterill et al., 2004; Simpson and Dean, 2002). In a parallel pathway, day length is perceived by the photoperiod pathway, and when the light period reaches a critical length in the spring, the transcription factor CONSTANS (CO) is produced, and serves to activate *FT* and *SOC1*, leading to the induction of flowering (Putterill et al., 1995; Samach et al., 2000). Another important sensory pathway, known as the autonomous pathway, is comprised of a collection of factors that repress *FLC* expression in response to diverse day length–independent stimuli, resulting in flowering (Simpson, 2004).

Interestingly, ARP4 and ARP6 have important, but separate roles in repressing the transition to flowering in *Arabidopsis*. Plants in which *ARP4* expression has been silenced by RNAi, show early flowering in long days, but not in short days, indicating that the photoperiod–dependent pathway is

conditions. (B) Fifty-day-old WT and *arp6-1* and *arp6-2* plants grown under short-day conditions. (C) Twenty-day-old WT and an ARP4 RNA interference silenced line (ARP4-Ri) grown under long-day conditions. (D) Sixty-eight-day-old WT and *ARP4-Ri* plant grown under short-day conditions. Long day = 16 h light/24 h. Short day = 9 h light/24 h. (E) A general outline depicting the flow of information for developmental pathways under ARP-dependent epigenetic control. (F) Specific model for the ARP4- and ARP6-dependent control of flowering time. ARP6-containing SWR1 complexes potentiate the expression of the central repressor of flowering FLC. In ARP6 mutants when FLC levels are down, the levels of the transcriptional activators of flowering FT, SOC1, LFY, and AP1 are up and the plants flower early. ARP4-mediated epigenetic control of other high-level regulators of flowering including PhyB and CO is proposed in this model.

aberrantly activated to promote flowering (Fig. 5.8C and D) (Kandasamy et al., 2005a). While the molecular basis of this phenotype is currently unknown, it is likely that ARP4-containing chromatin remodeling complexes may act to promote the expression of genes that repress *CO*, *CO-like genes*, or other regulatory genes, such as *PHYTOCHROME B* (Putterill et al., 1995). Alternatively, ARP4 may normally act to repress *CO-related* gene expression directly. In either case, *CO* could be activated inappropriately in ARP4-defective lines, leading to early flowering only under long-day conditions.

In contrast to the photoperiod–dependent *ARP4* phenotype, a null mutant (*arp6-1*) and a severe knockdown mutant (*arp6-2*) defective in *ARP6* expression result in early flowering under both long- and short-day photoperiods (Fig. 5.8A and B) (Choi et al., 2005; Deal et al., 2005; Martin-Trillo et al., 2006). This photoperiod–independent early flowering phenotype of *arp6* plants was shown to result from a drastic 5- to 10-fold reduction in the expression of *FLC*, indicating that ARP6 is normally required to promote the expression of *FLC*. As mentioned previously, yeast and mammalian ARP6 proteins function with the SWR1 and SRCAP complexes, respectively, which act to deposit the histone variant H2AZ into chromatin. In support for the activity of *Arabidopsis* ARP6 in a homologous complex, mutations in the *Arabidopsis* homologs of two other components of this complex, *PHOTOPERIOD-INDEPENDENT EARLY FLOWERING 1* (*PIE1*) and *SERRATED LEAVES AND EARLY FLOWERING* (*SEF*), also cause photoperiod–independent early flowering due to reduced *FLC* expression (March–Diaz et al., 2007; Noh and Amasino, 2003). Furthermore, we and others have recently shown that ARP6 and SEF interact with each other and with PIE1 (March–Diaz et al., 2007), and that ARP6 and PIE1 are required for deposition of H2AZ at the *FLC* locus (Deal et al., 2007). In addition, the loss of H2AZ from *FLC* chromatin in the *arp6* and *pie1* plants correlates with reduced *FLC* expression, indicating that plant H2AZ deposition in nucleosomes can potentiate transcriptional activation, similar to its role in yeast (Deal et al., 2007). These observations suggest that a SWR1–related complex is conserved in plants, and support a model in which dynamic ARP6/PIE1-mediated deposition of H2AZ is required for repression of flowering and maintenance of the vegetative growth phase.

A few subunits of ARP-containing chromatin remodeling complexes have roles in the phase transitions leading to animal organ and tissue development such as the development of bone, heart, striated muscle, T cells, and brain (Barak et al., 2004; Brown et al., 2007; Chi et al., 2002; Gebuhr et al., 2003; Lickert et al., 2004; Tromans, 2004; Yeh et al., 2002; Young et al., 2005). Solid evidence for the developmental roles for nuclear ARPs, however, is limited. Olave et al. (2002a) show that Arp4 isovariant Baf53b is first expressed in postmitotic neurons, and as part of a BAF

(SWI/SNF) complex Baf53b interacts with the transcriptional corepressor CtBP to repress glucocorticoid receptor expression and alter development.

As in plants, the phase transition in yeast from vegetative to reproductive development and in particular the yeast mating type switch are under strong and complex epigenetic control (Klar, 2007). The mating type switch requires both DNA rearrangement and transcription of the *MAT* locus, with both INO80 and SWR1 complexes being recruited to the region of DNA with DSBs. ARP8 mutants are defective in the end processing of DNA strands during DSB repair at *MAT* (van Attikum et al., 2007). In summary, nuclear ARPs play essential roles in developmental phase transitions, however, the severity of some ARP-defective phenotypes may hinder a more complete understanding of their importance in these subtle processes.

6.3. Senescence and PCD

In plants and animals, chromatin remodeling and histone modification are known to be key to the epigenetic control of senescence and PCD (Adams, 2007a; Burzynski, 2005; Lewis et al., 2006; Sarnowski et al., 2005; Wu et al., 2008). As illustrated in Fig. 5.9E, floral senescence is controlled by a complex pathway that is influenced by age, nutrient status, temperature, and dozens of transcription factors. Clear floral senescence phenotypes are demonstrated for two classes of ARP-defective plants. In most flowering plants, the shedding of sepals and petals generally follows fertilization of the flower and development of fruit and seeds. As a consequence, when wild-type *Arabidopsis* are grown under long-day conditions the inflorescence displays only four to five opened flowers that retain intact sepals and petals (Fig. 5.9A). This small number of flowers with sepals and petals remains essentially constant from the time the first fruits develop until as many as several dozen fruits develop on an older inflorescence. Knocking down ARP4 or ARP7 expression with RNA interference (Ri) results in plants with defects in this senescence phase of flower development and often produces inflorescences that are fully covered with flowers bearing sepals and petals (Fig. 5.9B) (Kandasamy et al., 2005a,b). These *ARP4-Ri* and *ARP7-Ri* plant lines maintain fully turgid sepals and petals on 12–20 or more flowers during long-day growth and even fully mature fruit may retain sepals and petals (Fig. 5.9B–D). During short-day growth, six to eight wild-type flowers retain these organs at any one time, whereas, in the ARP4-Ri and ARP7-Ri lines 20 or more flowers retain sepals and petals.

These senescence phenotypes are the result of a failure of the cluster of cells at the base of sepals and petals, known as the abscission zone, to die and produce the required organ release, but not from a failure to develop the abscission zone of tissue itself (Kandasamy et al., 2005b). PCD at the abscission zones of petals and sepals is thought to proceed by autophagous
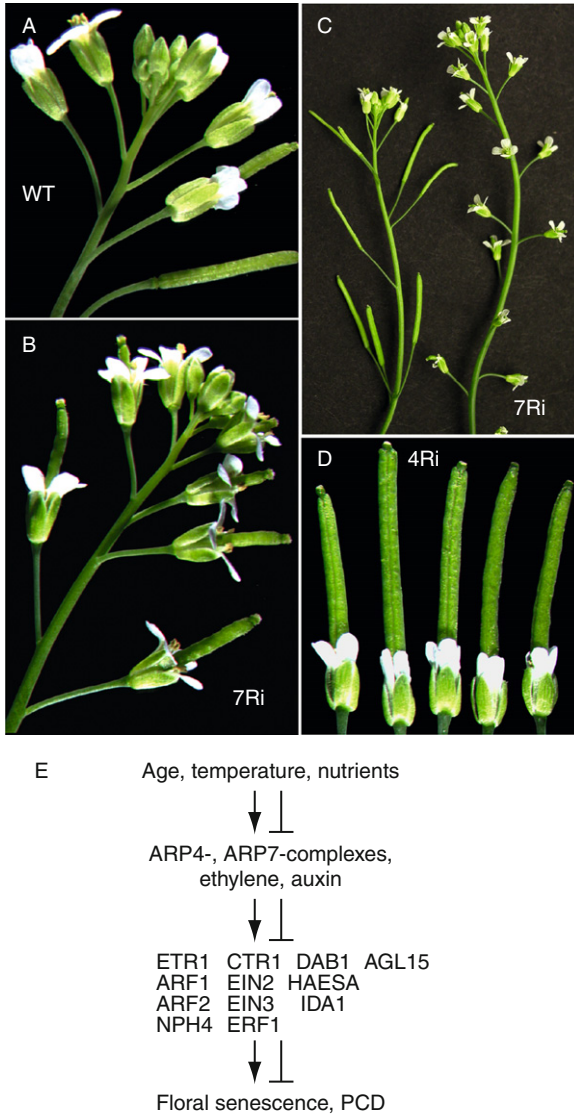
Figure 5.9 ARP4- and ARP7-defficient *Arabidopsis* plants display delayed floral organ senescence and abscission. (A) WT retains sepals and petals on only four to five flowers when grown under long-day conditions. (B) A moderate *ARP*7 RNA interference knockdown line (7Ri) retains petals and sepals after fertilization and even after the fruits are fully developed. (C) A strong *ARP*7 RNAi line (right) is relatively sterile and retains floral organs on all flowers as compared to wild type (left). (D) Close-up examination of developing fruits in a moderate ARP4 RNA interference line (4Ri) reveals retention of sepals and petals for a longer period than wild type (WT, A). (E) A general pathway proposed for the ARP4- and ARP7-dependent epigenetic control of floral organ senescence. A large number of transcription factors are known to control floral

mechanisms in which proteases are released from endoplasmic reticulum-derived vesicles to kill cells (Rogers, 2006). ARP4 and ARP7 may act within one or more chromatin modifying complexes to regulate the pathways of PCD leading to floral organ abscission. The hormone ethylene is known to play a central role in the regulation of flower senescence and abscission of floral organs in many plants (Bleecker and Patterson, 1997; Chang et al., 1993; Klee, 2002; Roberts, 2000). However, exogenous application of ethylene does not suppress the delayed floral organ abscission in ARP7-deficient lines (Kandasamy et al., 2005b) suggesting that ARP7 participates in controlling floral organ abscission in an ethylene–independent pathway. Epigenetic models for the normal action of ARP7-containing chromatin remodeling complexes may include the maintenance of *ETHYLENE RECEPTOR 1* (ETR1) in an activated state poised to respond to ethylene or regulation of any number of transcription factors activating or repressing floral senescence (Fig. 5.9E). We feel it is most likely that many of the other transcription factors known to control floral senescence will also fall under nuclear ARP control (Meagher et al., 2007).

Deficiencies, overexpression, and misexpression of various subunits and activators of mammalian ARP-containing chromatin remodeling and modifying complexes induce or suppress apoptosis and various pathways of senescence (Samuelson et al., 2005). Ectopic expression of a histone acetyltransferase–defective Tip60 complex in HeLa cells causes a defect in DNA DSB repair, leading to an inability to carry out apoptosis (Ikura et al., 2000; Jehn and Osborne, 1997). The human snf5-homolog Ini1 is a subunit of the SWI/SNF NR complex. Overexpression of Ini1 in human *ini1*-deficeint cell lines increased the rates of apoptosis and arrested many cells in G1 (Ae et al., 2002; Klochendler-Yeivin et al., 2006). In heterozygous *Ini1/ini1-null* mice, p53 overexpression causes increased rates of tumor formation over the rates of tumor formation in wild type. These results lead the authors to suggest that *Ini1* normally acts as a tumor suppressor. Similarly, overexpression of the Swi2 homolog Brg1 (Smarca4) increased p53 and retinoblastoma (Rb) expression and induced cell cycle arrest and apoptosis (Okazaki et al., 2008). Conversely, disruption of the Swi2-subunit homolog ATRX causes p53-mediated apoptosis (Seah et al., 2008). Normal SWI/SNF chromatin remodeling activity is essential to prevent apoptosis of cells undergoing DNA damage repair (Gong et al., 2008; Park et al., 2009).

In yeast cells, DSB repair is defective in ARP5- or ARP8-deficient cells or cells deficient in other subunits of the INO80 complex (van Attikum

---

senescence and it is likely that the influence of age, nutrients, and temperature are processed through ARP-dependent epigenetic mechanisms. ARP7-dependent chromatin remodeling activities function downstream of ethylene perception, whereas the sites of ARP4s activities are unclear (Meagher et al., 2007).

et al., 2004). RNAi silencing of the Swi2–related p400 in untransformed human fibroblasts causes G1 arrest, induction of p21, and increased levels of senescence–associated heterochromatic foci (Chan et al., 2005). Overexpression of Swi2–related Brg1 expression in mesenchymal stem cells induced a significant cell cycle arrest of MSCs in culture (Napolitano et al., 2007). The activities of both Rb and p53, commonly associated with senescence, are essential to this Brg1–mediated increase in stem cell senescence. Thus, there is strong direct and indirect evidence to suggest that mammalian nuclear ARP-containing chromatin remodeling complexes play roles in the control of apoptosis and senescence (Burzynski, 2005; Lin et al., 2006).

6.4. Cell proliferation and the cell cycle

Epigenetic controls over cell proliferation and the cell cycle are well established in animals, plants, and fungi (Chen et al., 2008; Francis, 2007). Roles for nuclear ARPs in cell cycle control are recently emerging as illustrated by a few studies in *Arabidopsis* and yeast, and for animal cells in culture. When grown under long-day conditions *A. thaliana (Columbia)* normally develops a rosette of about 12 leaves just prior to the initiation of flowering. The largest wild–type leaves average 4–5 cm in length at this developmental transition. *Arabidopsis* plants defective in ARP4, ARP5, ARP6, or ARP7 expression produce rosettes with leaves that are approximately half the size of wild type (Table 5.2, Fig. 5.10). Microscopic observations reveal that smaller leaves result from various abnormalities in leaf cell proliferation and/or expansion. Ri was used to generate stable epiallelic lines (*ARP4-Ri*), where ARP4 transcript levels are reduced to less than 20% of wild-type levels (Kandasamy et al., 2005a). The leaf epidermis of these strongly silenced epiallelic lines are composed of small cells that are less than half the size of wild type yet fairly normal in shape (Fig. 5.10A, D, and E). A null mutant lacking *ARP5* (*arp5-1*) produces stochastic patches of very small epidermal cells interspersed among moderately sized cells to produce small leaves (Fig. 5.10B and F) (Kandasamy et al., 2009). Strongly silenced *ARP7* RNAi lines (*ARP7-Ri*) also produce epidermal leaf cells that are essentially normally shaped, but average half the size of wild-type cells, with some clusters of very small cells (Fig. 5.10C and G) (Kandasamy et al., 2005b). Because of nonuniform epidermal cell expansion and clustering of extremely small and moderately sized cells and cell size differences on the abaxial and adaxial surfaces, *ARP5*– and *ARP7*–deficient leaves are often curled.

Stable knockout (*arp6-1*) and severe knockdown (*arp6-2*) lines of *Arabidopsis* were isolated that were defective in ARP6 expression (Deal et al., 2005). The ARP6-defective leaves were less than half the size of wild type (Fig. 5.10H). However, in contrast to defects in ARP4, ARP5,
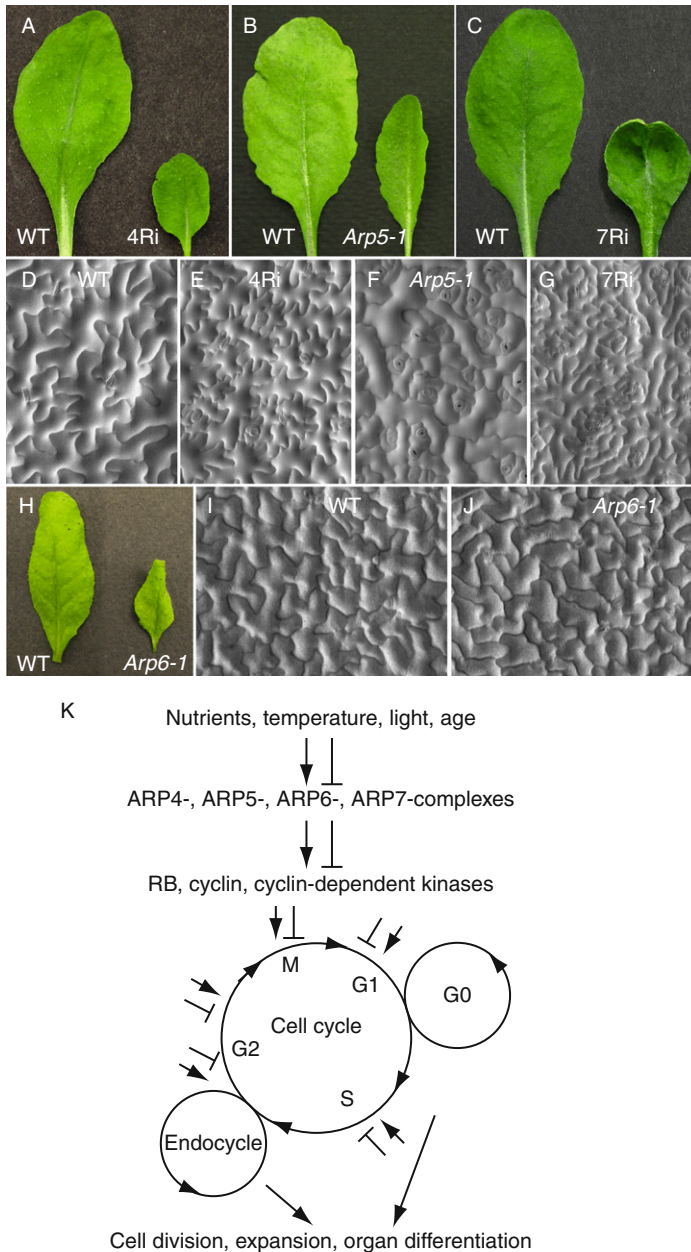
Figure 5.10 Nuclear ARP–defects alter the cell cycle and/or cell proliferation with effects on leaf morphology. ARP4–, ARP5–, ARP6–, and ARP7–deficient *Arabidopsis* plants all produce dwarf leaves, but the small organs result from different epidermal leaf cell morphologies. (A, D, E) ARP4–defective RNAi lines (4Ri) produce very small leaves composed of mixtures of small and tiny cells (E) compared to wild type (WT, D).

and ARP7, scanning electron microscopic examination of ARP6 mutant leaves reveals epidermal cell sizes and shapes that are indistinguishable from wild type (Fig. 5.10I and J). Thus, rather than producing smaller cells, ARP6-defective plants produce leaves composed of fewer total cells. These data suggest that during wild-type rosette leaf development, ARP6 promotes or extends the duration of cell proliferation to produce full-sized leaves. ARP4, ARP5, and ARP7 govern and balance rates of cell expansion, cell division, and the endocycle as suggested in the model pathway shown in Fig. 5.10K. We speculate that ARP deficiencies may produce these plant phenotypes, because of defects in epigenetic control including loss of normal chromatin remodeling essential for chromosomal segregation and changes in chromatin structure causing inappropriate expression of specific regulators of the cell cycle or endocycle including RBs, cyclins, and cyclin-dependent kinases (Francis, 2007; Meagher et al., 2007). Other than leaves, plant organs such as roots, stems, sepals, petals, stamens, and carpels are also smaller in these plants, but their cellular phenotypes have not yet been studied in detail.

Evidence from budding and fission yeast suggests that there is an essential role for nuclear ARPs in mitotic segregation, a process that impacts cell size and proliferation, which in multicellular organisms, helps determine organ size. In fission yeast, ARP4 and the DNA-dependent ATPase subunits of INO80 and SWI/SNF and SWR1 are all associated with centromeric heterochromatin. ARP4-defective cells are more sensitive to drugs known to inhibit progression through the cell cycle and arrest at the G2/M transition. The abnormally large budded ARP4-defective yeast cells display other mitotic phenotypes such as 2N DNA content and numerous broken spindles (Ogiwara et al., 2007b; Steinboeck et al., 2006). In addition, ARP4 associates with other known proteins in the kinetochore and is essential for its assembly. Fission yeast cells with defects in ARP4 expression also display

---

(B, F) The ARP5-defective null mutant *arp5-1* displays small, elongated leaves with mixtures of large and small poorly lobed cells and a significant excess of underdeveloped stomatal complexes relative to WT. (C, G) ARP7-defective RNAi lines (7Ri) develop small curled leaves composed of a few normal sized cells interspersed with large numbers of very small cells, as compared with the WT. (H–J) The ARP6 null mutant (*arp6–1*) produces small curled leaves composed of fewer cells, but of relatively normal cell sizes and with only slightly reduced number of lobes relative to wild type. (D–G, I, J) Scanning electron micrographs compare the epidermis of WT to ARP-deficient lines. All light and scanning microscope images were prepared using the largest rosette leaves from 3-week-old plants. (K) Possible pathways for epigenetic control of the cell cycle and endocycle are outlined. The phenotypes of ARP4-, ARP5-, ARP6-, and ARP7-defective plants suggest that cell division, cell expansion, and cell differentiation are under the influence of complex epigenetic control. By this model, ARP-containing chromatin remodeling machines respond to environmental influences and regulate the expression of transcription factors and signaling proteins controlling the cell cycle, cell proliferation, and cell and organ development.

mitotic phenotypes, including altered chromosome condensation and segregation and desilencing of centromeric transcription (Minoda et al., 2005). While a defect in ARP8 impairs the remodeling activity of INO80 and alters sister chromatid cohesion, it does not affect kinetochore assembly (Ogiwara et al., 2007a). Finally, ARP4-defective cells misregulated a number of genes in the TOR and NCR pathways that regulate cell growth (Steinboeck et al., 2006). Thus, it appears that ARP-containing complexes may be involved in the epigenetic control of chromatin remodeling and associated gene expression necessary for kinetochore assembly, chromosomal segregation, and progression through the cell cycle.

Strong indirect support also exists for the animal nuclear ARPs participating in the cell cycle and in cell proliferation. The ARP4 (BAF53)-containing mammalian BAF complexes were often classified as tumor suppressors (Sansam and Roberts, 2006) and by one view they may control the cell cycle by alternatively activating and repressing epigenetic states of the cell (Metivier et al., 2003). In flies and mammals, subunits of related SWI/SNF complexes act in the same pathway as E2F, a major regulator of cell cycle genes like the cyclins that impact, among other things, the G2/M transition (Staehling-Hampton et al., 1999). In human cell lines, subunits of the SWI/SNF complex interact with cyclin complexes and the tumor suppressor p53 to control cell cycle progression (Shanahan et al., 1999; Zhang et al., 2000). Human cultured cells expressing mutant forms of ARP4 show significant loss of viability and altered control of p53 (Lee et al., 2005). In addition, human ARP4 acts to repress p53-dependent p21-gene transcription by interacting directly with p53 (Wang et al., 2007) suggesting a specific role for this human ARP in the epigenetic control of the cell cycle and cell proliferation.

Using a combination of conditional mutations and drug inhibition of microtubule assembly, yeast ARP4 has now been shown to be associated with centromeric heterochromatin during the entire cell cycle and to be essential to cell division (Ogiwara et al., 2007b; Steinboeck et al., 2006). Moreover, defects in ARP4 cause arrest in the G2/M boundary of the cell cycle. These data suggest that perhaps the amount of ARP4 associated with the relatively small amount centromeric DNA was missed in previous microscopic localization studies showing that ARP4 was found concentrated in nucleoplasm of interphase cells.

7. NUCLEAR ARPs AND EPIGENETICS IN HUMAN DISEASE

Altered chromatin structure has been allied with human disease for the last 30 years (Crapper et al., 1979; Fujii et al., 1980; Smith et al., 1979; Voitenko, 1980). One may predict with confidence that loss in the

epigenetic control of gene expression for high-level transcription factors and the resulting alteration in tissue and organ development could account for many of the stochastic and complex properties associated with the onset of disease (Bottardi et al., 2003; Grewal and Moazed, 2003; Groudine et al., 1983; Nanney, 1958; Waddington, 1957). By considering epigenetic controls, we are better able to model how genes interact with the environment and how gene expression changes with the age of the individual. Otherwise, the influence of environment and age are difficult to interpret with purely genetic and biochemical models (Bjornsson et al., 2004; Ferluga, 1989; Graff and Mansuy, 2008; Mehler, 2008a; Weinhold, 2006). In the last decade, a strong connection has been made between epigenetic defects and diverse cancers and a variety of other human disorders including diabetes, cognitive dysfunction, autoimmune diseases, and neurobehavioral illnesses, all of which have age-related components associated with their frequency of onset (Adams, 2007b; Fraga et al., 2007; Garcia et al., 2005; Jirtle et al., 2000; Mehler and Purpura, 2008; Minucci and Pelicci, 1999; Remus et al., 2005; Robertson and Wolffe, 2000; Schulz et al., 2006; Shames et al., 2007; Soragni et al., 2008; Wong et al., 2007; Zeisig et al., 2008). ARP-containing chromatin remodeling complexes control directly or indirectly the majority of those changes to chromatin structure known to be associated with these diseases.

In particular, deficiencies in mutant forms of specific subunits of ARP-containing remodeling chromatin complex are linked to neoplastic cell growth and many subunits were initially identified as tumor suppressors (Olave et al., 2002b). DeCristofaro et al. (1999, 2001) and others have shown that a number of human tumors and immortal tumor-derived cells lines are deficient in subunits of the SWI/SNF family of complexes including defects in *snf5*, *baf57*, *brg-1*, and *brm-1*. For example, extracts from human adrenal gland carcinoma cells lack expression of the normally constitutive Swi2-related brg-1 and brm-1 proteins and form incomplete BAF and PBAF subcomplexes lacking ARP4 and actin. Transformation of the *brg-1* gene into these cells disrupts their neoplastic state of growth and these genetically complemented cells begin to differentiate (Liu et al., 2001). Among its numerous activities on target genes, the BAF complex binds to the promoter of *COLONY-STIMULATING FACTOR 1* (*CSF1*) promoter with a resulting alteration in DNA structure that appears essential for normal *CSF1* expression. In another example, Ruvbl1 (RUVB-like 1, TIP49), an ATPase subunit in an ARP4-containing remodeling complex, has been implicated as a cofactor for oncogenic transformation via its binding to β-catenin. β-Catenin mediates the neoplastic growth of cancer cells through its role in Wnt signaling that, among other things, affects T-cell factor (TCF)-mediated transcription. Expression of an ATPase-deficient mutant form of Ruvbl1 (TIP49D302N) substantially inhibited β-catenin cell transformation (Feng et al., 2003). As another example of

tumor suppressor activity, silencing the catalytic core subunits of SWI/SNF greatly reduces the ability of cells to carry out radiation–induced DSB repair and causes reduced survival of cells (Park et al., 2006).

DNA repair is essential to genome integrity and genetic inheritance, and inefficient or inaccurate repair results in mutations that may lead to carcinogenesis or inherited genetic diseases. Depending on the kind and severity of DNA damage, DNA repair proceeds through at least two major pathways: nucleotide excision repair (NER) and DSB repair. Evidence from diverse model systems suggests that reorganization of chromatin structure during NER and DSB repair may require the SWI/SNF, BAF, NEF, SWR1, RSC, INO80, SWR, and TIP60 complexes (Fritsch et al., 2004; Groth et al., 2007; Linger and Tyler, 2007; Morrison and Shen, 2006; Osley et al., 2007), whose compositions taken together include yeast and mammalian ARP4, ARP5, ARP6, ARP8, and yeast ARP7 and ARP9.

ARP4 is a common essential subunit of most of these complexes. The combined processes of chromatin remodeling and DNA damage repair have been modeled as proceeding through three major steps: *access*, *repair*, and *restore* (Smerdon and Lieberman, 1978). *Access* to the damaged site, arresting transcription, and arresting the cell cycle during DSB repair are accomplished by placing epigenetic marks on chromatin surrounding the damaged DNA. These marks include methylation, acetylation, ubiquitination, and phosphorylation of H2, H3, and/or H4 histone isovariants (Dinant et al., 2008). ARP4 is part of the TIP60 and NuA4 histone modifying complexes and is essential to localizing the yeast Nu4A complex to the sites of damaged DNA (Downs et al., 2004; Minoda et al., 2005). The early steps of *access* may also involve exchange of H2A, H2AX, and H2AZ isovariants within nucleosomes.

As mentioned earlier (Section 4.4), ARP4, ARP5, and ARP8 are essential components of the INO80 complex. INO80 is particularly associated with repair and phosphorylation of H2AX, a universal and well–characterized mark identifying DNA surrounding DSBs. Kitayama et al. (2009) have shown recently that human ARP5 partially complements the UV sensitivity of yeast ARP5 deletions. Silencing of human ARP5 in HeLa cells dramatically increases sensitivity to DNA DSBs. Furthermore, ARP5 depletion dramatically reduces phosphorylation of H2AX in these cells and the affinity of the Swi2–related Ino80 subunit of INO80 for DNA (Kitayama et al., 2009).

During the second step, *repair*, ARP8's activity in the INO80 complex is implicated in converting DSBs to ssDNA and to recombination repair (van Attikum et al., 2004). Phosphoryated H2AX is essential to the recruitment of the ARP6-containing SWR1 complex to DSB sites (van Attikum et al., 2007). Studies on the third step, *restore*, in which normal chromatin dynamics and DNA activities are resumed is just beginning. Following the repair process, ARP5- and ARP8-containing INO80 complexes aid in restarting

stalled replication forks (Shimada et al., 2008; Trujillo and Osley, 2008). These various steps of addressing DNA damage, *access*, *repair*, and *restore* require integrated activities of several nuclear ARPs and their chromatin remodeling complexes.

The nuclear ARPs themselves are described as tumor suppressors, because constituent ARP remodeling complexes activate genes with tumor suppressor activity. However, considering the complexity and dynamic nature of epigenetic control systems, it seems just as likely that ARP complexes may silence tumor suppressor genes as silence genes with other beneficial activities. For example, during ARP4 deficiency in budding yeast, a large number of stress response genes are increased or decreased in expression, relative to wild type (Gorzer et al., 2003; Shen et al., 2003a; Steinboeck et al., 2006). Similarly, ARP4–deficient fission yeast cells are defective in diverse histone H4 acetylation activities, resulting in the desilencing of genes linked to the centromere (Minoda et al., 2005).

ARP4 (Baf53) appears to be a necessary cofactor for c–Myc and p53 to participate in both tumor suppression and oncogenic transformation (Lee et al., 2005; Park et al., 2002; Wang et al., 2007). The cellular oncogenic proteins c–Myc and p53 play essential roles in the cell cycle, in DNA repair, and in apoptosis by regulating two relatively distinct and essential sets of genes and gene networks controlling these processes. Gene networks regulated by c–Myc and p53 and the normal expression of these two genes themselves are frequently disrupted in human and other animal cell cancers. ARP4 (Baf53) interacts with an N–terminal subdomain of c–Myc, the Myc–homology domain II (MBII) to form subcomplexes on chromatin and activate gene expression perhaps by recruiting ARP4–containing chromatin remodeling complexes to the promoters of these genes.

Mammalian ARP4 also interacts directly with p53 (Lee et al., 2005; Wang et al., 2007). Expression of a functional ARP4 protein with an intact N-terminal domain is essential for the normal expression of human p53. Alanine substitution at either the conserved Ser2 or Tyr6 residue in N-terminus of ARP4 inhibits human cell growth in culture, measured as reduced colony formation and growth rate (Lee et al., 2005). Expression of the Ser2Ala or Tyr6Ala forms show dramatically reduced transcription of p53. By contrast, the phosphomemetic form with Ser2Asp and Tyr6Glu substitutions complemented loss of ARP4 function restoring both normal cell growth and p53 expression levels to those of the parental cells. These data suggest that a phosphorylated form of ARP4 is essential for the control of the widely important activity of p53. Thus, ARP4 appears to be essential to regulating a secondary modification of p53 protein that affects p53's activity as a transcriptional activator (Wang et al., 2007).

The nuclear ARPs are ubiquitously expressed at low levels and have no known functions that do not require their interaction with other subunits of chromatin remodeling complexes. Hence, the few examples of ARP

expression levels being regulated in diseased cells are intriguing. Aging mice with the lethal yellow (*LY*) mutation in the agouti gene locus (*Ay*) show progressive obesity and reproductive dysfunction, similar to women with polycystic ovary syndrome (POS). When POS women are treated with insulin sensitizing agents like pioglitazone, they often have improved ovulatory function. Transcriptional array data on *AyLY* mice treated with pioglitazone revealed that a number of potentially important regulatory genes were misregulated, including a 50% drop in *ARP6* transcript levels (Brannian et al., 2008). It is unknown if altered ARP6 levels affect insulin responsiveness or ovarian function. However, any reduction in nuclear ARP levels is likely to have a significant effect on the chromatin remodeling in these cells. We found, for example, that the *Arabidopsis arp4-1* knockdown mutation, with only a 40% reduction in ARP4 levels throughout the plant, dramatically altered anther development and caused male sterility (Kandasamy et al., 2005a). Fission yeast expressing a temperature-sensitive *arp4* allele (*alp5-1134*) display serious mitotic phenotypes at the nonpermissive temperature, including missegregation of chromosomes due to altered structures in kinetochores (Minoda et al., 2005). These plant and fungal data suggest that downregulation of ARP4 homologs in mammalian cells could result in cancerous cell growth.

ARP-containing chromatin remodeling and modifying complexes are essential to normal epigenetic control of gene expression, chromosomal segregation, and DNA repair—basal functions necessary to human health. Significant roles for nuclear ARPs and the numerous other subunits of ARP complexes are emerging in cancer and many other human diseases. It is likely that the impact of aging and environment on human disease, in particular, act via nuclear ARP-mediated epigenetic controls.

8. Conclusions

Fungal, plant, animal, and many protist genomes encode several ancient classes of nuclear ARPs that participate in large macromolecular machines directing chromatin dynamics. The nuclear ARPs are variously required for the assembly and the activities of these complexes via their binding to the HSA domains of Swi2- and Vid21-related proteins with helicase and ATPase activities. The nuclear ARPs help these complexes bind to chromatin, and in the cases of ARP4, ARP5, and ARP8, the ARPs appear to bind nucleosomal histones directly. Nuclear ARP complexes carry out NR including nucleosomal phasing and HVE reactions and the chemical modifications of histone termini. These activities exert an epigenetic control over basal levels of transcription affecting cell division and proliferation in all eukaryotes, but in particular, in animals and plants

neoplastic cell growth and multicellular development. Genome integrity is maintained by the activities of nuclear ARP complexes in DNA replication, chromosome segregation, and DNA repair. In *Arabidopsis*, developmental pathways affecting nearly every plant tissue and organ and important organismal phase transitions require normal levels of ARP4, ARP5, ARP6, and/ or ARP7 expression, providing strong evidence for their epigenetic role in multicellular development. In animals, among many roles, specific ARP-containing complexes are essential to heart, T cell, and brain development, but most studies on the nuclear ARPs themselves have been restricted primarily to cultured cells. Diverse isoforms of ARP complexes in animals and plants may provide greater target gene specificity and a wider variety of chromatin modifying activities than found in single-celled organisms like yeast. We propose that the greater epigenetic control provided by increases in novel ARP-containing complex isoforms was a major factor in the macroevolution of new tissues and organs in higher plants and animals.

ACKNOWLEDGMENTS

REFERENCES

Adam, R.D., 2000. The *Giardia lamblia* genome. Int. J. Parasitol. 30, 475–484.

Adam, M., Robert, F., Larochelle, M., Gaudreau, L., 2001. H2A.Z is required for global chromatin integrity and for recruitment of RNA polymerase II under specific conditions. Mol. Cell. Biol. 21, 6270–6279.

Adams, P.D., 2007a. Remodeling chromatin for senescence. Aging Cell 6, 425–427.

Adams, P.D., 2007b. Remodeling of chromatin structure in senescent cells and its potential impact on tumor suppression and aging. Gene 397, 84–93.

Adl, S.M., Leander, B.S., Simpson, A.G., Archibald, J.M., Anderson, O.R., Bass, D., et al., 2007. Diversity, nomenclature, and taxonomy of protists. Syst. Biol. 56, 684–689.

Ae, K., Kobayashi, N., Sakuma, R., Ogata, T., Kuroda, H., Kawaguchi, N., et al., 2002. Chromatin remodeling factor encoded by *ini1* induces G1 arrest and apoptosis in *ini1*-deficient cells. Oncogene 21, 3112–3120.

Aoyama, N., Oka, A., Kitayama, K., Kurumizaka, H., Harata, M., 2008. The actin-related protein hArp8 accumulates on the mitotic chromosomes and functions in chromosome alignment. Exp. Cell Res. 314, 859–868.

Aparicio, S., Chapman, J., Stupka, E., Putnam, N., Chia, J.M., Dehal, P., et al., 2002. Whole-genome shotgun assembly and analysis of the genome of *Fugu rubripes*. Science 297, 1301–1310.

Auger, A., Galarneau, L., Altaf, M., Nourani, A., Doyon, Y., Utley, R.T., et al., 2008. Eaf1 is the platform for NuA4 molecular assembly that evolutionarily links chromatin acetylation to ATP-dependent exchange of histone H2A variants. Mol. Cell. Biol. 28, 2257–2270.

Bak, P., Paczuski, M., 1995. Complexity, contingency, and criticality. Proc. Natl. Acad. Sci. USA 92, 6689–6696.

Barak, O., Lazzaro, M.A., Cooch, N.S., Picketts, D.J., Shiekhattar, R., 2004. A tissue-specific, naturally occurring human SNF2L variant inactivates chromatin remodeling. J. Biol. Chem. 279, 45130–45138.

Bartee, L., Bender, J., 2001. Two *Arabidopsis* methylation-deficiency mutations confer only partial effects on a methylated endogenous gene family. Nucleic Acids Res. 29, 2127–2134.

Bendich, A.J., Drlica, K., 2000. Prokaryotic and eukaryotic chromosomes: what's the difference? Bioessays 22, 481–486.

Bezhani, S., Winter, C., Hershman, S., Wagner, J.D., Kennedy, J.F., Kwon, C.S., et al., 2007. Unique, shared, and redundant roles for the *Arabidopsis* SWI/SNF chromatin remodeling ATPases BRAHMA and SPLAYED. Plant Cell 19, 403–416.

Bird, A.W., Yu, D.Y., Pray-Grant, M.G., Qiu, Q., Harmon, K.E., Megee, P.C., et al., 2002. Acetylation of histone H4 by Esa1 is required for DNA double-strand break repair. Nature 419, 411–415.

Bjornsson, H.T., Fallin, M.D., Feinberg, A.P., 2004. An integrated epigenetic and genetic approach to common human disease. Trends Genet. 20, 350–358.

Bleecker, A.B., Patterson, S.E., 1997. Last exit: senescence, abscission, and meristem arrest in *Arabidopsis*. Plant Cell 9, 1169–1179.

Blessing, C.A., Ugrinova, G.T., Goodson, H.V., 2004. Actin and ARPs: action in the nucleus. Trends Cell Biol. 14, 435–442.

Bottardi, S., Aumont, A., Grosveld, F., Milot, E., 2003. Developmental stage-specific epigenetic control of human beta-globin gene expression is potentiated in hematopoietic progenitor cells prior to their transcriptional activation. Blood 102, 3989–3997.

Boyer, L.A., Peterson, C.L., 2000. Actin-related proteins (Arps): conformational switches for chromatin-remodeling machines? Bioessays 22, 666–672.

Brannian, J.D., Eyster, K.M., Weber, M., Diggins, M., 2008. Pioglitazone administration alters ovarian gene expression in aging obese lethal yellow mice. Reprod. Biol. Endocrinol. 6, 10.

Brown, E., Malakar, S., Krebs, J.E., 2007. How many remodelers does it take to make a brain? Diverse and cooperative roles of ATP-dependent chromatin-remodeling complexes in development. Biochem. Cell Biol. 85, 444–462.

Brzeski, J., Jerzmanowski, A., 2003. Deficient in DNA methylation 1 (DDM1) defines a novel family of chromatin-remodeling factors. J. Biol. Chem. 278, 823–828.

Burzynski, S.R., 2005. Aging: gene silencing or gene activation? Med. Hypotheses 64, 201–208.

Cai, Y., Jin, J., Florens, L., Swanson, S.K., Kusch, T., Li, B., et al., 2005. The mammalian YL1 protein is a shared subunit of the TRRAP/TIP60 histone acetyltransferase and SRCAP complexes. J. Biol. Chem. 280, 13665–13670.

Cai, Y., Jin, J., Gottschalk, A.J., Yao, T., Conaway, J.W., Conaway, R.C., 2006. Purification and assay of the human INO80 and SRCAP chromatin remodeling complexes. Methods 40, 312–317.

Cairns, B.R., 2004. Around the world of DNA damage INO80 days. Cell 119, 733–735.

Cairns, B.R., Erdjument-Bromage, H., Tempst, P., Winston, F., Kornberg, R.D., 1998. Two actin-related proteins are shared functional components of the chromatin-remodeling complexes RSC and SWI/SNF. Mol. Cell 2, 639–651.

Champion, K., Higgins, N.P., 2007. Growth rate toxicity phenotypes and homeostatic supercoil control differentiate *Escherichia coli* from *Salmonella enterica* serovar *Typhimurium*. J. Bacteriol. 189, 5839–5849.

Chan, H.M., Narita, M., Lowe, S.W., Livingston, D.M., 2005. The p400 E1A-associated protein is a novel component of the p53–> p21 senescence pathway. Genes Dev. 19, 196–201.

Chang, C., Kwok, S.F., Bleecker, A.B., Meyerowitz, E.M., 1993. *Arabidopsis* ethylene-response gene *ETR1*: similarity of product to two-component regulators. Science 262, 539–544.

Chen, Z.J., 2007. Genetic and epigenetic mechanisms for gene expression and phenotypic variation in plant polyploids. Annu. Rev. Plant Biol. 58, 377–406.

Chen, M., Shen, X., 2007. Nuclear actin and actin-related proteins in chromatin dynamics. Curr. Opin. Cell Biol. 19, 326–330.

Chen, Z., Tan, J.L., Ingouff, M., Sundaresan, V., Berger, F., 2008. Chromatin assembly factor 1 regulates the cell cycle but not cell fate during male gametogenesis in *Arabidopsis thaliana*. Development 135, 65–73.

Chi, T.H., Wan, M., Zhao, K., Taniuchi, I., Chen, L., Littman, D.R., et al., 2002. Reciprocal regulation of CD4/CD8 expression by SWI/SNF-like BAF complexes. Nature 418, 195–199.

Choi, E.Y., Park, J.A., Sung, Y.H., Kwon, H., 2001. Generation of the dominant-negative mutant of *hArpNbeta*: a component of human SWI/SNF chromatin remodeling complex. Exp. Cell Res. 271, 180–188.

Choi, K., Kim, S., Kim, S.Y., Kim, M., Hyun, Y., Lee, H., et al., 2005. *SUPPRESSOR OF FRIGIDA3* encodes a nuclear ACTIN-RELATED PROTEIN6 required for floral repression in *Arabidopsis*. Plant Cell 17, 2647–2660.

Choi, K., Park, C., Lee, J., Oh, M., Noh, B., Lee, I., 2007. *Arabidopsis* homologs of components of the SWR1 complex regulate flowering and plant development. Development 134, 1931–1941.

Conaway, R.C., Conaway, J.W., 2009. The INO80 chromatin remodeling complex in transcription, replication and repair. Trends Biochem. Sci. 34, 71–77.

Crapper, D.R., Quittkat, S., de Boni, U., 1979. Altered chromatin conformation in Alzheimer's disease. Brain 102, 483–495.

Csink, A.K., Henikoff, S., 1996. Genetic modification of heterochromatic association and nuclear organization in *Drosophila*. Nature 381, 529–531.

Cuzin, F., Grandjean, V., Rassoulzadegan, M., 2008. Inherited variation at the epigenetic level: paramutation from the plant to the mouse. Curr. Opin. Genet Dev. 18, 193–196.

Dang, W., Bartholomew, B., 2007. Domain architecture of the catalytic subunit in the ISW2-nucleosome complex. Mol. Cell. Biol. 27, 8306–8317.

Deal, R.B., Kandasamy, M.K., McKinney, E.C., Meagher, R.B., 2005. The nuclear actin-related protein ARP6 is a pleiotropic developmental regulator required for the maintenance of *FLOWERING LOCUS C* expression and repression of flowering in *Arabidopsis*. Plant Cell 17, 2633–2646.

Deal, R.B., Topp, C.N., McKinney, E.C., Meagher, R.B., 2007. Repression of flowering in *Arabidopsis* requires activation of *FLOWERING LOCUS C* expression by the histone variant H2A.Z. Plant Cell 19, 74–83.

Debril, M.B., Gelman, L., Fayard, E., Annicotte, J.S., Rocchi, S., Auwerx, J., 2004. Transcription factors and nuclear receptors interact with the SWI/SNF complex through the BAF60c subunit. J. Biol. Chem. 279, 16677–16686.

DeCristofaro, M.F., Betz, B.L., Wang, W., Weissman, B.E., 1999. Alteration of hSNF5/INI1/BAF47 detected in rhabdoid cell lines and primary rhabdomyosarcomas but not Wilms' tumors. Oncogene 18, 7559–7565.

DeCristofaro, M.F., Betz, B.L., Rorie, C.J., Reisman, D.N., Wang, W., Weissman, B.E., 2001. Characterization of SWI/SNF protein expression in human breast cancer cell lines and other malignancies. J. Cell Physiol. 186, 136–145.

Dinant, C., Houtsmuller, A.B., Vermeulen, W., 2008. Chromatin structure and DNA damage repair. Epigen. Chrom. 1, 9.

Dirscherl, S.S., Krebs, J.E., 2004. Functional diversity of ISWI complexes. Biochem. Cell Biol. 82, 482–489.

Downs, J.A., Allard, S., Jobin-Robitaille, O., Javaheri, A., Auger, A., Bouchard, N., et al., 2004. Binding of chromatin-modifying activities to phosphorylated histone H2A at DNA damage sites. Mol. Cell 16, 979–990.

Dryhurst, D., Thambirajah, A.A., Ausio, J., 2004. New twists on H2A.Z: a histone variant with a controversial structural and functional past. Biochem. Cell Biol. 82, 490–497.

Ebbert, R., Birkmann, A., Schuller, H.J., 1999. The product of the *SNF2/SWI2 paralogue INO80* of *Saccharomyces cerevisiae* required for efficient expression of various yeast structural genes is part of a high-molecular-weight protein complex. Mol. Microbiol. 32, 741–751.

Eckley, D.M., Schroer, T.A., 2003. Interactions between the evolutionarily conserved, actin–related protein, Arp11, actin, and Arp1. Mol. Biol. Cell 14, 2645–2654.

Eckley, D.M., Gill, S.R., Melkonian, K.A., Bingham, J.B., Goodson, H.V., Heuser, J.E., et al., 1999. Analysis of dynactin subcomplexes reveals a novel actin-related protein associated with the arp1 minifilament pointed end. J. Cell Biol. 147, 307–320.

Elango, N., Kim, S.H., Vigoda, E., Yi, S.V., 2008. Mutations of different molecular origins exhibit contrasting patterns of regional substitution rate variation. PLoS Comput. Biol. 4, e1000015.

Fan, J.Y., Rangasamy, D., Luger, K., Tremethick, D.J., 2004. H2A.Z alters the nucleosome surface to promote HP1alpha-mediated chromatin fiber folding. Mol. Cell 16, 655–661.

Feng, Y., Lee, N., Fearon, E.R., 2003. TIP49 regulates beta-catenin-mediated neoplastic transformation and T-cell factor target gene induction via effects on chromatin remodeling. Cancer Res. 63, 8726–8734.

Ferluga, J., 1989. Possible organ and age-related epigenetic factors in Huntington's disease and colorectal carcinoma. Med. Hypotheses 29, 51–54.

Ford, J., Odeyale, O., Shen, C.H., 2008. Activator-dependent recruitment of SWI/SNF and INO80 during INO1 activation. Biochem. Biophys. Res. Commun. 373, 602–606.

Fraga, M.F., Agrelo, R., Esteller, M., 2007. Cross-talk between aging and cancer: the epigenetic language. Ann. NY Acad. Sci. 1100, 60–74.

Francis, D., 2007. The plant cell cycle—15 years on. New Phytol. 174, 261–278.

Frankel, S., Sigel, E.A., Craig, C., Elgin, S.C., Mooseker, M.S., Artavanis-Tsakonas, S., 1997. An actin-related protein in *Drosophila* colocalizes with heterochromatin protein 1 in pericentric heterochromatin. J. Cell Sci. 110 (Pt 17), 1999–2012.

Fritsch, O., Benvenuto, G., Bowler, C., Molinier, J., Hohn, B., 2004. The INO80 protein controls homologous recombination in *Arabidopsis thaliana*. Mol. Cell 16, 479–485.

Fuchs, M., Gerber, J., Drapkin, R., Sif, S., Ikura, T., Ogryzko, V., et al., 2001. The p400 complex is an essential E1A transformation target. Cell 106, 297–307.

Fujii, K., Yonemasu, Y., Kitamura, K., Tsubota, Y., 1980. A genetic aspect of chromatin proteins of human brain tumors. J. Neurol. 223, 23–34.

Galarneau, L., Nourani, A., Boudreault, A.A., Zhang, Y., Heliot, L., Allard, S., et al., 2000. Multiple links between the NuA4 histone acetyltransferase complex and epigenetic control of transcription. Mol. Cell 5, 927–937.

Galkin, V.E., VanLoock, M.S., Orlova, A., Egelman, E.H., 2002. A new internal mode in F-actin helps explain the remarkable evolutionary conservation of actin's sequence and structure. Curr. Biol. 12, 570–575.

Garcia, B.A., Busby, S.A., Shabanowitz, J., Hunt, D.F., Mishra, N., 2005. Resetting the epigenetic histone code in the MRL-lpr/lpr mouse model of lupus by histone deacetylase inhibition. J. Proteome Res. 4, 2032–2042.

Gebuhr, T.C., Kovalev, G.I., Bultman, S., Godfrey, V., Su, L., Magnuson, T., 2003. The role of Brg1, a catalytic subunit of mammalian chromatin-remodeling complexes, in T cell development. J. Exp. Med. 198, 1937–1949.

Georgieva, M., Harata, M., Miloshev, G., 2008. The nuclear actin-related protein Act3p/Arp4 influences yeast cell shape and bulk chromatin organization. J. Cell Biochem. 104, 59–67.

Gong, F., Fahy, D., Liu, H., Wang, W., Smerdon, M.J., 2008. Role of the mammalian SWI/SNF chromatin remodeling complex in the cellular response to UV damage. Cell Cycle 7, 1067–1074.

Goodson, H.V., Hawse, W.F., 2002. Molecular evolution of the actin family. J. Cell Sci. 115, 2619–2622.

Gordon, J.L., Sibley, L.D., 2005. Comparative genome analysis reveals a conserved family of actin-like proteins in apicomplexan parasites. BMC Genom. 6, 179.

Gordon, J.L., Beatty, W.L., Sibley, L.D., 2008. A novel actin-related protein is associated with daughter cell formation in *Toxoplasma gondii*. Eukaryot. Cell 7, 1500–1512.

Gorzer, I., Schuller, C., Heidenreich, E., Krupanska, L., Kuchler, K., Wintersberger, U., 2003. The nuclear actin-related protein Act3p/Arp4p of *Saccharomyces cerevisiae* is involved in transcription regulation of stress genes. Mol. Microbiol. 50, 1155–1171.

Graff, J., Mansuy, I.M., 2008. Epigenetic codes in cognition and behaviour. Behav. Brain Res. 192, 70–87.

Grewal, S.I., Moazed, D., 2003. Heterochromatin and epigenetic control of gene expression. Science 301, 798–802.

Groth, A., Rocha, W., Verreault, A., Almouzni, G., 2007. Chromatin challenges during DNA replication and repair. Cell 128, 721–733.

Groudine, M., Kohwi-Shigematsu, T., Gelinas, R., Stamatoyannopoulos, G., Papayannopoulou, T., 1983. Human fetal to adult hemoglobin switching: changes in chromatin structure of the beta-globin gene locus. Proc. Natl. Acad. Sci. USA 80, 7551–7555.

Haig, D., 2004. The (dual) origin of epigenetics. Cold Spring Harb. Symp. Quant. Biol. 69, 67–70.

Harata, M., Karwan, A., Wintersberger, U., 1994. An essential gene of *Saccharomyces cerevisiae* coding for an actin-related protein. Proc. Natl. Acad. Sci. USA 91, 8258–8262.

Harata, M., Mochizuki, R., Mizuno, S., 1999a. Two isoforms of a human actin-related protein show nuclear localization and mutually selective expression between brain and other tissues. Biosci. Biotechnol. Biochem. 63, 917–923.

Harata, M., Oma, Y., Mizuno, S., Jiang, Y.W., Stillman, D.J., Wintersberger, U., 1999b. The nuclear actin-related protein of *Saccharomyces cerevisiae*, Act3p/Arp4, interacts with core histones. Mol. Biol. Cell 10, 2595–2605.

Harata, M., Oma, Y., Tabuchi, T., Zhang, Y., Stillman, D.J., Mizuno, S., 2000. Multiple actin-related proteins of *Saccharomyces cerevisiae* are present in the nucleus. J. Biochem. (Tokyo) 128, 665–671.

Harata, M., Nishimori, K., Hatta, S., 2001. Identification of two cDNAs for human actin-related proteins (Arps) that have remarkable similarity to conventional actin. Biochim. Biophys. Acta 1522, 130–133.

Harata, M., Zhang, Y., Stillman, D.J., Matsui, D., Oma, Y., Nishimori, K., et al., 2002. Correlation between chromatin association and transcriptional regulation for the Act3p/Arp4 nuclear actin-related protein of *Saccharomyces cerevisiae*. Nucleic Acids Res. 30, 1743–1750.

Harries, P.A., Pan, A., Quatrano, R.S., 2005. Actin-related protein2/3 complex component ARPC1 is required for proper cell morphogenesis and polarized cell growth in *Physcomitrella patens*. Plant Cell 17, 2327–2339.

Hedges, S.B., Blair, J.E., Venturi, M.L., Shoe, J.L., 2004. A molecular timescale of eukaryote evolution and the rise of complex multicellular life. BMC Evol. Biol. 4, 2.

Henderson, I.R., Jacobsen, S.E., 2007. Epigenetic inheritance in plants. Nature 447, 418–424.

Henikoff, S., 1979. Position effects and variegation enhancers in an autosomal region of *Drosophila melanogaster*. Genetics 93, 105–115.

Huanca-Mamani, W., Garcia-Aguilar, M., Leon-Martinez, G., Grossniklaus, U., Vielle-Calzada, J.P., 2005. CHR11, a chromatin-remodeling factor essential for nuclear proliferation during female gametogenesis in *Arabidopsis thaliana*. Proc. Natl. Acad. Sci. USA 102, 17231–17236.

Huang, M.E., Souciet, J.L., Chuat, J.C., Galibert, F., 1996. Identification of ACT4, a novel essential actin-related gene in the yeast *Saccharomyces cerevisiae*. Yeast 12, 839–848.

Ikura, T., Ogryzko, V.V., Grigoriev, M., Groisman, R., Wang, J., Horikoshi, M., et al., 2000. Involvement of the TIP60 histone acetylase complex in DNA repair and apoptosis. Cell 102, 463–473.

Iyer, L.M., Anantharaman, V., Wolf, M.Y., Aravind, L., 2008. Comparative genomics of transcription factors and chromatin proteins in parasitic protists and other eukaryotes. Int. J. Parasitol. 38, 1–31.

Jeddeloh, J.A., Stokes, T.L., Richards, E.J., 1999. Maintenance of genomic methylation requires a SWI2/SNF2-like protein. Nat. Genet. 22, 94–97.

Jehn, B.M., Osborne, B.A., 1997. Gene regulation associated with apoptosis. Crit. Rev. Eukaryot. Gene Exp. 7, 179–193.

Jiang, Y.W., Stillman, D.J., 1996. Epigenetic effects on yeast transcription caused by mutations in an actin-related protein present in the nucleus. Genes Dev. 10, 604–619.

Jin, J., Cai, Y., Yao, T., Gottschalk, A.J., Florens, L., Swanson, S.K., et al., 2005. A mammalian chromatin remodeling complex with similarities to the yeast INO80 complex. J. Biol. Chem. 280, 41207–41212.

Jirtle, R.L., Sander, M., Barrett, J.C., 2000. Genomic imprinting and environmental disease susceptibility. Environ. Health Perspect. 108, 271–278.

Johnson, L., Cao, X., Jacobsen, S., 2002. Interplay between two epigenetic marks. DNA methylation and histone H3 lysine 9 methylation. Curr. Biol. 12, 1360–1367.

Jonsson, Z.O., Jha, S., Wohlschlegel, J.A., Dutta, A., 2004. Rvb1p/Rvb2p recruit Arp5p and assemble a functional Ino80 chromatin remodeling complex. Mol. Cell 16, 465–477.

Kandasamy, M.K., McKinney, E.C., Meagher, R.B., 2003. Cell cycle-dependent association of *Arabidopsis* actin-related proteins AtARP4 and AtARP7 with the nucleus. Plant J. 33, 939–948.

Kandasamy, M.K., Deal, R.B., McKinney, E.C., Meagher, R.B., 2004. Plant actin-related proteins. Trends Plant Sci. 9, 196–202.

Kandasamy, M.K., Deal, R.B., McKinney, E.C., Meagher, R.B., 2005a. Silencing the nuclear actin-related protein AtARP4 in *Arabidopsis* has multiple effects on plant development, including early flowering and delayed floral senescence. Plant J. 41, 845–858.

Kandasamy, M.K., McKinney, E.C., Deal, R.B., Meagher, R.B., 2005b. *Arabidopsis* ARP7 is an essential actin-related protein required for normal embryogenesis, plant architecture, and floral organ abscission. Plant Physiol. 138, 2019–2032.

Kandasamy, M.K., McKinney, E.C., Meagher, R.B., 2008. *ACTIN-RELATED PROTEIN8* encodes an F-box protein localized to the nucleolus in *Arabidopsis*. Plant Cell Physiol. 49, 858–863.

Kandasamy, M.K., McKinney, L.C., Deal, R.B., Smith, A.P., Meagher, R.B., 2009. *Arabidopsis* actin-related protein ARP5 in multicellular development and DNA repair. Developmental Biology (In Press).

Kanno, T., Mette, M.F., Kreil, D.P., Aufsatz, W., Matzke, M., Matzke, A.J., 2004. Involvement of putative SNF2 chromatin remodeling protein DRD1 in RNA-directed DNA methylation. Curr. Biol. 14, 801–805.

Kato, M., Sasaki, M., Mizuno, S., Harata, M., 2001. Novel actin-related proteins in vertebrates: similarities of structure and expression pattern to Arp6 localized on *Drosophila* heterochromatin. Gene 268, 133–140.

Kawashima, S., Ogiwara, H., Tada, S., Harata, M., Wintersberger, U., Enomoto, T., et al., 2007. The INO80 complex is required for damage-induced recombination. Biochem. Biophys. Res. Commun. 355, 835–841.

Kehrer-Sawatzki, H., Cooper, D.N., 2007. Understanding the recent evolution of the human genome: insights from human-chimpanzee genome comparisons. Hum. Mutat. 28, 99–130.

Kitayama, K., Kamo, M., Oma, Y., Matsuda, R., Uchida, T., Ikura, T., et al., 2009. The human actin-related protein hArp5: nucleo-cytoplasmic shuttling and involvement in DNA repair. Exp. Cell Res. 315, 206–217.

Klar, A.J., 2007. Lessons learned from studies of fission yeast mating-type switching and silencing. Annu. Rev. Genet. 41, 213–236.

Klee, H.J., 2002. Control of ethylene-mediated processes in tomato at the level of receptors. J. Exp. Bot. 53, 2057–2063.

Klochendler-Yeivin, A., Picarsky, E., Yaniv, M., 2006. Increased DNA damage sensitivity and apoptosis in cells lacking the Snf5/Ini1 subunit of the SWI/SNF chromatin remodeling complex. Mol. Cell. Biol. 26, 2661–2674.

Kobor, M.S., Venkatasubrahmanyam, S., Meneghini, M.D., Gin, J.W., Jennings, J.L., Link, A.J., et al., 2004. A protein complex containing the conserved Swi2/Snf2-related ATPase Swr1p deposits histone variant H2A.Z into euchromatin. PLoS Biol. 2, E131.

Krogan, N.J., Keogh, M.C., Datta, N., Sawa, C., Ryan, O.W., Ding, H., et al., 2003. A Snf2 family ATPase complex required for recruitment of the histone H2A variant Htz1. Mol. Cell. 12, 1565–1576.

Kuo, L.J., Yang, L.X., 2008. Gamma-H2AX—a novel biomarker for DNA double-strand breaks. In Vivo 22, 305–309.

Kuroda, Y., Oma, Y., Nishimori, K., Ohta, T., Harata, M., 2002. Brain-specific expression of the nuclear actin-related protein ArpNalpha and its involvement in mammalian SWI/SNF chromatin remodeling complex. Biochem. Biophys. Res. Commun. 299, 328–334.

Kwon, C.S., Wagner, D., 2007. Unwinding chromatin for development and growth: a few genes at a time. Trends Genet. 23, 403–412.

Larochelle, M., Gaudreau, L., 2003. H2A.Z has a function reminiscent of an activator required for preferential binding to intergenic DNA. Embo. J. 22, 4512–4522.

Lazaro, A., Gomez-Zambrano, A., Lopez-Gonzalez, L., Pineiro, M., Jarillo, J.A., 2008. Mutations in the *Arabidopsis SWC6* gene, encoding a component of the SWR1 chromatin remodelling complex, accelerate flowering time and alter leaf and flower development. J. Exp. Bot. 59, 653–666.

Lee, J.H., Chang, S.H., Shim, J.H., Lee, J.Y., Yoshida, M., Kwon, H., 2003. Cytoplasmic localization and nucleo-cytoplasmic shuttling of BAF53, a component of chromatin-modifying complexes. Mol. Cells 16, 78–83.

Lee, J.H., Lee, J.Y., Chang, S.H., Kang, M.J., Kwon, H., 2005. Effects of *Ser2* and *Tyr6* mutants of *BAF53* on cell growth and p53-dependent transcription. Mol. Cells 19, 289–293.

Lee, K., Kang, M.J., Kwon, S.J., Kwon, Y.K., Kim, K.W., Lim, J.H., et al., 2007a. Expansion of chromosome territories with chromatin decompaction in BAF53-depleted interphase cells. Mol. Biol. Cell 18, 4013–4023.

Lee, K., Shim, J.H., Kang, M.J., Kim, J.H., Ahn, J.S., Yoo, S.J., et al., 2007b. Association of BAF53 with mitotic chromosomes. Mol. Cells 24, 288–293.

Lessard, J., Wu, J.I., Ranish, J.A., Wan, M., Winslow, M.M., Staahl, B.T., et al., 2007. An essential switch in subunit composition of a chromatin remodeling complex during neural development. Neuron 55, 201–215.

Lewis, M.W., Leslie, M.E., Liljegren, S.J., 2006. Plant separation: 50 ways to leave your mother. Curr. Opin. Plant Biol. 9, 59–65.

Li, B., Pattenden, S.G., Lee, D., Gutierrez, J., Chen, J., Seidel, C., et al., 2005. Preferential occupancy of histone variant H2AZ at inactive promoters influences local histone modifications and chromatin remodeling. Proc. Natl. Acad. Sci. USA 102, 18385–18390.

Lickert, H., Takeuchi, J.K., Von Both, I., Walls, J.R., McAuliffe, F., Adamson, S.L., et al., 2004. Baf60c is essential for function of BAF chromatin remodelling complexes in heart development. Nature 432, 107–112.

Lin, H.Y., Chen, C.S., Lin, S.P., Weng, J.R., 2006. Targeting histone deacetylase in cancer therapy. Med. Res. Rev. 26, 397–413.

Linger, J.G., Tyler, J.K., 2007. Chromatin disassembly and reassembly during DNA repair. Mutat. Res. 618, 52–64.

Liu, R., Liu, H., Chen, X., Kirby, M., Brown, P.O., Zhao, K., 2001. Regulation of CSF1 promoter by the SWI/SNF-like BAF complex. Cell 106, 309–318.

March-Diaz, R., Garcia-Dominguez, M., Florencio, F.J., Reyes, J.C., 2007. SEF, a new protein required for flowering repression in *Arabidopsis*, interacts with PIE1 and ARP6. Plant Physiol. 143, 893–901.

Martin-Trillo, M., Lazaro, A., Poethig, R.S., Gomez-Mena, C., Pineiro, M.A., Martinez-Zapater, J.M., et al., 2006. *EARLY IN SHORT DAYS 1 (ESD1)* encodes ACTIN-RELATED PROTEIN 6 (AtARP6), a putative component of chromatin remodelling complexes that positively regulates *FLC* accumulation in *Arabidopsis*. Development 133, 1241–1252.

McKinney, E.C., Kandasamy, M.K., Meagher, R.B., 2002. *Arabidopsis* contains ancient classes of differentially expressed actin-related protein genes. Plant Physiol. 128, 997–1007.

Meagher, R.B., 1995. The impact of historical contingency on gene phylogeny: plant actin diversity. In: Hecht, M., MacIntyre, R., Clegg, M. (Eds.), Evolutionary Biology, 28. NY, Plenum Press, pp. 195–215.

Meagher, R.B., McKinney, E.C., Kandasamy, M.K., 1999a. Isovariant dynamics expand and buffer the responses of complex systems: the diverse plant actin gene family. Plant Cell 11, 995–1006.

Meagher, R.B., McKinney, E.C., Vitale, A.V., 1999b. The evolution of new structures: clues from plant cytoskeletal genes. Trends Genet. 15, 278–284.

Meagher, R.B., Deal, R.B., Kandasamy, M.K., McKinney, E.C., 2005. Nuclear actin-related proteins as epigenetic regulators of development. Plant Physiol. 139, 1576–1585.

Meagher, R.B., Kandasamy, M.K., Deal, R.B., McKinney, E.C., 2007. Actin-related proteins in chromatin-level control of the cell cycle and developmental transitions. Trends Cell Biol. 17, 325–332.

Meagher, R.B., Kandasamy, M.K., McKinney, E.C., 2008. Multicellular development and protein–protein interactions. Plant Signal Behav. 3, 333–336.

Mehler, M.F., 2008a. Epigenetic principles and mechanisms underlying nervous system functions in health and disease. Prog. Neurobiol. 86, 305–341.

Mehler, M.F., 2008b. Epigenetics and the nervous system. Ann. Neurol. 64, 602–617.

Mehler, M.F., Purpura, D.P., 2008. Autism, fever, epigenetics and the locus coeruleus. Brain Res. Rev 59, 388–392.

Meneghini, M.D., Wu, M., Madhani, H.D., 2003. Conserved histone variant H2A.Z protects euchromatin from the ectopic spread of silent heterochromatin. Cell 112, 725–736.

Metivier, R., Penot, G., Hubner, M.R., Reid, G., Brand, H., Kos, M., et al., 2003. Estrogen receptor-alpha directs ordered, cyclical, and combinatorial recruitment of cofactors on a natural target promoter. Cell 115, 751–763.

Minoda, A., Saitoh, S., Takahashi, K., Toda, T., 2005. BAF53/Arp4 homolog Alp5 in fission yeast is required for histone H4 acetylation, kinetochore-spindle attachment, and gene silencing at centromere. Mol. Biol. Cell 16, 316–327.

Minucci, S., Pelicci, P.G., 1999. Retinoid receptors in health and disease: co–regulators and the chromatin connection. Semin. Cell Dev. Biol. 10, 215–225.

Mittelsten Scheid, O., Paszkowski, J., 2000. Transcriptional gene silencing mutants. Plant Mol. Biol. 43, 235–241.

Miura, A., Yonebayashi, S., Watanabe, K., Toyama, T., Shimada, H., Kakutani, T., 2001. Mobilization of transposons by a mutation abolishing full DNA methylation in *Arabidopsis*. Nature 411, 212–214.

Mizuguchi, G., Shen, X., Landry, J., Wu, W.H., Sen, S., Wu, C., 2004. ATP-driven exchange of histone H2AZ variant catalyzed by SWR1 chromatin remodeling complex. Science 303, 343–348.

Mohrmann, L., Verrijzer, C.P., 2005. Composition and functional specificity of SWI2/SNF2 class chromatin remodeling complexes. Biochim. Biophys. Acta 1681, 59–73.

Morgan, H.D., Sutherland, H.G., Martin, D.I., Whitelaw, E., 1999. Epigenetic inheritance at the agouti locus in the mouse. Nat. Genet. 23, 314–318.

Morrison, A.J., Shen, X., 2006. Chromatin modifications in DNA repair. Results Probl. Cell Differ. 41, 109–125.

Morrison, A.J., Highland, J., Krogan, N.J., Arbel-Eden, A., Greenblatt, J.F., Haber, J.E., et al., 2004. INO80 and gamma-H2AX interaction links ATP-dependent chromatin remodeling to DNA damage repair. Cell 119, 767–775.

Muller, G.B., Newman, S.A., 2005. The innovation triad: an EvoDevo agenda. J. Exp. Zool. B Mol. Dev. Evol. 304, 487–503.

Muller, J., Oma, Y., Vallar, L., Friederich, E., Poch, O., Winsor, B., 2005. Sequence and comparative genomic analysis of actin-related proteins. Mol. Biol. Cell 16, 5736–5748.

Nanney, D.L., 1958. Epigenetic control systems. Proc. Natl. Acad. Sci. USA 44, 712–717.

Napolitano, M.A., Cipollaro, M., Cascino, A., Melone, M.A., Giordano, A., Galderisi, U., 2007. Brg1 chromatin remodeling factor is involved in cell growth arrest, apoptosis and senescence of rat mesenchymal stem cells. J. Cell Sci. 120, 2904–2911.

Nie, Z., Xue, Y., Yang, D., Zhou, S., Deroo, B.J., Archer, T.K., et al., 2000. A specificity and targeting subunit of a human SWI/SNF family-related chromatin-remodeling complex. Mol. Cell. Biol. 20, 8879–8888.

Noh, Y.S., Amasino, R.M., 2003. PIE1, an *ISWI* family gene, is required for *FLC* activation and floral repression in *Arabidopsis*. Plant Cell 15, 1671–1682.

O'Dor, E., Beck, S.A., Brock, H.W., 2006. Polycomb group mutants exhibit mitotic defects in syncytial cell cycles of *Drosophila* embryos. Dev. Biol. 290, 312–322.

Ogiwara, H., Enomoto, T., Seki, M., 2007a. The INO80 chromatin remodeling complex functions in sister chromatid cohesion. Cell Cycle 6, 1090–1095.

Ogiwara, H., Ui, A., Kawashima, S., Kugou, K., Onoda, F., Iwahashi, H., et al., 2007b. Actin-related protein Arp4 functions in kinetochore assembly. Nucleic Acids Res. 35, 3109–3117.

Ohfuchi, E., Nishimori, K., Harata, M., 2002. Alternative splicing products of the gene for a human nuclear actin-related protein, hArpNbeta/Baf53, that encode a protein isoform, hArpNbetaS, in the cytoplasm. Biosci. Biotechnol. Biochem. 66, 1740–1743.

Ohfuchi, E., Kato, M., Sasaki, M., Sugimoto, K., Oma, Y., Harata, M., 2006. Vertebrate Arp6, a novel nuclear actin-related protein, interacts with heterochromatin protein 1. Eur. J. Cell Biol. 85, 411–421.

Okazaki, N., Ikeda, S., Ohara, R., Shimada, K., Yanagawa, T., Nagase, T., et al., 2008. The novel protein complex with SMARCAD1/KIAA1122 binds to the vicinity of TSS. J. Mol. Biol. 382, 257–265.

Olave, I., Wang, W., Xue, Y., Kuo, A., Crabtree, G.R., 2002a. Identification of a polymorphic, neuron-specific chromatin remodeling complex. Genes Dev. 16, 2509–2517.

Olave, I.A., Reck-Peterson, S.L., Crabtree, G.R., 2002b. Nuclear actin and actin-related proteins in chromatin remodeling. Annu. Rev. Biochem. 71, 755–781.

Oma, Y., Nishimori, K., Harata, M., 2003. The brain-specific actin-related protein ArpN alpha interacts with the transcriptional co-repressor CtBP. Biochem. Biophys. Res. Commun. 301, 521–528.

Ooi, S.L., Henikoff, S., 2007. Germline histone dynamics and epigenetics. Curr. Opin. Cell Biol. 19, 257–265.

Osley, M.A., Tsukuda, T., Nickoloff, J.A., 2007. ATP-dependent chromatin remodeling factors and DNA damage repair. Mutat. Res. 618, 65–80.

Papoulas, O., Beek, S.J., Moseley, S.L., McCallum, C.M., Sarte, M., Shearn, A., et al., 1998. The *Drosophila* trithorax group proteins BRM, ASH1 and ASH2 are subunits of distinct protein complexes. Development 125, 3955–3966.

Park, J., Wood, M.A., Cole, M.D., 2002. BAF53 forms distinct nuclear complexes and functions as a critical c-Myc-interacting nuclear cofactor for oncogenic transformation. Mol. Cell. Biol. 22, 1307–1316.

Park, J.H., Park, E.J., Lee, H.S., Kim, S.J., Hur, S.K., Imbalzano, A.N., et al., 2006. Mammalian SWI/SNF complexes facilitate DNA double-strand break repair by promoting gamma-H2AX induction. Embo J. 25, 3986–3997.

Park, J.H., Park, E.J., Hur, S.K., Kim, S., Kwon, J., 2009. Mammalian SWI/SNF chromatin remodeling complexes are required to prevent apoptosis after DNA damage. DNA Repair (Amst) 8, 29–39.

Peterson, C.L., Zhao, Y., Chait, B.T., 1998. Subunits of the yeast SWI/SNF complex are members of the actin-related protein (ARP) family. J. Biol. Chem. 273, 23641–23644.

Pien, S., Fleury, D., Mylne, J.S., Crevillen, P., Inze, D., Avramova, Z., et al., 2008. *ARABIDOPSIS TRITHORAX1* dynamically regulates *FLOWERING LOCUS C* activation via histone 3 lysine 4 trimethylation. Plant Cell 20, 580–588.

Pillus, L., Rine, J., 1989. Epigenetic inheritance of transcriptional states in *S. cerevisiae*. Cell 59, 637–647.

Poch, O., Winsor, B., 1997. Who's who among the *Saccharomyces cerevisiae* actin-related proteins? A classification and nomenclature proposal for a large family. Yeast 13, 1053–1058.

Putterill, J., Robson, F., Lee, K., Simon, R., Coupland, G., 1995. The *CONSTANS* gene of *Arabidopsis* promotes flowering and encodes a protein showing similarities to zinc finger transcription factors. Cell 80, 847–857.

Putterill, J., Laurie, R., Macknight, R., 2004. It's time to flower: the genetic control of flowering time. Bioessays 26, 363–373.

Raisner, R.M., Madhani, H.D., 2006. Patterning chromatin: form and function for H2A.Z variant nucleosomes. Curr. Opin. Genet. Dev. 16, 119–124.

Raisner, R.M., Hartley, P.D., Meneghini, M.D., Bao, M.Z., Liu, C.L., Schreiber, S.L., et al., 2005. Histone variant H2A.Z marks the 5′ ends of both active and inactive genes in euchromatin. Cell 123, 233–248.

Rando, O.J., Zhao, K., Janmey, P., Crabtree, G.R., 2002. Phosphatidylinositol-dependent actin filament binding by the SWI/SNF-like BAF chromatin remodeling complex. Proc. Natl. Acad. Sci. USA 99, 2824–2829.

Remus, R., Kanzaki, A., Yawata, A., Nakanishi, H., Wada, H., Sugihara, T., et al., 2005. DNA methylation in promoter regions of red cell membrane protein genes in healthy individuals and patients with hereditary membrane disorders. Int. J. Hematol. 81, 385–395.

Roberts, J.A., 2000. Abscission and dehiscence. Symp. Soc. Exp. Biol. 52, 203–211.

Robertson, K.D., Wolffe, A.P., 2000. DNA methylation in health and disease. Nat. Rev. Genet. 1, 11–19.

Rogers, H.J., 2006. Programmed cell death in floral organs: how and why do flowers die? Ann. Bot. (Lond) 97, 309–315.

Roux-Rouquie, M., 2000. Genetic and epigenetic regulation schemes: need for an alternative paradigm. Mol. Genet. Metab. 71, 1–9.

Ruhl, D.D., Jin, J., Cai, Y., Swanson, S., Florens, L., Washburn, M.P., et al., 2006. Purification of a human SRCAP complex that remodels chromatin by incorporating the histone variant H2A.Z into nucleosomes. Biochemistry 45, 5671–5677.

Samach, A., Onouchi, H., Gold, S.E., Ditta, G.S., Schwarz-Sommer, Z., Yanofsky, M.F., et al., 2000. Distinct roles of CONSTANS target genes in reproductive development of *Arabidopsis*. Science 288, 1613–1616.

Samuelson, A.V., Narita, M., Chan, H.M., Jin, J., de Stanchina, E., McCurrach, M.E., et al., 2005. p400 is required for E1A to promote apoptosis. J. Biol. Chem. 280, 21915–21923.

Sansam, C.G., Roberts, C.W., 2006. Epigenetics and cancer: altered chromatin remodeling via Snf5 loss leads to aberrant cell cycle regulation. Cell Cycle 5, 621–624.

Santisteban, M.S., Kalashnikova, T., Smith, M.M., 2000. Histone H2A.Z regulates transcription and is partially redundant with nucleosome remodeling complexes. Cell 103, 411–422.

Sardiu, M.E., Cai, Y., Jin, J., Swanson, S.K., Conaway, R.C., Conaway, J.W., et al., 2008. Probabilistic assembly of human protein interaction networks from label-free quantitative proteomics. Proc. Natl. Acad. Sci. USA 105, 1454–1459.

Sarnowski, T.J., Rios, G., Jasik, J., Swiezewski, S., Kaczanowski, S., Li, Y., et al., 2005. SWI3 subunits of putative SWI/SNF chromatin-remodeling complexes play distinct roles during *Arabidopsis* development. Plant Cell 17, 2454–2472.

Saze, H., Sasaki, T., Kakutani, T., 2008. Negative regulation of DNA methylation in plants. Epigenetics 3, 122–124.

Schulz, W.A., Steinhoff, C., Florl, A.R., 2006. Methylation of endogenous human retroelements in health and disease. Curr. Top. Microbiol. Immunol. 310, 211–250.

Seah, C., Levy, M.A., Jiang, Y., Mokhtarzada, S., Higgs, D.R., Gibbons, R.J., et al., 2008. Neuronal death resulting from targeted disruption of the Snf2 protein ATRX is mediated by p53. J. Neurosci. 28, 12570–12580.

Shaked, H., Avivi-Ragolsky, N., Levy, A.A., 2006. Involvement of the *Arabidopsis* SWI2/SNF2 chromatin remodeling gene family in DNA damage response and recombination. Genetics 173, 985–994.

Shames, D.S., Minna, J.D., Gazdar, A.F., 2007. DNA methylation in health, disease, and cancer. Curr. Mol. Med. 7, 85–102.

Shanahan, F., Seghezzi, W., Parry, D., Mahony, D., Lees, E., 1999. Cyclin E associates with BAF155 and BRG1, components of the mammalian SWI-SNF complex, and alters the ability of BRG1 to induce growth arrest. Mol. Cell. Biol. 19, 1460–1469.

Shen, X., Mizuguchi, G., Hamiche, A., Wu, C., 2000. A chromatin remodelling complex involved in transcription and DNA processing. Nature 406, 541–544.

Shen, J., Hsu, C.M., Kang, B.K., Rosen, B.P., Bhattacharjee, H., 2003a. The *Saccharomyces cerevisiae* Arr4p is involved in metal and heat tolerance. Biometals 16, 369–378.

Shen, X., Ranallo, R., Choi, E., Wu, C., 2003b. Involvement of actin-related proteins in ATP-dependent chromatin remodeling. Mol. Cell 12, 147–155.

Shimada, K., Oma, Y., Schleker, T., Kugou, K., Ohta, K., Harata, M., et al., 2008. Ino80 chromatin remodeling complex promotes recovery of stalled replication forks. Curr. Biol. 18, 566–575.

Simone, C., Forcales, S.V., Hill, D.A., Imbalzano, A.N., Latella, L., Puri, P.L., 2004. p38 pathway targets SWI-SNF chromatin-remodeling complex to muscle-specific loci. Nat. Genet. 36, 738–743.

Simpson, G.G., 2004. The autonomous pathway: epigenetic and post-transcriptional gene regulation in the control of *Arabidopsis* flowering time. Curr. Opin. Plant Biol. 7, 570–574.

Simpson, G.G., Dean, C., 2002. *Arabidopsis*, the Rosetta stone of flowering time? Science 296, 285–289.

Smerdon, M.J., Lieberman, M.W., 1978. Nucleosome rearrangement in human chromatin during UV-induced DNA- reapir synthesis. Proc. Natl. Acad. Sci. USA 75, 4238–4241.

Smith, H.S., Springer, E.L., Hackett, A.J., 1979. Nuclear ultrastructure of epithelial cell lines derived from human carcinomas and nonmalignant tissues. Cancer Res. 39, 332–344.

Soragni, E., Herman, D., Dent, S.Y., Gottesfeld, J.M., Wells, R.D., Napierala, M., 2008. Long intronic GAA*TTC repeats induce epigenetic changes and reporter gene silencing in a molecular model of Friedreich ataxia. Nucleic Acids Res. 36, 6056–6065.

Staehling-Hampton, K., Ciampa, P.J., Brook, A., Dyson, N., 1999. A genetic screen for modifiers of E2F in *Drosophila melanogaster*. Genetics 153, 275–287.

Stefanov, S.A., 2000. Further characterization of the actin-related protein Act3p/Arp4 of *S. cerevisiae* through mutational analysis. Mol. Biol. Rep. 27, 35–43.

Steinboeck, F., Krupanska, L., Bogusch, A., Kaufmann, A., Heidenreich, E., 2006. Novel regulatory properties of *Saccharomyces cerevisiae* Arp4. J. Biochem. (Tokyo) 139, 741–751.

Su, Y., Kwon, C.S., Bezhani, S., Huvermann, B., Chen, C., Peragine, A., et al., 2006. The N-terminal ATPase AT-hook-containing region of the *Arabidopsis* chromatin-remodeling protein SPLAYED is sufficient for biological activity. Plant J. 46, 685–699.

Sumi-Ichinose, C., Ichinose, H., Metzger, D., Chambon, P., 1997. SNF2beta-BRG1 is essential for the viability of F9 murine embryonal carcinoma cells. Mol. Cell. Biol. 17, 5976–5986.

Sunada, R., Gorzer, I., Oma, Y., Yoshida, T., Suka, N., Wintersberger, U., et al., 2005. The nuclear actin-related protein Act3p/Arp4p is involved in the dynamics of chromatin-modulating complexes. Yeast 22, 753–768.

Szerlong, H., Saha, A., Cairns, B.R., 2003. The nuclear actin-related proteins Arp7 and Arp9: a dimeric module that cooperates with architectural proteins for chromatin remodeling. EMBO J. 22, 3175–3187.

Szerlong, H., Hinata, K., Viswanathan, R., Erdjument-Bromage, H., Tempst, P., Cairns, B.R., 2008. The HSA domain binds nuclear actin-related proteins to regulate chromatin-remodeling ATPases. Nat. Struct. Mol. Biol. 15, 469–476.

Tamura, K., Dudley, J., Nei, M., Kumar, S., 2007. MEGA4: molecular evolutionary genetics analysis (MEGA) software version 4.0. Mol. Biol. Evol. 24, 1596–1599.

Tromans, A., 2004. Cardiovascular biology: how genes know their place. Nature 432, 29.

True, H.L., Berlin, I., Lindquist, S.L., 2004. Epigenetic regulation of translation reveals hidden genetic variation to produce complex traits. Nature 431, 184–187.

Trujillo, K.M., Osley, M.A., 2008. INO80 meets a fork in the road. Nat. Struct. Mol. Biol. 15, 332–334.

Ueno, M., Murase, T., Kibe, T., Ohashi, N., Tomita, K., Murakami, Y., et al., 2004. Fission yeast Arp6 is required for telomere silencing, but functions independently of Swi6. Nucleic Acids Res. 32, 736–741.

van Attikum, H., Fritsch, O., Hohn, B., Gasser, S.M., 2004. Recruitment of the INO80 complex by H2A phosphorylation links ATP-dependent chromatin remodeling with DNA double-strand break repair. Cell 119, 777–788.

van Attikum, H., Fritsch, O., Gasser, S.M., 2007. Distinct roles for SWR1 and INO80 chromatin remodeling complexes at chromosomal double-strand breaks. EMBO J. 26, 4113–4125.

van den Ent, F., Amos, L., Lowe, J., 2001. Prokaryotic origin of the actin cytoskeleton. Nature 413, 39–44.

Vasanthi, D., Mishra, R.K., 2008. Epigenetic regulation of genes during development: a conserved theme from flies to mammals. J. Genet. Genomics 35, 413–429.

Vignon, X., Zhou, Q., Renard, J.P., 2002. Chromatin as a regulative architecture of the early developmental functions of mammalian embryos after fertilization or nuclear transfer. Cloning Stem Cells 4, 363–377.

Voitenko, V.P., 1980. Aging, diseases and X-chromatin. Z. Gerontol. 13, 18–23.

Waddington, C.H., 1995. The strategy of the genes. In: The Strategy of the Genes. George Allen & Unwin Ltd, London, Ruskin House, p. 257.

Wagner, D., Meyerowitz, E.M., 2002. *SPLAYED*, a novel *SWI/SNF ATPase* homolog, controls reproductive development in *Arabidopsis*. Curr. Biol. 12, 85–94.

Walley, J.W., Rowe, H.C., Xiao, Y., Chehab, E.W., Kliebenstein, D.J., Wagner, D., et al., 2008. The chromatin remodeler SPLAYED regulates specific stress signaling pathways. PLoS Pathog. 4, e1000237.

Wang, W., Cote, J., Xue, Y., Zhou, S., Khavari, P.A., Biggar, S.R., et al., 1996a. Purification and biochemical heterogeneity of the mammalian SWI-SNF complex. EMBO J. 15, 5370–5382.

Wang, W., Xue, Y., Zhou, S., Kuo, A., Cairns, B.R., Crabtree, G.R., 1996b. Diversity and specialization of mammalian SWI/SNF complexes. Genes Dev. 10, 2117–2130.

Wang, M., Gu, C., Qi, T., Tang, W., Wang, L., Wang, S., et al., 2007. BAF53 interacts with p53 and functions in p53-mediated p21-gene transcription. J. Biochem. 142, 613–620.

Weber, V., Harata, M., Hauser, H., Wintersberger, U., 1995. The actin-related protein Act3p of *Saccharomyces cerevisiae* is located in the nucleus. Mol. Biol. Cell 6, 1263–1270.

Weinhold, B., 2006. Epigenetics: the science of change. Environ. Health Perspect. 114, A160–A167.

Williams, L., Fletcher, J.C., 2005. Stem cell regulation in the *Arabidopsis* shoot apical meristem. Curr. Opin. Plant Biol. 8, 582–586.

Wilson, A.C., Sarich, V.M., 1969. A molecular time scale for human evolution. Proc. Natl. Acad. Sci. USA 63, 1088–1093.

Wong, J.J., Hawkins, N.J., Ward, R.L., 2007. Colorectal cancer: a model for epigenetic tumorigenesis. Gut 56, 140–148.

Wu, W.H., Alami, S., Luk, E., Wu, C.H., Sen, S., Mizuguchi, G., et al., 2005. Swc2 is a widely conserved H2AZ-binding module essential for ATP-dependent histone exchange. Nat. Struct. Mol. Biol. 12, 1064–1071.

Wu, J.I., Lessard, J., Olave, I.A., Qiu, Z., Ghosh, A., Graef, I.A., et al., 2007. Regulation of dendritic development by neuron-specific chromatin remodeling complexes. Neuron 56, 94–108.

Wu, K., Zhang, L., Zhou, C., Yu, C.W., Chaikam, V., 2008. HDA6 is required for jasmonate response, senescence and flowering in *Arabidopsis*. J. Exp. Bot. 59, 225–234.

Yang, X., Zaurin, R., Beato, M., Peterson, C.L., 2007. Swi3p controls SWI/SNF assembly and ATP-dependent H2A–H2B displacement. Nat. Struct. Mol. Biol. 14, 540–547.

Yeh, J.H., Spicuglia, S., Kumar, S., Sanchez-Sevilla, A., Ferrier, P., Imbert, J., 2002. Control of *IL-2Ralpha* gene expression: structural changes within the proximal enhancer/core promoter during T-cell development. Nucleic Acids Res. 30, 1944–1951.

Young, D.W., Pratap, J., Javed, A., Weiner, B., Ohkawa, Y., van Wijnen, A., et al., 2005. SWI/SNF chromatin remodeling complex is obligatory for BMP2-induced, *Runx2-dependent skeletal gene* expression that controls osteoblast differentiation. J. Cell Biochem. 94, 720–730.

Yuan, G.C., Liu, Y.J., Dion, M.F., Slack, M.D., Wu, L.F., Altschuler, S.J., et al., 2005. Genome-scale identification of nucleosome positions in *S. cerevisiae*. Science 309, 626–630.

Zeisig, B.B., Cheung, N., Yeung, J., So, C.W., 2008. Reconstructing the disease model and epigenetic networks for MLL-AF4 leukemia. Cancer Cell 14, 345–347.

Zhang, H.S., Gavin, M., Dahiya, A., Postigo, A.A., Ma, D., Luo, R.X., et al., 2000. Exit from G1 and S phase of the cell cycle is regulated by repressor complexes containing HDAC–Rb–hSWI/SNF and Rb–hSWI/SNF. Cell 101, 79–89.

Zhang, J., Wang, L., Zhuang, L., Huo, L., Musa, S., Li, S., et al., 2008. Arp11 affects dynein-dynactin interaction and is essential for dynein function in *Aspergillus nidulans*. Traffic 9, 1073–1087.

Zhao, K., Wang, W., Rando, O.J., Xue, Y., Swiderek, K., Kuo, A., et al., 1998. Rapid and phosphoinositol-dependent binding of the SWI/SNF-like BAF complex to chromatin after T lymphocyte receptor signaling. Cell 95, 625–636.

Zhou, C., Miki, B., Wu, K., 2003. *CHB2,* a member of the *SWI3* gene family, is a global regulator in *Arabidopsis*. Plant Mol. Biol. 52, 1125–1134.

APPLICATION OF NEW METHODS FOR DETECTION OF DNA DAMAGE AND REPAIR

Maria P. Svetlova, Liudmila V. Solovjeva, *and* Nikolai V. Tomilin[1]

Contents

Institute of Cytology, Russian Academy of Sciences, 194064 St. Petersburg, Russian Federation
[1] Deceased on August 4, 2009

Abstract

New methods for detecting DNA damage and repair are reviewed and their potential significance is discussed. These include methods based on analysis of DNA damage-induced chromatin modifications, cytological detection of DNA repair synthesis, damage-induced immobilization of repair proteins and living cell imaging. Special attention is paid to current methods of detection of modifications of histones and other proteins associated with DNA double-strand breaks which represent most dangerous genome damage. New methods of analysis of DNA damage and repair may be useful in biodosimetry, early cancer diagnostics and in the analysis of efficiency of cancer radiation therapy and chemotherapy.

Key Words: DNA repair, DNA damage, Chromatin modifications, Genome damage, Detection methods.   © 2009 Elsevier Inc.

1. INTRODUCTION

Detection of DNA damage induced in chromosomes by radiation and chemical agents is critical for the evaluation of their genetic effects and the efficiency of different pathways of DNA repair in proliferating and non-proliferating cells. It is also important for evaluation of effects of cancer radiation therapy and chemotherapeutic anticancer drugs inducing DNA lesions in tumor cells.

DNA damage may be defined as a stable chemical modification of nitrogen bases in DNA or its sugar–phosphate backbone which leads to the inhibition of transcription, DNA replication, and cell proliferation. For example, irradiation of cells with short-wave ultraviolet (UV) light (254–280 nm) induces in DNA the dimerization of pyrimidine residues of two types: cylobutane pyrimidine dimers (CPDs) and 6-4 pyrimidine-pyrimidone photoproducts (6-4PPs) which suppress DNA replication and should be repaired. Some environmental chemical carcinogens induce bulky adducts to nitrogen bases, for example, benzo[*a*]pyrene–diol-epoxide–DNA adducts, 4-aminobiphenyl–DNA adducts, polycyclic aromatic hydrocarbon–DNA adducts, which inhibit DNA functions. Carcinogen–DNA adducts are considered as a biomarker for cancer risk (Rundle, 2006). Ionizing radiations (IRs) induce a wide spectrum of oxidative base modifications (e.g., thymine glycols; 8-oxoguanine, 8-oxoG) and breaks of sugar–phosphate DNA backbone, some of which can arise because of enzymatic processing of base damage through pathways of DNA repair.

Oxidative DNA damage can also arise spontaneously because of the action of intracellular reactive oxygen species (ROS), and its production is

suppressed by antioxidant systems. Some base modifications have the property of ambiquous pairing during replication: 8-oxoG can pair with cytosine and thymine that lead to C to T transitions. Double-strand DNA breaks (DSBs) induced by IRs disrupt chromosome integrity and can lead to chromosome aberrations and cell death (apoptosis, necrosis) or neoplastic growth (Weinstock et al., 2006).

Multiple DNA repair pathways are known to function in eukaryotic cells. Nucleotide excision repair (NER) has been extensively studied for four decades. NER eliminates damaged segments from duplex DNA through enzymatic cleavage of phosphodiester bonds adjacent to UV-induced pyrimidine dimers or carcinogen–induced DNA adducts. Two overlapping subpathways of NER are known. Global genome repair (GGR) is initiated by proteins deficient in Xeroderma pigmentosum complementation group C (XPC) patients and by UV-damaged DNA–binding protein (UV-DDB), deficient in some Xeroderma pigmentosum complementation group E (XPE) patients (Sugasawa et al., 2005). Second NER subpathway, transcription–coupled repair (TCR), is initiated by the UV-induced transcription block and requires proteins Cockayne syndrome group A (CSA) and Cockayne syndrome group B (CSB) deficient in Cockayne syndrome (CS) patients (Hanawalt and Spivak, 2008). Progressive multisystem degeneration, dwarfism, and segmental premature aging typical for CS illustrate importance of TCR for human health.

Base excision repair (BER) initiates elimination of many different damaged nitrogen bases using enzymes cleaving glycosidic bonds, DNA glycosylases (Barnes and Lindahl, 2004). BER is involved in elimination of endogenous nonoxidative damage like abasic (AB) sites or deaminated cytosines (Barnes and Lindahl, 2004), and oxidative DNA lesions arising due to the action of endogenous ROS are normally suppressed by antioxidant proteins and ATM protein kinase (Zha et al., 2008). BER is responsible for elimination of base lesions and single-strand DNA breaks (SSBs) induced by IRs and alkylating agents and operates through short-patch replacement (one nucleotide) and long-patch replacement subpathways (Fortini and Dogliotti, 2007). It is also recently established that DNA glycosylases and BER are involved in the elimination of 5-methylcytosine (5-meC) from duplex DNA, DNA demethylation (Gehring et al., 2009). 5-meC cannot be considered as a DNA damage but represents the major epigenetic DNA modification introduced enzymatically. In plants, two specific 5-meC-DNA glycosylases are identified (Morales–Ruiz et al., 2006), and in vertebrate embryos (zebrafish) cytosine deaminases assisted by the growth arrest and DNA damage inducible protein 45 (GADD45) are known, that can convert 5-meC into thymine followed by excision of thymine from the T::G mispair by a thymine DNA glycosylase (MBD4) and standard BER (Rai et al., 2008). Mechanism of GADD45 action in demethylation remains to be established (Jiricny and Menigatti, 2008), and

two reports suggest that GADD45a is not involved in DNA demethylation in vertebrates (Engel et al., 2009; Jin et al., 2008). However, mouse GADD45b is required for activity–induced demethylation of specific promoters in a mouse brain (Ma et al., 2009), and GADD45a gene knockout in mice leads to suppression of methyl methanesulfonate (MMS)–induced BER (Jung et al., 2007). Independently of getting the answer to the question about GADD45 involvement in demethylation, it seems likely that DNA repair is involved not only in elimination of DNA damage but also in regulation of major epigenetic genome modification.

Among the pathways involved in DSBs elimination, nonhomologous end joining (NHEJ) repair (Jeggo and Löbrich, 2005; Mahaney et al., 2009; van Gent and van der Burg, 2007) and repair by homologous recombination (HR) (Li and Heyer, 2008; Pierce et al., 2001) are well studied. Most of DSBs induced by IRs are eliminated by NHEJ, and this pathway is also involved in the repair of DSBs arising during site-specific recombination of immunoglobulin genes in normal development (Yan et al., 2007). In mammalian cells the minor fraction of induced DSBs is eliminated by HR, while this pathway is very important for suppression of carcinogenesis that is illustrated by HR deficiency in carriers of mutations in breast cancer succeptibility gene BRCA1 (Westermark et al., 2003). HR repair is hallmarked by involvement of central protein of HR Rad51 which ATPase activity is required for homology-directed DSB repair (Stark et al., 2002).

During the last decade a number of new, simple, and sensitive methods were developed for analysis of DNA damage and repair. The most important were findings of IR–induced foci of repair protein RAD50 (Maser et al., 1997) and specific phosphorylation of histone H2AX at genomic sites containing DSBs (Rogakou et al., 1998, 1999). DSBs represent the most toxic DNA lesions, and their detection is important in many fields of research and in medical diagnostics. Traditional methods of detection of DSBs like centrifugation in neutral sucrose gradients, neutral comet assay, and pulse–field gel electrophoresis are laborious, time–consuming, and have very low sensitivity. Counting of γH2AX foci in the nucleus allowed analysis of DSBs in human cells after very low doses of IR (Rothkamm and Löbrich, 2003), for example, at doses used during computer tomography examinations (Löbrich et al., 2005).

Another impressive technical achievement was detection of transient immobilization of NER protein ERCC1/XPF in living UV-irradiated cells using fluorescence redistribution after photobleaching (FRAP) assay which allowed the estimation of average time required for a single act of NER (Houtsmuller et al., 1999). UV-induced insolubilization of repair/replication protein proliferating cell nuclear antigen (PCNA) in methanol or Triton X–100 extracted non–S–phase cells has been demonstrated earlier (Celis and Madsen, 1986; Toschi and Bravo, 1988). Together, these observations

provided evidence that DNA repair proteins change their physical state during repair that is useful in indirect detection of DNA damage and repair.

Some DNA repair pathways (e.g., NER) include as an integral step of the limited resynthesis of one DNA strand, called DNA repair synthesis (DRS), which can serve as a signature of DNA damage and repair. Traditional radioautographic method of DRS detection in mammalian cells is time- consuming and has low spatial resolution. Usual indirect immunofluorescence detection of DNA synthesis through incorporation of 5-bromo- or 5-iododeoxyuridine (BrdU or IdU) has insufficient sensititvity for DRS, but the sensitivity can be increased using Tyramide system for signal amplification (de Haas et al., 1996; McKay et al., 1997). This system has been used for detection of DRS in non-S-phase cells after low doses of UV light and very short IdU labeling times (Svetlova et al., 1999b, 2002).

Recently, specific UV-induced changes of histone modifications in chromatin were demonstrated (Dinant et al., 2008; Nag and Smerdon, 2009), which may be useful in development of sensitive methods of detection of UV damage and repair. DNA damage-induced epigenetic changes of chromatin should be eliminated, otherwise they can result in stable alteration of patterns of gene expression and pathology.

2. INDIRECT DETECTION OF DOUBLE-STRAND DNA BREAKS AND HOMOLOGY-DEPENDENT REPAIR

2.1. Nuclear foci containing Rad51/BRCA1 and MRE11/Rad50

Nuclear foci containing mammalian Rad51 protein were first detected in cultured human cells treated with MMS, UV-irradiation, or ^{137}Cs gamma-rays (Haaf et al., 1995). In unirradiated S-phase human cells, Rad51 foci colocalize with the foci of breast cancer protein BRCA1 (Scully et al., 1997a). Replication arrest by hydroxyurea or treatment of cells with DNA damaging agents (UV, mitomycin C, gamma-irradiation) lead to the loss of BRCA1 and Rad51 protein from the foci and their reappearance at blocked replication forks marked by the presence of replication factor PCNA (Scully et al., 1997b). Apparently, BRCA1 and Rad51 are involved in homology-directed recombinational repair at stalled replication forks (Moynahan et al., 2001). It has been found recently that BRCA1 interacts with protein phosphatase 1 (PP1), and knockdown of the PP1 catalytic subunit (PP1alpha) using siRNA inhibits DNA damage-induced formation of Rad51 foci (Yu et al., 2008). However, the physiological target of PP1 in the mechanism of formation of Rad51 foci is not established. Analysis of Rad51 foci in S-phase cells containing DNA damage can be used for detection of homology-driven recombinational repair.

In non-S-phase mammalian cells, IR–induced foci are formed by DNA repair proteins Rad50 and MRE11 (Maser et al., 1997). Rad50 foci are not induced by UV, and their number strongly decreases in Ataxia teleangiectasia (AT) cells in contrast to Rad51 foci in which induction increases in AT cells (Maser et al., 1997). Rad50 foci are formed at DSBs in G1 and G2 cells, and MRE11/Rad50/NBS complex is suggested to be the main sensor of DSBs that bridges DNA ends together and initiates DSB repair (Buis et al., 2008; Stracker and Petrini, 2008; Williams et al., 2008). Therefore, MRE11/Rad50 foci can be used as indirect marker of DSBs. Fluorescence intensity correlation analysis increases sensitivity of detection of DSBs using simulteneous staining with Rad50 and MRE11 antibodies (Gerashchenko and Dynlacht, 2009). The detection of MRE11/Rad50 foci arising at transcription–coupled DSBs induced by a chemical agent Et743 might be useful to anticipate tumor response to chemotherapy (Guirouilh Barbat et al., 2008).

2.2. Phosphorylation of histone H2AX

Discrete nuclear foci containing γH2AX can be detected using indirect immunofluorescence with specific antibodies against C-terminal H2AX peptide containing phosphorylated Ser-139 as early as 3 min after treatment of cells with IR (Rogakou et al., 1999). These foci are formed in megabase chromatin domains the number of which corresponds to the number of induced DSBs (Rogakou et al., 1999). Therefore, a minor molecular event (the breakage of the two complementary strands of DNA) is strongly enhanced and represents highly amplified response. Amplification of phosphorylation of histone H2AX at DSBs is achieved through a cascade of biochemical reactions. Initially only two copies of the hMre11/hRad50/NBS1 complexes bind to two DNA ends and recruit ATM kinase which phosphorylates H2AX in nucleosomes near DSBs. Subsequent accumulation of many copies of this complex is triggered by phosphorylated MDC1 protein which directly binds to γH2AX (Spycher et al., 2008).

Many techniques were developed for detection of Ser-139 phosphorylated histone H2AX in different biological samples (Table 6.1) (Gavrilov et al., 2006; Ismail et al., 2007; Muslimovic et al., 2008; Nakamura et al., 2006; Olive, 2004; Pilch et al., 2004; Sedelnikova and Bonner, 2006). Flow cytometry-based assay of γH2AX detection in nonfixed peripheral blood cells was capable of recognizing DNA damage at levels 100-fold below the detection limit of the alkaline comet assay (Ismail et al., 2007; Muslimovic et al., 2008). Counting of γH2AX foci in the nuclei is an extremely sensitive method of analysis of DSBs with sensitivity several orders of magnitude higher than sensitivity of other methods of detection of DSBs (Rothkamm and Löbrich, 2003). Sensitivity of detection of radiation-induced DSBs is significantly limited by background level of γH2AX in unirradiated control cells. In some mammalian cell lines, this background is very low, allowing quantitation

Table 6.1 Modern methods of detection of DNA damage

Type of damage	Method	Sensitivity	References
DSBs	2D-gel analysis of H2AX	Moderate	Pilch et al. (2004)
DSBs	IF nuclear foci, anti-γH2AX Ab	High	Rogakou et al. (1999) and Rothkamm and Löbrich (2003)
DSBs	IF nuclear foci (IRIF), anti-Rad50, MRE11 Ab	High	Maser et al. (1997)
DSBs	Immunoblotting, anti-γH2AX Ab	Moderate	Nazarov et al. (2003) and Tomilin et al. (2001)
DSBs	Flow cytometry, anti-γH2AX Ab	Moderate	MacPhail et al. (2003) and Muslimovic et al. (2008)
Carcinogen–DNA adducts	Variable immunological	Moderate	Santella (1999)
UV-damage in DNA	Specific Ab, ELISA, IF staining	High	Cooke et al. (2003)
UV-damage in DNA	IF, insolubilization of XPA, PCNA	Low	Aboussekhra and Wood (1995) and Svetlova et al. (1999a)
UV-damage in DNA	IF, incorporation of BrdU, IdU, CldU without Tyramide	Low	Svetlova et al. (2005)
UV-damage in DNA	IF, incorporation of IdU plus biotin-Tyramide	High	Svetlova et al. (1999b, 2002)
8-Oxoguanine in DNA	Cytometry, avidin-FITC	High	Struthers et al. (1998)
8-OHdG in urea	HPLC	Moderate	Tagesson et al. (1995)
8-OHdG in urea	Capillary EF, amperometric detection	High	Xu et al. (2008)
AP sites in DNA	Biotinylated aldehyde-specific reagent	Moderate	Kow and Dare (2000)

of DSBs at cGy level (Rothkamm and Löbrich, 2003), but in many other cell lines the background is high. Nevertheless, H2AX is recommended as a top candidate protein biodosimeter for human exposure to IR (Marchetti et al., 2006). Using antibodies to γH2AX, DSBs were also detected after treatment of cells with anticancer drug bleomycin (Tomilin et al., 2001).

Phosphorylation of H2AX in megabase chromatin domains can lead to significant changes of gene expression, since some data indicate that transcription is inhibited at γH2AX foci in human cells (Svetlova et al., 2007). Figure 6.1 shows suppression of incorporation of BrUTP in the living
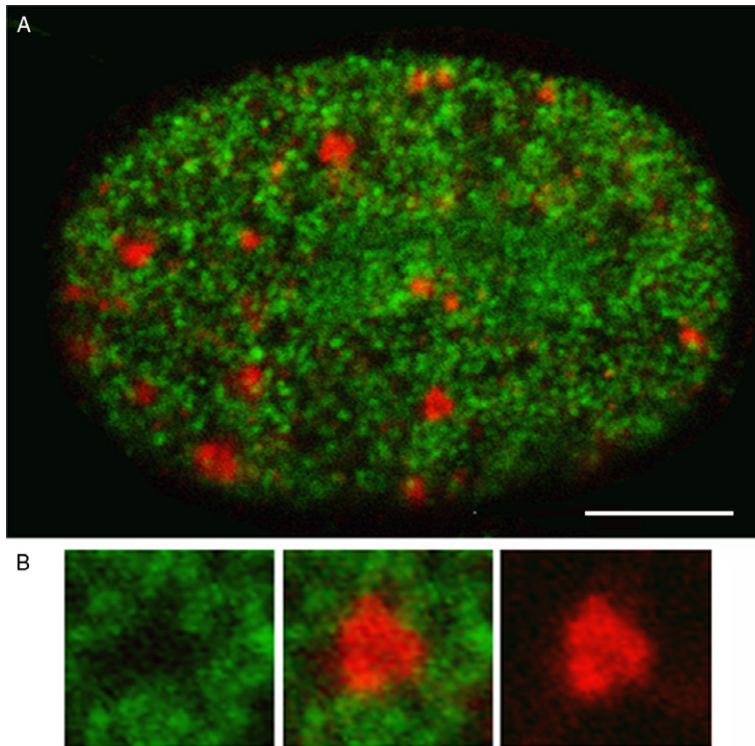
Figure 6.1 Simultaneous visualization of transcription (green) and histone γH2AX (red) in IR–treated human embryonal fibroblasts. (A) Confocal image of cell nucleus 1 h after 1 Gy irradiation and BrUTP incorporation (green signal, obtained using mouse anti–BrdU antibodies, biotinylated sheep antimouse IgG, and avidin–FITC) during subsequent 30 min. Transcription is suppressed at γH2AX foci (red signal, detected with rabbit anti–γH2AX antibodies, and Alexa Fluor 568-conjugated goat anti-rabbit IgG). (B) Represents enlarged segment of the nucleus containing single γH2AX focus (middle). Left, green channel; right, red channel; center, both channels. For technical details see Solovjeva et al. (2007). With kind permission from Springer Science+Business Media: Solovjeva et al. (2007), Figure 1B, Copyright 2007.

human embryonal fibroblasts at radiation–induced nuclear γH2AX foci. It is possible that γH2AX binds to RNA polymerase II engaged in transcription and suppresses its movement (Svetlova et al., 2007). Inhibition of transcription by actinomycin D induces γH2AX (Ljungman et al., 1999; Mischo et al., 2005), suggesting the existence of a tight link between induction of DSBs, inhibition of transcription and H2AX phosphorylation. However, γH2AX-comprising chromatin contains not only this modified histone but also many other proteins which may interfere with transcription.

Available evidence strongly suggests that γH2AX can also be formed spontaneously in the absence of IR (Banáth et al., 2004; Bartkova et al., 2005; McManus and Hendzel, 2005; Nazarov et al., 2003; Sedelnikova and Bonner, 2006; Warters et al., 2005; Yu et al., 2006). Elevated levels of endogenous γH2AX is general characteristic for cultured cancer cells, tumors, and premalignant lesions (Bartkova et al., 2005; Sedelnikova and Bonner, 2006). Therefore, γH2AX can serve as a potential biomarker for cancer diagnostics, prediction, and recurrence (Sedelnikova and Bonner, 2006). However, it remains unclear whether spontaneously formed γH2AX is actually associated with random DSBs in non–S-phase cancer cells. Some cervical cancer cell lines (HeLa, Caski, SW756) show >20 spontaneous γH2AX foci per nucleus (Banáth et al., 2004). It is likely that most of these foci arise at replication forks in S-phase cancer cells (Ward and Chen, 2001; Ward et al., 2004) and probably reflect an increased aberrant cell proliferation in preneoplastic and neoplastic tissues now called ''oncogenic stress'' (Bartkova et al., 2005) or ''replication stress'' (Sedelnikova and Bonner, 2006).

About 50 spontaneous DSBs are formed at replication forks during S phase resulting in ~ 10 spontaneous sister chromatid exchanges (SCEs) in each normally proliferating cell and to ~ 50 SCEs/cell in Bloom syndrome lymphocytes (Vilenchik and Knudson, 2003, 2006). In normal cells the majority of potential DSBs do not arise at all or are rapidly eliminated through nonrecombinational modes of repair which do not lead to formation of γH2AX. In cancer cells most of the potential DSBs do arise at replication forks and are poorly repaired, resulting in replication stress and γH2AX formation.

2.3. DSB-induced nuclear foci of other proteins

In damaged cells nuclear foci of p53-binding protein 1 (53BP1) (Schultz et al., 2000), mediator of DNA damage checkpoint 1 protein (MDC1) (Bekker-Jensen et al., 2006; Stewart et al., 2003), protein phosphatase 2A (PP2A) (Chowdhury et al., 2005), and Ring-finger ubiquitin ligase RNF8 (Huen et al., 2007; Kolas et al., 2007; Mailand et al., 2007) were detected. In unirradiated cells 53BP1 shows diffuse nuclear staining, but after treatment with IR discrete nuclear foci can be detected that colocalize with radiation-induced foci of MRE11 and γH2AX (Schultz et al., 2000).

Induction of 53BP1 foci does not depend on ATM kinase, and they are formed very rapidly after IR suggesting that 53BP1 functions early in the cellular response to DSBs, for example, in a checkpoint pathway (DiTullio et al., 2002; Schultz et al., 2000; Sengupta et al., 2004). 53BP1, but not MDC1 and BRCA1, mediates IR-induced ATM Serine-1981 autophosphorylation (Wilson and Stern, 2008), and, therefore, 53BP1 acts upstream of γH2AX, the formation of which depends on indicated ATM autophosphorylation (Bakkenist and Kastan, 2003). 53BP1 Ser-1219 is phosphorylated by ATM kinase upon DNA damage (Lee et al., 2009). It has been recently found that for stable retention of 53BP1 in chromatin its monoubiquitynation at lysine-1268 by Rad18 is required (Watanabe et al., 2009). 53BP1 foci can be used to identify DSBs not only in fixed but also in living cells (Jakob et al., 2009).

Formation of nuclear foci of the MDC1 protein requires γH2AX, and MDC1 form a complex with γH2AX (Stewart et al., 2003). MDC1 is phosphorylated by DNA damage-activated ATM kinase (Kolas et al., 2007). MDC1 also controls formation of DNA damage-induced foci of 53BP1, BRCA1, MRN complex (MRE11/Rad50/NBS1) (Stewart et al., 2003) and promotes the spread of H2AX phosphorylation in chromatin around DSBs (Bekker-Jensen et al., 2006; Lukas et al., 2004). Constitutive phosphorylation of MDC1 by casein kinase 2 is responsible for its ability to recruit MRE11/Rad50/NBS1 complex to γH2AX-containing chromatin (Spycher et al., 2008). MRN complex then activates ATM kinase (Lee and Paull, 2004). Therefore, MDC1 is the main amplificator of signals in cellular response to DSBs. Cells lacking MDC1 also fail to activate the intra–S–phase and G2/M phase cell–cycle checkpoints properly after exposure to IR, which was associated with an inability to regulate Chk1 (Stewart et al., 2003).

Ubiquitin ligase RNF8 binds to phosphorylated protein MDC1, and this is accompanied by an increase in DSB-associated ubiquitylation of 53BP1 and followed by its accumulation at repair foci (Huen et al., 2007; Kolas et al., 2007; Mailand et al., 2007). RNF8 also ubiquitylates histones H2A and H2AX, and their ubiquitylated forms colocalize with γH2AX foci in the nucleus (Mailand et al., 2007). Therefore, antibodies against RNF8 and ubiquitylated H2A can be used for detection of DSBs. Ubiquitylated histone H2A bind additional ubiquitin ligase RNF168 which acts with UBC13 to amplify RNF8-dependent histone ubiquitylation (Doil et al., 2009; Stewart et al., 2009). Mutation of RNF168 is identified in the RIDDLE syndrom characterized by immunodeficiency and radiosensitivity (Stewart et al., 2009).

PP1 and PP2A were suggested to be involved in dephosphorylation of γH2AX after DSB rejoining (Chowdhury et al., 2005; Nazarov et al., 2003).

PP2A colocalizes with radiation-induced γH2AX foci, and the recruitment of PP2A to DNA damage foci is H2AX-dependent (Chowdhury et al., 2005). Moreover, when PP2A catalytic subunit is inhibited or silenced by RNA interference, γH2AX foci persist, DNA repair is inefficient, and cells are hypersensitive to DNA damage (Chowdhury et al., 2005). Causes of inhibition of DNA repair upon inhibition of PP2A expression are unclear, since it is unknown if this protein phosphatase is required for DSB rejoining. Although it remains to be established how γH2AX elimination is coupled to DSB repair, the analysis of radiation-induced PP2A nuclear foci may be helpful in detection of DSBs.

3. Methods Based on Changes of Physical Properties of Proteins Involved in Nucleotide Excision and Postreplication Repair

3.1. Insolubilization of proliferating cell nuclear antigen (PCNA) during NER

NER is the main DNA repair pathway in mammals for removal of UV-induced lesions. NER involves the concerted action of more than 25 polypeptides. The most common types of DNA damage targeted by NER are cyclobutane pyrimidine dimers and 6-4PPs, both produced by the UV component of sunlight. It was suggested long time ago that NER operates in intact cells as a preassembled holocomplex that finds DNA damage by processive scanning of large genome segments. Repairosome-like holocomplex for NER has been identified in yeast (Svejstrup et al., 1995). An alternative view is that individual NER proteins act in a distributive fashion by diffusion and binding to sites of DNA damage: in this case, they can sequentially change their physical properties (e.g., solubility) during repair (Volker et al., 2001).

It has been found that DNA replication protein PCNA changes its solubility in methanol after its recruitment to DNA in undamaged S-phase cells (Madsen and Celis, 1985). In non-S-phase cells, PCNA becomes insoluble in methanol in G1/G2 cells only after UV-irradiation (Celis and Madsen, 1986), suggesting that this insolubilization may be associated with NER. During DNA replication, PCNA is loaded onto DNA by replication factor C (RFC) as a trimeric ring-like complex functioning as a sliding clamp for DNA polymerases delta/epsilon (Pol-delta/Pol-epsilon), nuclease FEN1, DNA ligase I and other replication proteins facilitating their movement along DNA (Moldovan et al., 2007).

In methanol-fixed or detergent-treated replicating cells, soluble PCNA is extracted and immobilized PCNA is detected in DNA replication centers using immunostaining and fluorescent microscopy (Bravo and MacDonald-Bravo, 1987; Madsen and Celis, 1985).

Changes of PCNA extractability can be detected following UV-irradiation in non–S-phase cells extracted by methanol (Celis and Madsen, 1986) or detergent Triton X-100 (Miura et al., 1992a; Toschi and Bravo, 1988). Rapid (within 30 min after irradiation) UV-induced insolubilization of PCNA, that is, the appearance of nonextractable PCNA foci after UV-irradiation in non–S-phase cells was interpreted as an indication of involvement of this protein in DNA resynthesis step of NER. This involvement is likely, since rapid PCNA insolubilization was found to depend on functional NER proteins XPA, XPG, XPF, XPG, XPB, and CSB (Aboussekhra and Wood, 1995; Balajee et al., 1998; Miura and Sasaki, 1996) and PCNA is known to be required for NER *in vitro* (Shivji et al., 1992). However, methanol-insoluble PCNA has been found in the XPA G1/G2 cells 3 h after UV irradiation, suggesting the existence of two different types of UV-induced PCNA complexes only one of which (rapidly formed) is indicative of NER (Miura et al., 1992b). Possible function of the slowly formed UV-induced insoluble PCNA remains unclear, but it can reflect long-term changes of chromatin in UV-damaged cells.

The mechanism of accumulation of PCNA at the sites of UV damage has been studied recently using DNA damage produced locally by UVA-laser micro-irradiation (365 and 405 nm) in HeLa cells (Hashiguchi et al., 2007). In DNA replication, trimeric PCNA is loaded onto DNA in an ATP-dependent fashion by RFC consisting of five subunits, the most important among them is the subunit RFC140 that binds to 3′ template-primer junction (Majka and Burgers, 2004). Local irradiation with 365 or 405 nm laser induces rapid accumulation of green fluorescent protein (GFP)-tagged PCNA and GFP-tagged RFC subunits in the nucleus (Hashiguchi et al., 2007). The 405 nm laser-induced local PCNA accumulation 2 or 5 min after irradiation can occur without assistance of RFC140 (Hashiguchi et al., 2007), indicating that the loading of trimeric PCNA ring around DNA is not required for its UV-induced accumulation. However, DRS *in vitro* requires RFC for loading of PCNA and Pol-delta (Mocquet et al., 2008). It remains unclear whether 405 and 365 nm laser UVA actually induce NER but not other types of repair (Dinant et al., 2007). Dinant et al. (2008) have shown that irradiation of Hoechst 33342-sensitized cells at 405 nm induces both DSBs and CPDs. It should be noted that PCNA interacts with a very large number (>100) of different proteins (Naryzhny, 2008) some of which can possibly mediate its unspecific binding to sites of UV damage in the nucleus without formation of trimeric ring on DNA.

3.2. Immobilization of ERCC1/XPF and other NER proteins (FRAP)

To study the nuclear organization and dynamics of NER, the endonuclease ERCC1/XPF (excision repair cross complementation group 1/Xeroderma pigmentosum group F) was tagged with GFP and its mobility was monitored in living Chinese hamster ovary cells (Houtsmuller et al., 1999). In the absence of DNA damage, the complex moved freely through the nucleus, with a diffusion coefficient consistent with its molecular size. UV light-induced DNA damage caused a transient dose-dependent immobilization of ERCC1/XPF, likely due to engagement of the complex in a single repair event. After 4 min the complex regained mobility. These results suggest that NER operates by assembly of individual NER factors at sites of DNA damage rather than by preassembly of holocomplexes and that ERCC1/XPF complex is involved in repair of DNA damage in a distributive fashion rather than by processive scanning of large genome segments.

The Xeroderma pigmentosum group A (XPA) protein has been suggested to function as a central organizer in NER. It is unknown how XPA finds DNA lesions and how the protein is distributed in time and space in living cells. Rademakers et al. (2003) have established that the majority of XPA moves rapidly through the nucleoplasm with a diffusion rate different from those of other NER factors tested, arguing against a preassembled XPA-containing NER complex. DNA damage induces a transient (approximately 5 min) immobilization of maximally 30% of XPA. Immobilization depends on XPC, indicating that XPA is not the initial lesion recognition protein *in vivo*. Moreover, loading of replication protein A (RPA) on NER lesions was not dependent on XPA. Thus, XPA participates in NER by incorporation of free diffusing molecules in XPC-dependent NER–DNA complexes. This study supports a model for a rapid consecutive assembly of free factors during early steps of NER, and a relatively slow simultaneous disassembly (Rademakers et al., 2003). However, these observations do not exclude a model in which another NER complex exists containing low mobility subunits like PCNA (Aboussekhra and Wood, 1995; Mocquet et al., 2008). Highly processive DNA replication complex contains very mobile subunits like DNA Pol-eta and Pol-iota and nuclease flap endonuclease 1 (Fen1) (Sabbioneda et al., 2008; Solovjeva et al., 2005).

Dynamic interactions of the DNA damage-binding protein 2 (DDB2) and cullin 4A (CUL4A) with UV-damaged DNA has been studied in living cells using EYFP-tagged DDB2 and EGFP-tagged CUL4A (Luijsterburg et al., 2007). DDB2 is involved in the global NER and interacts with CUL4A forming E3 ubiquitin ligase; this complex is bound to many more damaged sites than XPC, suggesting that there is little physical interaction between the two proteins (Luijsterburg et al., 2007). The distribution of DDB2-EYFP in non-UV-irradiated living fibroblasts is

homogeneous but UV-irradiated cells show regions of dense and less dense DDB2 fluorescence in the nucleus, similar to the uneven distribution of chromatin. This is not observed for other NER factors except TFIIH (Volker et al., 2001). In contrast, XPC protein readily associates with interphase and mitotic chromatin in the absence of DNA damage (Hoogstraten et al., 2008). Half-time of release of DDB2 at damaged sites demonstrated using fluorescence loss in photobleaching (FLIP) assay ($t_{1/2}$ of the FLIP curves) is found to be ~ 110 s at 37 °C in normal as well as in XPC cells in which GGR is suppressed. This observation indicates that the transient UV-induced recruitment of DDB2 to chromatin is not directly linked to GGR and reflects some chromatin changes in UV-irradiated cells, for example, their preparation for assembly of the NER complex (Luijsterburg et al., 2007). NER endonuclease XPG is recruited to UV-damaged DNA with a half-life of 200 s and is bound for 4 min in NER complexes (Zotter et al., 2006). The recruitment requires functional TFIIH but the binding of XPG to damaged DNA does not require the DDB2 protein, which is thought to enhance damage recognition by XPC protein. XPC constantly associates with and dissociates from chromatin in the absence of DNA damage, and after UV-irradiation its mobility decreases (Hoogstraten et al., 2008). Residence times of 28 and 45 s in UV-irradiated cells were found for XPC-EGFP and XPG-EGFP, respectively (Luijsterburg et al., 2007).

Solovjeva et al. (2005) studied mobility in living cells of the GFP-CSA protein that is required for TCR during NER and does associate with transcription foci after DNA damage (Kamiuchi et al., 2002). It was found that the high mobility of GFP-CSA (redistribution time < 4 s) did not change after UV-irradiation (Solovjeva et al., 2005).

3.3. UV-induced insolubilization of XPA and other NER proteins

UV-induced insolubilization was observed not only for PCNA but also for other NER proteins, including XPA, RPA, TFIIH, XPC, XPF, and UV-DDB (Oh et al., 2007; Rapić Otrin et al., 1998; Svetlova et al., 1999a; Volker et al., 2001; Wakasugi et al., 2002). It has been found using a local UV-irradiation approach that XPC/hHR23b repair complex is insolubilized first, TFIIH and XPA proteins associate relatively late, and XPA is required for anchoring of XPF/ERCC1 (Volker et al., 2001). This indicates that XPC works before XPA in NER. However, XPA and XPG are recruited to UV sites independently of XPB protein, a subunit of TFIIH (Oh et al., 2007). UV-DDB complex (heterodimer of p127 and p48) which greatly stimulates excision of CPDs *in vitro*, accumulates at UV-irradiated sites in the nucleus immediately after UV and independently of XPA and XPC proteins (Wakasugi et al., 2002). Structural studies indicate that

6-4PP photolesion in duplex DNA is exclusively recognized by WD40 propeller of the DDB2 (p48) protein, a small subunit of UV-DDB (Scrima et al., 2008).

Using electron microscopy it has been recently shown that XPC and XPA proteins rapidly accumulate in the perichromatin region after UV irradiation, whereas only XPC is also moderately enriched in condensed chromatin domains (Solimando et al., 2009). These observations suggest that DNA damage is detected by XPC throughout condensed chromatin domains, but DNA-repair complexes are preferentially assembled in the perichromatin region. It was proposed, therefore, that UV-damaged DNA inside condensed chromatin domains is relocated to the perichromatin region (Solimando et al., 2009). However, condensed chromatin is freely accessible to large macro-molecules in the mammalian nucleus (Verschure et al., 2003), and an absence of XPA in condensed chromatin is surprising, taking into account its very high diffusional mobility (Rademakers et al., 2003).

3.4. Protein dynamics in postreplication repair

Originally detected in fixed cells (Nakamura et al., 1986), DNA replication foci (RFi) were later visualized in living cells by using GFP-tagged prolif-erating cell nuclear antigen PCNA (Leonhardt et al., 2000). It has been shown using FRAP assay that focal GFP–PCNA slowly exchanges, suggest-ing the existence of a stable replication holocomplex (Leonhardt et al., 2000). Solovjeva et al. (2005) used the FRAP assay to study the dynamics of the GFP-tagged PCNA-binding proteins: Fen1 and DNA Pol-eta in Chinese hamster cells. In undamaged cells, GFP–Pol-eta and GFP–Fen1 are mobile with residence times at RFi approximately 2 and 0.8 s, respectively. After MMS damage, the mobile fraction of focal GFP–Fen1 decreased, and residence time increased, but then the mobility gradually recovered. The mobilities of focal GFP–Pol-eta and GFP–PCNA did not change after MMS. These data indicate that the normal replication complex contains immobile subunit (PCNA) and at least two mobile subunits (Pol-eta and Fen1). The decrease of the mobile fraction of focal GFP–Fen1 after DNA damage (Fig. 6.2) suggests that Fen1 exchange depends on the rate of movement of replication forks.

Diffusional mobility of Pol-eta and Pol-iota has also been studied in human cells (Sabbioneda et al., 2008). It has been found that both Y polymerases are highly mobile, and residence time of Pol-eta (but not of Pol-iota) associated with RFi is slightly increased after UV-irradiation but still remains very low, less than 1 s (Sabbioneda et al., 2008). The biological significance of this increase is unclear but it may reflect the time required for lesion bypass during replication.

Rad18 protein is required for monoubiquitination of PCNA and translesion synthesis during DNA lesion bypass in eukaryotic cells
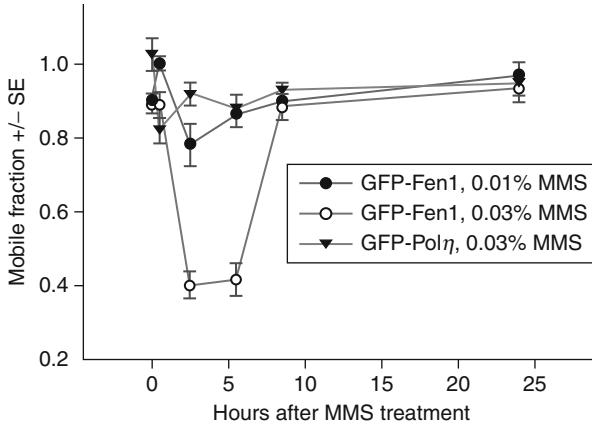
Figure 6.2 Mobility of focal GFP-Fen1 and GFP-Polη proteins in Chinese hamster V79 cells after treatment with methyl methanesulfonate (MMS). *Circles* (GFP-Fen1) and *triangles* (GFP-Polη) represent mobile fractions of indicated proteins at different times after MMS treatment calculated as described by Solovjeva et al. (2005). The mobile fraction of focal GFP-Fen1 is strongly decreased at 2–5 h after MMS treatment. Reprinted from Solovjeva et al. (2005), Copyright 2005, with permission from American Society for Cell Biology.

(Prakash et al., 2005). Rad18 is also involved in ubiquitination of the 9-1-1 checkpoint clamp (Fu et al., 2008) and RFC complex subunit RFC2 (Tomida et al., 2008). Rad18 protein rapidly translocates to the nuclei of UV-irradiated mammalian cells, accumulating at sites of stalled replication as discrete observable foci colocalizing with Pol-eta and PCNA (Watanabe et al., 2004). RAD18 also translocates to the nucleus in response to replication stress induced by dNTP depletion or after induction of DSBs where it can promote DSB repair in G1 cells through retention of 53BP1 (Watanabe et al., 2009). GFP-tagged human Rad18 expressed in Chinese hamster cells can be completely extracted from undamaged nuclei by Triton X-100 and methanol (Nikiforov et al., 2004). However, several hours after treatment with MMS, the Triton-insoluble form of GFP-Rad18 accumulates in S-phase nuclei where it colocalizes with PCNA (Fig. 6.3). This accumulation is suppressed by the inhibitor of protein kinases staurosporine (Svetlova et al., 1998) and wortmannin but is not effected by roscovitine (Nikiforov et al., 2004). It has also been found that MMS induces phosphorylation of Ser-317 in protein kinase Chk1 and Ser-139 in histone H2AX and stimulates formation of single-stranded DNA at RFi (Nikiforov et al., 2004). Together, these results suggest that MMS-induced accumulation of Rad18 protein at stalled replication forks involves protein phosphorylation which may be performed by S-phase checkpoint kinases.
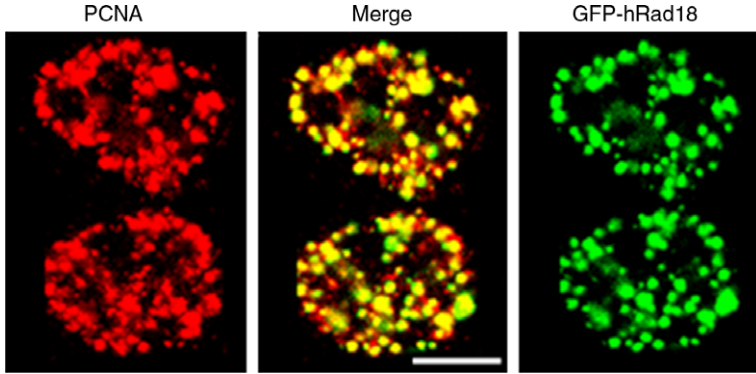
Figure 6.3 Accumulation of GFP-hRad18 at stalled replication forks in Chinese hamster cells treated with MMS. Cells transiently transfected with the plasmid encoding GFP-hRad18 were treated with 0.03% MMS for 1 h and then incubated without MMS for 4 h as described by Nikiforov et al. (2004). Before fixation transfected cells were extracted with a buffer containing Triton X-100 for elimination of soluble fractions of PCNA and hRad18. Triton-isoluble PCNA (red signal, visualized using mouse monoclonal antibodies against PCNA, biotinylated sheep anti-mouse IgG, and avidin–Texas Red) is associated with replication centers in S-phase cells (Toschi and Bravo, 1988). MMS treatment induces accumulation of hGFP-hRad18 at replication centers with stalled replication forks (Nikiforov et al., 2004). Reprinted from Nikiforov et al. (2004), Copyright 2004, with permission from Elsevier.

4. NEW METHODS FOR ANALYZING UV-INDUCED DNA REPAIR SYNTHESIS AND CHROMATIN MODIFICATIONS

4.1. Detection of incorporation of halogenated deoxyuridines in UV-irradiated cells

Tritium radioautography has been traditionally used for detection of DRS in UV-irradiated cells (Cleaver and Bootsma, 1975), and incorporation of BrdU has been widely used for detection of DNA replication using immunofluorescence (Nakamura et al., 1986). DNA RFi were also detected in mammalian cells by double labeling with two halogenated deoxyuridines: IdU and 5-chlorodeoxyuridine (CldU) (Manders et al., 1992, 1996). Immunofluorescent detection of incorporated IdU and CldU has been used for analysis of the UV-induced DRS in mammalian cells (Svetlova et al., 1999b, 2002, 2005). DRS-dependent incorporation of IdU is very low, but fluorescent signal can be amplified using Tyramide system (de Haas et al., 1996; McKay et al., 1997) allowing reliable detection of DRS in human cells at very short (10 min) IdU labeling times (Fig. 6.4A and B) after
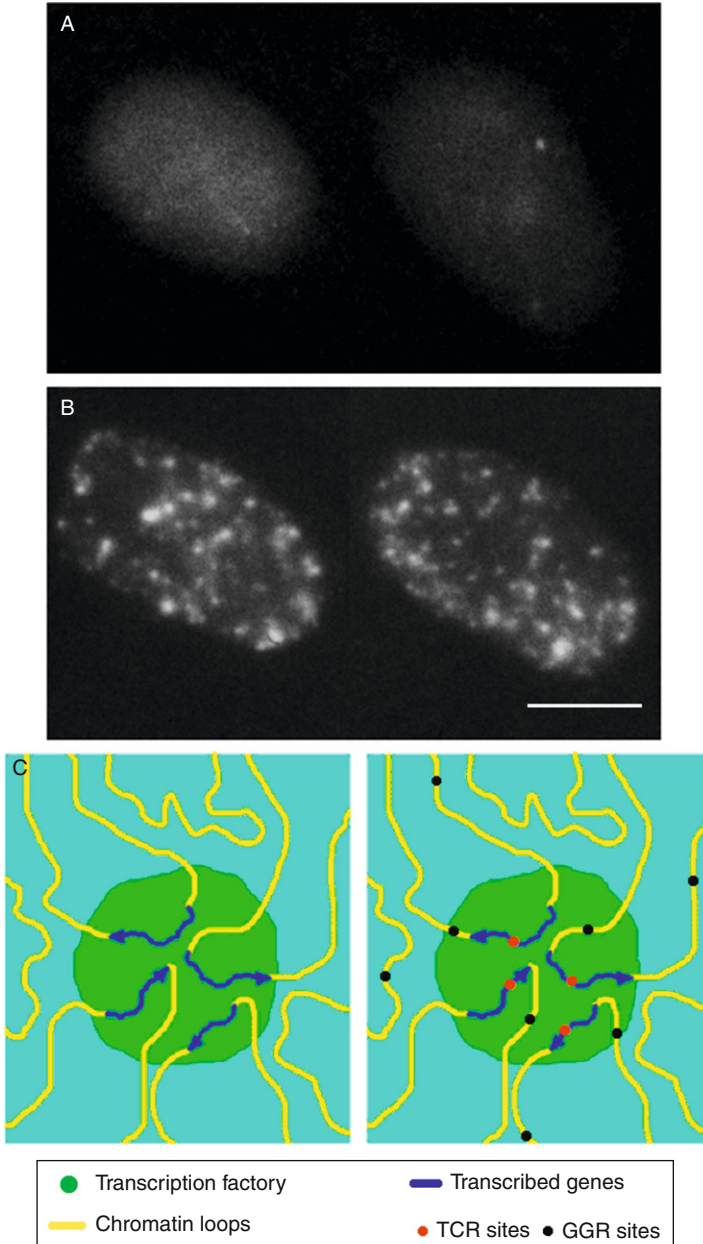
Figure 6.4 Focal sites of DNA repair synthesis in UV-irradiated human fibroblasts. Immediately after UV-irradiation (30 J/m^2), human quiescent fibroblasts were incubated for 10 min in the growth medium containing 5-iododeoxyuridine (IdU), and IdU was detected using antibodies against 5-bromodeoxyurine (BrdU) and signal amplified using Tyramide-biotin (de Haas et al., 1996; McKay et al., 1997) as described by Svetlova et al., 1999b, 2002. (A) Unirradiated control cells, (B) irradiated cells

UV-irradiation (Svetlova et al., 1999b, 2002). Since each individual repair synthesis patch is about 30-nt long (Bowman et al., 1997) and is not sufficent for detection using indirect immunofluorescence even with Tyramide amplification, it is likely that the detected discrete foci of DRS represent clusters of several DRS patches (Svetlova et al., 1999b, 2002). These DRS clusters can arise, for example, at clustered sites of transcription called transcription "factories" (Carter et al., 2008; Cook, 1999; Jackson et al., 1998; Mitchell and Fraser, 2008; Sexton et al., 2007) during TCR, a NER subpathway (Hanawalt and Spivak, 2008). In agreement with this view the number of observed DRS foci is independent of UV doses in the range 10–30 J/m^2 (Svetlova et al., 1999b) and their formation is suppressed in NER–proficient cells by transcription inhibitor alpha-amanitin and in CS cells deficient in TCR (Svetlova et al., 2002). The lack of UV dose dependence on the average DRS number per nucleus can be explained by a limited number of active transcription factories in a given type of cells (Mitchell and Fraser, 2008; Sexton et al., 2007). It is important that transcription factories remain in the absence of transcription (Mitchell and Fraser, 2008) and, therefore, should be conserved after UV-irradiation, when transcription is inhibited. Figure 6.4C shows a model of clustering of DRS events during NER in transcription factories. In this model, TCR-associated DRS patches concentrate at transcription factories, but DRS patches associated with GGR are not excluded from these nuclear compartments (Fig. 6.4C).

Since transcription factories may be enriched not only in the active form of RNA polymerase II but also in other transcription and repair factors, it is likely that GGR-associated DRS patches are also clustered in these compartments. This can explain detection of some DRS foci in the absence of TCR (in CS cells), which can only arise because of GGR (Svetlova et al., 2002). Recent *in vitro* observations suggest that the formation of DRS complex containing PCNA and RFC requires XPF 5′ incision, and positioning of RFC is facilitated by RPA and XPG; these proteins are released as soon as Pol–delta is loaded by the RFC/PCNA complex (Mocquet et al., 2008). Then Pol–delta can jump because of collision release (Langston and O'Donnell, 2008) filling different repair gaps spatially clustered in one transcription factory which should only contain RFC-loaded PCNA clamps (Langston and O'Donnell, 2008).

---

containing focal sites of DNA repair synthesis, and (C) a model explaining clustering of DNA repair synthesis events during transcription-coupled repair (TCR) in transcription factories. *Left*: the fragment of unirradiated cell with transcription factory and chromatin loops with transcribed genes. *Right*: the fragment of UV-irradiated cell containing TCR- and GGR-associated sites of DNA repair synthesis. This model explains the detection of repair-associated foci with Tyramide system in very short times of repair label incorporation. Bar is 10 μm.

4.2. Evidence for two pools of precursors for DRS

Double labeling of interphase and metaphase chromosomes by CldU and IdU was used in studies of the dynamics of DNA replication (Manders et al., 1992, 1996). Double labeling has also been used to analyze sites of DRS during NER in quiescent human fibroblasts (Svetlova et al., 2005). It has been found that when both precursors are added at the same time to UV-irradiated non–S-phase cells, they label different sites in the nucleus (Fig. 6.5B). In contrast, even very short periods of simultaneous IdU plus CldU labeling of S-phase cells produced mostly overlapped IdU and CldU RFi (Fig. 6.5A) in agreement with observations of other workers (Manders et al., 1992, 1996). The differential labeling of repair sites might be due to compartmentalization of IdUTP and CldUTP pools, or to differential utilization of these thymidine analogs by Pol-eta and Pol-epsilon. To explore the latter possibility, purified mammalian DNA polymerases were used in the *in vitro* experiments and it has been shown that IdUTP is efficiently utilized by both Pol-delta and Pol-epsilon (Svetlova et al., 2005). However, it has been found that the UV-induced incorporation of IdU is more strongly stimulated by treatment of cells with hydroxyurea than the incorporation of CldU. This indicates that there may be distinct IdU and CldU-derived nucleotide pools differentially affected by inhibition of the ribonucleotide reductase pathway of dNTP synthesis, and that is consistent
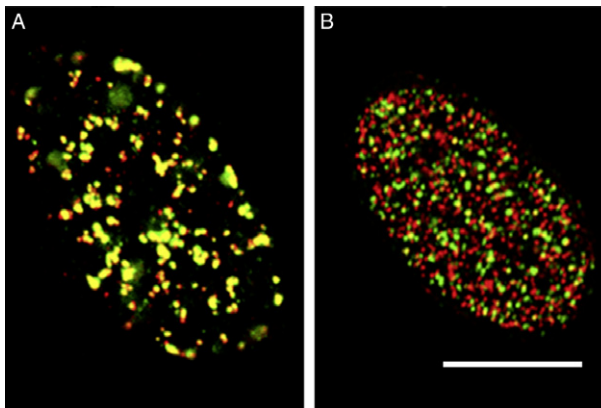
Figure 6.5   Visualization of CldU (green) and IdU (red) incorporated simultaneously in human fibroblasts. (A) Undamaged S-phase cell after incubation for 5 min with CldU and IdU (10 μM each). Colocalization (yellow) of red and green signals indicates simultaneous incorporation of CldU and IdU in the same nuclear domains (Manders et al., 1992, 1996). (B) A cell that incorporated CldU and IdU (10 μM each) during 3 h after UV-irradiatioin with the dose 30 J/m^2. Very little overlap of CldU and IdU foci is seen. Technical details can be found under Svetlova et al. (2005). Bar is 10 μm.

with the view that the differential incorporation of IdU and CldU during NER may be caused by the compartmentalization of IdU- and CldU-derived nucleotide pools (Svetlova et al., 2005). Biological significance of these observations remains to be established, but compartmentalization of the DRS nucleotide pools leads to differential IdU/CldU labeling of metaphase chromosomes (Fig. 6.6). Analysis of the distribution of IdU incorporated into metaphase chromosomes during UV-induced DRS in human VH-10 cells indicates that some clusters of DRS label coincide with the known clusters of expressed genes (e.g., at 4q21 and 5q31) (Svetlova et al., 2002).

4.3. UV-induced histone modification and histone deposition

Stimulation of UV-induced DRS by chromatin hyperacetylation was first detected 20 years ago (Ramanathan and Smerdon, 1989). However, UV-induced modifications of chromatin were clearly demonstrated only recently (Bergink et al., 2006; Dinant et al., 2008; Nag and Smerdon, 2009; Polo et al., 2006; Wang et al., 2006; Yu et al., 2005). UV-induced monoubiquitylation of histone H2A by the ubiquitin ligase Ring2 has been found to be NER-dependent (Bergink et al., 2006) but it is not required for
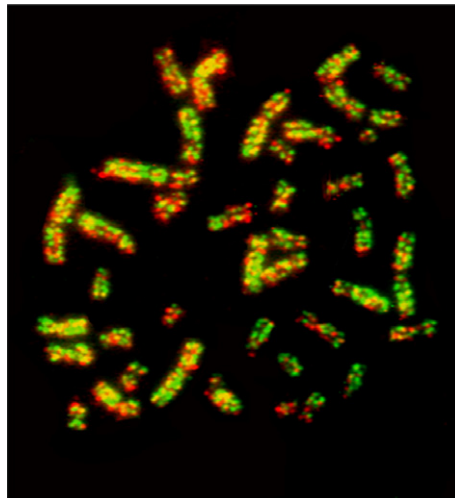
Figure 6.6 UV-induced sites of DNA repair synthesis after simultaneous incorporation of IdU and CldU in human fibroblasts. Quiescent fibroblasts were UV-irradiated with the dose 3 J/m^2, and CldU and IdU were incorporated during 2 h. Twenty hours later the cells were replated at low density for stimulation of cell division and cultivated for additional 24 h (Svetlova et al., unpublished). Metaphase plates were prepared according to standard protocol, and immunofluorescent staining of halogenated precursors was performed as described by Svetlova et al. (2005).

NER and because of its dependence on kinase ATR is considered to be a part of overall DNA damage response (Bergink et al., 2007). Ubiquitylation of H2A and H2AX dependent on the ubiquitin–conjugating enzyme Ubc13 and E3–ligase Ring–finger protein RNF8 was also observed after induction of DSBs (Huen et al., 2007; Ikura et al., 2007; Kolas et al., 2007; Mailand et al., 2007). DSB–associated ubiquitylation of H2AX depends on its phosphorylation and mobilization of mediator protein MDC1 which interacts directly with RNF8 (Mailand et al., 2007).

UV–irradiation also induces ubiquitylation of histones H3 and H4 catalyzed by the CUL4A–UV–DDB–ROC1 complex (Wang et al., 2006), and this modification can facilitate the assembly of NER complex on damaged chromatin (Luijsterburg et al., 2007). UV–induced hyperacetylation of Lys-9 and/or Lys-14 of histone H3 at the repressed MFA2 promoter in yeast and global hyperacetylation of histones H3 and H4 is found (Yu et al., 2005), but its association with NER is not demonstrated. Protein Rad16 is required for the UV–induced acetylation of histone H3, necessary for efficient global NER in yeast (Teng et al., 2008).

Some reports suggest that ATR–dependent H2AX phosphorylation can occur after UV–irradiation (Hanasoge and Ljungman, 2007; Matsumoto et al., 2007; O'Driscoll et al., 2003; Stiff et al., 2006). This phosphorylation depends on UV–induced replication stress and takes place at replication forks (Ward and Chen, 2001; Ward et al., 2004). Other studies show that γH2AX can also be detected in unirradiated and UV–irradiated G1 cells, but this phosphorylation produces only very small foci or diffuse staining of nuclei (Han et al., 2006; Marti et al., 2006; McManus and Hendzel, 2005). Significance of these observations remains unclear.

New H3.1 histones get incorporated *in vivo* at NER sites and this *de novo* deposition is dependent on NER, indicating that it occurs at a postrepair stage (Polo et al., 2006). This UV–induced deposition of H3.1 is catalyzed by chromatin assembly factor 1 (CAF1), but CAF1 knockdown does not inhibit NER in mammalian cells, suggesting that the deposition is a part of chromatin restoration step after DNA damage has been repaired (Dinant et al., 2008). Interestingly, the knockdown of p60 subunit of CAF1 abolishes formation of foci of ubiquitylated histone H2A in UV–irradiated cells (Zhu et al., 2009), suggesting that CAF1 (composed of the three subunits, p150, p60, and p48) may also be involved in H2A ubiquitylation. This ubiquitylation and H3.1 deposition can change epigenetic landscape in UV–irradiated cells (Corpet and Almouzni, 2009; Groth et al., 2007; Polo et al., 2006), but it remains to be established whether these chromatin changes are conserved during subsequent cell divisions or completely erased after repair.

Chromatin can also be altered during DNA repair in non–S–phase cells through histone exchange. For example, phosphorylated histone H2Av

induced at sites of DSBs is eliminated from *Drosophila* chromatin through its exchange with unmodified H2Av (Kusch et al., 2004). For this exchange the histone acetylation by dTIP60 protein and the activity of the adenosine triphosphatase Domino/p400 are required (Kusch et al., 2004). Mammalian TIP60 induces acetylation of histone H2AX (which depends on its ubiquitination) and stimulates release of γH2AX from damaged chromatin (Ikura et al., 2007). We found that GFP-H2AX has very low mobility in the nucleus that is not stimulated by DNA damage (Siino et al., 2002; Svetlova et al., 2007). However, even if the rate of H2AX exchange is slow, it could explain the slow elimination of γH2AX foci in the nucleus by histone exchange (Svetlova et al., 2007). Our attempts to detect stimulation of histone H2AX exchange after UV-irradiation were unsuccessful (Svetlova et al., unpublished).

5. DIRECT DETECTION OF DAMAGED NUCLEOTIDES USING SPECIFIC ANTIBODIES AND OTHER METHODS

5.1. Immunological detection of pyrimidine dimers and other lesions

Antibodies have been developed against UV-damaged DNA (Buma et al., 1995; Cooke and Robson, 2006; Cooke et al., 2003; Eggset et al., 1983) and the oxidized bases (Bruskov et al., 1999; Yin et al., 1995). Polyclonal antiserum prepared against DNA irradiated with short-wave UV-light (UVC) detects both CPDs and 6-4PPs (McCready, 2006). Mouse monoclonal antibodies TDM-2 specifically bind to cys-*syn*-cyclobutane dimers (Torizawa et al., 2000), and 6-4PPs can be detected with specific antibody Fab fragment 64 M2 (Yokoyama et al., 2000).

Monoclonal mouse Ab 1F7 and 1F11 which bind to 8-oxoG or 8-hydroxydeoxyguanosine (8-OHdG) in DNA were isolated (Yin et al., 1995). After immunoaffinity purification of 1F7 Ab, an ELISA quantitation method is developed which has sufficient sensitivity for detecting 8-OHdG in human DNA samples (Yin et al., 1995). A sensitive chemiluminescence enzyme immunoassay is also developed allowing the detection of several femtomoles of 8-oxoG in a 40 μg sample of DNA (Bruskov et al., 1999). It has been shown using this assay that nucleosides guanosine and inosine protect DNA against oxidation and heat-induced deamination and increase survival of lethally irradiated mice (Gudkov et al., 2006).

Antibodies were also prepared against a wide array of bulky carcinogen–DNA adducts, their sensitivity for the detection of DNA damage in humans has been demonstrated in many studies (Santella, 1999). An ultrasensitive detection and quantitation of carcinogen–DNA adducts is possible by ^{32}P-postlabeling assay, it has a wide range of applications in human, animal, and

in vitro studies, and can be used for a wide variety of classes of compounds and for the detection of adducts formed by complex mixtures (Phillips and Arlt, 2007).

5.2. Detection of 8-oxoG using avidin or HPLC

Avidin is shown to bind with high specificity to the oxidatively modified base, 8-oxoG (Conners et al., 2006; Struthers et al., 1998). The technique has been shown to be applicable to isolated DNA and to DNA in fixed cellular material and postmortem tissues. Different levels of oxidative damage can be demonstrated in both isolated DNA and cultured cells exposed to oxidative agents, and results can be quantitated using avidin-FITC conjugates and flow cytometry (Kropotov et al., 2006).

Urinary 8-OHdG is a marker of oxidative DNA damage which can be isolated by immunoaffinity chromatography and quantitated using antibodies or high–performance liquid chromatography (HPLC) with electrochemical detection (Degan et al., 1991). An automated analytical method has been developed for determination of 8-OHdG in human urine, based on coupled-column HPLC with electrochemical detection (Tagesson et al., 1995). High levels of urinary 8-OHdG were found in patients subjected to whole body irradiation, and in patients receiving chemotherapy with various cytostatic agents (Tagesson et al., 1995).

Recently, a simple and sensitive method for the analysis of urinary 8-OHdG by capillary electrophoresis with end-column amperometric detection has been developed allowing analysis of 8-OHdG in urine of healthy persons, patients with cancer, patients with diabetic nephropathy, and smokers (Xu et al., 2008).

5.3. New methods for detection of abasic sites

A biotinylated aldehyde-specific reagent, ARP, has been shown to react specifically with the aldehyde group present in AB sites, resulting in biotin-tagged AB sites in DNA. The biotin-tagged AB sites can then be determined colorimetrically with an ELISA-like assay, using avidin/biotin-conjugated horseradish peroxidase as the indicator enzyme. The ARP assay is thus a simple, rapid, and sensitive method for detection of AB sites in DNA (Kow and Dare, 2000). In another method the Redmond Red, a fluoropore containing a redox–active phenoxazine core, has been suggested as a new electrochemical probe for the detection of AB sites in double-stranded DNA (Buzzeo and Barton, 2008).

6. Conclusions and Perspectives

Apparent genome stability during long periods of geological time is surprising in view of its continuous damage by different environmental and endogenous factors. Not only protein- and RNA-coding sequences are conserved but also chromosome structures and nuclear architecture which is highly dynamic. In eukaryotic cells, excessive DNA damage initiates cell death indicating that genome maintenance mechanisms and DNA damage response are key regulators of cell cycle and cell proliferation. During the last decade, several new approaches were developed for detection and analysis of DNA damage and repair. In this chapter, we reviewed application of these approaches. The most important is the development of new cytological methods of detection of DSBs allowing localization and counting of these dangerous lesions in the nucleus. It is notable that cytological methods can be used for analysis of very different biological samples including tissue sections. Indirect methods of detection of DSBs have important current applications in medicine and basic research, and it is likely that their significance will grow in the future. The development of methods for the analysis of the dynamics of fluorescent protein-tagged DNA repair proteins and histones in living cells is very important. High mobility of repair proteins found in these studies anticipates the stochastic nature of transient assembly of repair complexes on DNA lesions or blocked replication forks. Low mobility of core histones is consistent with their central role in maintenance of epigenetic patterns. However, DNA damage-induced specific modifications of histones can effect epigenetic inheritance and gene expression and explain at least some of the known epigenetic effects of IR. Among other technical developments which may be useful for analysis of DNA repair are immunofluorescent methods of visualization of repair and chromatin proteins after partial UV-irradiation, and detection of DRS in fixed cells with high temporal and spatial resolution. These studies clearly demonstrate that at least some DRS events are regularly spaced (clustered) in the nucleus, like the transcription which is active in preassembled "factories" accommodating several chromatin loops.

REFERENCES

Aboussekhra, A., Wood, R.D., 1995. Detection of nucleotide excision repair incisions in human fibroblasts by immunostaining for PCNA. Exp. Cell Res. 221, 326–332.

Bakkenist, C.J., Kastan, M.B., 2003. DNA damage activates ATM through intermolecular autophosphorylation and dimer dissociation. Nature 421, 499–506.

Balajee, A.S., May, A., Dianova, I., Bohr, V.A., 1998. Efficient PCNA complex formation is dependent upon both transcription coupled repair and genome overall repair. Mutat. Res. 409, 135–146.

Banáth, J.P., Macphail, S.H., Olive, P.L., 2004. Radiation sensitivity, H2AX phosphorylation, and kinetics of repair of DNA strand breaks in irradiated cervical cancer cell lines. Cancer Res. 64, 7144–7149.

Barnes, D.E., Lindahl, T., 2004. Repair and genetic consequences of endogenous DNA base damage in mammalian cells. Annu. Rev. Genet. 38, 445–476.

Bartkova, J., Horejsí, Z., Koed, K., Krämer, A., Tort, F., Zieger, K., et al., 2005. DNA damage response as a candidate anti-cancer barrier in early human tumorigenesis. Nature 14, 864–870.

Bekker-Jensen, S., Lukas, C., Kitagawa, R., Melander, F., Kastan, M.B., Bartek, J., et al., 2006. Spatial organization of the mammalian genome surveillance machinery in response to DNA strand breaks. J. Cell Biol. 173, 195–206.

Bergink, S., Salomons, F.A., Hoogstraten, D., Groothuis, T.A, de Waard, H., Wu, J., et al., 2006. DNA damage triggers nucleotide excision repair-dependent monoubiquitylation of histone H2A. Genes Dev. 20, 1343–1352.

Bergink, S., Jaspers, N.G., Vermeulen, W., 2007. Regulation of UV-induced DNA damage response by ubiquitylation. DNA Repair (Amst) 6, 1231–1242.

Bowman, K.K., Smith, C.A., Hanawalt, P.C., 1997. Excision-repair patch lengths are similar for transcription-coupled repair and global genome repair in UV-irradiated human cells. Mutat. Res. 385, 95–105.

Bravo, R., MacDonald-Bravo, H., 1987. Existence of two populations of cyclin/proliferating cell nuclear antigen during the cell cycle: association with DNA replication sites. J. Cell Biol. 105, 1549–1554.

Bruskov, V.I., Masalimov, Z.K., Usacheva, A.M., 1999. Chemiluminescence enzyme immunoassay of 8-oxoguanine in DNA. Biochemistry (Mosc.) 64, 803–808.

Buis, J., Wu, Y., Deng, Y., Leddon, J., Westfield, G., Eckersdorff, M., et al., 2008. Mre11 nuclease activity has essential roles in DNA repair and genomic stability distinct from ATM activation. Cell 135, 85–96.

Buma, A.G.J., van Hannen, J.E.J., Roza, L., Velsdius, M.J.W., Gieskes, W.C., 1995. Monitoring ultraviolet B induced DNA damage in individual diatom cells by immunofluorescent thymine dimer detection. J. Phycol. 51, 314–321.

Buzzeo, M.C., Barton, J.K., 2008. Redmond red as a redox probe for the DNA-mediated detection of abasic sites. Bioconjug. Chem. 19, 2110–2112.

Carter, D.R., Eskiw, C., Cook, P.R., 2008. Transcription factories. Biochem. Soc. Trans. 36, 585–589.

Celis, J.E., Madsen, P., 1986. Increased nuclear cyclin/PCNA antigen staining of non S-phase transformed human amnion cells engaged in nucleotide excision repair. FEBS Lett. 209, 277–283.

Chowdhury, D., Keogh, M.C., Ishii, H., Peterson, C.L., Buratowski, S., Lieberman, J., 2005. Gamma-H2AX dephosphorylation by protein phosphatase 2A facilitates DNA double-strand break repair. Mol. Cell 20, 801–809.

Cleaver, J.E., Bootsma, D., 1975. Xeroderma pigmentosum: biochemical and genetic characteristics. Annu. Rev. Genet. 9, 19–38.

Conners, R., Hooley, E., Clarke, A.R., Thomas, S., Brady, R.L., 2006. Recognition of oxidatively modified bases within the biotin-binding site of avidin. J. Mol. Biol. 357, 263–274.

Cook, P.R., 1999. The organization of replication and transcription. Science 284, 1790–1795.

Cooke, M.S., Robson, A., 2006. Immunochemical detection of UV-induced DNA damage and repair. Methods Mol. Biol. 314, 215–228.

Cooke, M.S., Podmore, I.D., Mistry, N., Evans, M.D., Herbert, K.E., Griffiths, H.R., et al., 2003. Immunochemical detection of UV-induced DNA damage and repair. J. Imunol. Methods 280, 125–133.

Corpet, A., Almouzni, G., 2009. Making copies of chromatin: the challenge of nucleosomal organization and epigenetic information. Trends Cell Biol. 19, 29–41.

de Haas, R.R., Verwoerd, N.P., van der Corput, M.P., van Gijlswijk, R.P., Siitari, H., Tanke, H.J., 1996. The use of peroxidase-mediated deposition of biotin-tyramide in combination with time-resolved fluorescence imaging of europium chelate label in immunohistochemistry and in situ hybridization. J. Histochem. Cytochem. 44, 1091–1099.

Degan, P., Shigenaga, M.K., Park, E.M., Alperin, P.E., Ames, B.N., 1991. Immunoaffinity isolation of urinary 8-hydroxy-2′-deoxyguanosine and 8-hydroxyguanine and quantitation of 8-hydroxy-2′-deoxyguanosine in DNA by polyclonal antibodies. Carcinogenesis 12, 865–871.

Dinant, C., de Jager, M., Essers, J., van Cappellen, W. A., Kanaar, R., Houtsmuller, A. B., and Vermeulen, W., 2007. Activation of multiple DNA repair pathways by sub-nuclear damage induction methods. J. Cell. Sci. 120, 2731–2740.

Dinant, C., Houtsmuller, A.B., Vermeulen, W., 2008. Chromatin structure and DNA damage repair. Epigenet. Chromatin 12, 9.

DiTullio Jr, R.A., Mochan, T.A., Venere, M., Bartkova, J., Sehested, M., Bartek, J., et al., 2002. 53BP1 functions in an ATM-dependent checkpoint pathway that is constitutively activated in human cancer. Nat. Cell Biol. 4, 998–1002.

Doil, C., Mailand, N., Bekker-Jensen, S., Menard, P., Larsen, D.H., Pepperkok, R., et al., 2009. RNF168 binds and amplifies ubiquitin conjugates on damaged chromosomes to allow accumulation of repair proteins. Cell 136, 435–446.

Eggset, G., Volden, G., Krokan, H., 1983. UV-induced DNA damage and its repair in human skin *in vivo* studied by sensitive immunohistochemical methods. Carcinogenesis (London) 4, 745–750.

Engel, N., Tront, J.S., Erinle, T., Nguyen, N., Latham, K.E., Sapienza, C., et al., 2009. Conserved DNA methylation in Gadd45a(-/-) mice. Epigenetics 4 (in press).

Fortini, P., Dogliotti, E., 2007. Base damage and single-strand break repair: mechanisms and functional significance of short- and long-patch repair subpathways. DNA Repair (Amst) 6, 398–409.

Fu, Y., Zhu, Y., Zhang, K., Yeung, M., Durocher, D., Xiao, W., 2008. Rad6-Rad18 mediates a eukaryotic SOS response by ubiquitinating the 9-1-1 checkpoint clamp. Cell 133, 601–611.

Gavrilov, B., Vezhenkova, I., Firsanov, D., Solovjeva, L., Svetlova, M., Mikhailov, V., et al., 2006. Slow elimination of phosphorylated histone gamma-H2AX from DNA of terminally differentiated mouse heart cells in situ. Biochem. Biophys. Res. Commun. 347, 1048–1052.

Gehring, M., Reik, W., Henikoff, S., 2009. DNA demethylation by DNA repair. Trends Genet. 25, 82–90.

Gerashchenko, B.I., Dynlacht, J.R., 2009. A tool for enhancement and scoring of DNA repair foci. Cytometry A 75, 245–252.

Groth, A., Rocha, W., Verreault, A., Almouzni, G., 2007. Chromatin challenges during DNA replication and repair. Cell 128, 721–733.

Gudkov, S.V., Shtarkman, I.N., Smirnova, V.S., Chernikov, A.V., Bruskov, V.I., 2006. Guanosine and inosine display antioxidant activity, protect DNA *in vitro* from oxidative damage induced by reactive oxygen species, and serve as radioprotectors in mice. Radiat. Res. 165, 538–545.

Guirouilh Barbat, J., Redon, C., Pommier, Y., 2008. Transcription-coupled DNA double-strand breaks are mediated via the nucleotide excision repair and the Mre11-Rad50-Nbs1 complex. Mol. Biol. Cell 19, 3969–3981.

Haaf, T., Golub, E.I., Reddy, G., Radding, C.M., Ward, D.C., 1995. Nuclear foci of mammalian Rad51 recombination protein in somatic cells after DNA damage and its localization in synaptonemal complexes. Proc. Natl. Acad. Sci. USA 92, 2298–22302.

Han, J., Hendzel, M.J., Allalunis-Turner, J., 2006. Quantitative analysis reveals asynchronous and more than DSB-associated histone H2AX phosphorylation after exposure to ionizing radiation. Radiat. Res. 165, 283–292.

Hanasoge, S., Ljungman, M., 2007. H2AX phosphorylation after UV-irradiation is triggered by DNA repair intermediates and is mediated by the ATR kinase. Carcinogenesis 28, 2298–2304.

Hanawalt, P.C., Spivak, G., 2008. Transcription-coupled DNA repair: two decades of progress and surprises. Nat. Rev. Mol. Cell Biol. 9, 958–970.

Hashiguchi, K., Matsumoto, Y., Yasui, A., 2007. Recruitment of DNA repair synthesis machinery to sites of DNA damage/repair in living human cells. Nucleic Acids Res. 35, 2913–2923.

Hoogstraten, D., Bergink, S., Ng, J.M., Verbiest, V.H., Luijsterburg, M.S., Geverts, B., et al., 2008. Versatile DNA damage detection by the global genome nucleotide excision repair protein XPC. J. Cell Sci. 121, 2850–2859.

Houtsmuller, A.B., Rademakers, S., Nigg, A.L., Hoogstraten, D., Hoeijmakers, J.H., Vermeulen, W., 1999. Action of DNA repair endonuclease ERCC1/XPF in living cells. Science 284, 958–961.

Huen, M.S., Grant, R., Manke, I., Minn, K., Yu, X., Yaffe, M.B., et al., 2007. RNF8 transduces the DNA-damage signal via histone ubiquitylation and checkpoint protein assembly. Cell 131, 901–914.

Ikura, T., Tashiro, S., Kakino, A., Shima, H., Jacob, N., Amunugama, R., et al., 2007. DNA damage-dependent acetylation and ubiquitination of H2AX enhances chromatin dynamics. Mol. Cell. Biol. 27, 7028–7040.

Ismail, I.H., Wadhra, T.I., Hammarsten, O., 2007. An optimized method for detecting gamma-H2AX in blood cells reveals a significant interindividual variation in the gamma-H2AX response among humans. Nucleic Acids Res. 35 (5), e36.

Jackson, D.A., Iborra, F.J., Manders, E.M., Cook, P.R., 1998. Numbers and organization of RNA polymerases, nascent transcripts, and transcription units in HeLa nuclei. Mol. Biol. Cell 9, 1523–1536.

Jakob, B., Splinter, J., Durante, M., Taucher-Scholz, G., 2009. Live cell microscopy analysis of radiation-induced DNA double-strand break motion. Proc. Natl. Acad. Sci. USA 106, 3172–3177.

Jeggo, P.A., Löbrich, M., 2005. Artemis links ATM to double strand break rejoining. Cell Cycle 4, 359–362.

Jin, S.G., Guo, C., Pfeifer, G.P., 2008. GADD45A does not promote DNA demethylation. PLoS Genet. 4, e1000013.

Jiricny, J., Menigatti, M., 2008. DNA Cytosine demethylation: are we getting close? Cell 135, 1167–1169.

Jung, H.J., Kim, E.H, Mun, J.Y., Park, S., Smith, M.L., Han, S.S., et al., 2007. Base excision DNA repair defect in Gadd45a-deficient cells. Oncogene 26, 7517–7525.

Kamiuchi, S., Saijo, M., Citterio, E., de Jager, M., Hoeijmakers, J.H., Tanaka, K., 2002. Translocation of Cockayne syndrome group A protein to the nuclear matrix: possible relevance to transcription-coupled DNA repair. Proc. Natl. Acad. Sci. USA 99, 201–206.

Kolas, N.K., Chapman, J.R., Nakada, S., Ylanko, J., Chahwan, R., Sweeney, F.D., et al., 2007. Orchestration of the DNA-damage response by the RNF8 ubiquitin ligase. Science 318, 1637–1640.

Kow, Y.W., Dare, A., 2000. Detection of abasic sites and oxidative DNA base damage using an ELISA-like assay. Methods 22, 164–169.

Kropotov, A., Serikov, V., Suh, J., Smirnova, A., Bashkirov, V., Zhivotovsky, B., et al., 2006. Constitutive expression of the human peroxiredoxin V gene contributes to protection of the genome from oxidative DNA lesions and to suppression of transcription of noncoding DNA. FEBS J. 273, 2607–2617.

Kusch, T., Florens, L., Macdonald, W.H., Swanson, S.K., Glaser, R.L., Yates 3rd, J.R., et al., 2004. Acetylation by Tip60 is required for selective histone variant exchange at DNA lesions. Science 306, 2084–2087.

Langston, L.D., O'Donnell, M., 2008. DNA polymerase delta is highly processive with proliferating cell nuclear antigen and undergoes collision release upon completing DNA. J. Biol. Chem. 283, 29522–29531.

Lee, J.H., Paull, T.T., 2004. Direct activation of the ATM protein kinase by the Mre11/Rad50/Nbs1 complex. Science 304, 93–96.

Lee, H., Kwak, H.J., Cho, I.T., Park, S.H, Lee, C.H., 2009. S1219 residue of 53BP1 is phosphorylated by ATM kinase upon DNA damage and required for proper execution of DNA damage response. Biochem. Biophys. Res. Commun. 378, 32–36.

Leonhardt, H., Rahn, H.P., Weinzierl, P., Sporbert, A., Cremer, T., Zink, D., et al., 2000. Dynamics of DNA replication factories in living cells. J. Cell Biol. 149, 271–280.

Li, X., Heyer, W.D., 2008. Homologous recombination in DNA repair and DNA damage tolerance. Cell Res. 18, 99–113.

Ljungman, M., Zhang, F., Chen, F., Rainbow, A.J., McKay, B.C., 1999. Inhibition of RNA polymerase II as a trigger for the p53 response. Oncogene 18, 583–592.

Löbrich, M., Rief, N., Kühne, M., Heckmann, M., Fleckenstein, J., Rübe, C., et al., 2005. In vivo formation and repair of DNA double-strand breaks after computed tomography examinations. Proc. Natl. Acad. Sci. USA 102, 8984–8989.

Luijsterburg, M.S., Goedhart, J., Moser, J., Kool, H., Geverts, B., Houtsmuller, A.B., et al., 2007. Dynamic in vivo interaction of DDB2 E3 ubiquitin ligase with UV-damaged DNA is independent of damage-recognition protein XPC. J. Cell Sci. 120, 2706–2716.

Lukas, C., Melander, F., Stucki, M., Falck, J., Bekker-Jensen, S., Goldberg, M., et al., 2004. Mdc1 couples DNA double-strand break recognition by Nbs1 with its H2AX-dependent chromatin retention. EMBO J. 23, 2674–2683.

Ma, D.K., Jang, M.H., Guo, J.U., Kitabatake, Y., Chang, M.L., Pow-Anpongkul, N., et al., 2009. Neuronal activity-induced Gadd45b promotes epigenetic DNA demethylation and adult neurogenesis. Science 323, 1074–1077.

MacPhail, S.H., Banáth, J.P., Yu, T.Y., Chu, E.H., Lambur, H., Olive, P.L., 2003. Expression of phosphorylated histone H2AX in cultured cell lines following exposure to X-rays. Int. J. Radiat. Biol. 79, 351–358.

Madsen, P., Celis, J.E., 1985. S-phase patterns of of cyclin (PCNA) antigen staining resemble topographical patters of DNA synthesis. FEBS Lett. 193, 5–11.

Mahaney, B.L, Meek, K., Lees-Miller, S.P., 2009. Repair of ionizing radiation-induced DNA double-strand breaks by non-homologous end-joining. Biochem. J. 417, 639–650.

Mailand, N., Bekker-Jensen, S., Faustrup, H., Melander, F., Bartek, J., Lukas, C., et al., 2007. RNF8 Ubiquitylates Histones at DNA Double-Strand Breaks and Promotes Assembly of Repair Proteins. Cell 131, 887–900.

Majka, J., Burgers, P.M., 2004. The PCNA–RFC families of DNA clamps and clamp loaders. Prog. Nucleic Acid Res. Mol. Biol. 78, 227–260.

Manders, E.M., Stap, J., Brakenhoff, G.J., van Driel, R., Aten, J.A., 1992. Dynamics of three-dimensional replication patterns during the S-phase, analysed by double labelling of DNA and confocal microscopy. J. Cell Sci. 103, 857–862.

Manders, E.M., Stap, J., Strackee, J., van Driel, R., Aten, J.A., 1996. Dynamic behavior of DNA replication domains. Exp. Cell. Res. 226, 328–335.

Marchetti, F., Coleman, M.A, Jones, I.M., Wyrobek, A.J., 2006. Candidate protein biodosimeters of human exposure to ionizing radiation. Int. J. Radiat. Biol. 82, 605–639.

Marti, T.M., Hefner, E., Feeney, L., Natale, V., Cleaver, J.E., 2006. H2AX phosphorylation within the G1 phase after UV irradiation depends on nucleotide excision repair and not DNA doublestrand breaks. Proc. Natl. Acad. Sci. USA 103, 9891–9896.

Maser, R.S., Monsen, K.J., Nelms, B.E., Petrini, J.H., 1997. hMre11 and hRad50 nuclear foci are induced during the normal cellular response to DNA double-strand breaks. Mol. Cell. Biol. 17, 6087–6096.

Matsumoto, M., Yaginuma, K., Igarashi, A., Imura, M., Hasegawa, M., Iwabuchi, K., et al., 2007. Perturbed gap-filling synthesis in n ucleotide excision repair causes histone H2AX phosphorylation in human quiescent cells. J. Cell Sci. 120, 1104–1112.

McCready, S., 2006. A dot-blot immunoassay for measuring repair of ultraviolet photoproducts. Methods Mol. Biol. 314, 229–238.

McKay, J.A., Murray, G.I., Keith, W.N., McLeod, H.L., 1997. Amplification of fluorescent in situ hybridisation signals in formalin fixed paraffin wax embedded sections of colon tumour using biotinylated tyramide. Mol. Pathol. 50, 322–325.

McManus, K.J., Hendzel, M.J., 2005. ATM-dependent DNA damage-independent mitotic phosphorylation of H2AX in normally growing mammalian cells. Mol. Biol. Cell 16, 5013–5025.

Mischo, H.E., Hemmerich, P., Grosse, F., Zhang, S., 2005. Actinomycin D induces histone gamma-H2AX foci and complex formation of gamma-H2AX with Ku70 and nuclear DNA helicase II. J. Biol. Chem. 280, 9586–9594.

Mitchell, J.A., Fraser, P., 2008. Transcription factories are nuclear subcompartments that remain in the absence of transcription. Genes Dev. 22, 20–25.

Miura, M., Sasaki, T., 1996. Effect of XPA gene mutations on UV-induced immunostaining of PCNA in fibroblasts from Xeroderma pigmentosum group A patients. Mutat. Res. 364, 51–56.

Miura, M., Domon, M., Sasaki, T., Takasaki, Y., 1992a. Induction of proliferating cell nuclear antigen (PCNA) complex formation in quiescent fibroblasts from a xeroderma pigmentosum patient. J. Cell Physiol. 150, 370–376.

Miura, M., Domon, M., Sasaki, T., Kondo, S., Takasaki, Y., 1992b. Two types of proliferating cell nuclear antigen (PCNA) complex formation in quiescent normal and xeroderma pigmentosum group A fibroblasts following ultraviolet light (uv) irradiation. Exp. Cell Res. 201, 541–544.

Mocquet, V., Lainé, J.P., Riedl, T., Yajin, Z., Lee, M.Y., Egly, J.M., 2008. Sequential recruitment of the repair factors during NER: the role of XPG in initiating the resynthesis step. EMBO J. 27, 155–167.

Moldovan, G.L., Pfander, B., Jensch, S., 2007. PCNA, the maesto of replication fork. Cell 129, 665–679.

Morales-Ruiz, T., Ortega-Galisteo, A.P., Ponferrada-Marín, M.I., Martínez-Macías, M.I., Ariza, R.R., Roldán-Arjona, T., 2006. DEMETER and REPRESSOR OF SILENCING 1 encode 5-methylcytosine DNA glycosylases. Proc. Natl. Acad. Sci. USA 103, 6853–6858.

Moynahan, M.E., Cui, T.Y., Jasin, M., 2001. Homology-directed DNA repair, mitomycin–c resistance, and chromosome stability is restored with correction of a Brca1 mutation. Cancer Res. 61, 4842–4850.

Muslimovic, A., Ismail, I.H., Gao, Y., Hammarsten, O., 2008. An optimized method for measurement of gamma-H2AX in blood mononuclear and cultured cells. Nat. Protoc. 3, 1187–1193.

Nag, R., Smerdon, M.J., 2009. Altering the chromatin landscape for nucleotide excision repair. Mutat. Res. (in press).

Nakamura, H., Morita, T., Sato, C., 1986. Structural organizations of replicon domains during DNA synthetic phase in the mammalian nucleus. Exp. Cell Res. 165, 291–297.

Nakamura, A., Sedelnikova, O.A., Redon, C., Pilch, D.R., Sinogeeva, N.I., Shroff, R., et al., 2006. Techniques for gamma-H2AX detection. Methods Enzymol. 409, 236–250.

Naryzhny, S.N., 2008. Proliferating cell nuclear antigen: a proteomics view. Cell. Mol. Life Sci. 65, 3789–3808.

Nazarov, I.B., Smirnova, A.N., Krutilina, R.I., Svetlova, M.P., Solovjeva, L.V., Nikiforov, A.A, et al., 2003. Dephosphorylation of histone gamma-H2AX during repair of DNA double-strand breaks in mammalian cells and its inhibition by calyculin A. Radiat. Res. 160, 309–317.

Nikiforov, A., Svetlova, M., Solovjeva, L., Sasina, L., Siino, J., Nazarov, I., et al., 2004. DNA damage-induced accumulation of Rad18 protein at stalled replication forks in mammalian cells involves upstream protein phosphorylation. Biochem. Biophys. Res. Commun. 323, 831–837.

O'Driscoll, M., Ruiz-Perez, V.L., Woods, C.G., Jeggo, P.A., Goodship, J.A., 2003. A splicing mutation affecting expression of ataxia-telangiectasia and Rad3-related protein (ATR) results in Seckel syndrome. Nat. Genet. 33, 497–501.

Oh, K.S., Imoto, K., Boyle, J., Khan, S.G., Kraemer, K.H., 2007. Influence of XPB helicase on recruitment and redistribution of nucleotide excision repair proteins at sites of UV-induced DNA damage. DNA Repair (Amst) 6, 1359–1370.

Olive, P.L., 2004. Detection of DNA damage in individual cells by analysis of histone H2AX phosphorylation. Methods Cell Biol. 75, 355–373.

Phillips, D.H., Arlt, V.M., 2007. The 32P-postlabeling assay for DNA adducts. Nat. Protoc. 2, 2772–2781.

Pierce, A.J., Stark, J.M., Araujo, F.D., Moynahan, M.E., Berwick, M., Jasin, M., 2001. Double-strand breaks and tumorigenesis. Trends Cell Biol. 11, S52–S59.

Pilch, D.R., Redon, C., Sedelnikova, O.A., Bonner, W.M., 2004. Two-dimensional gel analysis of histones and other H2AX-related methods. Methods Enzymol. 375, 76–88.

Polo, S.E., Roche, D., Almouzni, G., 2006. New histone incorporation marks sites of UV repair in human cells. Cell 127, 481–493.

Prakash, S., Johnson, R.E., Prakash, L., 2005. Eukaryotic translesion synthesis DNA polymerases: specificity of structure and function. Annu. Rev. Biochem. 74, 317–353.

Rademakers, S., Volker, M., Hoogstraten, D., Nigg, A.L, Moné, M.J., Van Zeeland, A.A, et al., 2003. Xeroderma pigmentosum group A protein loads as a separate factor onto DNA lesions. Mol. Cell. Biol. 23, 5755–5767.

Rai, K., Huggins, I.J., James, S.R., Karpf, A.R., Jones, D.A., Cairns, B.R., 2008. DNA demethylation in zebrafish involves the coupling of a deaminase, a glycosylase, and Gadd45. Cell 135, 1201–1212.

Ramanathan, B., Smerdon, M.J., 1989. Enhanced DNA repair synthesis in hyperacetylated nucleosomes. J. Biol. Chem. 264, 11026–11034.

Rapić Otrin, V., Kuraoka, I., Nardo, T., McLenigan, M., Eker, A.P., Stefanini, M., et al., 1998. Relationship of the xeroderma pigmentosum group E DNA repair defect to the chromatin and DNA binding proteins UV-DDB and replication protein A. Mol. Cell. Biol. 18, 3182–3190.

Rogakou, E.P., Pilch, D.R., Orr, A.H., Ivanova, V.S., Bonner, W.M., 1998. DNA double-stranded breaks induce histone H2AX phosphorylation on serine 139. J. Biol. Chem. 273, 5858–5868.

Rogakou, E.P., Boon, C., Redon, C., Bonner, W.M., 1999. Megabase chromatin domains involved in DNA double-strand breaks in vivo. J. Cell Biol. 146, 905–916.

Rothkamm, K., Löbrich, M., 2003. Evidence for a lack of DNA double-strand break repair in human cells exposed to very low x-ray doses. Proc. Natl. Acad. Sci. USA 100, 5057–5062.

Rundle, A., 2006. Carcinogen-DNA adducts as a biomarker for cancer risk. Mutat. Res. 600, 23–36.

Sabbioneda, S., Gourdin, A.M., Green, C.M., Zotter, A., Giglia-Mari, G., Houtsmuller, A., et al., 2008. Effect of proliferating cell nuclear antigen ubiquitination and chromatin structure on the dynamic properties of the Y-family DNA polymerases. Mol. Biol. Cell 19, 5193–5202.

Santella, R.M., 1999. Immunological methods for detection of carcinogen-DNA damage in humans. Cancer Epidemiol. Biomarkers Prev. 8, 733–739.

Schultz, L.B., Chehab, N.H., Malikzay, A., Halazonetis, T.D., 2000. p53 binding protein 1 (53BP1) is an early participant in the cellular response to DNA double-strand breaks. J. Cell Biol. 151, 1381–1390.

Scrima, A., Koníčková, R., Czyzewski, B.K., Kawasaki, Y., Jeffrey, P.D., Groisman, R., et al., 2008. Structural basis of UV DNA-damage recognition by the DDB1-DDB2 complex. Cell 135, 1213–1223.

Scully, R., Chen, J., Plug, A., Xiao, Y., Weaver, D., Feunteun, J., et al., 1997a. Association of BRCA1 with Rad51 in mitotic and meiotic cells. Cell 88, 265–275.

Scully, R., Chen, J., Ochs, R.L., Keegan, K., Hoekstra, M., Feunteun, J., Livingston, D.M., 1997b. Dynamic changes of BRCA1 subnuclear location and phosphorylation state are initiated by DNA damage. Cell 90, 425–435.

Sedelnikova, O.A., Bonner, W.M., 2006. GammaH2AX in cancer cells: a potential biomarker for cancer diagnostics, prediction and recurrence. Cell Cycle 5, 2909–2913.

Sengupta, S., Robles, A.I., Linke, S.P., Sinogeeva, N.I., Zhang, R., Pedeux, R., et al., 2004. Functional interaction between BLM helicase and 53BP1 in a Chk1-mediated pathway during S-phase arrest. J. Cell Biol. 166, 801–813.

Sexton, T., Umlauf, D., Kurukuti, S., Fraser, P., 2007. The role of transcription factories in large-scale structure and dynamics of interphase chromatin. Semin. Cell. Dev. Biol. 18, 691–697.

Shivji, K.K., Kenny, M.K., Wood, R.D., 1992. Proliferating cell nuclear antigen is required for DNA excision repair. Cell 69, 367–374.

Siino, J.S., Nazarov, I.B., Svetlova, M.P., Solovjeva, L.V., Adamson, R.H., Zalenskaya, I.A., et al., 2002. Photobleaching of GFP-labeled H2AX in chromatin: H2AX has low diffusional mobility in the nucleus. Biochem. Biophys. Res. Commun. 297, 1318–1323.

Solimando, L., Luijsterburg, M.S., Vecchio, L., Vermeulen, W., van Driel, R., Fakan, S., 2009. Spatial organization of nucleotide excision repair proteins after UV-induced DNA damage in the human cell nucleus. J. Cell Sci. 122, 83–91.

Solovjeva, L., Svetlova, M., Sasina, L., Tanaka, K., Saijo, M., Nazarov, I., et al., 2005. High mobility of flap endonuclease 1 and DNA polymerase eta associated with replication foci in mammalian S-phase nucleus. Mol. Biol. Cell 16, 2518–2528.

Solovjeva, L.V., Svetlova, M.P., Chagin, V.O., Tomilin, N.V., 2007. Inhibition of transcription at radiation-induced nuclear foci of phosphorylated histone H2AX in mammalian cells. Chromosome Res. 15, 787–797.

Spycher, C., Miller, E.S., Townsend, K., Pavic, L., Morrice, N.A., Janscak, P., et al., 2008. Constitutive phosphorylation of MDC1 physically links the MRE11-RAD50-NBS1 complex to damaged chromatin. J. Cell Biol. 181, 227–240.

Stark, J.M., Hu, P., Pierce, A.J., Moynahan, M.E., Ellis, N., Jasin, M., 2002. ATP hydrolysis by mammalian RAD51 has a key role during homology-directed DNA repair. J. Biol. Chem. 277, 20185–20194.

Stewart, G.S., Wang, B., Bignell, C.R., Taylor, A.M., Elledge, S.J., 2003. MDC1 is a mediator of the mammalian DNA damage checkpoint. Nature 421, 961–966.

Stewart, G.S., Panier, S., Townsend, K., Al-Hakim, A.K., Kolas, N.K., Miller, E.S., et al., 2009. The RIDDLE syndrome protein mediates a ubiquitin-dependent signaling cascade at sites of DNA damage. Cell 136, 420–434.

Stiff, T., Walker, S.A., Cerosaletti, K., Goodarzi, A.A., Petermann, E., Concannon, P., et al., 2006. ATR-dependent phosphorylation and activation of ATM in response to UV treatment or replication fork stalling. EMBO J. 25, 5775–5782.

Stracker, T.H., Petrini, J.H., 2008. Working together and apart: the twisted relationship of the Mre11 complex and Chk2 in apoptosis and tumor suppression. Cell Cycle 7, 3618–3621.

Struthers, L., Patel, R., Clark, J., Thomas, S., 1998. Direct detection of 8-oxodeoxyguanosine and 8-oxoguanine by avidin and its analogues. Anal. Biochem. 255, 20–31.

Sugasawa, K., Okuda, Y., Saijo, M., Nishi, R., Matsuda, N., Chu, G., et al., 2005. UV-induced ubiquitylation of XPC protein mediated by UV-DDB-ubiquitin ligase complex. Cell 121, 387–400.

Svejstrup, J.Q., Wang, Z., Feaver, W.J., Wu, X., Bushnell, D.A., Donahue, T.F., et al., 1995. Different forms of TFIIH for transcription and DNA repair: holo-TFIIH and a nucleotide excision repairosome. Cell 80, 21–28.

Svetlova, M.P., Solovjeva, L.V., Nikiforov, A.A., Chagin, V.A., Lehmann, A.R., Tomilin, N.V., 1998. Staurosporine-sensitive protein phosphorylation is required for postreplication DNA repair in human cells. FEBS Lett. 428, 23–26.

Svetlova, M., Nikiforov, A., Solovjeva, L., Pleskach, N., Tomilin, N., Hanawalt, P.C., 1999a. Reduced extractability of the XPA DNA repair protein in ultraviolet light-irradiated mammalian cells. FEBS Lett. 463, 49–52.

Svetlova, M.P., Solovjeva, L.V., Pleskach, N.A., Tomilin, N.V., 1999b. Focal sites of DNA repair synthesis in human chromosomes. Biochem. Biophys. Res. Commun. 257, 378–383.

Svetlova, M., Solovjeva, L., Pleskach, N., Yartseva, N., Yakovleva, T., Tomilin, N., et al., 2002. Clustered sites of DNA repair synthesis during early nucleotide excision repair in ultraviolet light-irradiated quiescent human fibroblasts. Exp. Cell Res. 276, 284–295.

Svetlova, M., Solovjeva, L., Blasius, M., Shevelev, I., Hubscher, U., Hanawalt, P., et al., 2005. Differential incorporation of halogenated deoxyuridines during UV-induced DNA repair synthesis in human cells. DNA Repair (Amst) 4, 359–366.

Svetlova, M., Solovjeva, L., Nishi, K., Nazarov, I., Siino, J., Tomilin, N., 2007. Elimination of radiation-induced gamma-H2AX foci in mammalian nucleus can occur by histone exchange. Biochem. Biophys. Res. Commun. 358, 650–654.

Tagesson, C., Källberg, M., Klintenberg, C., Starkhammar, H., 1995. Determination of urinary 8-hydroxdeoxyguanosine by automated coupled-column high performance liquid chromatography: a powerful technique for assaying in vivo oxidative DNA damage in cancer patients. Eur. J. Cancer 31A, 934–940.

Teng, Y., Liu, H., Gill, H.W., Yu, Y., Waters, R., Reed, S.H., 2008. Saccharomyces cerevisiae Rad16 mediates ultraviolet-dependent histone H3 acetylation required for efficient global genome nucleotide-excision repair. EMBO Rep. 9, 97–102.

Tomida, J., Masuda, Y., Hiroaki, H., Ishikawa, T., Song, I., Tsurimoto, T., et al., 2008. DNA damage-induced ubiquitylation of RFC2 subunit of replication factor C complex. J. Biol. Chem. 283, 9071–9079.

Tomilin, N.V., Solovjeva, L.V., Svetlova, M.P., Pleskach, N.M., Zalenskaya, I.A., Yau, P.M., et al., 2001. Visualization of focal nuclear sites of DNA repair synthesis induced by bleomycin in human cells. Radiat. Res. 156, 347–354.

Torizawa, T., Yamamoto, N., Suzuki, T., Nobuoka, K., Komatsu, Y., Morioka, H., et al., 2000. DNA binding mode of the Fab fragment of a monoclonal antibody specific for cyclobutane pyrimidine dimer. Nucleic Acids Res. 28, 944–951.

Toschi, L., Bravo, R., 1988. Changes in cyclin/proliferating cell nuclear antigen distribution during DNA repair synthesis. J. Cell Biol. 107, 1623–1628.

van Gent, D.C., van der Burg, M., 2007. Non-homologous end-joining, a sticky affair. Oncogene 26, 7731–7740.

Verschure, P.J., van der Kraan, I., Manders, E.M., Hoogstraten, D., Houtsmuller, A.B., van Driel, R., 2003. Condensed chromatin domains in the mammalian nucleus are accessible to large macromolecules. EMBO Rep. 4, 861–866.

Vilenchik, M.M., Knudson, A.G., 2003. Endogenous DNA double-strand breaks: production, fidelity of repair, and induction of cancer. Proc. Natl. Acad. Sci. USA 100, 12871–12876.

Vilenchik, M.M., Knudson, A.G., 2006. Radiation dose-rate effects, endogenous DNA damage, and signaling resonance. Proc. Natl. Acad. Sci. USA 103, 17874–17879.

Volker, M., Moné, M.J., Karmakar, P., van Hoffen, A., Schul, W., Vermeulen, W., et al., 2001. Sequential assembly of the nucleotide excision repair factors in vivo. Mol. Cell 8, 213–224.

Wakasugi, M., Kawashima, A., Morioka, H., Linn, S., Sancar, A., Mori, T., et al., 2002. DDB accumulates at DNA damage sites immediately after UV irradiation and directly stimulates nucleotide excision repair. J. Biol. Chem. 277, 1637–1640.

Wang, H., Zhai, L., Xu, J., Joo, H.Y., Jackson, S., Erdjument-Bromage, H., et al., 2006. Histone H3 and H4 ubiquitylation by the CUL4–DDB–ROC1 ubiquitin ligase facilitates cellular response to DNA damage. Mol. Cell 22, 383–394.

Ward, I.M., Chen, J., 2001. Histone H2AX is phosphorylated in an ATR–dependent manner in response to replicational stress. J. Biol. Chem. 276, 47759–47762.

Ward, I.M., Minn, K., Chen, J., 2004. UV-induced ataxia-telangiectasia-mutated and Rad3-related (ATR) activation requires replication stress. J. Biol. Chem. 279, 9677–9680.

Warters, R. L., Adamson, P. J., Pond, C. D., Leachman, S. A., 2005. Melanoma cells express elevated levels of phosphjorylated histone H2AX foci. J. Invest. Dermatol. 124, 807–817.

Watanabe, K., Tateishi, S., Kawasuji, M., Tsurimoto, T., Inoue, H., Yamaizumi, M., 2004. Rad18 guides polη to replication stalling sites through physical interaction and PCNA monoubiquitination. EMBO J. 23, 3886–3896.

Watanabe, K., Iwabuchi, K., Sun, J., Tsuji, Y., Tani, T., Tokunaga, K., et al., 2009. RAD18 promotes DNA double-strand break repair during G1 phase through chromatin retention of 53BP1. Nucleic Acids Res. 37, 2176–2193.

Weinstock, D.M, Richardson, C.A., Elliott, B., Jasin, M., 2006. Modeling oncogenic translocations: distinct roles for double-strand break repair pathways in translocation formation in mammalian cells. DNA Repair (Amst) 5, 1065–1074.

Westermark, U.K., Reyngold, M., Olshen, A.B., Baer, R., Jasin, M., Moynahan, M.E., 2003. BARD1 participates with BRCA1 in homology-directed repair of chromosome breaks. Mol. Cell. Biol. 23, 7926–7936.

Williams, R.S., Moncalian, G., Williams, J.S., Yamada, Y., Limbo, O., Shin, D.S., et al., 2008. Mre11 dimers coordinate DNA end bridging and nuclease processing in double-strand-break repair. Cell 135, 97–109.

Wilson, K.A., Stern, D.F., 2008. NFBD1/MDC1, 53BP1 and BRCA1 have both redundant and unique roles in the ATM pathway. Cell Cycle 7, 3584–3594.

Xu, G., Shi, X., Mei, S., Yao, Q., Weng, Q., Wu, C., 2008. Capillary electrophoresis of oxidative DNA damage. Methods Mol. Biol. 384, 431–440.

Yan, C.T., Boboila, C., Souza, E.K., Franco, S., Hickernell, T.R., Murphy, M., et al., 2007. IgH class switching and translocations use a robust non-classical end-joining pathway. Nature 449, 478–482.

Yin, B., Whyatt, R.M., Perera, F.P., Randall, M.C., Jedrychowski, W., Cooper, Y., et al., 1995. Determination of 8-hydroxydeoxyguanosine by immunoaffinity chromatography-monoclonal antibody-based ELISA. Free Radic. Biol. Med. 18, 1023–1032.

Yokoyama, H., Mizutani, R., Satow, Y., Komatsu, Y., Ohtsuka, E., Nikaido, O., 2000. Crystal structure of the 64 M2 antibody Fab fragment in complex with a DNA dT(6-4)T photoproduct formed by ultraviolet radiation. J. Mol. Biol. 299, 711–723.

Yu, Y., Teng, Y., Liu, H., Reed, S.H., Waters, R., 2005. UV irradiation stimulates histone acetylation and chromatin remodeling at a repressed yeast locus. Proc. Natl. Acad. Sci. USA 102, 8650–8655.

Yu, T., MacPhail, S.H., Banáth, J.P., Klokov, D., Olive, P.L., 2006. Endogenous expression of phosphorylated histone H2AX in tumors in relation to DNA double-strand breaks and genomic instability. DNA Repair (Amst). 5, 935–946.

Yu, Y.M., Pace, S.M., Allen, S.R., Deng, C.X., Hsu, L.C., 2008. A PP1-binding motif present in BRCA1 plays a role in its DNA repair function. Int. J. Biol. Sci. 4, 352–361.

Zha, S., Sekiguchi, J., Brush, J.W., Bassing, C.H., Alt, F.W., 2008. Complementary functions of ATM and H2AX in development and suppression of genomic instability. Proc. Natl. Acad. Sci. USA 105, 9302–9306.

Zhu, Q., Wani, G., Arab, H.H., El-Mahdy, M.A., Ray, A., Wani, A.A., 2009. Chromatin restoration following nucleotide excision repair involves the incorporation of ubiquitinated H2A at damaged genomic sites. DNA Repair (Amst) 8, 262–273.

Zotter, A., Luijsterburg, M.S., Warmerdam, D.O., Ibrahim, S., Nigg, A., van Cappellen, W.A., et al., 2006. Recruitment of the nucleotide excision repair endonuclease XPG to sites of UV-induced DNA damage depends on functional TFIIH. Mol. Cell. Biol. 26, 8868–8879.

Index